United States Department of the Interior

U.S. GEOLOGICAL SURVEY

December 21, 2001

To: Wayne Praskins
Superfund Project Manager
EPA Region IX, Superfund Division
75 Hawthorn St (SFD-7)
San Francisco, CA 94015

Re: Final Carson River Mercury Report

Wayne,

I am pleased to be able to send you these three copies of our final Report entitled: "Methylmercury Formation and Degradation in Sediments of the Carson River System" in fulfillment of our prior contract [EPA Interagency Agreement # DW14955409-01-0]. As we have discussed previously, this earlier versions of this document was submitted as a USGS Administrative Report, and as such is still essentially "gray" literature. I went this route so that the contents can be readily dissected into a series of manuscripts that will be submitted to appropriate scientific journals, hopefully in the very near future. While I am sending copies of this report to the list of colleagues that we discussed, and to anyone who requests one, I am hoping that EPA will not post the contents of this report in any electronic format, until at least such time as the abovementioned manuscripts have been accepted by the appropriate journals. Thank you for funding this research. I look forward to our ongoing and future collaborations.

Sincerely,

Mark

Mark Marvin-DiPasquale
Microbial Ecologist, Ph.D.

Mark Marvin-DiPasquale / U.S. Geological Survey
345 Middlefield Rd. / MS 480 / Menlo Park, CA 94025
phone: 650-329-4442 / fax: 650-329-4463 / e-mail: mmarvin@usgs.gov

Methylmercury Formation and Degradation in Sediments of the Carson River System

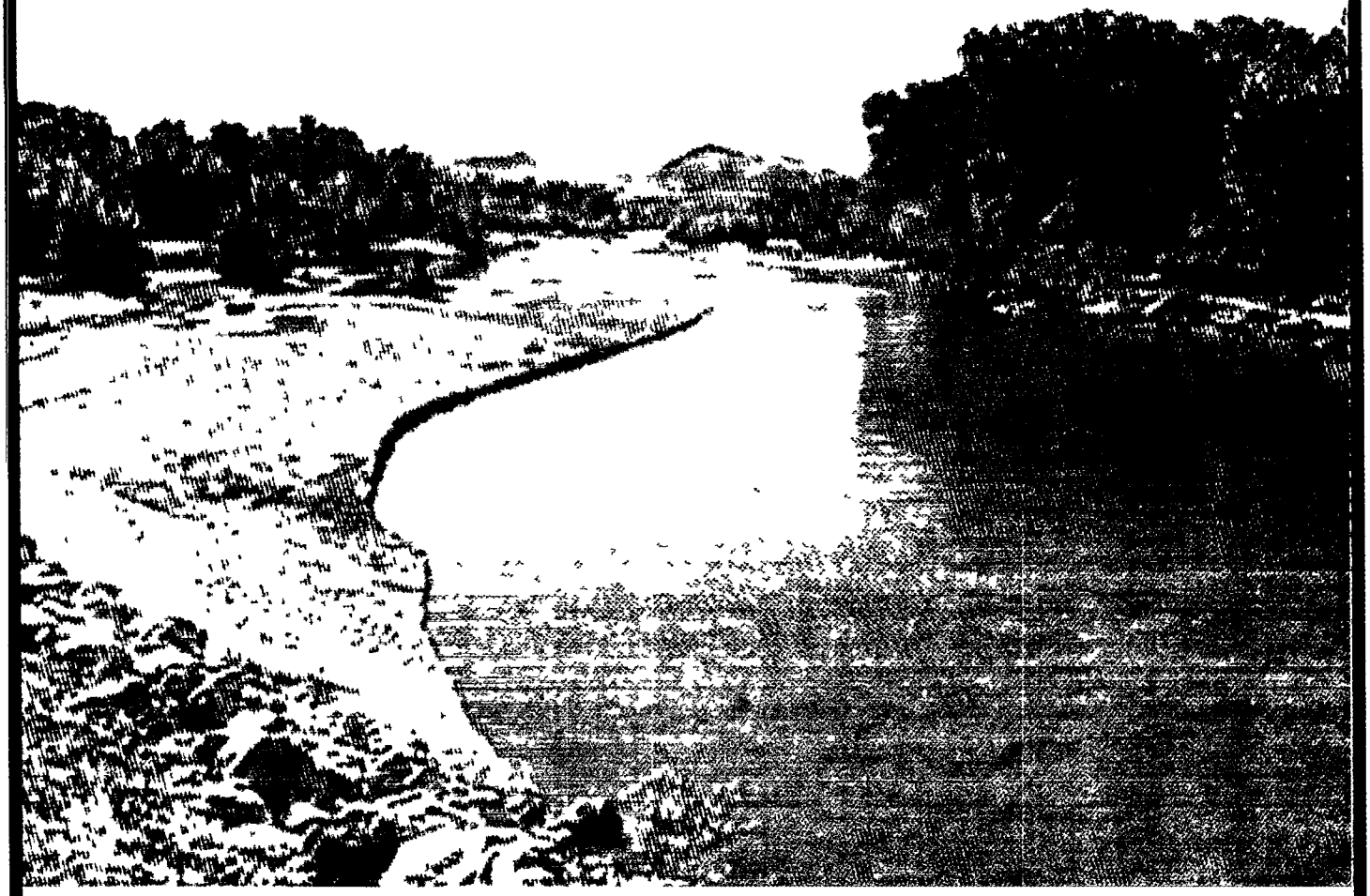

By:

Mark Marvin-DiPasquale, Jennifer Agee, David Krabbenhoft and Ronald S. Oremland

U.S. Geological Survey
Water Resources Division

Methylmercury Formation and Degradation in Sediments of the Carson River System

By:
Mark Marvin-DiPasquale[1], Jennifer Agee[1], Ronald S. Oremland[1] and David Krabbenhoft[2]

[1]U.S. Geological Survey
Water Resources Division
Menlo Park, CA 94025

[2]U.S. Geological Survey
Water Resources Division
Middleton, WI 53562

In Fulfillment of EPA Interagency Agreement: DW14955409-01-0

To:
Wayne Praskins
U. S. Environmental Protection Agency
Region IX, Superfund Division
San Francisco, CA 94105

December 17, 2001

TABLE OF CONTENTS

EXECUTIVE SUMMARY

Microbial mercury (Hg) transformations in sediments of the Carson River System (CRS), in central-western Nevada, were investigated both in the field (in-situ) and in the laboratory. Five distinct zones within the CRS were sampled on three occasions (October 1998, June and October 1999). The zones included: the Carson River proper, Lahontan Reservoir, Carson Sink (playa region), agricultural drains and wetlands. The latter three all lie in a heterogeneous region below the Lahontan Dam. Each zone, and individual site, has a unique hydrology and geochemistry that impacts microbial Hg-cycling. Preliminary assays were conducted on aged (3 mo.) surface sediment (0-4 cm) collected from 13 sites during October 1998 in order to decipher general spatial trends in Hg-speciation, microbiology and relevant biogeochemistry. During the second field campaign sample processing and incubations were conducted at ambient temperature within hours of sediment collection to provide a more accurate measure of in-situ process rates and analyte concentrations. The third field sampling (October 1999), involving 14 sampling and was conducted with a similar approach as in June 1999. The latter two data sets provide a direct seasonal comparison (summer/fall, high/lo flow conditions) of Hg-transformation dynamics in the CRS. Sediment depth profiles (0-16 cm) were investigated at four sites during June 1999 and at two of these four during October 1999. Eroding vertical bank material was sampled in the Hg-contaminated Fort Churchill region during both 1999 dates. Laboratory experiments were conducted using sediment collected during the latter two sampling dates.

Our primary goals were to a) identify important zones of net methylmercury (MeHg) production and consumption within the CRS, b) determine which environmental factors most strongly influence these processes and c) provide estimates of seasonal variability. Measurements were made of microbial Hg-transformations (via radiotracer) and in-situ Hg-speciation (total mercury (Hg_t), MeHg, and particle-associated acid-extractable Hg(II)). Acid-extractable Hg(II) was used as a surrogate measure for the Hg(II) most readily available to bacteria for methylation. A novel Hg-biosensor technique was also used to assess bioavailable Hg(II) in pore-water. A suite of ancillary microbial processes and sediment geochemical parameters were also measured to more fully characterize each site, and to relate these measurements to observed Hg-transformation rates and Hg-speciation.

Mercury Methylation

The key factors which determined the degree of net MeHg production at a given site included: a) acid-extractable Hg(II) concentration and its bioavailability to methylating bacteria, b) the intrinsic potential for the resident bacterial community to both methylate and demethylate mercury, c) the gross rate of MeHg degradation and d) indeterminate seasonal factors. Each of these was in turn affected by site-specific sediment geochemistry and microbiology. Calculated rates of in-situ MeHg production were typically greatest (> 50 pg MeHg • g wet sed^{-1} • d^{-1}) at Fort Churchill, the delta region of Lahontan Reservoir, and in the two agricultural drains. The lowest rates (< 5 pg MeHg • g wet sed^{-1} • d^{-1}) were consistently observed at the upstream control site (Lloyd's Bridge), north Lahontan Reservoir, and the Carson Sink playa. High in-situ MeHg production rates were primarily driven by high concentrations of bioavailable Hg(II), whereas low rates were driven by a combination of low levels of bioavailable Hg(II), low Hg-methylation potentials (i.e. rate constants), and/or high rates of gross MeHg degradation. Many within-site

temporal differences were noted, including a pronounced increase in the MeHg production in the agricultural drains and wetlands during October 1999 (low-water conditions) compared with June 1999 (high-water conditions). However, laboratory experiments suggested that variations in $^{203}Hg(II)$ amendment among sampling dates (due to variations in radioisotope specific activity) may partially account for temporal variations in calculated in-situ Hg-methylation rates.

Sediment Hg_t and MeHg concentrations were strongly correlated ($r^2 > 0.7$) for each sampling date. Significant positive correlations between Hg_t and Hg(II), as well as for Hg(II) and MeHg, were also observed ($r^2 = 0.5$ and 0.4, respectively). Spatial trends in MeHg concentration were generally similar among dates. Higher absolute MeHg concentrations were typically observed in fresh sediment (June/October 1999) as compared with 3-month storage of aged sediment (October 1998), as levels. Relatively small (5-500 m) differences in sampling-site location among dates led to large variations in MeHg and Hg_t concentrations in both the delta region of Lahontan Reservoir and in the Fort Churchill area. This heterogeneous distribution of Hg-species was largely due to variations in sediment grain size, with higher concentrations associated with smaller particles. Hg-species concentrations were highest at Fort Churchill (Dam) and in the Carson Lake agricultural drain, and low in the Carson Sink playa, north Lahontan Reservoir, and sites upstream of Fort Churchill. The southern delta inlet of Lahontan Reservoir was an important deposition zone for particle-bound mercury originating upstream, and had Hg_t concentrations 23 to 44-fold higher, and MeHg concentrations 2 to > 22 times higher, than northern Lahontan Reservoir. The Reservoir is an important transition zone with respect to mercury transport and cycling processes. Both agricultural drainage canals exhibited high levels of mercury contamination, and are a potentially important source of Hg_t and MeHg to the resident biota and larger wetland areas.

Comparative Mercury Methylation/Demethylation

Vertical depth profiles of bottom sediment were sampled at Lloyd's Bridge (LB, upstream control site), Fort Churchill Dam (F1, severely contaminated river site), south Lahontan Reservoir (LS), and Swan Check (SC, wetland/lake). Important spatial trends included: a) sub-surface maximum in MeHg concentration and production rates at all sites, b) a mid-depth minimum in MeHg production rates at SC that mirrors the maximum in reduced-S, c) an increase in Hg_t with depth at both F1 and SC, d) a large mid-depth (8-12 cm) maximum in Hg(II) (> 75 ng•g dry sed^{-1}) at F1, e) maximum MeHg degradation rates in SC and F1 surface sediment. High MeHg production rates at depth were dictated by sub-surface maximum in bioavailable Hg(II) and/or bacterial methylation potentials. MeHg diffusion across the sediment water interface may be limited in some locations (e.g. F1) due to active demethylation zones located above the horizon of maximal production, or due to oxidized surface sediment conditions which can bind MeHg. Rapid within sediment Hg-recycling is implied, a conclusion supported by low net MeHg production rates compared to gross demethylation rates.

Eroding wetted vertical bank material, collected during June 1999 in the Fort Churchill area, had Hg_t and MeHg concentrations that were at least 200X lower than those of the local sediment. While the fraction of acid-extractable Hg(II) in bank samples was comparatively high (4-9% Hg_t), MeHg production and degradation rates were low (< 4 pg • g wet sed^{-1} • d^{-1}) compared with most sediment sites. This was due to both low bioavailable Hg(II) concentrations and oxic conditions, which were presumably unfavorable to anaerobic methylating bacteria. These limited results suggest that the bank material was a minor source of Hg_t and MeHg to the immediate area. However, the contribution of this substrate to mercury contamination

downstream is undoubtedly a function of the erosion rate and the ultimate spatial redistribution of this material into various benthic zones. Hg_t levels in this material was similar to the upstream control site (i.e. $\leq$ 0.1 ppm) and was likely not representative of a mercury enriched mining debris, which is heterogeneously distributed in discrete layers in bank sediment. In contrast, loose dry bank material sampled during at the same site during October 1999 exhibited much higher levels of Hg_t (> 18.8 ppm), acid extractable Hg(II) (0.8 ppm), and MeHg (> 3.5 ppb) at a the lowest point (a bank-shelf) of the former vertical profile. This suggests that the sediment transport and deposition processes associated with these banks are temporally quite dynamic.

The majority of Hg(II) available for methylation was associated with sediment particles and not pore-water. The *mer-lux* biosensor data showed no detectable bioavailable Hg(II) in pore-water collected from fresh sediment (June 1999), while whole sediment acid-extractable Hg(II) concentrations varied widely (0.2 to 96 ng•g dry sed^{-1}). This latter surrogate measure of bioavailable Hg(II) typically represented < 2% of Hg_t, suggesting that only a small fraction of the total mercury in CRS sediment was available for methylation. However, since Hg_t concentrations varied >2000-fold, the absolute concentrations of Hg(II) available for methylation likewise varied greatly ($\approx$ 500-fold). This variability represented a primary factor dictating which areas of the system exhibit high or low net MeHg production, as there was a positive relationship between in-situ Hg concentration (both acid-extractable Hg(II) and Hg_t) and the Hg-methylation rate constant (k_{meth}).

In addition to the influence of Hg contamination of the sediment on k_{meth}, the spatial trend in this parameter indicated that environmental conditions for Hg-methylation were generally more favorable in the river and agricultural-drain sediments than in wetlands. Conditions for MeHg degradation were most favorable in the wetlands and agricultural drains. Overall, there was a consistent decrease in the methylation to demethylation (M/D) ratio for potential rate measurements along the transect from upstream (river sites) to downstream (wetland sites). We conclude that regional differences in sediment chemistry dictate these trends in at least two significant ways. First, sediment reduced-S content mediates the formation and speciation of inorganic Hg-S complexes, with more neutral species (e.g. HgS^0) formed at lower sulfide levels (e.g. in the upstream river), and charged species (e.g. HgS_2^{2-}) formed at higher sulfide levels (e.g. in the wetlands). Neutral Hg-S species are thought to be more readily methylated than are charged species, due to their ability to readily cross the bacterial cell membrane. Thus, the enhanced activity of sulfate-reducing bacteria in the wetlands leads to correspondingly high levels of reduced-S levels in these areas, which in turn leads to a decrease in Hg(II) availability via charged Hg-S complex formation. Evidence for this theoretical mechanism was supported by the field data, in which a significant decrease in Hg-methylation potential (as k_{meth}) was observed with increasing porewater sulfide concentration at all sites below Lahontan Reservoir and in wetland sediment depth profiles. This was also reflected in the significant positive relationship between sediment redox (E_h) and k_{meth} for data grouped by ecozone. The most oxidized sites (river grouping) had the highest average k_{meth}, while the most reduced sites (wetland grouping) had the lowest. In addition, a non-linear relationship between Hg(II) and reduced-S was also noted, where only at sites with very low reduced-S levels (< 0.2 µmol•g wet sed^{-1}) did acid-extractable Hg(II) (the operationally defined methylatable Hg(II) fraction) exceed 2% of Hg_t (up to 9%).

The second primary control on regional differences in potential M/D ratios is related to controls on MeHg degradation. In contrast to Hg-methylation, MeHg degradation was not

inhibited by reduced-S concentrations, but was positively correlated with increasing levels of both pore-water sulfide and whole sediment reduced-S. Sediment E_h was also negatively related to k_{deg}, with the most oxidized sites (river grouping) having the lowest degradation rates, and the most reduced sites (wetland grouping) with the highest rates. Further, the higher organic and nutrient content of the wetlands and drainage canals, led to enhanced rates of anaerobic microbial metabolism in general, and methanogenesis in particular. In addition to sulfate reducers, methanogens can also degrade MeHg. MeHg degradation rate constants were positively correlated with methanogenesis, as well as with sediment total carbon. Thus, in addition to reduced-S levels limiting Hg(II) availability for methylation in the wetlands, increased gross demethylation may further limit net methylation in this region, relative to the upstream river region.

The importance of wetland MeHg production should not be underestimated even though these sites often exhibited lower MeHg production potentials and M/D ratios than upstream river and irrigation drainage canal sites. Wetlands encompass a large spatial area within the CRS, support a complex food web, and represent critical habitat for resident and migratory birds. Thus, even comparatively low benthic MeHg production rates may represent a significant mass transfer of MeHg to the local food web when integrated over large spatial areas of critical habitat. Further, reducing conditions associated with wetland sediments may facilitate a more efficient MeHg flux to the water column, compared with upstream sites, which typically had more oxidized surface sediments. However, MeHg sediment/water-column flux dynamics were not assessed in the current study. Finally, because all three wetland sites were located in open water areas, as opposed to vegetated (root zone) areas, this sampling bias may have led to an underestimation of the importance of wetlands as a zone for MeHg-production in the CRS. We hypothesize that root zones may be a very important (yet unexplored) site for MeHg production because the associated microbial sulfate reduction presumably would be very active, while the build-up of potentially inhibitory reduced-S would be mitigated due to the transport of oxygen into the sediment by the plant during the day. Thus, had rooted zones within wetland region been included, we may well have conclude that the wetlands as a whole represent active areas of net MeHg production within the CRS. This possibility should be investigated in future work.

Oxidative demethylation (OD) was the primary pathway for anaerobic MeHg degradation throughout the CRS, as evidenced by the consistently high $^{14}CO2/^{14}C$-total gaseous end-product ratio observed from all incubations with ^{14}C-MeHg. This may have significant implications for Hg cycling in this system, because it has been previously speculated that the mercury end-product of MeHg degradation via OD is Hg(II). If true, than the effective residence time for mercury is enhanced in surface sediment, as this species may be readily remethylated or reacted with reduced-S. This situation contrasts one in which the *mer*-detoxification pathway dominates, leading to the formation of volatile Hg^0, which may more readily evade from the immediate environment.

Trace-Metal Relationships

Strong relationships between microbial Hg-transformation processes and microbial iron (Fe) and manganese (Mn) reduction rates were not evident in the current data set, although, the long incubation times necessary to measure these microbial processes (two weeks) compared to short incubation times used for Hg-transformation assays (6-24 hours), made direct comparison of results difficult. The potential influences of Fe and Mn biogeochemical cycle cycles on Hg

biogeochemistry are discussed in general terms. Significant positive relationships between Mn concentration and MeHg degradation rates, as well as between selenium (Se) concentration and MeHg degradation rates, were observed. However, bulk sediment concentrations of both Mn and Se were generally higher in agricultural drain and wetland sites than in upstream river sites, a spatial trend that paralleled that of k_{deg}. Thus, the positive relationship observed between these metals and MeHg degradation may have been due to covariation of these parameters across the system and not due to a direct effect of trace-metal concentration on microbial processes. No similar relationships between Se or Mn and MeHg-production rates were observed.

Experiments examining the effect of variable incubation time for both MeHg production and degradation radiotracer assays indicated that the standard short incubation time (ca. 6 hours) used during both 1999 sampling dates provided a much better estimate of the instantaneous Hg-transformation rates, than did the longer incubation time used with the October 1998 samples (ca. 24 hours). Increasing incubation time resulted in an underestimation of instantaneous rates, presumably due to the partitioning of the radiolabel amongst pools of differing bioavailability and due to non-linear microbial Hg-transformation kinetics.

Mercury Partitioning Characterization

The partitioning of the ^{203}Hg(II) radiolabel among acid and base-extractable sediment phases was examined (non-sequentially) at all sites. The percentage of ^{203}Hg(II) recovered by weak-acid extraction decreased significantly with increasing whole sediment reduced-S concentrations above 1 umol S•g wet sed^{-1} and with increasing sediment organic concentrations above 2% (as loss on ignition), while the percentage recovered by weak-base extraction linearly increased with increasing sediment reduced-S content. The acid-extractable ^{203}Hg(II) results parallel those for in-situ acid-extractable Hg(II) concentrations which were also substantially decreased with whole sediment reduced-S above 0.2 μmol S•g wet sed^{-1}, as noted above. This partially explains the lower calculated rates of in-situ Hg-methylation often observed in the reduced-S and organically enriched wetlands, compared with upstream river locations.

Sediments amended with ^{14}C-MeHg were subject to a sequential extraction regime that included water extraction followed by weak-acid then weak-base extraction. In the low organic river and reservoir sites, a majority of the ^{14}C-MeHg was recovered with the water and acid extraction. A much larger base-extractable and non-extractable pool was observed at organic rich wetland and drain sites downstream of Lahontan reservoir. As the sediment reduced-S and organic content increased amongst sites, the percentage of ^{14}C-MeHg recovered with weak-acid decreased and that recovered with weak-base increased. Further, as sediment organic content increase amongst sites the percentage of water extractable ^{14}C-MeHg decreased and the non-extractable pool size increased. These results suggest that a substantial fraction of MeHg produced in the organic rich wetland sediments may be organically bound and less available for microbial degradation. However, of the available MeHg pool, degradation by microbes appears to be most rapid in the wetlands region due to overall increased rates of anaerobic microbial metabolism.

Controls on Methymercury Production/Degradation: Laboratory Experiments

Laboratory experiments with agricultural drain (Carson Lake, CL), wetland (Stillwater Point Reservior, SP) and river (Fort Chruchill, F1) sediment demonstrated that both microbial rates of MeHg production and degradation increased throughout the environmental range of increasing temperature (from 6 to 27 °C). The increase was generally proportional so that the

M/D ratio stayed approximately constant in CL and SP sediment. However, F1 sediment appeared to have a modest (but statistitically non-significant) optimum M/D ratio at 20 °C. The response of both microbial MeHg production and degradation to increasing temperature was lowest for site CL and greatest (and similar) for sites F1 and SP. It is unclear why these spatial differences in temperature response exist, but likely are due to differences in microbial populations, and suggest that microbial Hg-transformations in both upstream river and wetland sediment respond strongly to seasonal temperature changes.

Controlled experiments further examined the relative influence of dissolved sulfate (SO_4^{2-}), oxygen (O_2), chloride (Cl^-) and reduced sulfur (as dissolved sulfide (S^{2-}) and solid phase iron-monosulfide (FeS)) on microbial Hg-transformation rates. Results were not consistent among sites. Hg-methylation was significantly inhibited (relative to unamended anoxic controls) by FeS, S^{2-}, and O_2 at river site F1 and drain site CL, while Cl^- and SO_4^{2-} had little to no influence. In contrast, Hg-methylation at wetland site SP was significantly stimulated by SO_4^{2-} and slightly stimulated by FeS, S^{2-}, Cl^- and O_2. The response of MeHg degradation was also similar at sites F1 and CL, such that this microbial process was significantly stimulated by SO_4^{2-} and FeS and inhibited by Cl^-, S^{2-}, O_2. Results at wetland site SP again differed from those of the other two sites with SO_4^{2-} and FeS slightly inhibiting, and Cl^-, S^{2-}, and O_2 significantly stimulating, MeHg degradation. These results suggest differences in the microbial community composition for both MeHg producing and degrading bacteria, with the agricultural drain being more similar to the upstream river locations than the wetland sites. This partially explains why the agricultural drains often exhibited the highest k_{meth} and in-situ rates of MeHg production. Further, these results reflect the complex effects of sediment redox conditions (as moderated by oxygen and reduced-S species) and sulfur speciation on microbial Hg-transformations.

The research presented illustrates that CRS sediment Hg-dynamics are mediated by a complex interaction of microbiology and geochemistry, coupled with the degree of sediment contamination. We have made significant progress towards our goal of explaining these interactions and identifying general "hot spots" for MeHg production. The following areas of the CRS should receive additional detailed study: the Lahontan Reservoir, agricultural drains, and root zones in the wetlands. The Lahontan Reservoir is an important transition zone, with comparatively high mercury species content and transformation rates in the depositional southern delta, relative to the northern reaches. Sampling in the Reservoir has been limited to two near-shore locations. Basic unanswered questions include: What is the spatial distribution and magnitude of benthic MeHg production in the deeper channel and in the middle lobe? To what extent does reservoir sediment acts as a MeHg source to downstream regions? Further investigation of Lahontan Reservoir is currently underway which attempts to more accurately assess the relative importance of MeHg production within this specific region of the CRS. This work is being conducted by a collaborative research group from EPA, USGS, CH2M-Hill, Univ. Nevada (Reno), and Univ. of Toronto.

Both our results and others (Hoffman & Thomas 2000) demonstrate that that agricultural drains are potentially an important source of Hg_t and MeHg to the wetlands, although, this conclusion is based on only a limited number of sites. More extensive sampling of these drains will allow for a better assessment of the extent and distribution of MeHg production within these channels. Such studies should focus on the anthropogenic factors (e.g. fertilizer use, organic enrichment, soil conservation practices, etc...) that influence MeHg production rates, and the ultimate influence of these drains on wetland mercury cycles.

Finally, root zones in wetland marshes represent a yet unexplored sub-system with the CRS that are potentially very active with respect to MeHg production (as discussed above). A direct comparison of these rooted sub-zones with non-rooted sub-zones within the Hg-impacted wetland regions should be a priority for further study. In addition a comparison of how these various wetland sub-regions respond to drying and reflooding events, with respect to both timing and duration, is a related area that also deserves priority attention. MeHg production within these areas may be mitigated if hydrologic management practices are implemented that leverage our scientific understanding of the natural processes at work.

1. INTRODUCTION

This report represents partial fulfillment of the interagency agreement between the U.S. Environmental Protection Agency (Region IX) and the U.S. Geological Survey (EPA/IAA # DW14955409-01-0) regarding investigations into microbial mercury transformations in the Carson River System (CRS). The overall goal of this project was to document the spatial and temporal trends of benthic MeHg production and degradation, and to investigate the environmental factors that give rise to these observed trends. Towards this end, the contents herein describe the results of field-work conducted in October 1998, June 1999, and October 1999, as well as laboratory experiments conducted during 1999 and 2000. This process-level information will be used to enhance the current mercury model for the CRS, and to aid EPA in evaluating potential remediation strategies aimed at mitigating mercury bioaccumulation in the local food web. Dr. Mark Marvin-DiPasquale directed this research program, under the auspices of Dr. Ronald S. Oremland (U.S. Geological Survey, Menlo Park, CA). Research collaborators included Dr. Mark Hines (Univ. of Alaska, Anchorage, AK) and Dr. David Krabbenhoft (U.S. Geological Survey, Madison, WI), who conducted assays of bioavailable Hg(II) and mercury speciation, respectively. The information gathered from this project will be jointly shared with Dr. John Warwick (Univ. of Florida, Gainesville), who is under ongoing contract with U.S. EPA (Region IX) to develop a mercury model for the CRS.

2. BACKGROUND

Aquatic and terrestrial biota and sediments of the CRS are contaminated with mercury (Ecology and Environment 1998, Hallock & Hallock 1993, Hoffman et al. 1989, Hoffman & Taylor 1998, Van Denburgh 1973, Wayne et al. 1996). This resulted from the use of the purified elemental form (Hg^0) in the milling of gold and silver ore mined from the surrounding Sierra Nevada Mountains from the mid to late 1800's. The primary source of mercury to the CRS is from contaminated mine tailings, distributed in the floodplain, channel banks and river sediment (Bonzongo et al. 1996a). Total mercury concentration in some areas of the CRS are among the highest recorded for any natural environment (i.e. > 800 $\mu g \cdot g$ dry sed^{-1}) (Wayne et al. 1996), and sediment downstream of the ore processing sites may exceed 200X background Hg levels (Van Denburgh 1973). This is of concern due to the potential for Hg bioaccumulation in aquatic food chains, and the potentially harmful human impacts resulting from fish consumption. As a consequence, the CRS was designated as a USEPA Superfund site in 1990. Since that time, an effort has been underway to develop management strategies aimed at ecosystem restoration.

Significant work has been done detailing the physical transport (Carroll et al. 2000, Heim & Warwick 1997, Hoffman & Taylor 1998, Miller et al. 1999, Miller et al. 1998, Wayne et al. 1996) and speciation of Hg in both water and sediment (Bonzongo et al. 1996a, Bonzongo et al. 1996b, Chen et al. 1996, Lechler et al. 1997). An extensive ecosystem level risk assessment has been conducted which considered bioaccumulation in aquatic and terrestrial food webs (Ecology

and Environment 1998). Most of this past work focused on the stretch of river from upstream of the historic mill locations to the Lahontan Dam **(Fig. 1)**. Less attention has been given to the region downstream of Lahontan Dam, which includes as series of wetlands, lakes, reservoirs and irrigation drainage canals, all of which provide critical habitat for local aquatic and terrestrial food webs. The information that does exist indicates that mercury contamination is evident for many biological species sampled downstream of Lahontan Dam (Hallock & Hallock 1993, Hoffman et al. 1989, Hoffman & Thomas 2000, Tuttle & Thodal 1997).

A large gap in our understanding of the Hg-cycle in the CRS and elsewhere results from the paucity of direct simultaneous measurements of microbial Hg-methylation and MeHg degradation. It is the competition between these two processes that ultimately dictates net MeHg production (Korthals & Winfrey 1987). While a few initial measurements of Hg-methlyation (Bonzongo et al. 1996b, Chen et al. 1996, Hines et al. 1999) and MeHg degradation (Hines et al. 1999, Oremland et al. 1995) have been made, no effort to date has been undertaken to assess these two processes simultaneously. The current project does just that, and thereby strengthens our understanding of how these opposing processes interact to control spatial and temporal variations in net MeHg production.

3. PROJECT OBJECTIVES

A. Identify important zones of net MeHg production and consumption within the CRS.

Radiotracer measurements of both MeHg production and degradation were simultaneously conducted at a diverse suite of sites throughout the system. In-situ rates were calculated from the resulting first-order rate constants for Hg-methylation and MeHg-degradation (k_{meth} and k_{deg}, respectively) and the in-situ concentrations of bioavailable Hg(II) and MeHg. Further, experiments were conducted to determine which MeHg degradation pathway (*mer*-detoxification or oxidative demethylation (OD)) dominates at each site, as the particular pathway may have a direct and significant impact on mercury residence time within the system.

B. Identify the key environmental factors and microbial groups that control these processes, both spatially and temporally.

To explain the observed spatial and temporal trends in MeHg production and degradation, a detailed investigation of the sediment geochemistry and microbiology was also conducted at each location. The selection of these ancillary measurements was based on previous research, which suggests that each might play a role in mediating microbial Hg-transformation rates. Pore-water and whole sediment geochemical analysis included nutrients and anions, organic carbon, reduced sulfur, trace-metals, pH and redox. Microbiological processes included sulfate, iron and manganese reduction, methanogenesis, and methane oxidation. Seasonal differences in Hg-cycling processes were investigated by conducting similar microbial rate measurements during periods of both high and low water flow conditions (June and October, 1999, respectively). Additional laboratory experiments were also conducted with various CRS sediment to directly examine the relative importance of various environmental parameters (e.g. temperature, oxygen, reduced-sulfur species, sulfate, chloride) on Hg-transformation rates under controlled conditions.

C. Provide qualitative and quantitative process information to the modeling group who will incorporate certain aspects of these findings into the Hg-model currently being developed for the CRS.

The scope, precision, accuracy, and predictability of the existing CRS Hg-model (and/or future models) may be greatly enhanced as a result of the measurements provided by the current study. Model algorithms may be added which predict benthic Hg-transformation rates based on Hg-concentration data and readily measured environmental parameters such as temperature, organic carbon content, reduced-S, etc...

D. Provide information and feedback to ecosystem managers regarding the feasibility of prospective restoration strategies.

Potential remediation strategies may be more thoughtfully assessed as a result of both the direct measurements conducted as part of this project and the improved Hg-model. This report, and the ensuing discussions with EPA Superfund managers and the modeling group, will serve as important platforms to facilitate assessment of these management options.

4. METHODS

4.1. Field Sampling

Sampling sites were selected based on our desire to investigate both a diverse and representative suite of locations within the CRS. When possible, sites sampled in previous investigations were selected to best leverage valuable background data regarding Hg concentration, speciation, and/or microbiological and geochemical factors. Five distinct hydrogeographic regions were investigated, **a)** the Carson River proper (from Carson City to Fort Churchill and one river site below Lahonton Dam), **b)** the Lahontan Reservoir, **c)** the Carson Sink (a seasonally wet saline playa), **d)** agricultural drains and **e)** wetland lakes in the Stillwater Wildlife Management Area. The latter three regions (**c-e**) are located in the heterogeneous region downstream of Lahontan Dam. A total of 14 sediment sites were sampled in all (**Fig. 1**). **Table 1** gives a brief description and exact coordinates of each.

A preliminary study was conducted in October 1998. Surface sediment (0-4 cm) was collected using acid-cleaned polycarbonate core tubes (9 cm i.d.). Sediment was immediately transferred to 1-liter acid washed mason jars (two per site), stored on wet ice, and transported back to the U.S. Geological Survey (USGS) facility in Menlo Park, CA. This material was held at 5 ^{0}C for three months prior to further processing. The primary objective of this study was to obtain an overview of microbial rates and sediment geochemistry at this suite of sites, and to develop the analytical methods outlined below. A second field sampling was conducted in June 1999 at all of the original sites, and at an additional eroding vertical bank site (F3) in the Fort Churchill area (between sites F1 and F2). Samples were collected at three depths (30 cm above, 10 cm below and 60 cm below the air/water interface. One-meter long steel reinforcing rods were driven into the cliff to mark the exact location where samples were collected. In addition to surface sediment (0-4 cm), depth profiles (0-16 cm in 4 cm intervals) were also investigated at four locations: Lloyd's Bridge (LB, upstream control site), Fort Churchill (F1, severely

contaminated river site), south Lahontan Reservoir (LS), and Swan Check (SC, wetland/lake). All June 1999 sediment was sub-sampled, incubated, and/or appropriately preserved, within hours of collection, to most accurately characterize in-situ rates and analyte concentrations. The third field campaign was conducted in October 1999, with sample processing and incubations again conducted within hours of collection. All original 13 sites were resampled, and an additional river site at Dayton (DY) was added. Depth profiles were conducted at F1 and SC only. The vertical bank at F3 was also re-sampled at the original top and bottom June 1999 horizons (the middle horizon was excluded). The water level had dropped more than two meters between sampling dates. Thus, all vertical bank material was completely dry during the October 1999 sampling, and the material at the bottom horizon was loose as opposed to compact.

While every attempt was made to sample the exact same sites (± 5 m) during all three dates, dangerous high-water conditions encountered during June 1999 made this impossible at two locations. Sampling was moved approximately 10-15 m at F2, from mid-channel (October 1998) to the shore edge (June 1999 and October 1999). Similarly, sampling at LS during June and October 1999 was located approximately 0.5 km up-stream from the original location sampled during October 1998. Further, the exact site varied about 10 m between the June and October 1999 sampling dates at LS, due to seasonal shoreline migration. Finally, dam reconstruction had occurred at F1 between June 1999 and October 1999. Since our original site had been clearly disturbed by bulldozer activity, the sampling location was moved from the north shore (June 1999) to the south shore and about 10-15 meters upstream (October 1999).

4.2 Sediment Processing

All initial sediment processing was conducted in a nitrogen gas (N_2) flushed glove bag to maintain anaerobic conditions. Sediment from a single site was transferred to a clean zip-lock bag and manually homogenized. Sub-samples, for each process or analyte were taken from this composite sample. Acid cleaned stainless steel tools were used for sub-sampling, and sediment was weighed (± 0.1 g precision) into the appropriate containers in the O_2-free glove bag. For October 1998 samples, pore-water was extracted under N_2 (O_2-free) by sediment squeezing (Reeburgh 1967), with in-line filtration using 0.45 µm polycarbonate membrane filters sandwiched between two paper pre-filters. This approach proved difficult and potentially problematic with respect to contamination (see **Section 5.2**), and was subsequently discontinued after the October 1998 sample processing. In June and October 1999, pore-water was collected by centrifugation (3000 rpm for 15 min.) of sediment in completely filled 50 cm^3 polystyrene screw-cap tubes. The resulting supernatant was collected via syringe and filtered (0.45 µm cellulose acetate in-line filter) inside an O_2-free glove bag. In cases where not enough pore-water was obtained, centrifuge tubes were first filled 2/3 with sediment and 1/3 with O_2-free ultrapure (Milli-Q) water. The mixture was shaken into a homogenous slurry, which was then centrifuged and the supernatant sampled as above. The exact weight of sediment and water added per tube was recorded, and subsequent pore-water analyte concentrations were calculated taking this pore-water dilution into account. A comparison of the sediment squeezing and centrifugation approaches was conducted (see **Section 5.2**).

Sub-sampling of October 1998 sediment was conducted in two phases: 93-95 days after initial field collection (for Hg-speciation and Hg-transformation rate assays), and 141-145 days after field collection (all other parameters). Sub-sampling in June and October 1999 was

conducted within 6 hours of sample collection. All samples were given a unique alpha-numeric code identifier (**Appendix I**). Samples collected for mercury speciation, bioavailable Hg(II) (via *mer-lux* biosensor), and grain size analysis were packed on dry ice or freezer packs, as appropriate, and shipped overnight to the respective analytical laboratory.

One heat-killed control was prepared for each site-specific sample set for the following microbial rate assays: MeHg production and degradation, sulfate reduction, and methane oxidation. Duplicate autoclaved killed controls were prepared for methanogenesis measurements. All microbial rate assays were conducted at room temperature (19-22 ^{0}C) for October 1998 samples, and at in-situ temperature (10-16 ^{0}C) for June and October 1999 samples. **Table 2** summarizes all microbial rates and ancillary parameters, describes the purpose and type of measurement, and provides methodological references. **Table 3** further summarizes the sample volume assayed, containers used, replication, incubation time and sample preservation method. More detailed standard operating procedure documentation is available upon request for any or all of the assays conducted.

4.3 Microbial Mercury Transformation Assays

A standard 1 μCi ^{203}Hg(II) amendment was used for the MeHg-production rate assay, which resulted in total Hg(II) amendments of 247 ng•g wet sed^{-1} (October 1998), 2350-2560 ng•g wet sed^{-1} (June 1999) and 833-901 ng•g wet sed^{-1} (October 1999). The difference in unlabeled Hg(II) amendment levels among sampling dates reflects the differences in ^{203}Hg stock solutions used and the specific activity (μCi•μg Hg) which is affected by the radioactive decay of the isotope (^{203}Hg(II); $t_{1/2}$ = 46.5 days). While these concentrations were often below in-situ Hg_t levels, they consistently exceeded in-situ acid-extractable Hg(II) concentrations (**Appendix II**). Similarly, standard ^{14}C-MeHg amendments (40 nCi for October 1998 and 9-10 nCi for June and October 1999), resulted in total MeHg additions (as Hg) of 51 ng•g wet sed^{-1} (October 1998) and 11-12 ng•g wet sed^{-1} (June and October 1999). These levels also exceeded in-situ MeHg concentrations in most cases (**Appendix II**). Thus, neither the ^{203}Hg nor ^{14}C-MeHg assay was a true tracer assay. The standard incubation time for both MeHg production and degradation assays was decreased from 24 hours (October 1998) to 6 hours (June and October 1999). We assumes that Hg(II)-methylation is a concentration dependent process, such that:

$$\mathbf{Hg(II)_t = Hg(II)_{t=0} \bullet EXP(-k_{meth} \bullet t)} \quad \text{Eq. 1}$$

where $\mathbf{Hg(II)_t}$ equals the concentration of Hg(II) at a given time (**t**), $\mathbf{Hg(II)_{t=0}}$ equals the concentration at an initial time (t = 0), and $\mathbf{k_{meth}}$ equals the first-order rate constant. Thus, the amount of Hg(II) methylated over a given time period can be expressed as:

$$\mathbf{Hg(II)_{methylated} = Hg(II)_{t=0} - Hg(II)_t} \quad \text{Eq. 2}$$

By combining Eq. 1 and Eq. 2, the amount of gross Hg(II) methylated for a given incubation time (t) and initial Hg(II) concentration, can thus be generally expressed as:

$$\mathbf{Hg(II)_{methylated} = Hg(II)_{t=0} - Hg(II)_{t=0} \bullet EXP(-k_{meth} \bullet t)} \quad \text{Eq. 3}$$

From the above expression, we solve for $\mathbf{k_{meth}}$, in terms of the radiotracer amendment, as follows:

$$\mathbf{k_{meth} = ln(1-f_m)/t} \quad \text{Eq. 4}$$

where: f_m equals the fraction radiolabeled $Me^{203}Hg$ produced from the $^{203}Hg(II)$ amendment, i.e.

$$f_m = Me^{203}Hg_t / {}^{203}Hg(II)_{t=0} \quad \text{Eq. 5}$$

A similar derivation can be carried out for MeHg degradation, assuming:

$$MeHg_t = MeHg_{t=0} \bullet EXP(-k_{deg} \bullet t) \quad \text{Eq. 6}$$

Where k_{deg} equals the MeHg degradation rate constant.

$$MeHg_{degraded} = MeHg_{t=0} - MeHg_t \quad \text{Eq. 7}$$

By combining Eq. 6 and Eq. 7, the amount of gross MeHg degraded for a given incubation of duration time (t), for any initial MeHg concentration, can thus be generally expressed as:

$$MeHg_{degraded} = MeHg_{t=0} - MeHg_{t=0} \bullet EXP(-k_{deg} \bullet t) \quad \text{Eq. 8}$$

Solving for k_{deg} in terms of the ^{14}C-MeHg radiotracer amendment and degradation end-products ($^{14}CH_4 + {}^{14}CO_2$) we get:

$$k_{deg} = \ln(1-f_d)/t \quad \text{Eq. 9}$$

where:

$$f_d = ({}^{14}CH_4 + {}^{14}CO_2)_t / {}^{14}C\text{-}MeHg_{t=0} \quad \text{Eq. 10}$$

Thus, in-situ methylation and demethylation daily rates were calculated from equations 3 and 8, respectively, by applying the radiolabel-derive k_{meth} and k_{deg} rate constants, Hg-species in-situ concentrations ($Hg(II)_{t=0} = Hg(II)_{in\text{-}situ}$ and $MeHg_{t=0} = MeHg_{in\text{-}situ}$), and a t value of 1 day. The whole sediment acid-extractable Hg(II) measurement was used for $Hg(II)_{in\text{-}situ}$, while the whole sediment total MeHg concentration was used for $MeHg_{in\text{-}situ}$. Potential rates for both processes were calculated in exactly the same manner, except that the $Hg(II)_{t=0}$ and $MeHg_{t=0}$ values used were calculated as the combined total of in-situ concentrations plus the amount of Hg(II) or MeHg added as part of the radiolabel amendment (as given above).

4.4 Additional Experiments

4.4.1 Time Courses

While our standard $^{203}HgCl_2$ and ^{14}C-MeHg incubations consisted of only one time point (6 or 24 hours), we also investigated the effect of varying incubation time on calculated k_{meth} and k_{deg} values using site F1 sediment (0-4 cm, collected June 1999). Parallel sets of Hg-methylation and MeHg degradation samples were prepared as described above. Radioisotope amendments were 1 µCi (467 ng•g wet sed^{-1}, total Hg) for $^{203}HgCl_2$ and 9.4 nCi (12 ng•g wet sed^{-1}, as Hg) for ^{14}C-MeHg. Incubations were conducted at room temperature (19-20 °C) and individual sample sets were arrested at nine time points over a five-day period. Samples were assayed for radiolabeled end-products (e.g. $CH_3{}^{203}Hg$, $^{14}CH_4$ and $^{14}CO_2$) as previously described (Table 2). Each time point set represented two live sediment samples and one control which was heat sterilized (autoclaved).

4.4.2 Variation in $^{203}HgCl_2$ Specific Activity

Due to the relatively short half-live (46.5 days) of the ^{203}Hg(II) isotope used for the microbial Hg-methylation rate assay, and because field samples were always amended with a constant amount of activity (1 μCi•sample^{-1}), the actual amount of Hg(II) added to each sample varied among assay dates as a function of the injection solution specific activity (μCi•μg Hg(II)). We were thus interested in determining how this variation in the total Hg(II) amendment might affect measured values of k_{meth} and subsequently calculated Hg-methylation rates (both *in-situ* and potential rates). Sediment samples from site LS (collected October 1999) were prepared as above, and were amended with 1 μCi $^{203}HgCl_2$ at four treatment levels of specific activity (in μCi•μg Hg(II); 1.58, 1.00, 0.50, 0.11), which resulted in the following total Hg(II) amendment concentrations (in μg Hg(II)•g wet sed^{-1}; 0.21, 0.33, 0.67, 3.03, respectively). For comparison, fresh sediment from site LS had *in-situ* concentrations of 9.8 μg•g wet sed^{-1} total-Hg and 0.02 μg•g wet sed^{-1} acid-extractable Hg(II). All samples were incubated for 22 hours. Incubations were arrested by freezing, and samples were assayed for $CH_3{}^{203}$Hg by toluene extraction and gamma counting (Table 2). Each treatment set consisted of duplicate live sediment samples and one heat-killed control.

4.4.3 Radiolabel Partitioning

One assumption in using radiolabeled compounds to elucidate microbial Hg-transformation processes is that the added label acts similarly to its naturally occurring non-labeled counterpart. Like the unlabeled fraction, not all of the radiolabel added to a sample may be available for microbial biotransformation. Thus, we were interested to determine how the two radiolabels (^{203}Hg(II) and ^{14}C-MeHg) distributed themselves, upon addition to sediment, among readily extractable phases. Such measurements subsequently give us some idea of how the naturally occurring in-situ pools of Hg(II) and MeHg may be distributed. Experiments were conducted on aged (ca. 4 months) surficial sediment (0-4 cm) from all sites (except F3). Sediment had been originally collected during the October 1999 field campaign and was stored in seal mason jars at 5 ^{0}C prior to sub-sampling. The approaches used for assessing ^{203}Hg(II) and ^{14}C-MeHg partitioning differed somewhat.

In the first case, $^{203}HgCl_2$ was added (1 μCi; 584 ng Hg(II)•g wet sed^{-1}) to 3.0 g sediment samples (n = 2 to 3 per site), which had been previously autoclaved (heat-sterilized). After thorough mixing, and allowing at least 15-30 minutes for equilibration, the ^{203}Hg(II) was extracted from the sediment with weak acid. Sediment first was washed from the original serum bottles into fluoropolymer (FEP) centrifuge tubes (four 0.06 N HCl washes at 10 ml each = 40 ml HCl total). The resulting slurry was mixed on a rotating shaker for 10 minutes, and then centrifuged for 10 minutes. A 15-20 ml aliquot of the resulting aqueous acid-extracted phase was filtered (0.45 μm, nylon in-line syringe filter) and assayed for ^{203}Hg(II) via gamma counting.

In a separate set of similarly prepared and $^{203}HgCl_2$ amended autoclaved samples, ^{203}Hg(II) was base-extracted with 0.01 N KOH (again 40 ml). The resulting slurry was similarly mixed, centrifuged, and 4-10 ml aliquots were assayed for ^{203}Hg(II) via gamma counting. This base-extractable fraction primarily represents Hg-organic (both fulvic and humic acid) complexes, while the acid-extractable fraction primarily represents exchangeable Hg(II) from solid phase organic matter, minerals or (hydr)oxides (Wallschläger et al. 1998).

The ^{14}C-MeHg extraction experiment was conducted with three sequential extractant phases (water → weak acid → weak base), as opposed to acid and base extractions (only) on separate samples, as per the above ^{203}Hg(II) method. Duplicate sediment sub-samples (3.0 g) were amended with ^{14}C-MeHg (83 nCi; 102 ng•g wet sed^{-1} as Hg), vortexed for 2 minutes, and allowed to equilibrate for 15-30 minutes. Sediment was rinsed from the glass serum bottles into FEP centrifuge tubes with four 5 ml aliquots of Milli-Q water. The resulting slurry was vigorously mixed by hand-shaking (1 min), and the phases separated by centrifugation. The aqueous phase was decanted into a second FEP centrifuge tube, and a 1.0 ml filtered (0.45 μm, nylon in-line syringe filter) sub-sampled was transferred into scintillation vial containing an appropriate scintillation cocktail (8 ml). A second 20 ml portion of water was added to the original sediment, and the shaking, centrifugation, decanting, sub-sampling and filtration steps repeated. This was followed by a similar extraction procedure of the same sediment sample with 0.06 N HCl (two 40 ml extractions), with each aqueous acid-extraction phase being sub-sampled into separate scintillation vials. The sediment was then rinsed with two 20 ml portions of Milli-Q water (not sampled for ^{14}C activity). Finally two 40 ml base-extractions were conducted with 0.01 N KOH on the same samples, with each aqueous base-extraction phase being appropriately sub-sampled for ^{14}C-MeHg. All extraction fractions were then counted for ^{14}C activity on a beta liquid scintillation counter.

4.4.4 The Effect of Temperature on Microbial Hg-Transformations

A variable temperature experiment was simultaneously conducted on sediment from three sites (F1, CL, SP; collected October 1999) amended with either ^{203}Hg(II) (1.5 μCi, 82 ng Hg(II)•g wet sed^{-1}) or ^{14}C-MeHg (9 nCi, 12 ng•g wet sed^{-1} as Hg) to determine whether or not this global parameter impacted microbial rates of MeHg production and degradation similarly. Samples were incubations at 6, 15, 20, 27 ^{0}C for 18-19 hours and subsequently assayed for radiolabeled end-products as previously noted. Each time point set consisted of two live samples and one heat-killed control. The temperature response of most microbial reaction rates is typically non-linear, and can be described by the Arrhenius equation. The linear form of the model was fit to the Hg-transformation rate and temperature data to examine the site-specific temperature influence on microbial MeHg production and degradation:

$$\mathbf{ln(Hg\text{-}Rate) = (-E_a/R) \bullet T^{-1} + ln(A)} \qquad \text{Eq. 11}$$

where Hg-Rate is either the MeHg production or degradation potential rate (ng Hg•g wet sed^{-1}•d^{-1}), T is temperature (^{o}K), A is a pre-exponential factor, E_a is the activation energy (kJ•mol^{-1}), and R is the gas constant (0.008314 kJ•mol^{-1} • ^{o}K^{-1}). E_a is frequently calculated as a measure of the temperature response of metobolic reaction rates. Increasing E_a values reflect an increase in the temperature response for a given process. A similar measure is Q_{10}, calculated as:

$$\mathbf{Q_{10} = (R1/R2)^{[(T2-T1)/10]}} \qquad \text{Eq. 12}$$

where T1 = 10 °C, T2 = 20 °C, R1 and R2 represent the corresponding high and low Hg-transformation rates calculated from Eq. 11, using T1 and T2, respectively, and model-fit values of E_a and A. Like E_a, Q_{10} increases with increasing temperature response. The general rule of thumb for Q_{10} value is that microbial reaction rates increase approximately two-fold for every 10 °C increase in temperature. The Q_{10} values calculated here for the three representative sites, can be used to further refine existing and future temperature dependent Hg-models for the CRS.

4.4.5 The Effect of Key Parameters on Microbial Hg-Transformations

A suite of key environmental variables (chloride, sulfate, sulfide, solid-phase reduced-sulfur (FeS), and oxygen) was simultaneously investigated with respect to their relative influence on rates of MeHg production and degradation. Sediment from three sites (F1, CL, SP; collected October 1999) were subject to six separate treatments, which consisted of 3.0 g of whole sediment plus one of the following (1 ml) amendments: anoxic Milli-Q water, 5-108 µmol Cl^-, 4-7 µmol SO_4^{2-}, 4-7 µmol HS^-, 4-11 mg FeS, or O_2-saturated Milli-Q water. All treatments had an anaerobic N_2 gas phase except the O_2-saturated water treatments, which had a gas phase of room air. The exact Cl^-, SO_4^{2-}, HS^-, and FeS amendment levels for each site was based on the background concentration of that constituent at each site. Parallel samples from each site/treatment set were amended with either $^{203}Hg(II)$ (1.5 µCi, 111 ng Hg(II)•g wet sed^{-1}) or ^{14}C-MeHg (11 nCi, 14 ng•g wet sed^{-1} as Hg). Samples were incubations at 20 ^{0}C for 18-19 hours and subsequently assayed for radiolabeled end-products as previously noted. Each time point treatment set consisted of two live samples and one heat-killed control.

4.5 Disposal of Investigation Derived Waste

Disposal of radioactive waste material was conducted according current USGS regulations (USGS 1998a, USGS 1998b) as required by our NRC radioisotope user site license (Oremland Project, Permit No. 8). New World Technology (Livermore, CA) carried out the collection and disposal of long-lived radioactive waste (^{14}C). Non-radioactive waste (e.g. acids, bases, heavy metal amended environmental samples, etc...) was stored in plastic or glass containers in a ventilation hood until collection by the USGS Hazardous Materials Officer. This waste was ultimately packaged, transported and disposed of by Laidlaw Environmental Services (San Jose, CA) according to EPA specified regulations.

5. QUALITY CONTROL

Quality control for all processes and parameter measurements included sample preservation, replication, matrix spikes, reagent and equipment blanks, certified analytical standards and killed controls, where appropriate. **Table 4** compares requested quantitation limits and holding times with those actually achieved, and summarizes individual assay precision and accuracy measured in this study. Commercially prepared standards were used whenever possible.

The efficiency of the extraction procedure used to separate of $Me^{203}Hg$ from $^{203}HgCl_2$ amended samples (Gilmour & Riedel 1995, Guimaraes et al. 1995) was assessed for each site/depth and for all sampling dates. ^{14}C-MeHg was added to replicate (n = 2 to 3) heat-killed samples, which were then subjected to the organic extraction. Extraction efficiencies ranged from 56-96% and the appropriate value was used to calculate the final k_{meth} measured via the $^{203}HgCl_2$ assay. Both $^{14}CH_4$ combustion and $^{14}CO_2$ trapping efficiencies were also tested before and after assaying the ^{14}C-MeHg degradation samples. In both cases efficiencies were > 90%. Liquid scintillation (beta) counting was calibrated with quench curve industry standards.

An experiment was conducted with October 1998 sediment to determine if pore-water parameter measurements were affected by the collection method (i.e. squeezing versus centrifugation). While all but one site (SC) was originally sampled by sediment squeezing, a second sub-sampling of all pore-water constituents was conducted by both methods in parallel, using site CL sediment **(Appendix II)**. Compared to centrifugation, sediment squeezing resulted in 5-fold higher NO_3^- and 29-fold higher SO_4^{2-} concentration. This would suggest that reduced nitrogen and sulfur species were partially oxidized during the squeezing method. However, samples from the same pore-water fraction (collected by squeezing) had slightly higher sulfide levels (7.6 ± 2.6 μM) than those collected by centrifugation (4.3 ± 1.0 μM). This would contradict the reduced-S oxidation hypothesis. Further, even if completely oxidized, these sulfide concentrations could not account for the difference in SO_4^{2-} measured by the two methods. Sulfate contamination was an unlikely possibility, although, an earlier squeezer equipment blank did give a sulfate value (0.9 μM) slightly higher than the detection limit (< 0.5 μM). No significant difference among methods was noted for pore-water Cl^- or DOC values. Pore-water PO_4^{3-} concentrations via squeezing were 23% lower than those collected via centrifugation. It is unclear what accounted for these contradictory results. The sediment squeezing approach was abandoned after October 1998, and all subsequent pore-water was collected via centrifugation.

Original data and detailed notes on methods development were kept in ringed binders and bound laboratory notebooks, respectively. Original chart recorder and integrator printouts will be archived for a minimum of five years after completion of this project. Dr. Marvin-DiPasquale checked all technician laboratory notebooks for completeness. The Quality Assurance Officer (Larry Miller, USGS Menlo Park, CA) spot-checked electronic data entry (Microsoft Excell spreadsheets) and calculations for accuracy and completeness. All primary data is tabulated in **Appendix II**.

6. RESULTS & DISCUSSION

6.1 Sediment Mercury Speciation and Spatial Distribution

The relative spatial distribution of mercury species (Hg_t, MeHg and Hg(II)) in 0-4 cm surface sediment was generally consistent among sampling dates **(Figs. 2-9)**, with some notable exceptions (discussed below). Species concentrations were spatially correlated **(Fig. 10)**, with the strongest relationship between Hg_t and MeHg (r^2 = 0.72- 0.77; n = 12-27), followed by Hg_t and Hg(II) (r^2 = 0.68-0.69; n = 20-27), and Hg(II) and MeHg (r^2 = 0.39-0.59; n = 20-27). The lack of significant relationships for October 1998, in these latter two cases, may reflect the possibility

that MeHg and Hg(II) concentrations changed during the > 3 month storage period (prior to sub-sampling).

The strong correlation between Hg_t and MeHg in CRS sediments is in contrast to the mercury-impacted Florida Everglades, where the relationship between MeHg and Hg_t is weak (r^2 = 0.08) (Gilmour et al. 1998a). This may be partially due to the much larger range and higher Hg_t concentrations in the CRS (1-21 ppm in 44% of the samples) compared to the Everglades (< 0.4 ppm maximum). These high Hg_t concentrations in the CRS presumably lead to high concentrations of microbially available Hg(II), and subsequently high MeHg.

6.1.1 Total Mercury (Hg_t)

The range of Hg_t concentrations varied over three orders of magnitude (0.008 to 21.3 ppm) for the complete data set. During October 1998, 0-4 cm sediment concentrations were highest at F1 (12.7 ppm), while substantially lower less than one kilometer downstream at F2 (0.8 ppm) **(Fig. 2a)**. In contrast, both sites were similarly elevated in Hg_t (10.7-15.7 ppm) in June 1999 **(Fig. 2b)**, but returned to a down-gradient decrease during October 1999 (12.6 ppm and 1.9 ppm respectively, **Fig 2c)**. These variations are attributed to the relocation of both F1 and F2 sampling spots between dates (as described in **Section 4.1** and **Table 1)**, and linked to variations in sediment grain size over small spatial scales (see **Section 6.3.3.4**). Similar variations were noted for the southern Lahontan Reservoir (LS) delta region, where 0-4 cm Hg_t concentrations were highest (2.7-21.3 ppm) in fine grain substrate (October 1998 and '99), and lowest (0.5 ppm) in courser sand (June 1999). Both agricultural drains (CL and SS) also exhibited elevated Hg_t (3.3-9.7 ppm) during all sampling dates. Similar elevated mercury levels have been previously reported for Fort Churchill, south Lahontan Reservoir and the agricultural drains (Ecology and Environment 1998, Hoffman et al. 1989, Hoffman & Thomas 2000). Other sites with consistently high Hg_t (> 0.4 ppm) included CD and the three wetland-lakes (LL, SP, SC). The two most upstream locations (LB and DR) had comparatively low Hg_t levels (< 0.14 ppm), while the Dayton site (DY) was only slightly higher (0.38 ppm, sampled October 1999 only). Finally, the northern portion of Lahontan Reservoir (LN) and the Carson Sink (CS) exhibited the lowest Hg_t (≤ 0.06 ppm).

Among-site differences in Hg_t depth profiles for June '99 **(Fig. 7a)** were similar to those observed in surface sediments (i.e. F1 >> SC > LS > LB). Increasing Hg_t with depth, at both F1 and SC, suggest sub-surface horizons of historically deposited mercury, which are currently being buried at these locations. However, this trend was not repeated at SC in the October 1999 sample, which showed nearly constant Hg_t with depth **(Fig. 7b)**. Decreasing Hg_t with depth at LS suggests that Hg-enriched material, transported from upstream, is accumulating in the Lahontan Reservoir southern delta. This region acts as an important catchment zone for particle-bound mercury, as evidenced by the 23 to 414-fold higher Hg_t levels in LS compared to LN (surface 0-4 cm, all sampling dates). Vertical bank (F3) material had low Hg_t (≤ 0.1 ppm) compared to Fort Churchill sediments, with a maximum just below the June 1999 air/water interface **(Fig. 9a)**. When the top and bottom intervals at F3 were resampled in October, the water level had fallen more than two meters and the same horizons were completely dry. While the upper-most interval (D1) exhibited only slightly higher Hg_t levels compared to the June sample, the bottom-most interval (D3) was considerably higher (> 18.5 ppm). This sample was composed of loose dry sand/clay that had either fallen from above or had been transported from up-stream and deposited

on the small ledge at D3. Thus, this loose material was not representative of the compact vertical bank, which had been sampled four months earlier.

6.1.2 Methylmercury

Spatial trends in surface sediment (0-4 cm) MeHg were similar between October 1998 and June 1999, with highest concentrations (6-26 ppb) at F1 and CL **(Figs. 3a,b)**. These two sites were again elevated in MeHg in October 1999, as were sites LS, SP, and SS (all above 5 ppb) **(Fig. 3c)**. MeHg was typically higher when sediment was sub-sampled and preserved within hours of collection (June and October 1999), compared to sediment aged for 3 months (October 1998). Thus, while spatial trends were apparently maintained, absolute MeHg levels may have decreased during refrigerated storage. MeHg concentrations were consistently lowest in CS and LN ($\leq$ 0.1 ppb). In Lahontan Reservoir, concentrations were 2X (October 1998) to > 80X (October 1999) higher at LS than at LN, further indicating that the southern delta is an important zone of MeHg production for the Reservoir as a whole. Average MeHg concentrations for all sites sampled in Stillwater Wildlife Refuge (LL, SP, SC and SS) were 1.6 $\pm$ 0.5 ppb in June 1999 and 4.1 $\pm$ 3.3 ppb in October 1999. These averages were not significantly different at $P < 0.1$, and were in the same range (<0.1 to 5 ppb) as those for the mercury impacted Everglades wetland (Gilmour et al. 1998b).

June 1999 depth profiles showed a sub-surface MeHg maximum at all sites, with F1 sediment exceeding 32 ppb in the 4-12 cm horizon **(Fig. 7c)**. In October 1999, maximum MeHg levels occurred at the sediment surface at wetland site SC (1.2 ppb), but increased with depth to 13.5 ppb at the relocated F1 site **(Fig. 7d)**. In F3 vertical bank material, MeHg was much lower (< 0.3 ppb) than local F1 and F2 sediments at all depths during June 1999 and at D1 during October 1999 **(Fig. 9b)**. The loose sandy material collected at D3 during October 1999 had a 10-fold higher MeHg content (3.9 ppb), again suggesting that this substrate was different from the previously sampled bank material at this depth. As a percentage of Hg_t, MeHg was consistently highest (up to 2.3 %) at the control site (LB), while all other sites were consistently > 1% MeHg **(Figs. 4, 7e, and 9c)**.

6.1.3 Acid-Extractable Hg(II)

The vast majority of Hg(II) available to bacteria for methylation was associated with sediment particles and not pore-water. This was deduced from the *mer-lux* biosensor data, which showed small amounts (< 0.4 to 6.1 $ng \cdot l^{-1}$) of bioavailable Hg(II) in pore-water collected from aged (October 1998) sediment, but no detectable amounts (limit = 0.2 $ng \cdot l^{-1}$) in pore-water from fresh sediment (June 1999) **(Appendix II)**. These concentrations were negligible compared to the whole sediment concentrations (0.1 to 780 ppb, **Figs. 5, 8a,b, 9d**) measured using weak acid-extraction of Hg(II). This was one of the first attempts to use the *mer-lux* probe method with sediment pore-water. Prior uses of this approach have been with oxygenated overlying water (Rasmussen et al. 2000, Selifonova et al. 1993). The lack of detectable Hg(II) and large errors associated with the *mer-lux* data in the current study may have been due to the inability of the aerobic E-coli bacteria, used in the microprobe, to function under the low oxygen to anoxic and/or sulfidic conditions typical of sediment pore-water. Subsequently, the operationally defined weak acid-extractable Hg(II) pool was our standard surrogate measure of bioavailable

Hg(II), and was used for calculating *in-situ* MeHg production rate (i.e. **Equation 3**). Spatial trends for Hg(II) generally followed those for Hg_t and MeHg **(Fig. 10b,c)**, with highest levels (> 20 ppb) measured at Fort Churchill (F1 & F2), south Lahontan Reservoir (LS) and the agricultural drains (CL and SS) **(Fig. 5)**. While June 1999 depth profiles for Hg(II) were nearly vertical for LB, LS, and SC, a large mid-depth (8-12 cm) maximum (78 ppb) was evident at F1 **(Fig. 8a).** A smaller distinct mid-depth maximum was again observed in the relocated F1 site in October 1999 **(Fig. 8b)**. Vertical bank (F3) sediment was highest (≈ 7 ppb) just above and below the air/water interface, and decreased sharply at the lowest depth in June 1999 **(Fig. 9d)**. In contrast, this lowest depth (D3) had exceedingly high Hg(II) levels (780 ppb) in October 1999. Again, this loose sand matrix differed from the compact bank material sampled in June, and may represent newly eroded bank material generated during the previous high-flow period (Carroll et al. 2000). If so, the high Hg(II) and MeHg concentrations associated with this sample would confirm the hypothesis that eroding bank deposits are significant sources of reactive Hg to downstream locations.

Acid-extractable Hg(II) typically represented < 2% of Hg_t in 0-4 cm sediments **(Figs. 6a,b).** The two exceptions both represented large grain (sandy), oxic, organic poor sediments, with %Hg(II) values of 4.8% (F2 - October 1998) and 6.6% (LN - June 1999). In both cases, the exact sampling location was moved between sampling dates due to high water conditions. Subsequently, these high %Hg(II) values were not reproduced at either site, as specific sediment characteristics (i.e. grain size, redox, organic content) varied between sampling dates. While %Hg(II) varied little with sediment depth at LB, F1 and SC, a distinct increase (1.2% to 4.5%) was observed in the LS profile **(Fig. 8c)**. Vertical bank (F3) material had the highest %Hg(II) content (9.0% to 4.2%) **(Fig. 9e)**. Overall, these results indicate that only a very small fraction of the total mercury in CRS sediment is available for methylation. This assumes that acid-extractable Hg(II) is a reasonable surrogate measure of bioavailable Hg(II). It has been recently suggested, however, that relying on the acid-extractable pool only as may underestimate the true microbial available Hg(II) pool size, as the addition of weak acid will cause a precipitation of dissolved organic matter in pore-water, and a potential complexation of previously dissolved Hg(II) (N. Bloom, pers. comm.). Thus, the in-situ rates calculated in this report should be considered as minimum estimates.

6.2 Microbial Mercury Transformations

6.2.1 Rate Constants – Assumptions and Spatial/Temporal Trends

Radiotracer derived rate constants (k_{meth} and k_{deg}) provide a measure of how readily Hg(II) is methylated or MeHg is degraded back to inorganic species. These measurements are influenced by substrate concentrations (Hg(II) and MeHg, respectively), abiotic sediment conditions and the general activity of the resident microbial community. Assumptions inherent in these k values include: a) the radiotracer (^{203}Hg(II) or ^{14}C-MeHg) acts as a surrogate for the in-situ pools of Hg(II) or MeHg, b) factors which impact the in-situ Hg-species availability to bacteria, may similarly impact the radiotracer (i.e. complexation with organics, Hg-S species formation, solid phase binding, etc...), c) factors which impact general microbial activity consequently impact k's (i.e. temperature, electron donor or acceptor availability, sediment pH and redox conditions, etc...), d) above ambient levels of radiolabled Hg and MeHg are not

inhibitory to sediment microbes and e) transformations are governed by first-order kinetics. Further, k_{meth} values, calculated from long-term incubations (e.g. 24 hours during October 1998), are assumed to reflect net MeHg production because the $^{203}Hg(II)$-methylation reaction is reversible, and k_{deg}'s are comparatively rapid. In contrast, k_{deg} values reflect gross rates, as this reaction is essentially non-reversible because the potential for $^{14}CO_2$ or $^{14}CH_4$ end-products to be reincorporated into ^{14}C-MeHg is negligible. Further, our experimental data, and that of other researchers (Wallschläger et al. 1998), supports the assumption that the added radiolabel rapidly (within minutes) distributes itself amongst various geochemical fractions within the sediment matrix (i.e. dissolved, organically-complexed, particle bound, etc...). For the purposes of interpretation, we assume that this distribution of the radiolabel is in the same ratio as the natural Hg-species. Thus, the measured k's indicate the transformation rates of the Hg(II) and MeHg pools most readily available to the bacteria.

Surficial sediment (0-4 cm) k_{meth} values ranged from $< 1x10^{-4}$ d^{-1} to $2.8x10^{-2}$ d^{-1}, and were spatially and temporally variable **(Fig. 11)**. In October 1998, values appeared highest ($\geq 1x10^{-2}$ d^{-1}) in the upstream river (LB, DR and F1), and low in the wetland sites (LL, SP and SC). In June 1999, k_{meth} was noticeably lower than previous measured at most sites, highest at F1 ($7x10^{-3}$ d^{-1}), and low ($\leq 3x10^{-3}$ d^{-1}) at all other sites. In October 1999, k_{meth} was highest at LS. Wetlands and agricultural drain values were 4 to 44-fold larger than the values similarly measured during June 1999. The situation for k_{deg} was somewhat less erratic. Surface sediment values of k_{deg} were much higher than those for k_{meth}, and ranged from $3.2x10^{-2}$ d^{-1} to 7.2 d^{-1} **(Fig. 12).** Values of k_{deg} were also typically higher in fresh sediment (June and October 1999) than in aged sediment (October 1998). The highest k_{deg} values were downstream of Lahontan Dam in the wetlands and agricultural drains, for all sampling periods, and at LS during both October 1998 and 1999. Vertical trends for both k_{meth} and k_{deg} varied among sites, but general trends were similar among the two sampling dates **(Fig. 13)**. A below surface maximum in k_{meth} was often observed, while k_{deg} was typically highest in the surface sediment, most noticeably at the wetland site (SC). Both k_{meth} and k_{deg} decreased with depth in the June 1999 vertical bank F3 profile **(Fig. 14)**. Only k_{deg} in the loose sandy D3 interval was above our detection limit during October 1999.

6.2.2 Rate Constants – Methodological Considerations

The spatial and temporal variations in k_{meth} and k_{deg} may reflect the natural variation in specific environmental variables that impact these rate constants **(Section 6.3)**. Thus, given an adequate understanding of ancillary processes, ratiotracer derived rate constants are extremely useful in elucidating which factors control spatial and temporal microbial Hg-transformations in natural systems. However, a number of methodological factors may also contribute to observed differences in k's. For example, the higher incubation temperatures used in October 1998 (20 ^0C) would tend to increase overall microbial rates and k values (see **Section 6.5),** compared to the in-situ incubation temperatures (10-17.5 ^0C) used in June and October '99. We did observe generally higher k_{meth} values, but not k_{deg} values, at the higher incubation temperature **(Figs. 11-12)**. Variations in $^{203}Hg(II)$ specific activity, among sampling dates, may also have impacted observed k_{meth} values. While 1 μCi of $^{203}Hg(II)$ per sample was consistently our target amendment, specific activity of the radiotracer varied substantially among dates: [in μCi/μg Hg(II)] October '98 (0.96), June '99 (0.14), October '99 (0.38). Thus, unlabeled Hg(II) was added in the order of: [in μg Hg(II) per 3 g sample] October '98 (1.0) < October '99 (2.6) < June

'99 (7.1). The effect of adding increasing levels of Hg(II) may result in a number of potential responses, including a) stimulation of concentration dependent Hg-methylation (increased k_{meth}), b) inhibition of bacteria due to toxic effects (decreased k_{meth}), or c) a decrease in calculated k_{meth} simply due to a smaller fraction of the Hg(II) amendment as radiotracer ^{203}Hg(II) (i.e. isotope dilution). Results from the controlled specific activity experiment, using site LS sediment (collected October 1999), suggest that decreasing specific activity (increasing unlabeled Hg(II)) resulted in a decrease in observed k_{meth} **(Fig. 15a)**, presumably due to simple isotope dilution. At the lowest specific activity (highest Hg(II) amendment), k_{meth} was below the detection limit. If isotope dilution was the only effect of decreasing specific activity, we would predict that calculated potential rates would remain constant (i.e. no effect on microbial populations), as the decrease in k_{meth} is off-set by the increase in the total Hg(II) amendment in Eq. 3. Alternatively, potential rates might increase due to first-order stimulation of k_{meth}. However, since the calculated potential methylation rate decreased **(Fig. 15b)**, a partial inhibitory effect at high mercury amendment levels is suggested. Since the decrease in k_{meth} was larger (6.7-fold) than the decrease in the potential rate (2.1-fold), between specific activity levels of 1.58 to 0.5 μCi/μg Hg(II), it would appear that isotope dilution was more significant than was toxic inhibition. These results may partially explain the seasonal differences observed in Hg-methylation rates, such that the generally lower k_{meth} values observed during June 1999, compared with October 1999, were due primarily to an isotope dilution effect and possibly a partial inhibition of resident microbes at the higher total Hg(II) amendment during June **(Figs. 11b,c)**.

Since the specific activity of the ^{14}C-MeHg stock solutions remains essentially unchanged, due to the exceedingly long half-life of the isotope (5730 years), the above concerns regarding isotope decay do not apply for the MeHg degradation experiments. However, the four-fold lower ^{14}C-MeHg amendments used in June and October '99, compared to October 1998, could potentially have resulted in an increase in k_{deg} values, as has been previously observed in other studies (Marvin-DiPasquale & Oremland 1998). We did indeed observe generally higher k_{deg}'s when the lower MeHg amendments were used **(Fig. 12)**. This effect may again be linked to partial inhibition of bacterial communities at the higher MeHg amendment levels.

The absolute effect on k's of using aged sediment in October 1998 is unknown, as this may decrease the activity of some microbial groups while increasing the activity of others. The decrease in incubation time from 24 hours (October 1998) to 6 hour (June and October 1999) potentially resulted in k_{meth} and k_{deg} values that were both higher and more accurate. This was demonstrated with the time course experiment using F1 sediment **(Fig. 16)**. Instantaneous values of k calculated from the initial linear slope of the percentage of ^{203}Hg-methylated (or ^{14}C-MeHg degraded) versus time plots **(Figs. 16a,c)**, reflect the transformation rates for the most readily bioavailable pools of Hg(II) and MeHg in a given sediment. After a certain time the slope begins to decrease, as the bioavailable fraction of each radiotracer begins to decrease and/or steady state is reached (in the case of ^{203}Hg-methylaton/demethylation only). Corresponding plots **(Figs. 16b,d)** show a rapid time-dependent decrease in values of k_{meth} and k_{deg} calculated from individual time points. The values calculated from the standard 6-hour incubation compared reasonably well with the initial instantaneous slope calculated from the multi-point time course. The k's calculated from the 24-hour single time point were significantly lower. This suggests that k_{meth} and k_{deg} values obtained for June and October 1999 (6 hour incubations) provided a reasonable measure of bioavailable Hg(II) and MeHg transformations, respectively. In contrast, k's calculated for the October 1998 (24 hour incubations) likely underestimated maximum potential rates. It is difficult to know precisely how the combined influence of these multiple

factors affected the observed differences between sampling dates for site-specific k_{meth} and k_{deg}. Clearly, working with freshly collected sediment at in-situ temperature, and conducting short incubations, provides the most accurate measurements.

6.2.3 In Situ MeHg Production and Degradation Rates

Site-specific in-situ rates of MeHg production **(Figs. 17, 19a,b and 20)** were calculated from **Eq. 3** using the appropriate radiotracer derived k_{meth} **(Figs. 11, 13a,b, and 14a)** and the in-situ concentration of acid-extractable Hg(II) **(Figs. 5, 8a,b and 9d)**. MeHg production in surface (0-4 cm) sediment was consistently high at F1 (90-150 pg•g wet sed^{-1}•d^{-1}) during all sampling periods, while rates for the nearby F2 site were less consistent **(Fig. 17)**. Similarly, methylation rates in Lahontan Reservoir delta (site LS) varied widely (3-200 pg•g wet sed^{-1}•d^{-1}) among sampling periods. Much of the variation at both LS and F2 was undoubtedly due to the differences in the exact sampling location between dates (as discussed above). However, rates for LS were consistently higher (8-2000X) than for LN, indicating that the delta region of the Lahontan Reservoir is an important zone for MeHg production. The agricultural drain sites CL and SS also typically exhibited significantly higher MeHg production than the wetland and playa sites. All depth profiles showed maximum MeHg production below the 0-4 cm surface horizon **(Figs. 19a,b)**. In contrast to June 1999, enhanced MeHg production in the 0-4 cm interval was evident in the October 1999 depth profile for SC. MeHg production in vertical bank (F3) material decreased with depth during June 1999 **(Fig. 20)**, but was undetectable during October 1999 when the substrate was dried out. The June rates were 50-100X lower than the sediment methylation rates at F1 and F2, indicating the MeHg production in the wetted vertical bank material was minor compared to production in the sediment.

Site-specific in-situ rates of MeHg degradation **(Figs. 18, 19c,d and 20)** were calculated from **Eq. 8** using the appropriate radiotracer derived k_{deg} **(Figs. 12, 13c,d, and 14b)** and the in-situ concentration of MeHg **(Figs. 3, 7c,d and 9b)**. Spatial trends for MeHg degradation in surface sediment **(Fig. 18)** were similar among sampling dates, with the highest rates at F1, LS, CD, the agricultural drains (CL and SS), and the wetland sites (LL, SP, and SC). Degradation rates measured in fresh sediment (July and October 1999) were about 10X higher than rates measured in aged sediment (October 1998), possibly due to the inhibitory effects of higher ^{14}C-MeHg amendment levels used in 1998 (as discussed above). Strong differences were observed between June 1999 and October 1999 at site LS, presumably due to the differences in substrate (i.e. sand versus fine-grained silt/clay). MeHg degradation at F1 and SC was highest at the sediment surface and decreased with depth, for both sampling dates **(Figs. 19c,d)**. In contrast, rates were low (< 0.1 ng•g wet sed^{-1}•d^{-1}) and essentially constant with depth at LB and LS during June 1999. As with Hg-methylation, vertical bank (F3) material had degradation rates at least 100X lower than the adjacent sediment sites (F1 and F2), with a maximum just below the air/water interface during June 1999 **(Fig. 20)**. MeHg degradation rates were below detection during October 1999 in the dried F3 substrate.

Since calculated in-situ MeHg production rates **(Fig. 17)** in surficial sediments were small compared to in-situ MeHg degradation rates **(Fig. 18)**, a rapid recycling of Hg within the sediment is suggested. This conclusion is partially based on the assumption that the measured k_{meth} reflects net methylation of the ^{203}Hg-radiotracer, and k_{deg}'s reflect gross ^{14}C-MeHg degradation, as described in **Section 6.2.1**. The time course experiment conducted with F1

sediment gives us some insight into these assumptions. After an initial (≈ 12 hour) rapid linear increase, the % ^{203}Hg(II) methylated over time reached a plateau at about 2.5% **(Fig. 16a)**. One interpretation of this is that opposing methylation-demethylation reactions reached steady state after the initial 12 hour period. This would suggest that k_{meth} values calculated from incubations > 12 hours (i.e. October 1998) reflect true net methylation rate constants, and that k_{meth}'s calculated from shorter incubations (i.e. June 1999) do not. Alternatively, the plateau may reflect the distribution of the radiotracer into bioavailable (≈ 2.5%) and non-available (≈ 97.5%) Hg(II) pools. The initial linear slope would then reflect the methylation rate of the most bioavailable pool only. Acid-extractable Hg(II) measured for site F1 (0-4 cm) was 0.1% to 0.3 % of Hg_t (all dates, **Fig. 6**). If the second interpretation of the % Hg-methylated versus time plot is correct, and the distribution of ^{203}Hg(II) is proportional to the actual distribution of methylatable-Hg(II), than the operationally defined acid-extracted Hg(II) pool would appear to underestimate the actual pool size of methylatable-Hg(II). This would raise the estimates of MeHg production by approximately10-fold in the case of site F1. However, it is unknown how closely the added radiotracer mimics the natural distribution of in-situ Hg(II). Thus, it is subsequently unclear whether or not ^{203}Hg radiotracer derived MeHg production rates reflect true net measurements. Additional experiments are necessary to further explore these questions.

The situation with respect to ^{14}C-MeHg is less equivocal. Because this reaction is essentially non-reversible (with respect to the gaseous ^{14}C end-products), the radiotracer derived k_{deg} clearly does reflect gross demethylation. Further, no similar plateau was observed in the MeHg degradation time course **(Fig. 16c)**, although the rate of degradation did slow over time. This may reflect either the concentration-dependent nature of MeHg degradation enzyme kinetics, and/or a similar distribution of the radiolabel between readily available and less available MeHg pools.

6.2.4 Potential Rates and M/D Ratios

There currently exists no definitive way to assess how much of the total Hg(II) in sediment is available to bacteria for methylation, and which geochemical fraction this pool is associated with. Similarly, it is unknown how much of the total MeHg is actually available for demethylation, and with which geochemical fraction(s) this bioavailable pool is associated. Research is currently underway in our laboratory, and in many others, to address these important uncertainties. In light of these uncertainties, a number of assumptions were needed to calculate the above in-situ rates, including that weak acid-extractable Hg(II) represents the pool most readily methylated by bacteria, and that all of the measured in-situ MeHg was available for demethylation. If we consider the methylation to demethylation (M/D) ratio for the resulting in-situ rates in sediments (excluding F3 bank material) we calculate a range of ratios from 4.8×10^{-4} to 2.0, with a median and mean of 3.7×10^{-2} and 0.12, respectively (all data, n= 64, not shown). Of these only one site/depth had an M/D ratio > 1 (F2/Oct. '99/0-4 cm; M/D = 2.0). This would imply that in-situ demethylation exceeds Hg-methylation in almost all cases. Clearly this is not the situation or else there would be no net MeHg production. Thus, the calculated in-situ Hg-methylation rates apparently underestimate either k_{meth} or the bioavailable Hg(II) pool. Alternatively, the in-situ rate of MeHg degradation may be too high due to either an overestimation of k_{deg} or that the assumption that all of the measured MeHg was available for demethylation was false. Finally, erroneously low M/D ratios would result if the Hg-methylation term represents a net measurement, as opposed to a gross measurement (as discussed above).

Making sense of the relative importance of Hg-methylation versus MeH-demethylation is thus confounded by these uncertainties.

One approach to simplifying the analysis is to consider potential rates of microbial Hg-transformations. While both in-situ and potential rates rely on radiolabel derived values of k_{meth} and k_{deg}, the calculation of the latter uses the amendment plus the in-situ Hg-species pools, as opposed to in-situ Hg-species concentration only. Since the amount of Hg(II) or MeHg added to each sample was constant across all sites and depths for a given sampling date, and typically larger than the in-situ pools, variations in calculated potential rates due to spatial changes in Hg-species pool size are minimized. Subsequently, the spatial trend among sites for potential rates (not shown) would essentially track that of the k_{meth} or k_{deg} values alone **(e.g. Figs. 11-12)**, for any given date. When we examine the M/D ratios calculated from calculated potential rates, an overall trend of decreasing ratios going from the upstream river to the downstream sites is apparent **(Fig. 21)**. This strongly suggests that locations upstream of Lahontan Dam have a higher potential for net Hg-methylation, than do areas below Lahontan Dam, regardless of in-situ Hg(II) concentrations. This trend was generally reproducible for all sampling dates, but strongest during July and October 1999, when fresh sediment was assayed. Depth profiles of M/D ratios calculated from potential rates indicate that net Hg-methylation was typically greatest below the surface interval at nearly all sites **(Fig. 22)**. Many more sites exhibited M/D > 1 when potential rate data was used to calculate ratios than when in-situ rate data was used. However, all sites below Lahontan Dam still exhibited M/D values < 1, even when potential rates were used. This should not be interpreted to mean that sites below Lahontan Reservior are net demethylation zones, as uncertainties regarding the gross versus net status of the k_{meth} measurement still applies. It is the down-gradient decrease trend in M/D that is of greatest importance in these initial results.

6.3 Biogeochemical Controls on Net Methylmercury Production

The key determinants of the degree of net MeHg production at a given site were: a) Hg(II) concentration and its bioavailability to methylating bacteria, b) the intrinsic potential for the resident bacterial community to both methylate and demethylate mercury, and c) the gross rate of MeHg degradation. Each of these determinants is in turn affected by the overall sediment microbiology and geochemistry of a particular site. Extensive effort was thus put forth to understand the interplay between benthic microbiological processes and physical/geochemical sediment characteristics. While a written description of the entire ancillary data set is beyond the scope of this report, the following discussion highlights the important aspects of these biotic and abiotic processes, and details their influence on CRS Hg-cycling.

6.3.1 General Description of CRS Regions

There is distinct shift in sediment characteristics going from the high-energy river environment upstream to the low-energy wetlands environment. This transition results in larger particles being deposited upstream and finer particles downstream, as well as a transition from low to high zones of primary production. Sediment in the Carson River proper (LB, DR, DY, F1, F2 and CD), Lahontan Reservoir (LS and LN), and Carson Sink (CS) were generally characterized as sandy **(Fig. 43)**, organic-poor **(Fig. 54,55)**, low porosity **(Figs. 45, 46)** and often

oxidized **(Figs. 47, 48)**. In contrast, wetland (LL, SP, and SC) and agricultural drain (CL and SS) sediments were comparatively fine-grained, carbon-rich, high porosity and reducing.

6.3.2 Bioavailable Hg(II)

The total amount of Hg(II) available to methylating bacteria represents a primary factor mediating absolute rates of MeHg production. There was a positive relationship between k_{meth} and in-situ Hg concentration (both acid-extractable Hg(II) and Hg_t) noted for both June and October 1999 data sets **(Fig. 23)**. These results indicate that there is a trend towards increasing natural populations of Hg-methylating bacteria with increasing Hg contamination across the CRS. This positive relationship was comparatively weak during June 1999, and markedly more pronounced during October 1999. This temporal difference may reflect the partial inhibition of Hg-methylation during June 1999 due to increased $^{203}Hg(II)$ amendment levels, as discussed above **(Section 6.2.2)**. Further, the lack of a similar positive relationship in October 1998 (not shown) may reflect the depletion of sulfate, and the subsequent inhibition of the sulfate reducing bacteria, during the extended period of sediment storage and prior to the Hg-methylation assay. Since the relationship between Hg_t and k_{meth} **(Fig. 23d)** was somewhat tighter than the relationship between acid-extractable Hg(II) and k_{meth} **(Fig. 23b)**, this may suggest that the acid-extractable Hg(II) fraction does not encompass all of the microbially available (methylatable) Hg(II), and that Hg_t is a better indicator of methylatable-Hg(II) in the CRS. More work in this area is necessary to better quantify the elusive microbially available Hg(II) fraction.

The current observation of increasing k_{meth} with increasing Hg concentration would seem to contradict the earlier findings of Chen et. al. (1996), who suggested that high levels of Hg (> 15 $\mu g \cdot g$ dry sed^{-1}) may have an inhibitory affect on Hg-methylating bacteria, and that this could partially explain the low MeHg/Hgt ratios often observed in the CRS. MeHg/Hgt ratios from the current data set typically ranged from 0.0001 to 0.003 (or as % MeHg [e.g. $MeHg/Hg_t$ ratio x 100] 0.01% to 0.3% as depicted in **Fig. 4**). The exceptions being the two most upstream control sites (LB and DR) which exhibited values from 0.7% to 2.4% MeHg. By comparison, the downstream $MeHg/Hg_t$ ratios were similar to sediment values for other freshwater systems directly and acutely impacted by Hg, such as Clear Lake (California) (< 0.4% MeHg) (Suchanek et al. 1998) and mining impacted sites throughout the western U.S. (< 0.4% MeHg) (Mark Marvin-DiPasquale, unpublished data), but were low compared to systems that receive Hg inputs from diffuse (e.g. atmospheric) sources, such as comparatively pristine lakes in Sweden (Regnell et al. 1997) and the Florida Everglades (Gilmour et al. 1998b) where the % MeHg often exceeds 1%. Thus, the inhibition hypothesis seems plausible for heavily Hg-contaminated systems such as the CRS. Sites where in-situ Hg_t levels were highest (e.g. > 5 ppm, **Fig. 2**) include F1, LS, CL, and SS. However, we see that these are the same sites that typically had the highest k_{meth} values **(Fig. 11)**, not the lowest. In only two cases did we see Hg_t levels > 15 ppm, the level suggested to be inhibitory by Chen et. al.. In the first case (site F2, June 1999), the corresponding k_{meth} was comparable to other sites, with much lower Hg_t levels, sampled during the same period. In the second case (site LS, October 1999), the corresponding k_{meth} was the highest we measured for that sampling period. Thus, high concentrations of Hg_t in sediments do not seem to correspond with an inhibition of Hg-methylation potentials. The fact that the CRS and other similarly heavily Hg-impacted sites appear to have low $MeHg/Hg_t$ ratios (or % MeHg values) may simply reflect the fact that only a small fraction of Hg_t is actually methylatable-Hg(II), and while Hg_t may increase over a 1000-fold range the pool of methylatable-Hg(II) likely does not. The result

of this is that there is some restriction on how much MeHg can be made, which is linked to restrictions on methylatable-Hg(II) concentrations, which is not a linear function of Hg_t concentration. Therefore, higher Hg_t values result in lower the $MeHg/Hg_t$ ratios. However, we do argue that the generally lower k_{meth} values observed in the June 1999 data, compared to the October 1999 data, may be due to partial inhibition of Hg-methylating bacteria by the higher Hg amendment level used during the earlier sampling date (see Section 6.2.2). The difference between this argument and the one put forward by Chen et. al. lies in the time frame under consideration. For buried Hg-contaminated sediments, the resident microbial community that is eventually selected for is one that is best adapted to whatever the local Hg-concentration is. Conversely, when we spike sediment with a slug of Hg(II), and conduct an immediate short-term incubation on the time scale of hours, an partial inhibition of the resident microbial community is certainly possible, especially if the Hg-amendment level is high. Thus, even in the natural environment, when rapid deposition of highly Hg-contaminated debris occurs, as in the case of spring high flow or flood events, there may be an initial inhibition affect on the resident Hg-methylating microbes. This inhibition may subside after enough time has elapsed to allow for a more Hg-tolerant microbial population to naturally develop. Chen et. al. does suggest that such an eposidic pulse of high Hg-deposition to the sediments occurs during spring and results in (at least temporary) inhibition. Our results are consistent with this interpretation.

The above uncertainties regarding the size of the complete methylatable Hg(II) pool notwithstanding, the acid-extractable Hg(II) fraction is currently the surrogate measure of choice. Much can be learned about the environmental factors which influence Hg(II) availability for methylation by examining which other factors are associated with this fraction. Clearly, the primary factor controlling the absolute concentration of acid-extractable Hg(II) among sites was Hg_t, as these two parameters were strongly correlated among sites **(Fig. 10b)**. Typically, less than 2% of Hg_t in CRS sediment was associated with the acid-extractable Hg(II) fraction **(Fig. 6)**. However, since Hg_t concentrations varied >2000-fold, the absolute concentrations of Hg(II) likewise varied greatly (> 500-fold), although, among-site differences in Hg(II) do not necessarily translate to similar spatial variations in MeHg production. Thus, a location may have very high levels of Hg(II), but also have sediment conditions unfavorable for methylation (e.g. aerobic or organic substrate limited). Alternatively, conditions for methylation may be favorable, but Hg(II) availability may be limited due to organic matter complexation, solid phase binding, or abiotic reaction with reduced-S.

Radiolabel extraction experiments were conducted using October 1999 sediment to investigate the relative influence of in-situ reduced-S and organic matter content on Hg(II) binding. Strong regional differences were observed in the amount of weak acid (0.06 M HCl) or weak base (0.01 M KOH) extractable $^{203}Hg(II)$ that was recovered from $^{203}HgCl_2$ amended heat-sterilized sediments. The weak acid fraction primarily reflects exchangeable $^{203}Hg(II)$ originally bound to organics, minerals and/or metal-(hydr)oxides, while the weak base fraction consists primarily of extractable organics (Hg(II)-humics and Hg(II)-fulvic acid complexes) (Wallschläger et al. 1996). Less than 1% of the radiolabel was recovered in the acid-extractable fraction for sites F1, LS, or any site below the Carson Dam, while recoveries of 3-40 % were obtained for the majority of sites upstream of the Dam **(Fig. 24a)**. When compared to in-situ concentrations of solid-phase acid-volatile reduced sulfur (AVS) and organic matter (measured as percent weight loss on ignition (% LOI)), it is apparent that the lowest recoveries (those < 1%) were observed when AVS was above 1 $\mu mol \cdot g$ wet sed^{-1} and/or LOI was above 2% **(Figs. 25a,b)**. While both AVS and LOI generally increase along the transect from the river to wetland

sites, the correlation between these two parameters was poor ($r = 0.42$), and a linear relationship was not significant at $P < 0.10$ for the 0-4 cm October 1999 data **(not shown)**. A non-linear power function was better fit to the AVS vs % acid-extractable $^{203}Hg(II)$ data ($r^2 = 0.70$) than the LOI vs % Acid-extractable $^{203}Hg(II)$ data ($r^2 = 0.55$). However, both AVS and organic content undoubtedly impact the overall solid-phase binding of Hg(II) in the transition from sites upstream of Lahontan Dam to sites downstream.

In contrast to the acid-extractable fraction, more base-extractable $^{203}Hg(II)$ was recovered from sites below Lahontan Dam (14-36%) than sites upstream of the Dam (1-11%) **(Fig. 24b)**. This indicates that a larger fraction of $^{203}Hg(II)$ was bound to extractable organic matter in the areas below Carson Dam, which is not surprising since the overall organic content is highest in these downstream sites **(Figs. 54 and 55)**. However, no significant relationship was evident between LOI and the % base-extractable $^{203}Hg(II)$ ($P > 0.2$), while AVS versus % base-extractable $^{203}Hg(II)$ did show a significant positive relationship ($P < 0.05$) **(Figs. 25c,d)**. We interpret this to mean that binding of the radiolabel was influenced both by the amount of organic matter and the amount of reduced-S. This pattern likely reflects the fact that these extractions were carried out on parallel samples, and not as sequential extractions of the same sample. Thus, it is uncertain how much of the recovered radiolabel was common in both acid and base extractions. Nonetheless, this extraction experiment does suggest that Hg(II) is associated with both reduced-S and organic ligands to a greater extent in sites downstream of Lahontan Dam than in upstream river sites.

From these results we might predict that the availability of Hg(II) for methylation is more limited in the wetlands, relative to other sites, due to enhanced Hg(II) binding to organic and reduced-S solid phases. This would support our initial assumption, that the most bioavailable Hg(II) fraction is associated with readily exchangeable pools (i.e. weak acid-extractable), and would account for the comparatively low k_{meth} values observed in the wetland sites during October 1998 **(Fig. 11)**. However, wetland k_{meth} values appeared comparable to most upstream sites during June 1999, and were often among the highest measured during October 1999. Thus, the control on Hg(II) availability to bacteria, as reflected by k_{meth}, is more complicated than these operationally defined pools might suggest.

6.3.3 Microbial and Abiotic Controls

6.3.3.1 Sulfate Reduction and Reduced Sulfur

The influence of microbial sulfate reduction (SR) on the benthic Hg-cycle is two-fold. First, sulfate-reducing bacteria (SRB) are the primary methylators of Hg in both freshwater and saline systems (Compeau & Bartha 1985, Gilmour et al. 1992). Second, the reduced-S produced as a result of SR can control the availability of Hg(II) for methylation. The CRS is very heterogeneous with respect to sulfur biogeochemistry. Microbial SR was highest in agricultural drains, but also clearly active at most other sites in October 1998 samples **(Fig. 26a)**. Rates measured in this preliminary study likely underestimated the original in-situ rates due to SO_4^{2-} depletion that undoubtedly occurred during the 3-month sediment storage. Indeed, concentrations of surficial (0-4 cm) SO_4^{2-} were consistently higher in fresh (1999) sediment than in aged (October 1998) sediment **(Figs. 59 and 60)**. The 1999 data provides a more accurate representation of in-situ SR rates, as these samples were incubated within hours of collection. Depth profiles for both 1999 dates show that SR was significantly higher in the wetland site (SC)

than in upstream river and reservoir sites **(Figs. 26b,c)**. Rates decreased with increasing depth at all sites except LS (June 1999), where SR was barely above detection. The high concentration of reduced-S **(Figs. 27-29)** in the wetlands and agricultural drains, support the conclusion that SR is most active in these organic-rich areas. However, even though SR rates were typically highest in the areas downstream of the Lahontan Dam, the potential for Hg-methylation was often lower in these areas compared with sites upstream of the Dam **(Figs. 17, 19, and 21)**. The build-up of reduced-S in the organic rich sites partially explains this apparent paradox.

Recent modeling efforts suggest that neutral HgS dominates Hg-S complex formation at low sulfide concentrations (Benoit et al. 2001a, Benoit et al. 2001b, Benoit et al. 1999). This neutral species is thought to readily cross the cell membrane of Hg-methylating bacteria. Methylation is limited at high sulfide levels, as charged Hg-S species (e.g. HgS_2H^-, HgS_2^{2-}) form, which do not readily cross the cell membrane. Thus, the potential for Hg-methylation may be optimal under conditions in which SRB are active, but in-situ reduced-S concentrations are minimal (Benoit et al. 1998, Gagnon et al. 1996), as was the situation for most sites upstream of the Lahontan Dam. In contrast, the three wetland-lakes had the highest pore-water sulfide levels **(Fig. 29a)** and among the lowest MeHg production rates **(Fig. 17a)**. The correlation between sulfide and k_{meth} was not significant when all sites were compared (October 1998, 0-4 cm data). However, a negative logarithmic relationship ($r^2 = 0.67$) was apparent when the analysis was limited to the seven sites downstream of Lahontan Dam (i.e. CD → CS) **(Fig. 30a)**. Further, a similar negative relationship between sulfide and k_{meth} was evident for depth profile data at the wetland site (SC), during both June and October 1999 **(Fig. 30b)**. No significant relationships were found between sulfide and k_{meth} in 1999 depth profile data from the three upstream sites (LB, F1 and LS), which had substantially lower sulfide concentrations.

Solid phase reduced-S may bind Hg(II) (Gagnon et al. 1997), thus decreasing its availability to methylating bacteria. As with sulfide, bulk sediment AVS was typically highest in agricultural drains and wetland sites **(Figs. 27 and 28).** A non-linear relationship between acid-extractable Hg(II) and AVS was also observed for the complete data set (all dates), in which only sites with low reduced-S levels (< 0.2 μmol•g wet sed^{-1}) was acid-extractable Hg(II) ever in excess of 2% Hg_t (up to 9%) **(Fig. 30c)**. These results for in-situ Hg(II) are similar to those found for the ^{203}Hg(II) weak acid extraction experiments discussed above **(Fig. 25a)**. Taken together, these results indicate that both dissolved and solid phase reduced-S play an important roll in mediating Hg-methylation in the CRS, with most favorable conditions upstream of the Lahonton Dam. This was generally reflected in the M/D ratio data **(Fig. 21)**.

6.3.3.2 Methanogenesis and its Relationship to Sulfate Reduction

Methane (CH_4) producing bacteria (MPB or methanogens) are not known to methylate Hg, but can degrade MeHg (Marvin-DiPasquale & Oremland 1998, Oremland et al. 1991). Because SRB can effectively out-compete MPB for mutually used substrates (e.g. hydrogen and acetate), the zone of maximum MPB activity is often below the active sulfate reduction zone in sediments. However, when non-competitive organic substrates for MPB are present (e.g. trimethylamine, methanol), these two bacterial groups can effectively both thrive in the same sediment horizon (Oremland & Polcin 1982). Thus, the spatial distribution, competition, and coexistence of both SRB (MeHg producers and degraders) and MPB (MeHg degraders) within sediments, all play an important role in mediating the degree of net MeHg production.

Methane production rates were highest in the organic rich wetlands and agricultural drains in October 1998 aged sediment **(Fig. 31a)**. Depth profiles of freshly collected sediment (both 1999 dates), exhibited high and comparable CH_4-production rates in both the wetland site (SC) and the highly contaminated river site (F1). The profiles for these two sites differed, with maximum rates in surface sediments at SC and in deeper sediments at F1 **(Figs. 31b,c)**. Rates were generally lower in the control site (LB) and below detection in the sandy reservoir site (LS) during June 1999. In-situ concentrations of CH_4 **(Fig. 32)** generally followed the spatial distribution of CH_4-production rates during all sampling periods. Since SR activity was likely limited in sulfate depletion aged sediment, the competition between SRB and MPB would have been alleviated somewhat in the 1988 samples, resulting in the generally higher CH_4-production rates compared to both 1999 dates. Additionally, the higher incubation temperature (20 ^{0}C, room temperature) used in the 1998, compared to both 1999 studies (12-16 ^{0}C, in-situ temperatures), may have also partially contributed to higher observed CH_4-production in the first case. In either case, the 1999 data was more reflective of in-situ rates, as was also noted above for SR.

A number of relevant observations are evident when spatial trends of both SR **(Fig. 26)** and CH_4-production **(Fig. 31)** are compared: a) both processes are active at common site/depths in a majority of cases, b) both share a mid-depth maximum (4-8 cm) at site LB and a surface (0-4 cm) maximum in wetland site SC (June '99), c) at F1 (June/Oct. '99) SR is high at depths where CH_4 production is low (but not zero), and d) both are minimal or absent in comparatively organic-poor, oxic, sandy sediments (e.g. F2 – Oct. '98, LS – June '99). These results suggest: a) the presence of non-competitive substrates allows for the simultaneously activity of both SRB and MPB within most sediment horizons, b) some degree of substrate competition exists between these microbial groups at a number of sites (e.g. F1) leading to spatially separate zones of maximum activity; and c) conditions in certain oxidized, organic-poor, sandy sediments were not conducive to either anaerobic respiratory process. Comparing the millimoles of sulfate reduced versus the millimoles CH_4 produced (on a per $cm^3 \cdot d^{-1}$ basis), we conclude that much more of the overall carbon flow goes through methanogenesis than through SR, which is typical of SO_4^{-2} limited freshwater systems (Capone & Kiene 1988). This calculation assumes that two moles of idealized organic matter (CH_2O) is consumed for each mole of either SO_4^{-2} reduced or CH_4 produced (Marvin 1995).

Implications of the above findings, with respect to microbial Hg-transformations, include: a) bacteria responsible for both the production and degradation of MeHg are typically active within the same sediment horizon, which would imply rapid recycling of Hg between methylated and inorganic forms, b) the vertical distribution of maximal rates of MeHg production versus degradation may be influenced by the degree of competition between SRB and MPB due to the relative availability of competitive and non-competitive substrates, and c) demethylation by MPB may represent a dominant control on net MeHg production in the CRS because the overall activity of these bacteria, with respect to carbon flow, far exceeds the activity of SRB. Determining the specific amount of MeHg degraded by MPB alone is complicated due to the fact the SRB can also degrade MeHg. However, the dominant influence of MPB was suggested by the significant positive relationship detected between the rate of CH_4 production and the MeHg degradation rate constant k_{deg} in the October 1998 data set **(Fig. 61a, see Section 6.3.4).** Similar positive relationships were not apparent between SR rates and k_{meth}, which may reflect the fact that the Hg-methylation radiotracer assay is a net, as opposed to gross, measurement.

6.3.3.3 Iron and Manganese Reduction

Microbial dissimilatory iron (Fe) and manganese (Mn) reduction refers to biologically mediated reactions in which specific bacteria groups obtain energy from the conversion of oxidized Fe(III) and Mn(IV) to their respective reduced forms (*viz.*, Fe(II) and Mn(II)). Iron-reducing bacteria may also be capable of MeHg production (Gilmour et al. 1996), although their relative contribution in natural systems is unknown, but is likely minor compared to that of SRB. The primary importance of Fe-reducers, as well as Mn-reducers, may be the ability of both groups to dissolve solid-phase oxidized Fe and Mn minerals. This in-turn affects the partitioning of various Hg-species between the solid and aqueous phases, and subsequently the release of Hg(II) and MeHg from the sediment to the water column (Gagnon et al. 1997, Gagnon et al. 1996). We did not measure sediment/water Hg-exchanges as part of the current research program. However, by investigating the spatial distribution of these microbial processes, as well as dissolved and solid-phase Fe and Mn concentrations, we attempted to provide some insight into where Hg-repartioning might be greatest.

Initial microbial-rate measurements (October 1998) were conducted on sediment slurries (5:3 = water:sediment volume ratio), which were initially oxygenated by placing them uncapped on a rotating shaker (100 rpm) for three hours prior to incubation. This was done to partially re-oxidize some of the reduced Fe(II) and Mn(II) that might have built-up during the three month storage period. The incubation was conducted anoxically at room temperature for 14 days. Subsamples were taken at the beginning and end of the incubation period, and assayed for weak acid (0.5 M HCl) extractable Fe(II) and Mn(II). A net increase in these constituents was used as an index of microbial reduction reactions, whereas a net decrease suggested either a re-oxidation of reduced species or the net precipitation of Fe(II) and/or Mn(II) into non-acid-extractable fractions (eg. FeS_2). A hydroxylamine (0.25 M) extraction was also preformed on separate subsamples to test for microbially available (reducible) Fe(III) (Lovley & Phillips 1987) as a compliment to the acid-extractable Fe(II) analysis. A net decrease in Fe(III) would similarly indicate Fe-reduction activity. The net change in microbially available Fe(III) generally mirrored that for Fe(II) **(Figs. 33a,b)**. Taken together, results indicate that Fe-reduction was greatest downstream of Lahontan Dam at the CD river site, wetland sites LL and SP, and in the CL drain. It is noteworthy that while most all samples had measurable quantities of microbially available Fe(III) at the beginning of the experiment **(Fig. 35a)** only the sites noted above exhibited clear evidence of Fe-reduction. This suggests that either Fe-reducers were out-competed by other microbial groups (eg. denitrifiers) for commonly used substrates, or some other necessary growth factor was limiting. Significant Mn-reduction occurred at F1 and LL only **(Fig. 36a)**. To our knowledge, a similar complimentary assay for microbially available Mn(IV) does not exits.

We repeated the Fe and Mn reduction assays during June and October 1999 at depth profiles sites (only). Fresh whole-sediment, as opposed to sediment slurries, was used in these latter instances. In contrast to the October 1998 sample set, these samples were not oxidized prior to incubation in order to maintain initial in-situ redox conditions. Results were quite variable **(Figs. 34, 36b-c)**. Fe-reduction was only evident at F1 and LS surface sediment (0-4 cm) during June 1999, based on net changes in both Fe(II) and microbially available Fe(III). Acid-extractable Mn(II) also increased at these two site/depths. In contrast, no net increase in Fe(II) or Mn(II) was detected at site F1 during October 1999. Further, while Fe(II) increased at site SC in all but the 4-8 cm depth interval, the amount of microbially available Fe(III) was below detection in all October 1999 samples, suggesting that changes in the Fe(II) pool may have been due to

abiotic chemical processes during the incubation. Further, Mn(II) typically decreased during the October 1999 incubation at both SC and F1, suggesting net incorporation of reduced-Mn into solid phase matrices which were not readily extracted with weak acid. Such unquantified side-reactions are one drawback to the simple approach of measuring the increase in Fe(II) and Mn(II) associated with microbial dissimilatory reduction pathways over a long time course. The two 1999 samplings of Fe and Mn-reduction (using fresh unamended sediment) were probably more reflective of in-situ rates than were 1998 measurements, due to the methodological manipulations invoked in 1998 (e.g. pre-oxidation of samples, sediment slurry matrix). However, the preliminary slurry experiment provided a reasonable assessment of potential rates at all sites, while spatial comparisons made during the latter two sampling dates were more limited.

In-situ Fe and Mn concentration measurements in both whole sediment and pore-water provide further insight into the spatially variable geochemistry of these two metals and compliment the microbial reduction measurements described above. Whole sediment Fe concentrations were high (ca. 15-40 ppt) throughout the system, but exhibited no distinct spatial trend and were nearly constant with depth **(Fig. 37)**. In contrast, pore-water Fe (primarily reduced Fe(II)) was typically highest upstream of Lahonton Reservoir and in the CL drain, and lowest in wetland sites **(Fig. 38)**. A similar pattern was observed for Mn, with only moderate spatial variability in whole sediment (highest in drain sites) **(Fig. 39)**, and low pore-water concentrations in the wetlands **(Fig. 40)**. These trends reflects the potential for precipitation of Fe(II) and Mn(II) into reduced-S mineral phases. Thus, in upstream locations where SR is comparatively low, there is little reduced-S formed and Fe(II) and Mn(II) build-up in anoxic pore-water. In contrast, where SR is rapid (e.g. the wetlands) the abundant sulfide produced precipitates Fe(II) and Mn(II), and pore-water concentrations of these substances are minimal.

The interaction of these biogeochemical cycles of S, Fe, and Mn can have a number of direct impacts on net Hg-methylation and MeHg flux. In the comparatively oxidized sediments upstream of Lahontan Dam, the excess dissolved Fe(II) and Mn(II) helps keep sulfide concentrations low, and may thus enhance MeHg production by favoring the formation of neutrally charged HgS complex (Benoit et al. 1999). In the organic rich wetlands, there is not enough Fe(II) and Mn(II) to precipitate all of the sulfide formed from SR, so the latter builds-up to high concentrations, a situation which favors charged Hg-S complex formation and limits MeHg production. However, the upstream areas presumably have higher concentrations of solid phase Fe(III) and Mn(IV)-oxides, since these sediments are more oxidized **(Figs. 47-48)**, and since the reoxidation of dissolved Fe(II) and Mn(II) is more rapid than for solid phase metal-sulfides. This assumption was supported by the higher concentrations of microbially available Fe(III) in the three upstream sediments (LB, F1, LS), relative to the wetland site (SC), observed in the freshly collected July 1999 samples **(Fig. 35b)**. Inorganic Hg(II) is readily absorbed onto Fe and Mn oxide particles in oxidized surface sediment. As this layer is buried, Hg(II) is released when metal oxides become reduced (Gobeil & Cossa 1993), leading to higher rates of MeHg production at depth. This was evident from depth profiles of in-situ MeHg concentration, which exhibited below-surface maximum at all three upstream sites (LB, F1, LS), but not the wetland site (SC) during June 1999 **(Fig. 7c)**. MeHg may also bind to metal-oxides (Gagnon et al. 1997), and Mn has been suggested as an important species in the solid/aqueous phase partitioning of MeHg in the water column of the Carson River (Bonzongo et al. 1996b). Furthermore, the relative flux of MeHg across the sediment/water interface may be limited in the oxidized upstream areas to a greater extent than in the comparatively reducing wetland areas. This hypothesis should be directly tested in future work.

6.3.3.4 Selenium

The impact of selenium (Se) on Hg biogeochemistry is unique and complex, as Se may mitigate the build-up of Hg in the foodwebs (Henny et al. (in prep.), Nuutinen & Kukkonen 1998, Turner & Rudd 1983). Further, low concentrations (< 10 nM SeO_4^{2-}) have been shown to stimulate Hg-methylation in CRS sediments, while higher concentrations (> 270 nM SeO_4^{2-}) inhibited methylation, presumably by inhibiting microbial SR (via a SO_4^{2-} analog substitution reaction) (Chen et al. 1997). Our original intention was to determine if natural variation in either whole sediment or pore-water Se was related to observed variation in any Hg-transformations being investigated. Initial attempts at Se quantification via inductively coupled plasma emissions spectroscopy (ICP-ES) and graphite furnace atomic adsorption spectroscopy (GF-AAS) were unsuccessful due to matrix interferences with high levels of Fe and Mn. Quantification of Se was finally achieved via ICP-mass spectromety (ICP-MS), although analysis was limited to July 1999 whole sediment samples only **(Fig. 42)**. Concentrations of Se in bulk sediment varied over a fairly narrow range (0.25 to 0.81 ppm dry wt.) in 0-4 cm surface sediments, with highest concentrations generally in the agricultural drains and wetland sites. Depth profiles were generally constant with depth for most sites (LB, F1, and LS), but showed increased levels of Se in surface sediment at the wetland site (SC). There was no relationship detected between bulk sediment Se concentration and either k_{meth} or in-situ Hg-methylation rates. However, there was a positive relationship between Se and in-situ rates of MeHg degradation **(Fig. 62)**, as discussed below (see **Section 6.3.4**). Thus, due to the narrow range of Se concentrations, the comparatively large range of Hg-methylation rates, and the lack of an observed relationship between the two measures, the current data set does not support the hypothesis that Se is a primary factor controlling Hg-methylation rates in the CRS. However, further measurements with respect to Se-speciation and pore-water concentrations would be useful in verifying the current conclusions.

6.3.3.5 Sediment Grain Size and Percent Water

Wetland and agricultural drain sediments were composed of a larger proportion of fine-grained (< 62 μm) particles than river, reservoir or playa region sediments **(Fig. 43)**. There was a weak positive linear relationship ($r^2 = 0.21$, $P = 0.10$) between decreasing grain size and total-Hg concentration (as LOG[Hg_t]) for the October 1998 0-4 cm samples (all sites, data not shown). Similar within-site relationships were stronger, as decreasing grain size was correlated with increasing Hg_t and Hg(II) in the Fort Churchill area, and with Hg_t (only) in LS (June 1999) **(Figs. 44a-c)**. Thus, grain size may be an important factor controlling the within-site spatial distribution of Hg_t (Miller et al. 1999) and subsequently methylatable-Hg(II) concentration. This partially explains the high variability in Hg_t concentration over small spatial distances (< 1 km) and among sampling dates for sites F1 and F2 **(Fig. 2)**. No grain size measurements were made on October 1999 samples. However, direct observation indicated that the October 1999 Lahontan southern delta (site LS) sample was much finer than the sandy (large grain) sample taken at this site during June 1999. While these two samples were taken only a few meters apart, Hg_t and MeHg concentrations were 43-fold and 19-fold higher in October 1999, respectively **(Figs. 2-3)**. Although local variations in Hg_t were clearly linked to variations in grain size, there were no significant among-site relationships detected between grain size and Hg-methylation rates.

However, a clear negative relationship between grain size and k_{deg} was observed (see **Section 6.3.4).**

A parameter closely associated with to sediment grain size is percent water **(Figs. 45-46)**. These two parameters were strongly correlated ($r = -0.98$, $n = 28$; not shown). As the grain size decreased, the sediment percent water content increased, with the highest values in wetland sites and agricultural drain sites. The among-date variation in specific sampling location for sites F1, F2 and LS were evident in the sediment % water data. A similar relationship between increasing sediment water content and k_{deg} was also noted (linear $r^2 = 0.67$, $n = 12$; $P < 0.001$, not shown) (see **Section 6.3.4.)**

6.3.3.6 Sediment Redox

Sediment redox (E_h) is an empirical measure of the ratio of total oxidized to reduced species dissolved in pore-water, as measured by a platinum electrode, relative to a normal hydrogen reference electrode (the potential of which is zero by definition). Thus, E_h is not a controlling environmental variable itself, but an operationally defined parameter. It is useful for assessing the net balance that results from the diffusion of oxidized species (eg. O_2, NO_3^-, SO_4^{2-}, etc...) into the sediment from the overlying water, and the generation of reduced species (e.g. HS^-, Fe(II), Mn(II), etc..) from organic matter decomposition within the sediment. Variations in the relative concentrations of these oxidized/reduced species (as reflected by E_h) can impact mercury cycling by controlling the depth at which certain microbial groups are most active, and by affecting the aqueous/solid phase partitioning of individual Hg species. Sulfate reducers are strict anaerobes, largely inhibited when oxygen (O_2) is present (i.e. highly oxidized conditions). The production of MeHg by these bacteria may thus be limited under oxic conditions (Regnell et al. 1996). A number of sandy, low water content, upstream sites had oxidized (although not necessarily O_2 containing) sediment (e.g. sites DR, F2, LN, **Figs. 47-48**). The among-date variation in sediment E_h at a number of these sites reflects the above noted among-date variation in the exact site location. Sites downstream of Lahontan Reservoir were generally reducing (negative E_h). There was no relationship between microbial SR rates and E_h in October 1998 data, although oxidized sites typically had microbial SR rates that were comparatively small to below detection.

Data plots of E_h versus k_{meth}, k_{deg}, and M/D ratios were constructed **(Fig. 49)** to investigate how variable redox conditions affect microbial Hg-transformation rates in surface (0-4 cm) sediment. Since there was considerable variability in the data, a 3-point running average was calculated to more clearly illustrate trends. A number of trends were evident, including: a) maximum k_{meth} values typically occurred near the redox discontinuity region ($E_h = 0$ mV), between –100 mV and +100 mV, b) k_{deg} values were consistently low at $E_h > +100$ mV and increased with decreasing E_h, and c) the resulting M/D ratio was very low at $E_h < -100$ mV and had maximum between roughly –50 to +150 mV. When all 0-4 cm data was averaged by region, for the complete data set, significant linear relationships were evident for the three parameters (k_{meth}, k_{deg}, and M/D ratio) as a function of sediment redox **(Fig. 50)**. The river and Lahanton Reservior sites had the highest average E_h ($\approx +140$ mV) and had the highest average values of k_{meth} and M/D ratios, and the lowest k_{deg} values. Conversely, the wetland, drain, and playa sites were much more reducing (average $E_h = -10$ to -100 mV) with low average k_{meth} and M/D ratios and high k_{deg} values. Thus, while the variability in these measurements is large, sediment E_h may

serve as a readily obtainable measurement for the cursory prediction of where net MeHg production may be greatest.

6.3.3.7 Sediment pH

MeHg production is generally enhanced in low pH freshwater sediments (Winfrey & Rudd 1990). Among-site differences in pH may potentially influence the sediment/pore-water partitioning (and thus availability) of both Hg(II) and MeHg (Yin et al. 1997a, Yin et al. 1996), and may impact the optimal growth conditions for key bacterial groups involved in Hg-transformations. However, sediment pH in the CRS was near-neutral to slightly alkaline and varied over a fairly narrow range (6.8 to 8.2, mean = 7.5 ± 0.5, all data), with highest values in the playa region (sites CS) and the lowest value in the vertical bank material (F3 June '99) **(Figs. 51-52)**. There was a general increase in k_{meth} with decreasing pH apparent during all sampling periods , and a weak negative relationship between pH and k_{meth} on a regional basis ($r^2 = 0.34$; n = 5) **(Figs. 53a,b)**. Similar regional relationships between pH and k_{deg} or M/D ratio were not found. We conclude that among-site differences in pH had only a subtle impact on observed Hg-dynamics in the CRS.

6.3.3.8 Organic Matter

Sediment organic matter is a key factor mediating Hg-transformations due to its ability to bind both Hg(II) and MeHg, thus impacting availability, and its role in mediating the rate and distribution of various heterotrophic (carbon-utilizing) microbial processes. In the Carson system, this second influence is reflected in the higher overall rates of anaerobic microbial metabolism (e.g. SR and methanogenesis) in the particulate carbon (PC) enriched wetlands and agricultural drains **(Fig. 54)**. Sediment PC was measured at all sites and depths for the first two sampling periods, but only for the two depth profile sites during October 1999. Sediment weight loss upon ignition (LOI) at 500 ^{0}C was assayed at all sites and depths during all sampling periods **(Fig. 55)**, as an additional surrogate measure of total organic matter, and as a compliment to PC. These two parameters were highly correlated (r = 0.92, all data), and subsequently paralleled each other with respect to spatial trends. There was also little within-site variation among sampling dates for both PC and LOI, except in cases where the exact sampling site was necessarily moved (e.g. LS)

The adsorption/desorption kinetics of Hg(II) on the solid phase component of soils and sediments is largely controlled by organic content, with a decrease in desorption capacity associated with increasing organic matter (Yin et al. 1997b, Yin et al. 1997c). We might thus predict that Hg(II) is more strongly bound, and therefore less available to methylating bacteria, in the organic rich wetland and drain sites, and that this might partially account for the typically lower k_{meth} and M/D ratios at these sites. There was an overall decrease in both k_{meth} and M/D ratio with increasing PC in surface sediment for the October 1998 samples **(data not shown),** although a statistically significant relationship at $P < 0.1$ was not detected, and no comparable trend was observed in June 1999. Significant relationships between PC and k_{meth} (or the M/D ratio) were also <u>not</u> detected for within-site multiple-depth data for either June 1999 or October 1999, or when all 0-4 cm data was grouped by region. Similar non-significant results were

obtained when LOI was used instead of PC. In contrast, k_{meth} generally increased with organic content during October 1999, as evident from three-point-average trendline of LOI versus k_{meth} **(data not shown)** and the high k_{meth} values in the wetland and drain sites during this sampling period **(Fig. 11c)**, but this relationship was not significant at $P < 0.10$. Thus, the hypothesis that solid phase organic content was the dominant factor controlling net MeHg production was not consistently supported by the data.

In contrast, a consistent trend of increasing k_{deg} with increasing solid-phase organic content (both PC and LOI) in 0-4 cm surface sediment was noted for all sampling periods, and significant ($P < 0.01$) regional relationships were detected **(Fig. 56)**. The selective adsorption of MeHg onto organic matter has been cited as a control on the partitioning of MeHg between the pore-water and solid phases (Mucci et al. 1995). However, the current data suggests that the potential for enhanced partitioning of MeHg onto solid phase organics in the wetland and drain sites did not offset the increased activity of MeHg-degrading microbes in these regions. Hence, microbial activity may have a more direct control on MeHg degradation than is the case for Hg-methylation, the latter being more impacted by abiotic processes mediating Hg(II) availability.

In addition to solid phase organic matter, the concentration and form of dissolved organic matter may play an important role in the sediment/pore-water partitioning, transport, and microbial availability of Hg-species. Increased levels of dissolved organic carbon (DOC) have been shown to reduce the availability of Hg(II) for methylation (Barkay et al. 1997). In particular, Hg(II) has a strong affinity for humic acids, owing to the often abundant reduced-S ligands associated with this material (Wallschläger et al. 1998, Wallschläger et al. 1996). MeHg also strongly binds to high molecular weight humic acids (Hintelmann et al. 1995), thus potentially affecting its availability for demethylation. Pore-water DOC was assayed at all October 1998 sampling sites and at the depth profile sites only for the two subsequent samplings **(Fig. 57)**. Concentrations across all sites ranged from 5ppm (site F2) to 58 ppm (site LN) for the 0-4 cm October 1998 samples, with no clear regional trends apparent. Subsequent depth profiles showed similar DOC concentrations (ca. 20-50 ppm) in the top 12 cm of sites LB, F1 and SC, while LS exhibited a 100 ppm surface maximum and a marked decreased with depth. We initially speculated that contamination from paper pre-filters, mistakenly used with the pore-water squeezers, could have led to the high DOC levels observed in LN (October 1998) sediment. However, both June and October 1999 samples were processed via centrifugation (as opposed to pore-water squeezers), and similar high DOC concentration was again observed for Lahontan Reservoir (albeit a different site). Further, equipment blanks showed no contamination, indicating that the high DOC levels in the October 1998 LN sample was likely legitimate. We noted the formation of a brown precipitate in a number of the wetland pore-water samples. Since these samples were originally filtered (0.45 um), preserved with 0.1 M HNO_3, and stored refrigerated, we suspected that this material was humic acids precipitating upon acidification (Wallschläger et al. 1998). However, we were unable to redissolve the precipitate by adjusting the pH upward (> 7) with NaOH or by heating, and it was subsequently filtered out of the sample prior to the DOC analysis. It is possible that the precipitate was humic material that was irreversibly transformed upon acidification. The removal of this material from the sample would clearly have lowered our DOC measurements by some unknown amount.

No significant relationships between DOC and k_{meth}, k_{deg} or M/D ratios were evident for the October 1998 data when assessed across all sites or when data was grouped by region. However, a significant non-linear decrease in the amount of acid-extractable in-situ Hg(II) with

increasing DOC was evident **(Fig. 58)**. This may reflect increased desorption of bioavailable Hg(II) induced by complexation with DOC. Alternatively, this may reflect the loss of dissolved Hg(II) at high DOC levels, due to dissolved humic precipitation as a result of sample acidification. This latter possibility would thus represent a methodological artifact and cause an underestimation of Hg(II) with increasing DOC. It is unknown if this is the case, but further experiments with various sequential extraction regimes are warranted.

DOC has also been shown to be able to abiotically reduce Hg(II) to dissolved gaseous elemental Hg^0 (Allard & Arsenie 1991, Matthiessen 1998). The extent to which this happens in CRS pore-water or overlying water is unknown, and quantifying this reaction was not part of the current investigation. However, this abiotic Hg-transformation is a potentially important step in the overall cycling of Hg in the CRS, and an assessment of this reaction should be considered in future CRS research.

6.3.3.9 Pore-Water Anions

The high pore-water Cl^- concentration in the wetlands, agricultural drains and CS **(Figs. 59-60)** reflects the arid nature of the terminal river basin, were high evaporation rates concentrate salts. Elevated Cl^- in these areas may reduce the availability of Hg(II) for methylation, by shifting dominant Hg speciation from neutral inorganic complexes (i.e. $HgCl_2$, $Hg(OH)_2$, and HgClOH) at low Cl^- concentrations, to charged $HgCl_3^-/HgCl_4^{2-}$ at high salinity (Barkay et al. 1997). As discussed above, the neutral Hg(II) species are thought to be more available for methylation due to their ability to readily to cross microbial cell membranes. Thus, we postulate that the strong shift in Cl- ion concentration, going from river to wetland sediments, partially accounts for the comparatively low k_{meth} and M/D ratios often observed for the downstream locations. The Cl^- concentration at SC was only about half as high in October 1999 (ca. 10 mM), compared with October 1998 and June 1999 (ca. 20 mM). Interestingly, a previous report indicated that an appreciable shift from particle-bound to dissolved Hg at Cl^- levels equal to or above 20mM (Wang et al. 1991). Further, Hg-speciation modeling of that data indicated that there was a substantial increase in dissolved charged Hg-Cl complexes (e.g. $HgCl_3^-$, $HgCl_4^{2-}$) and a corresponding decrease in neutral complexes (e.g. $HgCl_2^0$, $Hg(OH)_2^0$) as Cl^- concentration increased from 10 mM to 20 mM. Assuming that charged Hg-Cl complex are less able to cross the bacterial cell wall than are neutral complexes, the lower pore-water Cl^- concentrations during October 1999 may partially explain the higher k_{meth} values of observed at that time, relative to June 1999, for the wetland site **(Fig. 11)**. This would be akin to a partial the partial inhibition of Hg-methylation at high sulfide levels, discussed above **(Section 6.3.3.1)**. In addition to these direct affects on Hg(II) speciation, Cl^- ion concentration can also impact the solid/aqueous partitioning of both Hg(II) and MeHg (Yin et al. 1997a, Yin et al. 1996). As evidence, the addition of Cl^- to wetland site SP sediment clearly stimulated MeHg degradation in controlled laboratory experiments **(Section 6.3.5, Fig. 67f)**.

Pore-water SO_4^{2-} clearly plays an important role in MeHg production, as it is the electron acceptor for sulfate reducing bacteria, who's activity may be SO_4^{2-} limited in freshwater systems (Capone & Kiene 1988). Increasing SO_4^{2-} concentrations thus lead to increasing rates of sulfate reduction, and presumably MeHg production. This is only true up to the point where increasing levels of reduce-S end-products begin to inhibit Hg(II) methylation (see **Section 6.3.3.1**). At some sites (e.g. F2 and CS), rates of sulfate reduction were low **(Fig. 26a)** although SO_4^{2-}

concentrations were high **(Fig. 59b)**, due to oxidizing sediment conditions **(Fig. 47a)** that were unfavorable to these bacteria. Concentrations of SO_4^{2-} were low (< 100 μM) in most October 1998 samples, which likely reflected SO_4^{2-} depletion relative to original in-situ levels, which occurred during sediment storage. Surface sediment (0-4 cm) concentrations were significantly higher in June 1999 samples **(Fig. 60b)**, where SO_4^{2-} exhibited the classic depletion with depth at three of the four sites. In wetlands site SC, a less typical mid-depth (4-8 cm) minimum was observed, with increasing concentrations below this zone.

The high PO_4^{3-} concentrations in the wetlands and agricultural **(Figs. 59c-60c)** drains reflects the organic rich conditions of these zones, as this nutrient is sequestered by plants and subsequently released during organic matter decay. Aside from its importance in overall bacterial growth, there were no apparent relationships between PO_4^{3-} levels and Hg-dynamics in the CRS. A similar conclusion was reached regarding Hg-cycling in the Florida Everglades (Gilmour et al. 1998b, Marvin-DiPasquale & Oremland 1998).

Like PO_4^{3-}, NO_3^- can be an important nutrient in overall bacterial growth, and serves as the electron acceptor for microbial denitrification (NO_3^- reduction to N_2). High NO_3^- levels may partially inhibit sulfate reduction and methanogenesis, as denitrifiying bacteria compete with these other bacterial groups for organic substrates. In this way, NO_3^- may have a secondary affect on Hg-cycling (Marvin-DiPasquale & Oremland 1998). However, there were no readily apparent relationships between NO_3^- levels and Hg-dynamics in the CRS. There were few striking among-site differences in pore-water NO_3^-, apart from the elevated levels in oxidized surface sediments (e.g. F2 and CS) **(Fig. 59d)** and at depth at the SC wetland site **(Fig. 60d)**. Elevated NO_3^- likely reflects zones of active microbial nitrification (NH_4^+ oxidation to NO_3^-), a process typically coupled to denitrification (Bodelier et al. 1996). While common in oxidized surface sediment, the suggestion of nitrification at 12-16 cm depth in wetland site SC (June 1999) was curious. There was a corresponding increase in sediment E_h **(Fig. 48a)**, elevated levels of SO_4^{2-}, PO_4^{3-} and DOC **(Figs. 60b,c and 57c)**, and a decrease in reduced-S pools **(Figs. 28a and 29b)** at this horizon. These observations indicate that the 12-16 cm layer at SC was qualitatively different from those above. This may reflect the influence of the local emergent macrophyte root zone, or possibly ground water influx. Interestingly, MeHg concentration **(Fig. 7c)** and production rate **(Fig. 19a)** were also highest at this depth. These profiles illustrate how within-site variations in geochemistry and microbiology may strongly influence the depth of the dominant MeHg production zone.

6.3.4 Methylmercury Degradation

Gross MeHg degradation is a primary control on net MeHg production (Korthals & Winfrey 1987, Matilainen et al. 1991). It is important then to determine what factors mediate MeHg degradation in the CRS. In contrast to Hg-methylation, which is primarily mediated by sulfate reducing bacteria, MeHg degradation may be carried out by sulfate reducers, methanogens, aerobes, and possibly other anaerobic bacterial groups (Marvin-DiPasquale & Oremland 1998, Oremland et al. 1991). Increased rates of anaerobic metabolism in the organic rich wetlands and agricultural drains leads to increased MeHg degradation. Specifically, k_{deg} values were correlated with methanogenesis ($r^2 = 0.43$), as well as with sediment percent carbon ($r^2 = 0.63$) **(Figs. 61a-b)**. A similar relationship between MeHg decradation and sediment organic content was previously noted in oligotrophic lake sediments (Korthals & Winfrey 1987).

While increased levels of reduced-S can inhibit Hg(II)-methylation **(Section 6.3.3.1)**, this was clearly not the case with respect to MeHg degradation, as k_{deg} values were also positively correlated with pore-water sulfide ($r^2 = 0.39$) and whole sediment reduced-S ($r^2 = 0.57$) **(Figs. 61c-d)**. The strong spatial trend of higher k_{deg} values in wetland and agricultural drain sites was reflected in a number of other significant relationships, such as the negative linear relationship between k_{deg} and sediment grain size ($r^2 = 0.63$, $P < 0.005$), and the closely related positive relationship between k_{deg} and sediment water content ($r^2 = 0.68$, $P < 0.001$) (Oct. 1998 data, not shown). Further, significant positive relationships were also noted between in-situ MeHg degradation rates and sediment Mn and Se concentrations **(Fig. 62)**. Clearly, many of these relationships simply represent the natural among-site distribution of covarying parameters (e.g. grain size, % water content, trace-metal concentrations, etc...), and not a true cause and effect relationship between these measures and MeHg degradation dynamics. It is difficult to tease apart variables that truly control microbial processes, from those that simply covary with the controlling variable. Without evidence to the contrary, we conclude that it is primarily the higher overall rates of anaerobic microbial metabolism that is responsible for the increased rates of MeHg degradation in the downstream regions. Further, this increased MeHg degradation represents a primary factor limiting net MeHg production in the wetlands.

In addition to these regional aspects, the importance of MeHg degradation as a control on net MeHg production is illustrated in the vertical depth profiles. As noted above, MeHg production typically exhibited a sub-surface rate maximum **(Figs. 19a,b)** which was driven to a large degree by the vertical trend in bioavailable Hg(II) **(Figs. 8a,b)** and/or site-specific methylation potentials (i.e. k_{meth} values, **Figs. 13a,b**). In contrast, maximum rates of MeHg degradation were often observed in the top-most depth interval **(Figs. 13c,d and 19c,d)**. Thus, MeHg diffusion across the sediment water interface may be limited in some locations due to active demethylation zones located above the horizon of maximal production.

A positive correlation between the degree of mercury contamination (as Hg_t) and k_{deg}'s was apparent in the October 1998 data **(Fig. 63)**. A similar trend was seen in an earlier (three-site) Carson River study (Oremland et al. 1995) and in a comparison among and within different ecosystems (Marvin-DiPasquale et al. 2000). This would imply that the activity of the MeHg degrading microbial community was enhanced in response to increasing mercury contamination. This relationship was more pronounced in the wetlands than in all other sites (combined), indicating that MeHg degrading bacteria in the wetland may be particularly responsive to mercury contamination, which may further explain the low net MeHg production in the wetland areas. However, no similar positive relationship between k_{deg} and Hg_t (and/or MeHg) was evident in June or October 1999 data. Thus, the relationship observed in the October 1998 data was either spurious or the trend during the later dates was obscured by other factors that exert more influence on microbial MeHg degradation.

For all three sampling dates, 75-100% of the ^{14}C-MeHg degradation end-product was recovered as $^{14}CO_2$ in all but two cases (data not shown). Even for these exceptions (LB and F2, October 1998) % $^{14}CO_2$ was still > 20%. This result indicates that oxidative demethylation (OD) is the primary pathway for MeHg degradation throughout the CRS. This may have significant implications on Hg cycling for the Carson River system. It has been previously speculated that the mercury species end-product of MeHg degradation via OD is Hg(II) (Marvin-DiPasquale & Oremland 1998). If true, than the effective residence time for mercury in the sediment is enhanced under conditions favoring OD, as Hg(II) can be readily remethylated or reacted with

reduced-S. This prolonged residence time would lead to a higher probability that mercury will be incorporation into the local food chain. This is in contrast to the situation where *mer*-detoxification dominates MeHg degradation, as would be indicated if all or most of the ^{14}C-gaseous end-product were $^{14}CH_4$ (Marvin-DiPasquale et al. 2000). The *mer*-pathway results in the formation of volatile Hg^0 (Robinson & Tuovinen 1984) that may more readily evade from the system. While we did not evaluate Hg^0 production from either Hg(II) or MeHg in the current project, methods are currently being developed to quantify both processes. Such measurements in the future will help fill gaps in our understanding of Hg-transformations in the CRS.

It has recently been suggested that the $^{14}CO2$ production, observed from ^{14}C-MeHg degradation assays, actually reflects the anaerobic oxidation of $^{14}CH_4$ that was previously released from ^{14}C-MeHg via *mer*-detoxification (Pak & Bartha 1998). We reject this hypothesis base on direct evidence from the CRS. In two-day incubation experiments of microbial methane oxidation no $^{14}CO_2$ production was detected, at any site, in $^{14}CH_4$ amended samples, with the sole exception of site SP **(Appendix II)**. Even in this case, the rate constant for MO was extremely small (0.0009 d^{-1}) and could not account for the more than 90% $^{14}CO_2$ end-product measured for MeHg degradation at this site. Further, the site F1 time course experiment showed a nearly constant % $^{14}CO_2$ end-product ($\approx$ 60%) fraction, after a small initial increase from 40%, throughout the five-day incubation **(Fig. 16c)**. If *mer*-detoxification was the sole MeHg degradation pathway, we would have expected to see no $^{14}CO_2$ produced (only $^{14}CH_4$). If both *mer*-detoxification and OD were equally important processes, we would expect the % $^{14}CO_2$ decrease over time, as the contribution of $^{14}CH_4$ from *mer*-detoxification became an increasingly larger fraction of the total ^{14}C-end-product pool (Marvin-DiPasquale et al. 2000). The fact that the % $^{14}CO_2$ remained nearly constant throughout the incubation suggests that OD was the primary (if not sole) degradation pathway.

A primary factor that will undoubtedly influence the rate of MeHg degradation is the relative availability of MeHg to the microbial community, a situation analogous to the availability of Hg(II) to the methylating bacteria. For the purposes of calculating in situ MeHg degradation rates, we assumed that all of the whole sediment MeHg measured was available for degradation **(Section 4.3)**. However, MeHg associated with various fractions of the sediment matrix (i.e. aqueous, organically complexed, particle bound, etc...) may very well have different availabilities to MeHg-degrading bacteria. Thus, determining how in-situ MeHg is actually distributed in the sediment is important in better refining our understanding of the MeHg degradation processes. Towards this end, we amended sediment from all sites with the ^{14}C-MeHg analog, and then subjected these samples to a sequential extractions procedure to determine how the radiotracer distributed itself in the sediment matrix **(Section 4.4.3)**. The overall spatial trend indicated that sites upstream of Lahontan Dam (e.g. LB → LN) had most of the extractable ^{14}C-MeHg associated with the readily exchangeable (acid-extractable) and dissolved (water-extractable) fractions, and much less associated with the organic (base-extractable) fraction **(Fig. 64)**. Downstream of Lahontan Dam, particularly in the agricultural drain sites (CL and SS) and wetland sites (LL, SP, and SC), the acid-extractable fraction decreased and a much larger percent of ^{14}C-MeHg was associated with the base-extractable fraction. The hypersaline playa region (site CS) was unique in that majority of the extractable radiolabel was associated with the water-extractable fraction. We further examined the results of this MeHg extraction experiment by plotting the percent ^{14}C-MeHg recovered against site-specific reduced-S (i.e. AVS) or organic content (i.e. as LOI) **(Fig. 65)**. Both linear and non-linear curve-fitting approaches were used to find meaningful relationships in the data. The

percentage of ^{14}C-MeHg recovered decreased for both water-extractable and acid-extractable fractions with increasing organic content **(Figs. 65b,d)**. The percent recovery via acid-extraction also decreased with increasing AVS **(Fig. 65c)**. In contrast, ^{14}C-MeHg recovery via base-extraction increased with both LOI and AVS **(Figs. 65e,f)**. Thus not unexpectedly, an increasing fraction of the MeHg is bound to base-extractable organics in the spatial transition from the organic poor river sites to organic (and AVS) rich wetland sites. We could assume that the combination of the water, weak-acid and weak-base extractable fractions represent the majority of the MeHg that may be readily degraded by bacteria, and that the balance is primarily not available for degradation. In general, the amount of non-extractable ^{14}C-MeHg was larger in the downstream drains and wetlands than in the upstream river and reservoir **(Fig. 64)**, and there was a clear increase in the non-extractable pool size was associated with increasing organic content **(Fig. 65h)**. However, recalling that k_{deg} was generally highest in the drains and wetland sites, this would suggest that while a larger fraction of total MeHg may be available for degradation in the upstream sites, the rate of degradation of available MeHg is greatest in the wetlands, presumably due to increased rates of general microbial metabolism. Thus, based on these experimental results, much of the in-situ MeHg may not be readily available for degradation, which suggests that degradation rates calculated using the total MeHg value may overestimate the actual in-situ rate.

6.3.5 Multi-Factor Comparisons: Controlled Experiments

It is often difficult with field data to directly assess the which factors mediate a particular microbial process, as multiple controlling variables potentially come into play, which vary in both time and space. Laboratory experiments are thus useful in limiting the number of variables and as a way of comparing the relative effect of a few key parameters on the microbial process of interest. We took this approach with respect to determining which factors (dissolved O_2, SO_4^{2-}, S^{2-}, Cl^- or solid-phase FeS) had the greatest influence on MeHg production and degradation rates in three representative CRS sediments (river site F1, drain site CL, wetland site SC). Potential rates of MeHg production in unamended anoxic controls fell within a fairly narrow range (0.75 – 1.06 ng•g wet sed^{-1}•d^{-1}) and followed the spatial trend CL < SP < F1 **(Fig. 66a)**. Potential rates of MeHg degradation in the control samples increased in the downstream direction (F1 < CL < SP; range = 1.7 – 11.0 ng•g wet sed^{-1}•d^{-1}) **(Fig. 66b)**. These spatial trends generally followed those previously observed in the field data **(Figs. 11-12)**. Results for treatment amended samples were expressed as the percent change in either MeHg production or degradation relative to these unamended controls **(Fig. 67)**. Observed treatment effects were not consistent among sites. Hg-methylation was significantly inhibited by FeS, S^{2-}, and O_2 at sites F1 and CL, while the effect of added Cl^- and SO_4^{2-} was minor **(Figs. 67a,b)**. In contrast, Hg-methylation at wetland site SP was significantly stimulated by SO_4^{2-} while the effect of all other treatments was minor **(Fig. 67c)**. MeHg degradation was also similar at F1 and CL, such that rates were significantly stimulated by SO_4^{2-} and FeS and generally inhibited by Cl^-, S^{2-}, and O_2 **(Figs. 67d,e)**. Wetland site SP again showed the mirror image, with degradation rates stimulated by Cl^-, S^{2-}, and O_2, and slightly inhibited by SO_4^{2-} and FeS **(Fig. 67f)**. Thus, microbiological and/or geochemical factors that controlled Hg-transformations appeared similar at sites F1 and CL, but quite different in the wetland site SP. This may partially explain why the agricultural

drains often exhibited the high k_{meth} values and in-situ rates of MeHg production, similar to upstream river sites.

A scenario consistent with the above discussion regarding controls on Hg-transformations can largely explain the results of this controlled amendment experiment. High levels of pore-water S^{2-} can inhibit Hg-methylation in some cases (e.g. sites F1 and CL), due the formation of dissolved charged Hg-S complexes that do not readily cross the cell membrane of methylating bacteria **(Section 6.3.3.1)**. The observed affect of such a S^{2-} amendment may have been mitigated in the organic rich wetland (site SP) if the in-situ pore-water S^{2-} concentration was already high (unknown), as is typical of wetland sediment. The inhibition of Hg-methylation at F1 and CL was likely linked to the binding of the $^{203}Hg(II)$ substrate to the FeS particle surface. Competition with dissolved organic matter binding to the same FeS particle surface may have mitigated of this process in the wetlands site. The O_2 treatment likely inhibited strictly anaerobic SRB, and thus Hg-methylation, at site F1 and CL. However, if pore-water S^{2-} was elevated at site SP, as suspected, then most or all of the O_2 spike would have been readily consumed in the oxidation of S^{2-} back to SO_4^{-2}. This increase in SO_4^{-2} would subsequently stimulate microbial SR and potentially Hg-methylation. There was evidence of this as there was a slight increase in amount of Hg-methylated, relative to the control, for the O_2 treatment at site SP **(Fig. 67c).** Further, the stimulation of methylation due to the direct addition of SO_4^{-2} at this same site confirms that microbial SR was SO_4^{-2} limited in the wetland sample. Sulfate reducers were apparently not similarly SO_4^{-2} limited at sites F1 and CL, as suggested by the lack of significant stimulation of Hg-methylation. Alternatively, SR was stimulated by the addition of SO_4^{-2} at F1 and CL, but the corresponding increase in net Hg-methylation was not observed due to a simultaneous increase in MeHg-degradation also associated with SO_4^{-2} addition at F1 and CL **(Figs. 67d,e).** It has been shown that SRB as well as methanogens can degrade MeHg (Oremland et al. 1991), although, much less is known about the abiotic geochemical conditions that regulate this process. The inhibition of MeHg degradation by S^{2-} in F1 and CL sediments may be linked to the formation of charged MeHg-S complexes (akin to the charged Hg-S complexes) that limits the movement of this molecule across the membrane of MeHg-degrading bacteria. However, the opposite effect of added S^{2-} in the wetlands site (SP) is puzzling, as is the muted and/or slightly inhibitory effect of added SO_4^{-2} at SP. An alternative possibility is that the S^{2-} amendment level used at sites F1 and CL (ca. 2 mM) was inhibitory to the resident MeHg-degrading bacteria, but not to the bacteria at site SP, which are likely acclimated to higher S^{2-} levels. Further, if anaerobic SRB are important MeHg-degrading bacteria in the CRS, then the inhibition of degradation at F1 and CL by added O_2 makes sense. Again, if site SP had high S^{2-} concentrations to begin with, then the O_2 addition at this would have been consumed in the reoxidation of S^{2-} to SO_4^{-2}, and the effect would be to stimulate MeHg-degradation by stimulating SR. The stimulation of MeHg-degradation with solid-phase FeS at sites F1 and CL, and with dissolved Cl^- at site SP, suggests that various reactions can occur which involve MeHg-Cl^- complex formation, changes in the solid-phase adsorption/desorption kinetics of MeHg, and possible MeHg interactions with and dissolved and particulate organic matter. All of these processes will impact the availability of MeHg for degradation. However, the specific mechanisms behind these abiotic controls are poorly understood at this time.

6.4 Regional Aspects of the Benthic Mercury Cycling Within the CRS

We have thus far outlined the spatial trends in Hg-species concentrations and transformation rates, and have discusses how contributing factors of contamination, microbiology, and physical geochemistry interact to regulate Hg-dynamics. We now take a broad view of this information to draw conclusions about benthic Hg-cycling and general remediation strategies for specific regions of the CRS.

6.4.1 Upstream: The Carson River

River sediments appear particularly conducive to MeHg production due to active sulfate reduction, low reduced-S and comparatively low MeHg degradation rates. This, in addition to areas of extremely high Hg(II) concentrations, leads to very high localized rates of MeHg production, particularly in the Fort Churchill region. Such "hot spots" may be an important source of MeHg to areas downstream, although, oxidized surface sediment conditions in sandy sections of the river likely mitigate the flux of MeHg across the sediment/water interface somewhat. Direct flux measurements, or more depth discrete sampling of Hg-species in the surface sediment, would be needed to determine the relative importance of these areas as sources of MeHg to the water column. Localized remediation efforts may prove effective. However, those involving sediment removal risk exposing deeper zones containing high levels of MeHg and bioavailable Hg(II), which are slowly being buried and may be semi-effectively trapped, due to surface sediment redox conditions. Disturbing this zone could potentially worsen downstream contamination, at least in the short term.

6.4.2 Vertical Bank Sediment

Eroding bank material had much lower MeHg production rates compared to local sediments in the Fort Churchill area in June 1999. This was presumably due to both comparatively low acid-extractable Hg(II) concentrations and to oxic sediment conditions, unfavorable to anaerobic methylating bacteria. The dry conditions encountered during October 1999 were also not conducive to the bacterial production of MeHg. These limited results indicate that the bank sediment sampled was a minor source of MeHg to the immediate water column. However, more detailed spatial sampling would be needed to fully evaluate the potential for Hg-methylation associated with this substrate. It is likely that the consolidated bank material sampled during June 1999 was more representative of naturally occurring sediment than of historic mining debris. However, subsequent sampling during October 1999 showed extremely high concentrations of both Hg_t (19 ppm) and Hg(II) (780 ppb) in loose bank material left behind after the high water had subsided **(Fig. 9)**. Thus, a significant amount of microbially available Hg(II) may be transported downstream during episodic high erosion periods (Hoffman & Taylor 1998). Modeling efforts are currently underway to determine if this material is a significant source of inorganic mercury to downstream areas (Carroll et al. 2000, Warwick & James 2000a, Warwick & James 2000b, Warwick & James 2000c). If this is the case, bank erosion abatement may be an effective remediation strategy. Alternatively, the effective mitigation of high water flows, via the construction of upsteam reservoirs in the Sierra Nevada, may significantly limit

erosion and subsequently the downstream transport of methylatable-Hg (J. Warwick, pers. comm.).

6.4.3 Lahontan Reservoir

The Lahontan Reservoir may retain as much as 80 to 90% of the total Hg originating from the upstream point sources (Diamond 1999, Hoffman & Taylor 1998). Estimates suggest that the Reservoir contains over 300,000 kg of Hg in sediments, with over half of this load in the delta and deep channel regions (Miller et al. 1995). The Reservoir is thus a potentially important zone of MeHg production. An earlier investigation concluded that the contaminated stretch of river above the reservoir is a net source of MeHg, and that the Reservoir is a net MeHg sink (Ecology and Environment 1998). This conclusion was based on a) lower water-column MeHg concentrations in the Reservoir than in the upstream river, b) a mercury mass balance model, which demonstrated that water-column MeHg concentrations in the Reservoir could be maintained by the flux of MeHg originating upstream (Diamond 1999), and c) evidence of significant MeHg production in the upstream river during low-flow, warm, anoxic periods. One possible implication of these conclusions is that the Reservoir sediments are not a significant source of MeHg to the water column. This view seems inconsistent with the data presented in the current report that shows not only very high Hg_t, acid-extractable Hg(II), and MeHg levels in delta (LS) sediments, but also very high potentials for MeHg production **(Fig. 11)**. One possible explanation for this apparent inconsistency is that while there might be significant MeHg production within the sediment, very little of it is crossing the sediment water interface. While it is doubtful that sediment/water MeHg flux would be minor in the face of such high MeHg concentrations and production rates, direct flux measurements are needed to assess this possibility. A second possibility is that the sediments are a significant source of MeHg to the water column, but processes which subsequently degrade MeHg (e.g. photo- and microbial degradation) in the water column are also significant and result in the overall model results. Again, direct measurements of these specific water-column processes are needed.

While the reservoir undoubtedly acts as a large catchment area for particles, its ultimate effect may be to only slow the progression of Hg_t and MeHg downstream (Hoffman & Taylor 1998), and the view of the reservoir as a net sink for MeHg is really one of short versus long time scales. Since the southern delta appears to still be accumulating particle-bound Hg from upstream, as suggested by the Hg_t profile **(Fig. 7a)**, increasing loads over time will potentially increase the importance of this region as a MeHg source. Subsequently, strategies that reduce the total amount of mercury entering the delta region be prioritized.

More focused studies of the Lahonton Reservoir are recommended. These studies should include the above-mentioned measurements of sediment/water flux of Hg-species, and water column Hg-transformation processes of MeHg photodegradation, microbial degradation, and Hg(II) photoreduction to Hg^0. Since our sampling of this important catchment/transition zone was limited to two nearshore sites at the either end, it is unclear if the observed spatial trends in benthic Hg-transformation rates are representative of deeper channel and mid-Reservoir regions. Thus, the spatial network of these potential rate measurements should also be expanded.

6.4.4 Agricultural Drains

Agricultural drainage canals represent an important source of Hg_t and MeHg to the larger wetland areas (Hallock & Hallock 1993). High MeHg production rates were driven by high levels of Hg(II) available for methylation, even though corresponding demethylation rates and solid phase reduced-S pools were also high. This may be due to elevated solid phase and dissolved Fe and Mn concentrations, which can scavenge dissolved sulfide and helps to keep the Hg-S complexes in a form that is most readily methylated (e.g. as neutral HgS^0). It is possible that localized mercury clean up efforts of the agricultural drains may be beneficial, but again, any dredging of these canals may also remobilize buried mercury and worsen the situation in the wetlands over the short term. However, if agricultural drains are indeed a primary source of Hg_t and MeHg to the wetlands, then site-specific remediation of these areas, and other "hot spots", may prove more cost effective than system-wide remediation efforts.

6.4.5 Wetlands

Rates of MeHg production in the wetland sediments were typically lower than rates at upstream "hot-spots" (e.g. F1 and LS) and the drainage canals (CL and SS) **(Fig. 17)**. This was primarily due to lower acid-extractable Hg(II) concentration, high levels of reduced-S, and high rates MeHg degradation. However, the importance of wetland MeHg production should not be underestimated. MeHg flux across the sediment /water interface may be enhanced in this region, due to reducing surface sediment conditions, compared to upstream sites which often exhibit oxidized surface sediments. The bioturbation activity of benthic infauna in the wetlands may further enhance MeHg flux to the water column (Gagnon et al. 1996). The current research program does not directly assess mercury transfer to the resident biota, although, bioaccumulation is clearly taking place in the wetlands food web, as evidenced from earlier reports demonstrating high levels of mercury in numerous CRS wetland plant and animal species (Hallock & Hallock 1993, Hoffman et al. 1989, Tuttle & Thodal 1997). Considering the large spatial extent, and the key role wetlands play in providing critical habitat to a complex food web, the importance of this region as a critical area for mercury bioaccumulation is obvious. Any potential remediation effort in the wetlands would likely be costly and difficult, due to their complex and spatially extensive nature of this. Efforts focused on limiting further mercury input to the wetlands may be the best strategy. It is currently unknown how long it would take for a decrease in Hg input to the wetlands to translate into a measurable decrease in wildlife. However, remediation focused on the drains, which empty into the wetlands, may be the most effective near-term focus for the future.

6.4.6 Carson Sink – Playa Region

MeHg production in the Carson Sink was low, primarily because there was little bioavailable "acid-extractable" Hg(II). However, only one playa region site was sampled. Our findings may have been markedly different if Hg(II) was found to be abundant, as this region appears to be conducive to active MeHg production. Microbial sulfate reduction was active, while reduced-S species and MeHg degradation potentials (k_{deg} values) were low relative to other sampling sites. Conversely, MeHg flux to the overlying water column would be mitigated to the

extent surface sediment is oxidized. More extensive spatial sampling of the playa region would be needed to determine its importance as a zone of net MeHg production. While less species-diverse than the wetlands, large fish and piscivorous birds (cormorants and pelicans) were bountifully evident in this region during our field sampling. Thus, if localized "hot spots" of MeHg production do exist, these species would be most affected. No remediation recommendations are offered for the playa region at this time.

6.5 Seasonal Aspects of the Benthic Mercury Cycling Within the CRS

The comparison of the June and October 1999 data sets give a snapshot of seasonal (high flow/low flow) differences in Hg-transformation processes. The most striking difference among these two dates is the much higher k_{meth} values observed in wetlands and agricultural drains observed in October 1999 compared to the June sampling **(Fig. 11)**. While overall higher k_{meth} values might have been predicted for October, due to the lower $^{203}Hg(II)$ amendment level used **(Section 6.2.2)**, this trend was not consistent among sites. The fact that k_{meth} values were similar among dates at a majority of site the upstream of Lahontan Dam, but higher downstream of the dam in October 1999, suggests a biogeochemical change in the system downstream. Temperature was ruled out as a driving parameter, because among-date differences were generally small (3-5 ^{o}C) and the June sampling actually had the higher temperature in the downstream regions **(Appendix II)**. A number of other factors may have accounted for the seasonal difference in k_{meth}. First, MeHg-degradation rates (as k_{deg}) were lower in the downstream region during October 1999 **(Fig. 12)**. Second, microbial SR was lower in October 1999 in the one wetland sited examined (SC), and the corresponding pore-water S^{2-} and bulk sediment AVS was also lower in surface (0-4 cm) sediment **(Appendix II)**. The higher SR rates during June reflect the higher wetland temperatures, but also likely reflect the fact that a large quantity of fresh (labile) material was deposited to the sediment surface during the high flow period. As much of this labile organic matter is consumed over the summer, rates of SR begin to slow and levels of reduced-S constituents also begin to drop in surface sediments. This leads to a lessening of the inhibitory affect of reduced-S on Hg-methylation, which results in increased MeHg production rates. The generally higher rates of anaerobic metabolism in June 1999, compared to October 1999, were also reflected in the CH_4 production rate profiles **(Figs. 31b,c).** Finally, the third factor contributing to higher Hg-methylation rates in October 1999, relative to June, may be partially related to differences in porewater Cl^- concentration, which was higher during June. As discussed above **(Section 6.3.3.9)**, it is right around the 10 mM to 20 mM Cl- transition that there is a substantial shift from neutral to charged Hg-Cl complexes. Akin to the inhibition of Hg-methylation by high levels of sulfide, these charged complexes are less likely to cross the bacterial cell wall and become methylated. Finally, the possibility cannot be excluded that small-scale difference in specific sampling locations among dates may have contributed to the observed seasonal difference in Hg-transformation. Thus, the observed seasonal differences in Hg-methylation rates may reflect a combination of the reasons discussed above.

While temperature did not seem to explain the seasonal differences described above, it is most certainly a key parameter mediating Hg-transformation rates in this and all systems. The in-situ temperatures observed in this study spanned only a moderate range (10.0 - 17.5 ^{o}C). From

the perspective of Hg-model development however, it is desirable to know how these processes are affected over a more comprehensive temperature range. Thus, controlled experiments were undertaken to assess this at three of the five major ecozones, namely the upstream river (site F1), an agricultural drain (site CL) and a wetland (site SP). Not surprisingly, rates of both MeHg production and degradation increased throughout the applied temperature range (6 to 27 °C) at all sites **(Figs. 68a,b)**. As is also typical of microbial reaction rates, the increase was non-linear, but the two opposing processes were generally proportional so that the resulting M/D ratio stayed approximately constant in CL and SP sediment **(Fig. 68c)**. Site F1 sediment appeared to have a modest (but statistitically non-significant) optimum M/D ratio at 20 °C. Two common measures used to compare the temperature response for a given microbial process are to calculate either the activation energy (E_a) or the Q_{10}. These two parameters are related **(Section 4.4.4)** and subsequently follow the same general trend. The E_a is derived from the linear slope of the Arrhenius plots **(Figs. 69a,b)**. Site specific Q_{10} values are then calculated from the resulting Arrhenius model fit to the transformed rate and temperature data. Q_{10} values of approximately 2.0 are common for microbial reactions, and this simply means that the given reaction rate doubles for a 10 °C increase in temperature. The temperature response for Hg-methylation was high and similar at sites F1 and SP (Q_{10} = 2.4 to 2.5), and low at the agricultural drain site CL (Q_{10} = 1.5). Likewise, the temperature response for MeHg-degradation was similar at sites F1 and SP (Q_{10} = 1.9 to 2.1), and low at the agricultural drain site CL (Q_{10} = 1.6). It is unclear why these spatial differences in temperature response exist, but are likely related to differences in microbial populations. These results indicate that microbial Hg-transformations in both the river and wetland sediment respond more strongly than the agricultural drain sediment to increased temperature. Further, the temperature response of Hg-methylation is stronger than that for MeHg-degradation in the wetland and river sites, but not so in the agricultural drain. This implies that, all other factors being equal, Hg-methylation rates in the river and wetlands should be greatest during the warmest part of the year due to a temperature-dependent uncoupling of MeHg production and degradation.

7. CONCLUSION

Site-specific MeHg production rates in the CRS are mediated by the interplay between the extent of Hg-contamination, benthic-microbiological processes and physical/geochemical sediment and hydrodynamic characteristics. High MeHg production rates were primarily driven by high concentrations of bioavailable Hg(II), whereas low rates were limited by a combination of low levels of bioavailable Hg(II), low Hg-methylation potentials (i.e. rate constants), and/or high rates of gross MeHg degradation (particularly in the wetlands). The result is a complex and heterogeneous mercury cycle that may be understood in general, and sometimes incomplete, terms. In the current project we have detailed both benthic-mercury dynamics and ancillary biogeochemical factors that are important in regulating the CRS mercury cycle. This is the first such extensive spatial study of directly measured microbial benthic Hg-transformations in the CRS. Important preliminary findings include a) localized high rates of MeHg production in the upstream river and reservoir sediments and comparatively low rates in wetland sediments b) low rates of MeHg degradation in the upstream river sediments and high rates in the wetlands, c) gross MeHg degradation strongly impacting net MeHg production, d) microbial sulfate reduction and resulting reduced-S concentrations mediating Hg-transformations, e) oxidative

demethylation dominanting MeHg degradation pathway in the CRS, f) agricultural drains potentially serving as an important source of mercury to the larger wetland areas, and g) distinct spatial trends in microbial Hg-dynamics reflecting the immediate environmental conditions with respect to organic matter, sediment redox, pore-water anions, and overall anaerobic microbial activity. We conclude that any remediation plan that is based solely on lowering Hg_t concentrations, without careful consideration of biogeochemical and microbiological Hg-cycling dynamics and Hg-bioavailability, is likely to prove ineffective in the long term.

8. ACKNOWLEDGEMENTS

This research was funded by U.S. EPA - Region IX (Interagency Agreement #DW-14955409-01-0). The authors wish to thank W. Praskins (USEPA, Region IX) for assistance with the Field Plan development; M. Olson, J. DeWild, and S. Olund (USGS, Madison, WI) for mercury speciation analysis; M. Hines and E. Bailey (Univ. of AK, Anchorage) for bioavailable Hg(II) analysis via the *mer-lux* biosensor; C. Kendall and S. Silva for particulate carbon analysis; A. Mlodnosky (USGS, Salinas, CA) for sediment grain size analysis; S. Hoeft, R. Huddleston, B. Topping, C. McGowan (USGS, Menlo Park, CA) for technical assistance; W. Henry (US Fish and Wildlife Service, Fallon, NV), R. Hoffman and K. Thomas (USGS, Carson City, NV) for field and logistical support; and Larry Miller (USGS, Menlo Park, CA) technical guidance and quality assurance monitoring.

9. REFERENCES

Allard B, Arsenie I (1991) Abiotic reduction of mercury by humic substances in aquatic system - An Important process for the mercury cycle. Water Air Soil Pollut. 56:457-464

Barkay T, Gillman M, Turner RR (1997) Effects of dissolved organic carbon and salinity on bioavailability of mercury. Appl. Environ. Microbiol. 63:4267-4271

Benoit JM, Gilmour CC, Mason RP (2001a) Aspects of bioavailability of mercury for methylation in pure cultures of Desulfobulbus propionicus (1pr3). Appl. Environ. Microbiol. 67:51-58

Benoit JM, Gilmour CC, Mason RP (2001b) The influence of sulfide on solid-phase mercury bioavailability for methylation by pure cultures of *Desulfobulbus propionicus* (1pr3). Environ. Sci. Technol. 35:127-132

Benoit JM, Gilmour CC, Mason RP, Heyes A (1999) Sulfide controls on mercury speciation and bioavailability to methylating bacteria in sediment porewaters. Environ. Sci. Technol. 33:951-957

Benoit JM, Gilmour CC, Mason RP, Riedel GS, Riedel GF (1998) Behavior of mercury in the Patuxent River estuary. Biogeochem. 40:249-265

Bloom N (1989) Determination of picogram levels of methylmercury by aqueous phase ethylation, followed by cryogenic gas chromatography with cold vapour atomic fluorescence detection. Can. J. Fish. Aquati. Sci. 46:1131-1140

Bodelier PLE, Libochant JA, Blom CWPM, Laanbroek HJ (1996) Dynamics of nitrification and denitrification in root-oxygenated sediments and adaptation of ammonia-oxidizing bacteria to low-oxygen or anoxic habitats. Appl. Environ. Microbiol. 62:4100-4107

Bonzongo JC, Heim KJ, Warwick JJ, Lyons WB (1996a) Mercury levels in surface waters of the Carson River-Lahontan Reservoir system, Nevada: Influences of historic mining activities. Environ. Pollut. 92:193-201

Bonzongo J-CJ, Heim KJ, Chen Y, Lyons WB, Warwick JJ, Miller GC, Lecher PJ (1996b) Mercury pathways in the Carson River-Lahontan Reservoir system, Nevada, USA. Environ. Toxicol. Chem. 15:677-683

Caetano M, Falcão M, Vale C, Bebianno MJ (1997) Tidal flushing of ammonium, iron and manganese from inter-tidal sediment pore waters. Mar. Chem. 58:203-211

Capone DG, Kiene RP (1988) Comparison of microbial dynamics in marine and freshwater sediments: Contrasts in anaerobic carbon catabolism. Limnol. Oceanogr. 33:725-749

Carroll RWH, Warwick JJ, Heim KJ, Bonzongo JC, Miller JR, Lyons WB (2000) Simulation of mercury transport and fate in the Carson River, Nevada. Ecological Modelling 125:255-278

Chen Y, Bonzongo JC, Miller GC (1996) Levels of methylmercury and controlling factors in surface sediments of the Carson River system, Nevada. Environ. Pollut. 92:281-287

Chen Y, Bonzongo JCJ, Lyons WB, Miller GC (1997) Inhibition of mercury methylation in anoxic freshwater sediment by group VI anions. Environ. Toxicol. Chem. 16:1568-1574

Cline JD (1969) Spectrophotometric determination of hydrogen sulfide in natural waters. Limnol. Oceanogr. 14:454-458

Compeau GC, Bartha R (1985) Sulfate-reducing bacteria: Principal methylators of mercury in anoxic estuarine sediment. Appl. Environ. Microbiol. 50:498-502

Culbertson CW, Zehnder AJB, Oremland RS (1981) Anaerobic oxidation of acetylene by estuarine sediments and enrichment cultures. Appl. Environ. Microbiol. 41:396-407

Dalziel JA (1995) Reactive mercury in the eastern North Atlantic and southeast Atlantic. Mar. Chem. 49:307-314

Diamond ML (1999) Development of a fugacity/aquivalence model of mercury dynamics in lakes. Water Air Soil Pollut. 111:337-357

Dionex (1992) Installation Instructions and Troubleshooting Guide for the IONPAC^{O} AG4A-SC Guard Column / IONPAC^{O} AS4A-SC Analytical Column. Sunnyvale, CA, Dionex Corporation Document No. 034528

Ecology and Environment I (1998) Ecological Risk Assessment Carson River Mercury Site. San Francisco, California, Prepared for the U.S. Environmental Protection Agency Document Control No. ZS3490

Gagnon C, Pelletier E, Mucci A (1997) Behaviour of anthropogenic mercury in coastal marine sediments. Mar. Chem. 59:159-176

Gagnon C, Pelletier E, Mucci A, Fitzgerald WF (1996) Diagenetic behavior of methylmercury in organic-rich coastal sediments. Limnol. Oceanogr. 41:428-434

Gill GA, Fitzgerald WF (1987) Picomolar mercury measurements in seawater and other materials using stannous chloride reduction and two-stage gold amalgamation with gas phase detection. Mar. Chem. 20:227-243

Gilmour CC, Henry EA, Mitchell R (1992) Sulfate stimulation of mercury methylation in freshwater sediments. Environ. Sci. Technol. 26:2281-2287

Gilmour CC, Heyes A, Benoit J, Riedel G, Bell JT (1998a) Distribution and Biogeochemical Control of Mercury Methylation in the Florida Everglades. St. Leonard, MD, The Academy of Natural Sciences,Data Report: March 1995 through July 1997

Gilmour CC, Riedel GS (1995) Measurement of Hg methylation in sediments using high specific activity 203Hg and ambient incubation. Water Air Soil Pollut. 80:747-756

Gilmour CC, Riedel GS, Coates JD, Lovley D (1996) Mercury methylation by Iron(III)-Reducing Bacteria. Abstracts of the Amer. Soc. Microbiol. 96th General Meeting, May 19-23, 1996, New Orleans, LA. Abstract: (98) O-15:356

Gilmour CC, Riedel GS, Ederington MC, Bell JT, Benoit JM, Gill GA, Stordal MC (1998b) Methylmercury concentrations and production rates across a trophic gradient in the northern Everglades. Biogeochem. 40:327-345

Gobeil C, Cossa D (1993) Mercury in sediments and sediment pore water in the Laurentian Trough. Can. J. Aquat. Sci. 50:1794-1800

Guimaraes JRD, Malm O, Pfeiffer WC (1995) A simplified radiochemical technique for measurements of net mercury methylation rates in aquatic systems near goldmining areas, Amazon, Brazil. Sci. Total Environ. 175:151-162

Guy HP (1969) Laboratory theory and methods for sediment analysis. Techniques of Water-Resource Investigations of the United States Geological Survey U.S. Government Printing Office, Washington D.C. Book 5, Chapt. C1, Book 5.

Hallock RJ, Hallock LL (1993) Detailed Study of Irrigation Drainage In and Near Wildlife Management Areas, West-Central Nevada, 1987-90, Part B, Effect on Biota in Stillwater and Fernley Wildlife Management Areas and Other Nearby Wetlands. Carson City, NV, U.S. Geological Survey,Water Resources Investigations Report 92-4042B

Heim KJ, Warwick JJ (1997) Simulating sediment transport in the Carson River and Lahontan Reservoir, Nevada, USA. Wat. Res. Bull. 33:1-15

Henny CJ, Hill EF, Hoffman DJ, Spalding MG, Grove RA ((in prep.)) Mercury Hazard to Fish-Eating Birds: Fledglings at Risk -- Demethylation Protects Adults.

Hines ME, Nadig S, Barkay T, Bonzongo JCJ, Bailey EA (1999) Mercury Methylation/Demethylation and the mer Operon in the Carson River, Nevada. ASM 99th General Meeting (May 30-June 3, 1999)

Hintelmann H, Welbourn PM, Evans RD (1995) Binding of methylmercury compounds by humic and fulvic acids. Water Air Soil Pollut. 80:1031-1034

Hoffman RJ, Hallock RJ, Rowe TG, Lico MS, Burge HL, Thompson SP (1989) Reconnaissance investigation of water quality, bottom sediment, and biota associated with Stillwater Wildlife Management Area, Churchill county, Nevada, 1986-87. Carson City, NV, U. S. Geological Survey,Water-Resources Investigations Report 89-4105

Hoffman RJ, Taylor RL (1998) Mercury and suspended sediment, Carson River Basin, Nevada, - Loads to and from Lahontan Reservoir in flood year 1997 and deposition in Reservoir prior to 1983. Carson City, NV, U. S. Geological Survey,Fact Sheet FS-001-98

Hoffman RJ, Thomas KA (2000) Methylmercury in Water and Bottom Sediment Along the Carson River System, Nevada and California, September 1998. Carson City, NV, U.S. Geological Survey,Water-Resources Investigations Report 00-4013

Knott JM, Sholar CJ, Matthes WJ (1992) Quality assurance guidelines for the analysis of sediment concentration by U.S. Geological Survey sediment laboratories. Denver, CO, U.S. Geological Survey,Open-File Report 92-33

Korthals ET, Winfrey MR (1987) Seasonal and spatial variations in mercury methylation and demethylation in an oligotrophic lake. Appl. Environ. Microbiol. 53:2397-2404

Lechler PJ, Miller JR, Hsu LC, Desilets MO (1997) Mercury mobility at the Carson River Superfund Site, west-central Nevada, USA: Interpretation of mercury speciation data in mill tailings, soils, and sediments. J. Geochem. Explor. 58:259-267

Lovley DR, Phillips EJP (1987) Rapid Assay for microbially reducible ferric iron in aquatic sediments. Appl. Environ. Microbiol. 53:1536-1540.

Marvin MC (1995) Controls on the Spatial and Temporal Trends of Benthic Sulfate Reduction and Methanogenesis Along the Chesapeake Bay Central Channel. MEES Program. College Park, MD, University of Maryland

Marvin-DiPasquale M, Agee J, McGowan C, Oremland RS, Thomas M, Krabbenhoft D, Gilmour C (2000) Methyl-mercury degradation pathways: A comparison among three mercury-impacted ecosystems. Environ. Sci. Technol. 34:4908-4916

Marvin-DiPasquale MC, Oremland R S (1998) Bacterial methylmercury degradation in Florida Everglades peat sediment. Environ. Sci. Technol. 32:2556-2563

Matilainen T, Verta M, Niemi M, Uusi-Rauva A (1991) Specific rates of net methylmercury production in lake sediments. Water Air Soil Pollut. 56:595-605

Matthiessen A (1998) Reduction of divalent mercury by humic substances - kinetic and quantitative aspects. Sci. Total Environ. 213:177-183

Miller J, Barr R, Grow D, Lechler P, Richardson D, Waltman K, Warwick J (1999) Effects of the 1997 flood on the transport and storage of sediment and mercury within the Carson River Valley, West-Central Nevada. J. Geol. 107:313-327

Miller JR, Lechler PJ, Desilets M (1998) The role of geomorphic processes in the transport and fate of mercury in the Carson River basin, west-central Nevada. Environ. Geol. 33:249-262

Miller JR, Lechler PJ, Rowland J, Desilets M, Hsu L-C (1995) An integrated approach to the determination of the quantity, distribuion, and dispersal of mercury in Lahontan Reservoir, Nevada, USA. J. Geochem. Explor. 52:45-55

Mucci A, Lucotte M, Montgomery S, Plourde Y, Pichet P, Tra HV (1995) Mercury remobilization from flooded soils in a hydroelectric reservoir of northern Quebec, La Grande-2: results of a soil resuspension experiment. Can. J. Fish. Aquat. Sci. 52:2507-2517

Nuutinen S, Kukkonen JVK (1998) The effect of selenium and organic material in lake sediments on the bioaccumulation of methylmercury by Lumbriculus variegatus (Oligochaeta). Biogeochem. 40:267-278

Oremland RS, Culbertson CW, Winfrey MR (1991) Methylmercury decomposition in sediments and bacterial cultures: Involvement of methanogens and sulfate reducers in oxidative demethylation. Appl. Environ. Microbiol. 57:130-137

Oremland RS, Miller LG, Dowdle P, Connell T, Barkey T (1995) Methylmercury oxidative degradation potentials in contaminated and pristine sediments of the Carson River, Nevada. Appl. Environ. Microbiol. 61:2745-2753

Oremland RS, Polcin S (1982) Methanogenesis and sulfate reduction: Competitive and noncompetitive substrates in estuarine sediments. Appl. Environ. Microbiol. 44:1270-1276

Ouddane B, Martin E, Boughriet A, Fischer JC, Wartel M (1997) Speciation of dissolved and particulate manganese in the Seine river estuary. Mar. Chem. 58:189-201

Pak K, Bartha R (1998) Products of mercury demethylation by sulfidogens and methanogens. Bull. Environ. Contam. Toxicol. 61:690-694

Qian J, Mopper K (1996) Automated high-performance, high-temperature combustion total organic carbon analyzer. Anal. Chem. 68:3090-3097

Rasmussen LD, Turner RR, Barkay T (1997) Cell-density-dependent sensitivity of a mer-lux bioassay. Appl. Environ. Microbiol. 63:3291-3293

Rasmussen LD, Sorensen SJ, Turner RR, Barkay T (2000) Application of a mer-lux biosensor for estimating bioavailable mercury in soil. Soil Biol. Biochem. 32:639-646

Reeburgh WS (1967) An improved interstitial water sampler. Limnol. Oceanogr. 12:163-165

Regnell O, Ewald G, Lord E (1997) Factors controlling temporal variation in methyl mercury levels in sediment and water in a seasonally stratified lake. Limnol. Oceanogr. 42:1784-1795

Regnell O, Tunlid A, Ewald G, Sangfors O (1996) Methyl mercury production in freshwater microcosms affected by dissolved oxygen levels: Role of cobalamin and microbial community composition. Can. J. Fish. Aquat. Sci. 53:1535-1545

Robinson JB, Tuovinen OH (1984) Mechanisms of microbial resistance and detoxification of mercury and organomercury compounds: Physiological, biochemical, and genetic analyses. Microbiol. Rev. 48:95-124

Selifonova O, Burlage R, Barkay T (1993) Bioluminescent sensors for detection of bioavailable Hg(II) in the environment. Appl. Environ. Microbiol. 59:3083-3090

Soltanpour PN, Johnson GW, Workman SM, Benton Jones JJ, Miller RO (1996) Inductively coupled plasma emission spectrometry and inductively couples plasma-mass spectrometry. In: Bigham JM (ed.) Methods of soil analysis. Part 3. Chemical methods. Soil Science Society of America and American Society of Agronomy, , Vol. SSSA Book Series No. 5 p 91-139.

Suchanek TH, Mullen LH, Lamphere BA, Richerson PJ, Woodmansee CE, Slotton DG, Harner EJ, Woodward LA (1998) Redistribution of mercury from contaminated lake sediments of Clear Lake, California. Water Air Soil Pollut. 104:77-102

Teasdale PR, Minett AI, Dixon K, Lewis TW, Batley GE (1998) Practical improvements for redox potential (E-H) measurements and the application of a multiple-electrode redox probe (MERP) for characterising sediment in situ. Anal. Chim. Acta 367:201-213

Turner MA, Rudd JWM (1983) The English-Wabigoon River system: III. Selenium in lake enclosures: Its geochemistry, bioaccumulation, and ability to reduce mercury bioaccumulation. Can. J. Fish. Aquat. Sci. 40:2228-2240

Tuttle PL, Thodal CE (1997) Field screening of water quality, bottom sediment, and biota associated with irrigation in and near the Indian Lakes Area, Stillwater Wildlife Management Area, Churchill County, West-Central Nevada, 1995. Carson City, NV, U.S. Geological Survey,Water Resources Investigations Report 97-4250

Ulrich GA, Krumholz LR, Suflita JM (1997) A rapid and simple method for estimating sulfate reduction activity and quantifying inorganic sulfides. Appl. Environ. Microbiol. 63:1627-1630

USEPA (1996) Compilation of EPA's Sampling and Analysis Methods, Second Edition. Keith LH CRC Press Inc., New York

USGS (1998a) ALARA (As Low As Reasonably Achievable) Proceedures: USNRC Licence No. 04-06674-07. Use Permit No. 8. Menlo Park, CA, U.S. Geological Survey

USGS (1998b) Radiation Safety Manual for Licensed Material. Menlo Park, CA, U.S. Geological Survey, Western Region

Van Denburgh AS (1973) Mercury in the Carson and Truckee River Basins of Nevada. Carson City, Nevada, U.S. Geological Survey,Open-File Report 73-352

Verardo DJ, Froelich PN, McIntyre A (1990) Determination of organic carbon and nitrogen in marine sediments using the Carlo Erba NA-1500 Analyzer. Deep-Sea Res. 37:157-165

Wallschläger D, Desai MVM, Spengler M, Windmoller CC, Wilken RD (1998) How humic substances dominate mercury geochemistry in contaminated floodplain soils and sediments. J. Environ. Quality 27:1044-1054

Wallschläger D, Desai MVM, Wilken RD (1996) The role of humic substances in the aqueous mobilization of mercury from contaminated floodplain soils. Water Air Soil Pollut. 90:507-520

Wang JS, Huang PM, Liaw WK, Hammer UT (1991) Kinetics of the desorption of mercury from selected freshwater sediments as influenced by chloride. Water Air Soil Pollut. 56:533-542

Warwick JJ, James A (2000a) Analysis of Spatial Variation In Predicted Lateral Bank Erosion. Gainsville, FL, University of FL,Draft #1 - Report to EPA Region IX

Warwick JJ, James A (2000b) Carson River System Mercury Model. Gainsville, FL, Univ. of Florida,Documentation Draft #1 - Report to EPA Region IX

Warwick JJ, James A (2000c) Modeling Total and Methyl Mercury in the Carson River, Nevada. Model Documentation: Detailed Output. Gainsville, FL, Univ. of Florida,Report to EPA Region IX

Wayne DM, Warwick JJ, Lechler PJ, Gill GA, Lyons WB (1996) Mercury contamination in the Carson River, Nevada: A preliminary study of the impact of mining wastes. Water Air Soil Pollut. 92:391-408

Winfrey MR, Rudd JWM (1990) Environmental factors affecting the formation of methylmercury in low pH lakes. Environ. Toxicol. Chem. 9:853-869

Yin Y, Allen HE, Huang C-P, Sanders PF (1997a) Effects of pH, chloride and calcium (II) on adsorption of monomethylmercury by soils. Environ. Toxic. Chem. 16:2457-2462

Yin YJ, Allen HE, Huang CP, Sanders PF (1997b) Adsorption/desorption isotherms of Hg(II) by soil. Soil Sci. 162:35-45

Yin YJ, Allen HE, Huang CP, Sparks DL, Sanders PF (1997c) Kinetics of mercury(II) adsorption and desorption on soil. Environ. Sci. Technol. 31:496-503

Yin YJ, Allen HE, Li YM, Huang CP, Sanders PF (1996) Adsorption of mercury(II) by soil: Effects of pH, chloride, and organic matter. J. Environ. Quality 25:837-844

Table 1. Carson River System sampling locations. All sites repeatedly sampled during October 19-23, 1998, June 2-9, 1999 and October 10-15, 1999, unless otherwise noted. All sites sampled within ± 5 meters of given coordinates.

Name	Code	Latitude (N)	Longitude (W)	Description
Lloyd's Bridge	LB	39 08.53'	119 42.33'	Background control site near Carson City, NAWQA site [c]
Deer Run Road	DR	39 10.92	119 41.64'	Historic mill tailing deposits in this area, but upstream from major contaminated reach; NAWQA and Superfund site [c]
Dayton	DY	39 15.00'	119 35.08'	Within the vicinity of historic Rock Point stamp mill (built in 1861). NAWQA site.[c] Sampled October '99 only.
Fort Churchill (Upstream Dam)	F1	Oct. '98 / June '99 39 17.57' Oct. '99 39 17.54'	Oct. '98 / June '99 119 18.84' Oct. '99 119 18.96'	Within major contaminated reach, fine grained sediment; Sampling moved from north (Oct. '98/ June '99) to south (Oct. '99) shore due to disturbance of original site due to dam restoration. USGS site [a]
Fort Churchill (Weeks Bridge)	F2	Oct. '98 39 17.88' mid-channel June/Oct. '99 along southern shoreline	Oct. '98 119 15.50' mid-channel June/Oct. '99 along southern shoreline	Within major contaminated reach, < 0.5 miles from F1, course grained sandy sediment; Exact sampling location varied due to dangerous water conditions encountered during June '99. USGS-NAWQA and EPA Superfund site [c]. Coordinates given were taken from the southern shoreline during the Oct. '98 sampling only, when sediment was collected in the mid-channel (approx. 5-10 m from shore). Subsequently, June/Oct. '99 samples were taken right at the waters edge where the sediment was much finer than the encountered during the previous Oct. 98 sampling.
Fort Churchill (Vertical Bank)	F3	39 17.42'	119 17.51'	Vertical Bank located between F1 and F2 on north shore; Sampled in June '99 and October '99 only.
Lahontan Reservoir (South)	LS	Oct. '98 39 20.83' June '99 39 20.77'	Oct. '98 119 08.20' June '99 119 08.20'	Delta region at the head of the reservoir, major deposition zone for river derived suspended particulate matter. Exact sampling location varied.
Lahontan Reservoir (North)	LN	39 27.74'	119 04.22'	Immediately upstream of dam, particle retention area, additional particulate input from the Truckee Canal. USGS site [a]
Carson Diversion Dam	CD	39 29.41'	118 59.97'	River location downstream of Lahontan Res., 0.2 km upstream of Carson Diversion Dam, vegetated area [c]
Carson Lake (Sprig Pond)	CL	39 19.56'	118 44.63'	Immediately at the end of the principal drain to Carson Lake wetlands, a NIWQP site, open water / wetland area, terminal lake, high levels of total Hg and MeHg in surface water [c,d]
South Lead Lake	LL	39 36.96'	118 31.22'	Within SWR, slightly alkaline, moderate salinity, low Se lake [b,d]
Stillwater Point Reservoir	SP	39 30.68'	118 30.96'	Within SWR, USGS water storage reservoir downstream from wetlands, important source of irrigation water [d]
Stillwater Slough Cutoff Drain	SS	39 33.06'	118 31.75'	Irrigation canal within SWR [c]
Swan Check	SC	39 38.15'	118 26.92'	Wetland lake within SWR
Carson Sink	CS	39 46.06'	118 44.38'	A seasonally wet playa area, high concentrations of evaporated salts and naturally occurring trace elements

[a] (Oremland et al. 1995), [b] (Steinberg & Oremland 1990), [c] (Hoffman et. al. 1989, 2000), [d] (Hallock & Hallock 1993)

Table 2. Analytical Methods Summary. All assays were conducted by the USGS (Menlo Park, CA) group, unless otherwise indicated. All microbial rate measurements were conducted using anoxic bottle incubations of whole sediment.

Parameter (CODE)	Purpose for Measurement	Analytical Method	Reference
I. Microbial Hg-Transformation Rates			
MeHg Production **(MP)**	Hg form of primary concern, produced in anoxic sediments by SO_4^{2-} reducing bacteria, Identify zones of high and low activity within the CRS	$^{203}HgCl_2$ incubation with organic extraction and gamma counting of $CH_3{}^{203}Hg^+$	(Gilmour & Riedel 1995, Guimaraes et al. 1995)
MeHg Degradation **(MD)**	Hg form of primary concern, complimentary reverse pathway to MP, Identify zones of high and low activity within the CRS	$^{14}CH_3HgI$ incubation with gaseous ^{14}C end product quantification via $^{14}CH_4$ combustion → $^{14}CO_2$ trapping → LSC (beta counting)	(Marvin-DiPasquale & Oremland 1998)
II. Ancillary Microbial Process Rates			
Sulfate Reduction **(SR)**	SO_4^{2-} reducing bacteria both produce and degrade MeHg, Produces reduced-S endproducts which can mediate Hg bioavailability	$^{35}SO_4^{2-}$ incubation → distillation and trapping of reduced ^{35}S species via chromium reduction and acid volatilization → reduced ^{35}S quantificaiton via LSC.	(Ulrich et al. 1997)
Methanogenesis **(ME)**	Methanogenic bacteria can degrade MeHg	Net in-situ CH_4 production → quantification via GC-FID	(Culbertson et al. 1981, Oremland & Polcin 1982)
Methane Oxidation **(MO)**	Verification that this process does not significantly contribute to $^{14}CO_2$ counted in MD assay	$^{14}CH_4$ incubation → $^{14}CO_2$ quantification via trapping and LSC	(Marvin-DiPasquale & Oremland 1998)
Iron Reduction **(IR)**	Fe reducing bacteria may methylate Hg, Capacity to degrade MeHg is unknown, May be important in overall sediment biogeochemistry of the CRS	Unspiked sediment slurry incubation → net in-situ Fe^{2+} production / Fe^{3+} depletion quantified colorometrically	(Lovley & Phillips 1987)
Manganese Reduction **(MR)**	May be important to the overall sediment biogeochemistry of the CRS	Unspiked sediment incubation → net in-situ dissolved Mn^{+2} production quantified via ICP	(Ouddane et al. 1997)

Table 2. (Continued)

Parameter (CODE)	Purpose for Measurement	Analytical Method	Reference
III. Whole Sediment Parameters			
Total mercury [a] **(Mt)**	Used to assess trends in concentration compared to rates of microbial tranformations	Acid digestion → BrCl oxidation,→Sn reduction → CVAFS detection	(Gill & Fitzgerald 1987)
Methylmercury [a] **(MM)**	Used to calculate in-situ MeHg consumption rates and to assess trends in concentration compared to microbial Hg-transformation rates	Gas phase ethylation → GC separation → pyrolization → CVAFS detection	(Bloom 1989)
Acid-labile 'reactive'- Hg(II) [a] **(RM)**	Used to calculate in-situ MeHg production rates and to assess trends in concentration compared to microbial Hg-transformation rates	Adjustment of sample pH to 1.2 →Sn reduction → CVAFS detection	(Dalziel 1995)
Bioavailable Hg(II) via the *mer-lux* biosensor [b] **(BM)**	Compare to RM, Provide an independent measure of bioavailable Hg using a newly developed technology	*E. Coli* culture grown containing *mer-lux* DNA plasmid, biosensor exposed to porewater → light emission quantifed	(Rasmussen et al. 1997)
Bulk density **(BD)**	Needed to normalize Hg concentration to sediment dry weight	Calculated from sediment wet and dry weight determinations	(Marvin-DiPasquale & Oremland 1998)
Porosity **(POR)**	Needed to normalize Hg concentration to sediment dry weight	Calculated from sediment wet and dry weight determinations	(Marvin-DiPasquale & Oremland 1998)
Grain size [c] (<62 μm) **(GS)**	Sediment characterization parameter, Differences among sites may influence Hg concentration and availability	Wet sediment sieving (62 μm) → % dry weight	(Guy 1969, Knott et al. 1992)
Redox Potential **(Eh)**	Sediment characterization parameter, May influence Hg bioavailability to microbes	Eh Pt-electrode placed directly into sediment	(Teasdale et al. 1998)
Sediment pH **(pH)**	Sediment characterization parameter, May influence Hg bioavailability to microbes	pH electrode placed directly into sediment	EPA Method 1625 (USEPA 1996)
Total particulate carbon **(PC)**	Sediment characterization parameter, May influence Hg bioavailability to microbes	Grind dry sediment sample (< 62 μm) → weigh subsample → run on automated CHN analyzer	(Verardo et al. 1990), EPA Method 415.1 (USEPA 1996)

Table 2. (Continued)

Parameter (CODE)	Purpose for Measurement	Analytical Method	Reference
Total selenium **(Se)**	Se has been shown to mediate Hg bioaccumulation, although its impact on microbial Hg cycling is unknown	Strong acid digestion → graphite furnace atomic absorption spectrophotometry	(Soltanpour et al. 1996), EPA Method xxxx (USEPA 1996)
Methane **(CH4)**	Sediment characterization parameter, Endproduct of microbial methanogenesis	Sediment sub-sampling into crimp sealed container → autoclave → GC/FID quantification	(Culbertson et al. 1981)
Total iron **(Fe)**	Solid phase Fe-oxyhydroxides may bind Hg	Strong acid digestion → inductively coupled plasma emission spectroscopy detection	EPA Method 6010 (USEPA 1996)
Total manganese **(Mn)**	Solid phase Mn-oxyhydroxides may bind Hg	Strong acid digestion → inductively coupled plasma emission spectroscopy detection	EPA Method 6010 (USEPA 1996)
Acid volatile reduced sulfur **(RS)**	Primarily FeS which may bind Hg and partially mediate Hg microbial bioavailability	Cold HCl extraction → ZnS trapping → methylene blue colorimetric detection	(Cline 1969, Ulrich et al. 1997)
IV. Sediment Pore-Water Parameters			
Chloride **(Cl)**	Pore water anion which may partially mediate Hg(II) bioavailability to bacteria	Anoxic sediment squeezing → pore water filtration → ion chromotography	EPA Method 300.0 (USEPA 1996)
Sulfate **(SO4)**	Pore water anion needed to calculate in-situ rates of SO_4^{2-} reduction	Anoxic sediment squeezing → pore water filtration → ion chromotography	EPA Method 300.0 (USEPA 1996)
Inorganic nitrogen **(NO2, NO3)**	Pore water anions which indicate both sediment redox condition and nutrient status	Anoxic sediment squeezing → pore water filtration → ion chromotography	(Dionex 1992)
Phosphate **(PO4)**	Pore water anion which indicates sediment nutrient status, , may compete with Hg for binding sites on Fe-(oxy)-hydroxide minerals	Anoxic sediment squeezing → pore water filtration → ion chromotography	(Dionex 1992)
Sulfide **(SU)**	Endproduct of SO_4^{2-} reduction, may mediate HgS formation or facilitate Hg binding to solid phase thiols	Anoxic sediment squeezing → pore water filtration → "fix" as ZnS → methylene blue colorometric assay	(Cline 1969)

Table 2. (Continued)

Parameter (CODE)	Purpose for Measurement	Analytical Method	Reference
Iron (**Fe**)	Needed for assessment of microbial Fe- reduction processes	Anoxic sediment squeezing or centrifugation → pore water filtration → acidification → flame AA quantification	EPA Method 243.1 (USEPA 1996)
Manganese (**Mn**)	Needed for assessment of microbial Mn- reduction processes	Anoxic sediment squeezing or centrifugation → pore water filtration → acidification → flame AA quantification	(Caetano et al. 1997), EPA Method 243.1 (USEPA 1996)
Dissolved organic carbon (**OC**)	May bind various forms of Hg, indicator of relative organic substrate available to fuel heterotrophic bacteria	Anoxic sediment squeezing → pore water filtration → high temperature non-catalytic oxidation with IR detection	(Qian & Mopper 1996), EPA Method 415.1 (USEPA 1996)

[a] Conducted by Dr. David Krabbenhoft et al. (USGS, Madison , WI).
[b] Conducted by Dr. Mark Hines et al. (Univ. of Alaska, Anchorage, AK).
[c] Conducted by Allan Mlodnosky (USGS Sediment Laboratory, Salinas, CA).

Table 3. Sample preparation with respect to sample size, assay container type, replication, killed controls, and preservation method.

Parameter Code [a]	Sample Size (cc)	Vial Type [b] (cc)	Incubation Time (d)	Replication / Killed Controls [c]	Preservative
I. Microbial Hg-Transformation Rates					
MP	3.0 ± 0.1	SB (13)	0.25-1.0	R1-3, k	Freeze
MD	3.0 ± 0.1	SB (13)	0.25-1.0	R1-4, k	1 ml 3 M NaOH
II. Ancillary Microbial Process Rates					
SR	1.5 ± 0.1	SB (120)	0.2	R1-2, k	6 ml 10% ZnAc, Freeze
ME	3.0 ± 0.1	SB (13)	7-14	(Ti & Tf)x2	Freeze
MO	3.0 ± 0.1	SB (13)	1.9	R1-2, k	1 ml 3 M NaOH
IR [e]	3.0 ± 0.1	CT (15)	14	(Ti & Tf)x2	Assay immediately
MR [e]	3.0 ± 0.1	CT (15)	14	(Ti & Tf)x2	Freeze pore-water Mn
III. Whole Sediment Parameters					
Mt, MM, RM [d]	5-10	SV-QA (20)	NA	R1-2	Freeze
BM	5-10	SV-QA (20)	NA	R1-2	Refrigerate
GS	5-10	SV (20)	NA	R1-2	Refrigerate
PC, BD, POR[d]	≈ 3	SV (20)	NA	R1-2	Freeze
CH4 [f]	3.0 ± 0.1	SB (13)	NA	R1-2	Freeze
Fe, Mn, Se [d]	5-10	SV-QA (20)	NA	R1-2	Freeze
RS	1.5 ± 0.1	SB (120)	NA	R1-2	6 ml 10% ZnAc, Freeze
pH	≈ 10	SV (20)	NA	R1-2	Refrigerate
Eh	≈ 10	SV (20)	NA	R1-2	Refrigerate
IV. Sediment Pore-Water Parameters					
Cl, SO4, NO3, NO2, PO4 [d]	5-10	SB (13)	NA	R1-2	Freeze
SU	5-10	SB (13)	NA	R1-2	1 ml 10% ZnAc, Refrig.
DOC	5-10	SV (20)	NA	R1-2	1 ml HNO_3, pH =1, Refrig.
Fe, Mn [d]	5-10	SV-QA (20)	NA	R1-2	1 ml HNO_3, pH =1, Refrig.

[a] Parameter codes as per Table 2.

[b] Vial Type Code: SV = glass scintillation vial, SB = glass serum bottle, CT = polypropylene centrifuge tube, QA = commercially pre-cleaned quality assurance

[c] R# = replicate, k = autoclaved killed control, Ti and Tf = time points initial and final, respectively.

[d] All constituents from the same sample.

[e] IR and MR were taken from same sub-sample, but differ in preservation method.

[f] Taken as the pair of Ti samples from net methanogenesis (ME) assay.

Table 4. Analytical Methods - Quality Assurance/Quality Control.

Parameter Code [a]	Quantitation Limit - Requested	Quantitation Limit - Measured	Requested Max Holding Time (d)	Actual Holding Time (d) [b]	Accuracy Measured [c]	Precision Measured [e]
I. Microbial Hg-Transformations						
MP	0.2 % $^{203}HgCl_2$ amendment methylated	$^{203}HgCl_2$ amendment methylated: 10/98 = 0.01% 6/99 = 0.01% 10/99 = 0.01%	46 (one isotope half-life)	10/98 = 23-35 6/99 = 34-44 10/99 = 23-33	NA [d]	all sample sets: 10/98 = ±(2-24%) 6/99 = ± (6-136%) 10/99 = ± (0-103%)
MD	0.5 % ^{14}C-MeHg amendment degraded	^{14}C-MeHg amendment degraded: 10/98 = 0.1% 6/99 = 0.3% 10/99 = 0.2%	90	10/98 = 10-27 6/99 = 28-56 10/99 = 18-51	NA [d]	all sample sets: 10/98 = ±(1-24%) 6/99 = ±(1-97%) 10/99 = ± (2-56%)
II. Ancillary Microbial Processes						
SR	0.5 % $^{35}SO_4^{2-}$ amendment reduced	$^{35}SO_4^{2-}$ amendment reduced: 10/98 = 0.002% 6/99 = 0.015% 10/99 = 0.009%	87 (one isotope half-life)	10/98 = 8 6/99 = 30-34 10/99 = 52-53	NA [d]	all sample sets: 10/98 = ±(8-99%) 6/99 = ±(11-89%) 10/99 = ±(59-80%)
ME	0.5 nmol CH_4 • cc sed^{-1} • d^{-1}	(nmol CH_4 • cc sed^{-1} • d^{-1}) 10/98 = 0.1 6/99 = 0.2-1.7 10/99 = 0.11-0.88	60	10/98 = 1-8 6/99 = 23-28 10/99 = 50-51	NA [d]	all sample sets: 10/98 = ±(1-112%) 6/99 = ±(4-135%) 10/99 = ±(1-10%)
MO	0.5% $^{14}CH_4$ amendment oxidized	$^{14}CH_4$ amendment oxidized: 10/98 = 0.15%	60	10/98 = 1-11 6/99 = not conducted 10/99 = not conducted	NA [d]	10/98 = ±17%, (n=2) 6/99 = not conducted 10/99 = not conducted
IR	2% change in dissolved Fe^{2+} concentration over the incubation period	Increase (or decrease) in dissolved Fe^{2+} concentration over the incubation period: 10/98 = 0.7 ug • cc $slurry^{-1}$ • d^{-1} 6/99 = 3.1 ug • g wet sed^{-1} • d^{-1} 10/99 = 3.6 ug • g wet sed^{-1} • d^{-1}	180	10/98 = 0 6/99 = 0 10/99 = 0	NA [d]	all sample sets: 10/98 = ±(0-36%) 6/99 = ±(21-266%) 10/99 = ±(30-104%)

Table 4. (continued)

Parameter Code [a]	Quantitation Limit - Requested	Quantitation Limit - Measured	Requested Max Holding Time (d)	Actual Holding Time (d) [b]	Accuracy Measured [c]	Precision Measured [e]
MR	2% change in dissolved Mn^{2+} concentration over the incubation period	Change in dissolved Mn^{2+} concentration over the incubation period: 10/98 = 0.01 ug • cc slurry^{-1} • d^{-1} 6/99 = 0.39 ug • g wet sed^{-1} • d^{-1} 10/99 = 0.41 ug • g wet sed^{-1} • d^{-1}	180	10/98 = 240 6/99 = 225 10/99 = 92-93	NA [d]	all sample sets: 10/98 = ±(1-143%) 6/99 = ±(5-57%) 10/99 = ±(22%)
III. Whole Sediment Parameters						
Mt	1 pg Hg (absolute limit for CVAFS)	Absolute (pg Hg): 10/98 = 5 6/99 = 9 10/99 0.3 g sample (pg • g wet sed^{-1}) 10/98 = 17 6/99 = 30 10/99 -	28	10/98 = 78-113 6/99 = 69-76 10/99 = 74-80	CRM [f]: 10/98 = 97%, (n=4) 6/99 = 96%, (n=6) 10/99 = 92%, (n=5) CRM [j]: 10/99 = 103%, (n=4) Matrix Spike (0.5 ng): 10/98 = 106% (n=10) 6/99 = 101% (n=8) 10/99 = 98% (n=7)	CRM [f]: 10/98 = ±4 %, (n=4) 6/99 = ±16 %, (n=6) 10/99 = ± 5%, (n=5) CRM [j]: 10/99 = ± 10%, (n=4) all sample sets: 10/98 = ±(2-23%) 6/99 = ±(0-68%) 10/99 = ±(0-31%)
MM	1 pg Hg (absolute limit for CVAFS)	Absolute (pg Hg): 10/98 = 2 6/99 = 10 10/99 = 3 0.3 g sample (pg • g wet sed^{-1}) 10/98 = 7 6/99 = 33 10/99 = 10	28	10/98 = 78-113 6/99 = 69-85 10/99 = 71-142	CRM [g]: 10/98 = 180%, (n=6) 6/99 = 173%, (n=6) 10/99 = 180%, (n=7) Matrix Spike (0.1 ng): 10/98 = 123% (n=8) 6/99 = 104% (n=10) 10/99 = 124% (n=14)	CRM [g]: 10/98 = ±2 %, (n=6) 6/99 = ±31%, (n=6) 10/99 = ±7 %, (n=7) all sample sets: 10/98 = ±(2-108%) 6/99 = ±(0-27%) 10/99 = ±(5-112%)
RM	1 pg Hg (absolute limit for CVAFS)	Absolute (pg Hg): 10/98 = 5 6/99 = 9 10/99 = 6 0.3 g sample (pg • g wet sed^{-1}) 10/98 = 17 6/99 = 30 10/99 = 22	28	10/98 = 78-113 6/99 = 56-79 10/99 = 67-74	Matrix Spike (10 ppb $HgCl_2$): 10/98 = 101%, (n=5) 6/99 = 99%, (n=8) 10/99 = 103%, (n=6)	10 µg/l Hg(II) spike: 10/98 = ±4 %, (n=6) 6/99 = ±8 %, (n=8) 10/99 = ±4 %, (n=6) all sample sets: 10/98 = ± (5-65%) 6/99 = ± (5-83%) 10/99 = ± (1-69%)

Table 4. (continued)

Parameter Code [a]	Quantitation Limit - Requested	Quantitation Limit - Measured	Requested Max Holding Time (d)	Actual Holding Time (d) [b]	Accuracy Measured [c]	Precision Measured [e]
BM	7 pM Hg^{2+}	Hg(II) (pM): 10/98 = 2 6/99 = 1	28	10/98 = 75-92 6/99 = 8-16	NA [d]	all sample sets: 10/98 = ±(28-141%) 6/99 = none detected
BD	NA	NA	30	10/98 = 21 6/99 = 25 10/99 = 28	NA [d]	all sample sets: 10/98 = ±(0-3%) 6/99 = ±(0-21%) 10/99 = ±(0-8%)
POR	NA	NA	30	10/98 = 21 6/99 = 25 10/99 = 28	NA [d]	all sample sets: 10/98 = ±(1-8%) 6/99 = ±(1-21%) 10/99 = ±(0-11%)
CH4	5 nmol CH_4 • cc wet sed^{-1}	(nmol CH_4 • cc wet sed^{-1}) 10/98 = 1 6/99 = 2 10/99 = 1	60	10/98 = 2 6/99 = 23-28 10/99 = 50-51	Matrix Spike (800 ppm CH_4): 10/98 = 94%, (n=6) 6/99 = 78%, (n=4) 10/99 = not conducted	all sample sets: 10/98 = ±(9-16%) 6/99 = ±(0-89%) 10/99 = ±(0-35%)
GS	1% < 63 µm	< 63 µm: 10/98 = 1% 6/99 = 1% 10/99 = not conducted	10	10/98 = 30 6/99 = 6 10/99 = not conducted	NA [d]	all sample sets: 10/98 = ±(0-14%) 6/99 = ±(0-20%) 10/99 = not conducted
E_h	NA	NA	0	10/98 = 9 6/99 = 0 10/99 = 0	bias in redox potential change between 86-263 mV: 10/98 = -4 mV 6/99 = -2 mV 10/99 = 2mV	At 238 mV, Zobell's solution 10/98 = ± 0 mV, (n=1) 6/99 = ±3 mV, (n=7) 10/99 = ±1mV, (n=5) all sample sets: 10/98 = ±(5-132%) 6/99 = ±(1-114%) 10/99 = ±(0-74%)

Table 4. (continued)

Parameter Code [a]	Quantitation Limit - Requested	Quantitation Limit - Measured	Requested Max Holding Time (d)	Actual Holding Time (d) [b]	Accuracy Measured [c]	Precision Measured [e]
pH	NA	NA	0	10/98 = 0 6/99 = 0 10/99 = 0	bias at pH = 7 02 10/98 = -0 01 pH units 6/99 = +0 02 pH units 10/99 = -0 02 pH units	At pH = 7 02 10/98 = ± 0 1 pH units (n=3) 6/99 = ± 0 02 pH units (n=8) 10/99 = ± 0 55 pH units (n=5) all sample sets 10/98 = ±(0-4%) 6/99 = ±(0-3%) 10/99 = ± (0-1%)
PC	0 1% C	10/98 = 0 06 % C 6/99 = 0 02%C 10/99 = 0 35%C	28	10/98 = 66 6/99 = 63-70 10/99 = 72-73	Matrix Spike (0 4-0 9 mg EDTA) 10/98 = n d 6/99 = 103%, (n=6) 10/99 = 104%, n=6)	all sample sets 10/98 = ±(1-39%) 6/99 = ±(0-64%) 10/99 = ±(1-9%)
Se	2 ppb	6/99 = 1 ppb	180	532	Matrix Spike (30 ng Se) 6/99 = 103%, (n=2)	all sample sets 6/99 = ±(2-21%)
RS	0 01 µmol S • g wet sed $^{-1}$	(µmol S • g wet sed $^{-1}$) 10/98 = 0 002 6/99 = 0 003 10/99 = 0 005	60	10/98 = 15 6/99 = 48-55 10/99 = 58-66	Matrix Spike (1 5 µmol ZnS) 10/98 = 77%, (n=3) 6/99 = n d 10/99 = n d	All sample sets 10/98 = ±(0-35%) 6/99 = ±(0-133%) 10/99 = ±(0-38%)
Fe	7 µg • liter $^{-1}$ in extractent	In whole sediment (dry weight) 10/98 = 26 ppb 6/99 = 870 ppb 10/99 = 300ppb	180	10/98 = 156-163 6/99 = 79-89 10/99 = 83-88	Matrix Spike (27-37 mg Fe) 10/98 = 99%, (n=4) 6/99 = 91%, (n=6) 10/99 = 132% (n=2) CRM [h] 10/98 = 54%, (n=3) 6/99 = 50%, (n=3) 10/99 = 61% (n=2) CRM [i] 6/99 = 88%, (n=3) 10/99 = 93% (n=2)	CRM [h] 10/98 = ±1% (n=3) 6/99 = ±1% (n=3) 10/99 = ±1% (n=2) CRM [i] 6/99 = ±3% (n=3) 10/99 = ±4% (n=2) all sample sets 10/98 = ±(0-17%) 6/99 = ±(0-53%) 10/99 = ±(1-8%)

Table 4. (continued)

Parameter Code [a]	Quantitation Limit - Requested	Quantitation Limit - Measured	Requested Max Holding Time (d)	Actual Holding Time (d) [b]	Accuracy Measured [c]	Precision Measured [e]
Mn	2 µg • liter^{-1} in extractent	In whole sediment (dry weight) 10/98 = 3 ppb 6/99 = 113 ppb 10 99 = 30ppb	180	10/98 = 156-163 6/99 = 79-89 10/99 = 83-88	Matrix Spike (0 5 mgMn) 10/98 = 129%, (n=4) 6/99 = 127% (n=6) 10/99 = 133% (n=2) CRM [h] 10/98 = 58%, (n=3) 6/99 = 54% (n=3) 10/99 = 61% (n=2) CRM [i] 6/99 = 88%, (n=3) 10/99 = 49% (n=2)	CRM [h] 10/98 = ±1% (n=3) 6/99 = ±0 4% (n=3) 10/99 = ±2% (n=2) CRM [i] 6/99 = ±2% (n=3) 10/99 = ±1% (n=2) all sample sets 10/98 = ±(1-12%) 6/99 = ±(0-30%) 10/99 = ±(0-7)
IV. Pore-Water Parameters						
Cl	5 µM	10/98 = 1 7 µM 6/99 = 1 2 µM 10/99 = 0 5 µM	28	10/98 = 52-59 6/99 = 55-68 10/99 = 69-76	Matrix Spike (25-32 ppm Cl) 10/98 = 96%, (n=2) 6/99 = 154%, (n=2) 10/99 = 117% (n=2)	All sample sets 10/98 = ±(1-28%) 6/99 = ±(2-38%) 10/99 = ±(8-30%)
SO4	5 µM	10/98 = 0 5 µM 6/99 = 0 4 µM 10/99 = 0 4 µM	28	10/98 = 52-59 6/99 = 55-68 10/99 = 69-76	Matrix Spike (37-39 ppm SO_4^{2}) 10/98 = 98%, (n=2) 6/99 = 123%, (n=2) 10/99 = 103% ,(n=2)	all sample sets 10/98 = ±(0-60%) 6/99 = ±(2-65%) 10/99 = ±(2-55%)
NO2	5 µM	10/98 = 1 6 µM 6/99 = 0 3 µM 10/99 = 0 6 µM	28	10/98 = 52-59 6/99 = 55-68 10/99 = 69-76	Matrix Spike (1-2 ppm NO_2) 10/98 = 111% , (n=2) 6/99 = 107%, (n=1)	all sample sets 10/98 = ±(7%) 6/99 = ±(12-16%)
NO3	5 µM	10/98 = 0 8 µM 6/99 = 0 3 µM 10/99 = 0 4 µM	28	10/98 = 52-59 6/99 = 55-68 10/99 = 69-76	Matrix Spike (3 ppm NO_3) 10/98 = 110%, (n=2) 6/99 = 117%, (n=1) 10/99 = 93% (n=2)	all sample sets 10/98 = ±(1-80%) 6/99 = ±(2-88%) 10/99 = ±(13-74%)
PO4	5 µM	10/98 = 0 5 µM 6/99 = 0 6 µM 10/99 = 0 6 µM	28	10/98 = 52-59 6/99 = 55-68 10/99 = 69-76	Matrix Spike *1 ppm PO_4^{3}) 10/98 = 65%, (n=2) 6/99 = 95%, (n=1) 10/99 = 38% (n=2)	all sample sets 10/98 = ±(3-19%) 6/99 = ±(2-85%) 10/99 = ±(0-82%)

Table 4. (continued)

Parameter Code [a]	Quantitation Limit - Requested	Quantitation Limit - Measured	Requested Max Holding Time (d)	Actual Holding Time (d) [b]	Accuracy Measured [c]	Precision Measured [e]
SU	1 µM	10/98 = 0.3 µM 6/99 = 0.2 µM 10/99 = 0.7 µM	60	10/98 = 8-12 6/99 = 42-49 10/99 = 161-162	Matrix Spike (10-180 µM ZnS): 10/98 = 105%, (n=2) 6/99 = 88%, (n=2) 10/99 = n.d.	all sample sets: 10/98 = ±(4-74%) 6/99 = ±(1-80%) 10/99 = ±(2-40%)
Fe	10 µg*liter^{-1}	10/98 = 7 µg • liter^{-1} 6/99 = 9 µg • liter^{-1} 10/99 = 3 µg • liter^{-1}	180	10/98 = 231 6/99 = 147-154 10/99 = 91-92	Matrix Spike (200 ng Fe): 10/98 = 67%, (n=2) 6/99 = 101%, (n=1) 10/99 = 73%, (n=1)	all sample sets: 10/98 = ±(1-131%) 6/99 = ±(1-81%) 10/99 = ±(0-40%)
Mn	10 µg*liter^{-1}	10/98 = 4 µg • liter^{-1} 6/99 = 3 µg • liter^{-1} 10/99 = 1 µg • liter^{-1}	180	10/98 = 230 6/99 = 114-121 10/99 = 91-92	Matrix Spike (6 ng Mn): 10/98 = 133%, (n=2) 6/99 = n.d. 10/99 = 236%, (n=2)	all sample sets: 10/98 = ±(0-82%) 6/99 = ±(0-43%) 10/99 = ±(4-20%)
DOC	3 µM C	10/98 = 61 µM C 6/99 = 23 µM C 10/99 = 20 µM C	28	10/98 = 31 6/99 = 63-70 10/99 = 53-54	Matrix Spike (13-18 ppm DOC): 10/98 = 100% (n=2) 6/99 = 98%, (n=3) 10/99 = 94%, (n=1)	all sample sets: 10/98 = ±(0-16%) 6/99 = ±(3-57%) 10/99 = ±(1-23%)

[a] Parameter codes as per Table 2 and Appendix 1.

[b] Represents holding time from sub-sampling and/or incubation date to final analyte analysis date. For October 1998 samples (10/98), sediment was collected in the field (Oct. 20-22, 1999) and stored in filled mason jars at 5 ^{0}C for 93-95 days (MD, MP, BM, Hgt, MM, RM) or 141-145 days (all other parameters) before being sub-sampled. For June 1999 samples (6/99), sediment was sub-sampled and incubated the day of collection.

[c] Given as % Recovery unless otherwise indicated.

[d] A direct assessment of accuracy is not relevant for this assays as no certified standards exist.

[e] Given as % Relative Standard Deviation unless otherwise indicated.

[f] Certified Reference Material = IAEA-356, marine sediment, certified value: 7.62 µg Hg_t • g dry wt^{-1}.

[g] Certified Reference Material = IAEA-356, marine sediment certified value: 5.45 ng MeHg • g dry wt^{-1}). A number of independent laboratories have also observed high MeHg recoveries with this particular item. It is believed that the certified value may be in error (too low). This possibility is being investigated.

[h] Certified Reference Material = PACS-2 marine sediment (NRCC), certified at 58.5 mg Fe • g dry wt^{-1} and 440 µg Mn • g dry wt^{-1}.

[i] Certified Reference Material = SRM-2709 San Joaquin soil (NIST), certified at 35.0 mg Fe • g dry wt^{-1} and 538 µg Mn • g dry wt^{-1}.

[j] Certified Reference Material = MESS-2, marine sediment, certified value: 0.092 µg Hg_t • g dry wt^{-1}.

Table 5. ^{14}C-MeHg degradation enrichment cultures from Carson River (site F1). Each entry represents a given electron donor and acceptor pair growth condition (n=1). The first number reflects the total % ^{14}C-MeHg degraded after 13 days. The second number, in { }, represents the $^{14}CO_2/(^{14}CH_4 + ^{14}CO_2)$ end-product ratio (%).

Electron Acceptors	Electron Donors					
	Acetate		Lactate		Glucose	
O_2	52	{0}	54	{0}	46	{0}
Fe(III)	7	{50}	10	{46}	5	{0}
NO_3^-	8	{0}	5	{0}	3	{0}
SO_4^{2-}	13	{12}	9	{0}	3	{0}
SeO_4^{2-}	18	{0}	11	{0}	5	{0}
$As\ O_4^{2-}$	1	{0}	2	{0}	2	{0}

List of Figures

List of Figures (continued)

List of Figures (continued)

Figure 1. Sampling sites in the Carson River System

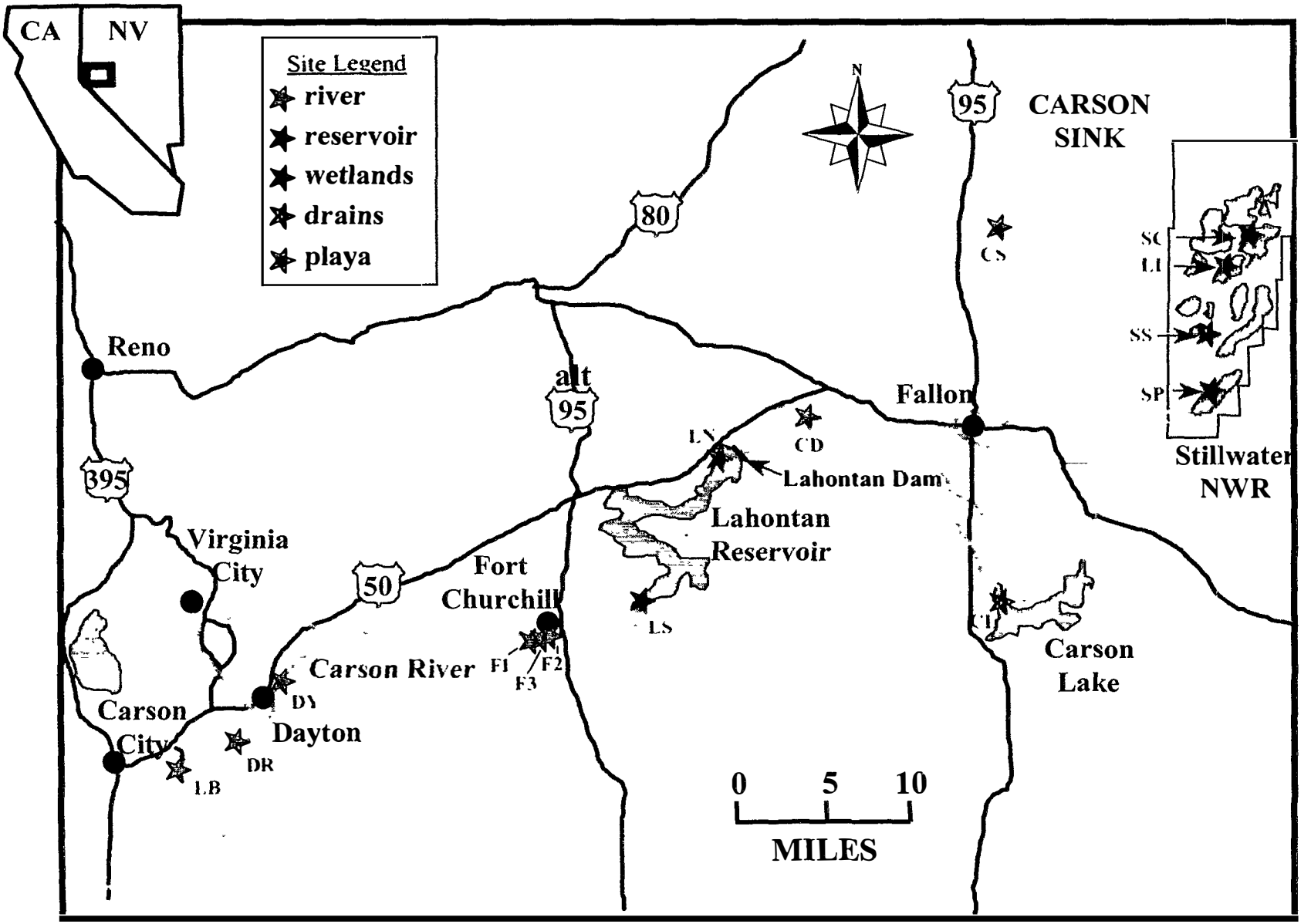

Figure 2. Total Mercury - Surface Sediment (0-4 cm)

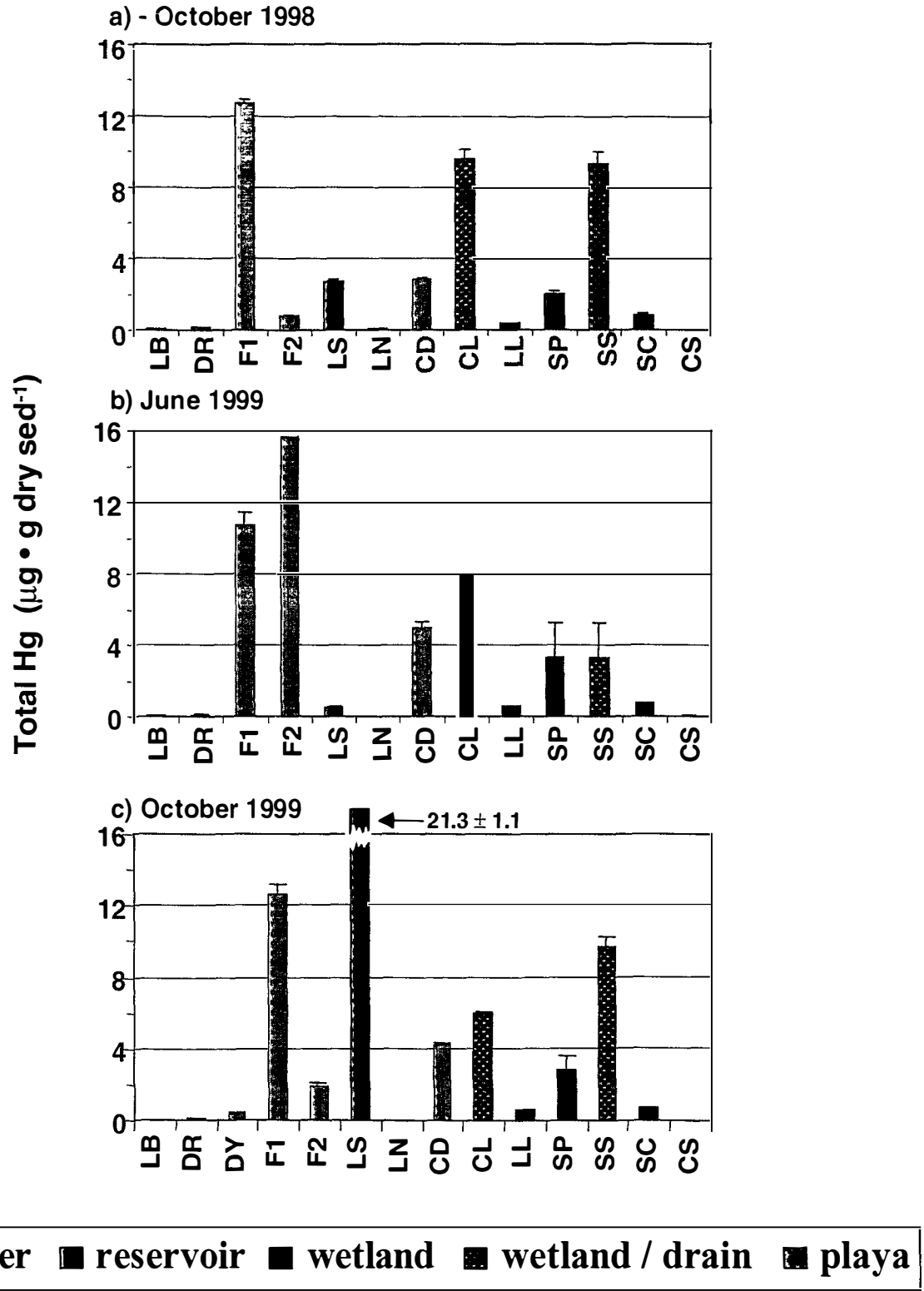

Figure 3. Methylmercury - Surface sediment (0-4 cm)

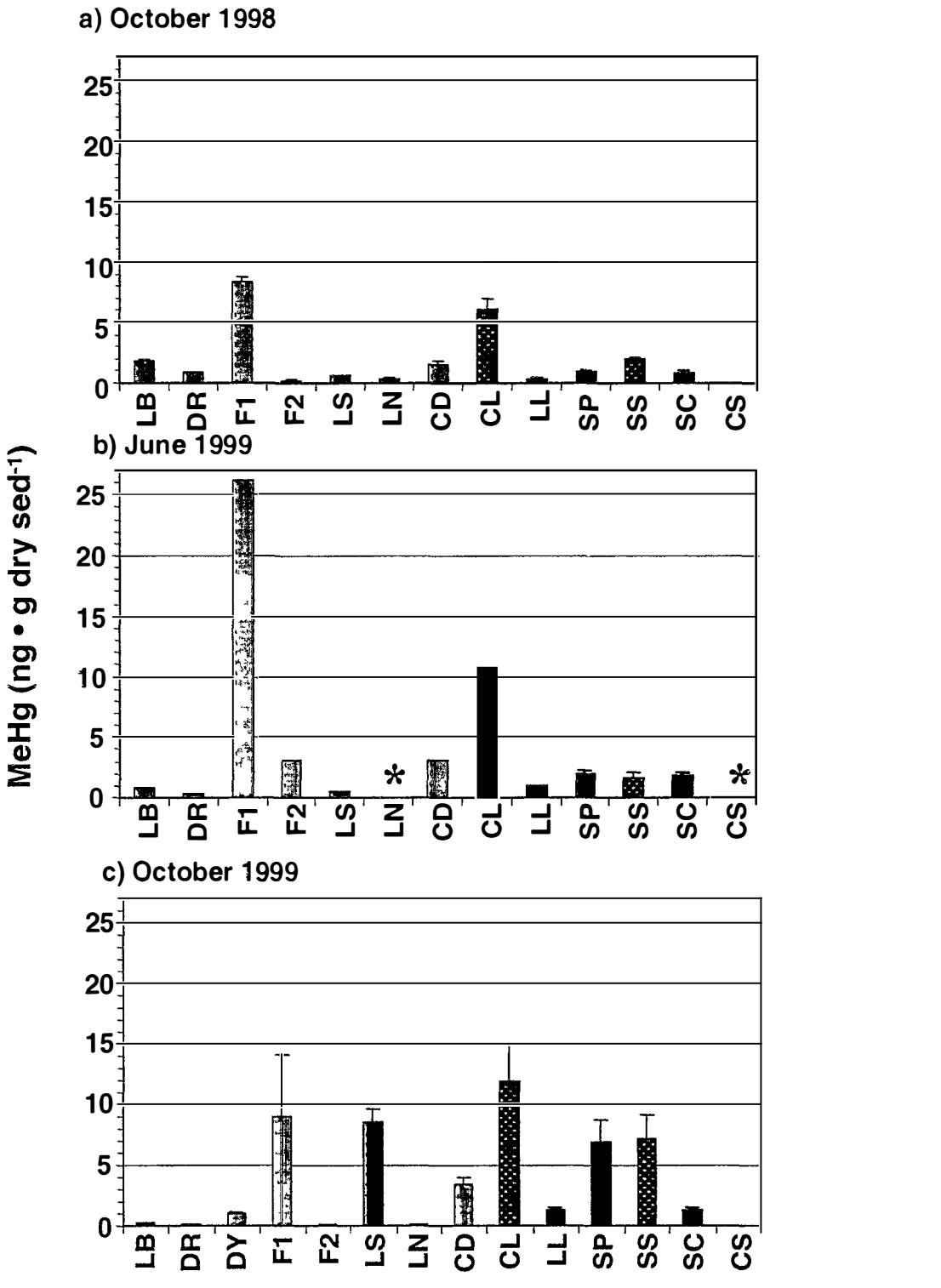

Figure 4. Percent Methylmercury - Surface sediment (0-4 cm)

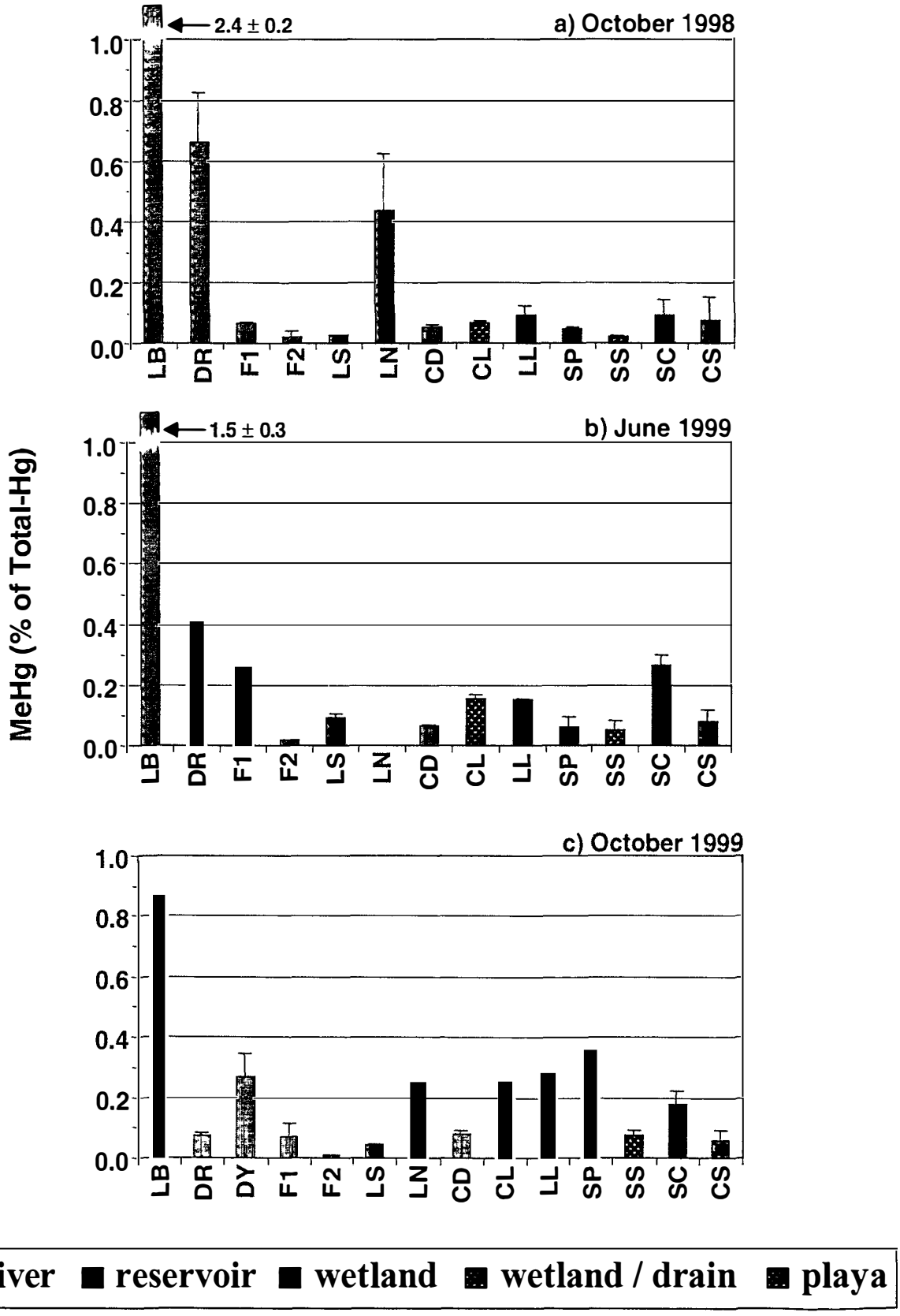

Figure 5. Acid-Extractable "Reactive" Hg(II) - Surface Sediment (0-4 cm)

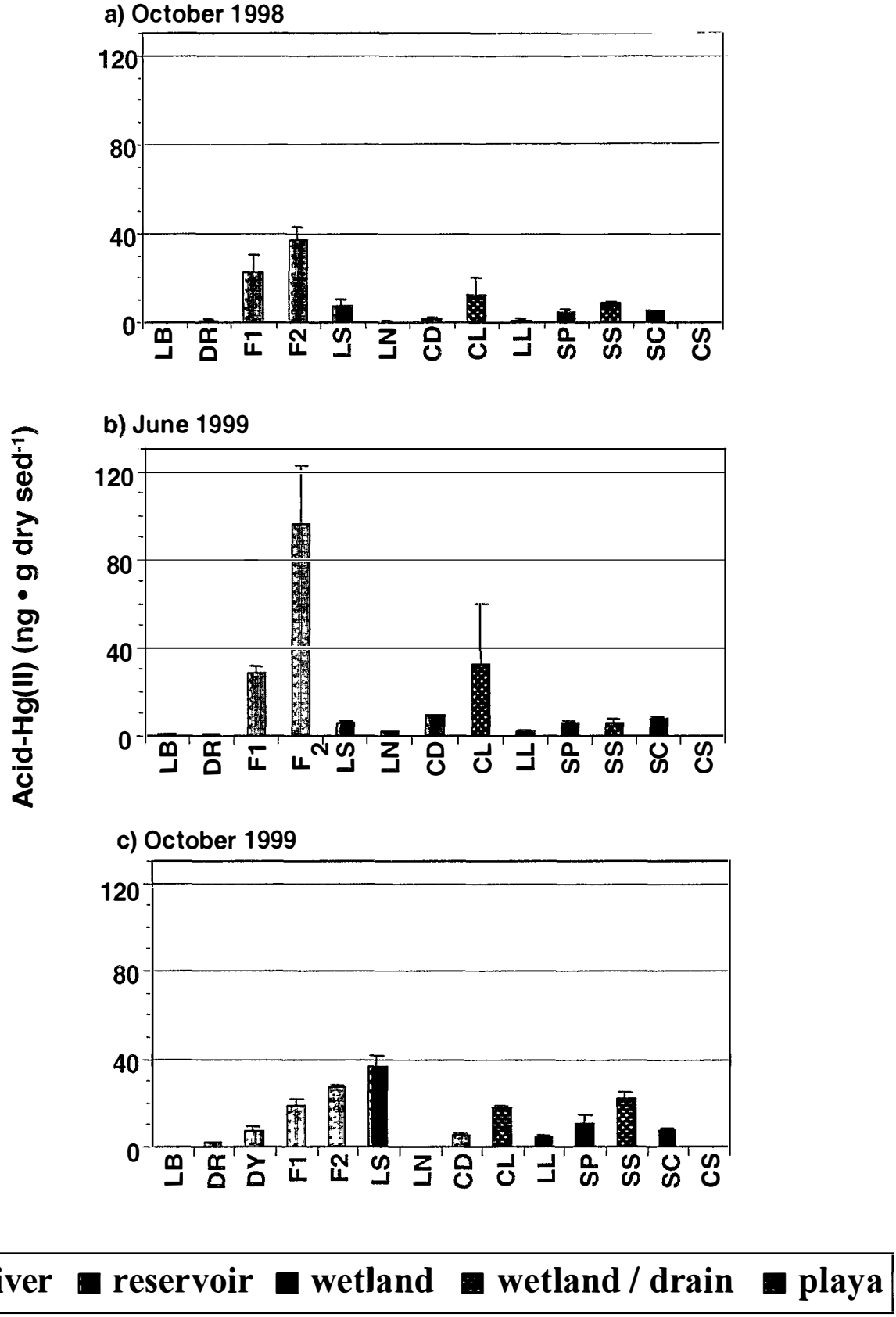

Figure 6. Percent Acid-Extractable "Reactive" Hg(II) Surface Sediment (0-4 cm)

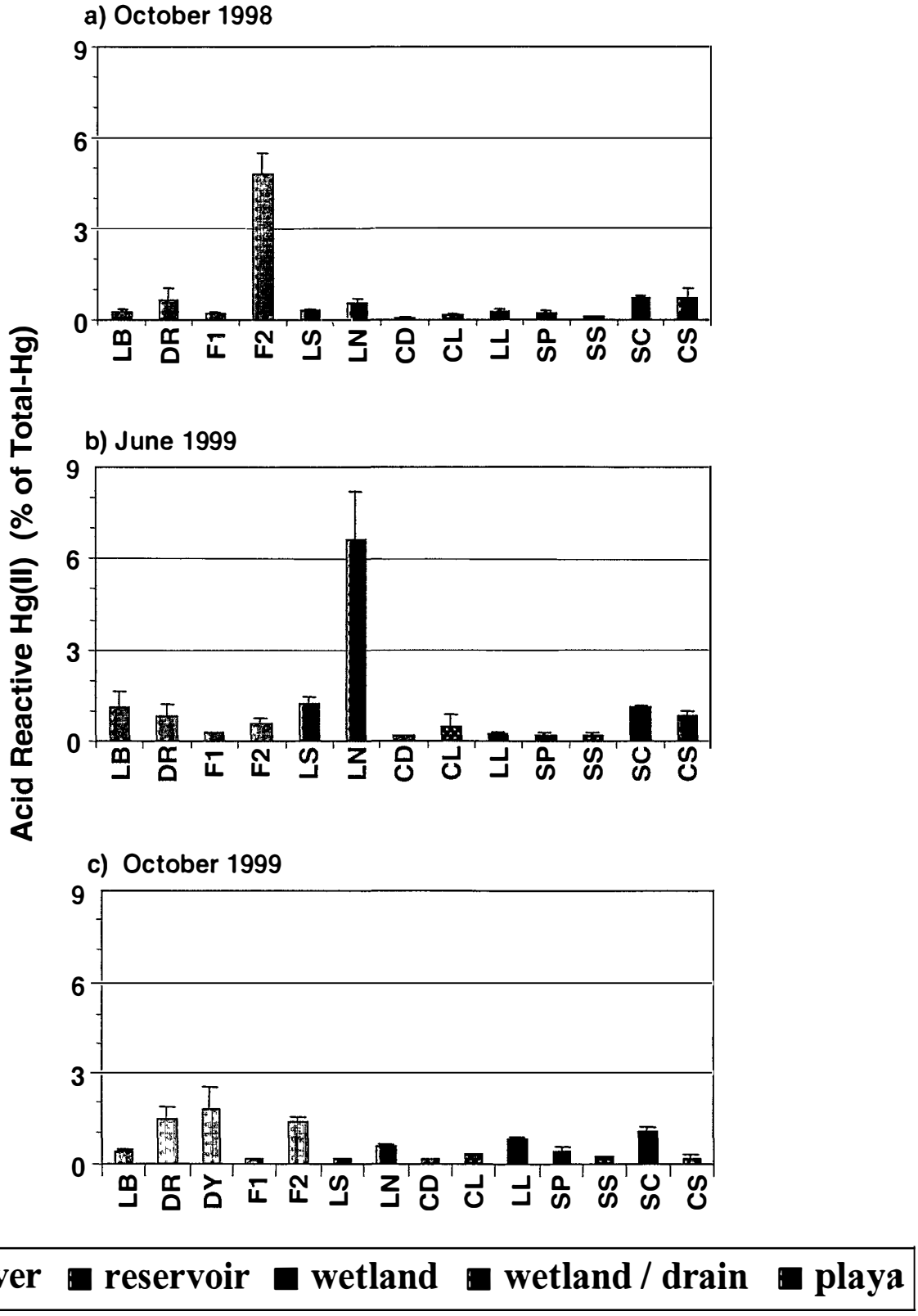

Figure 7. Depth Profiles of Total Mercury & Methylmercury

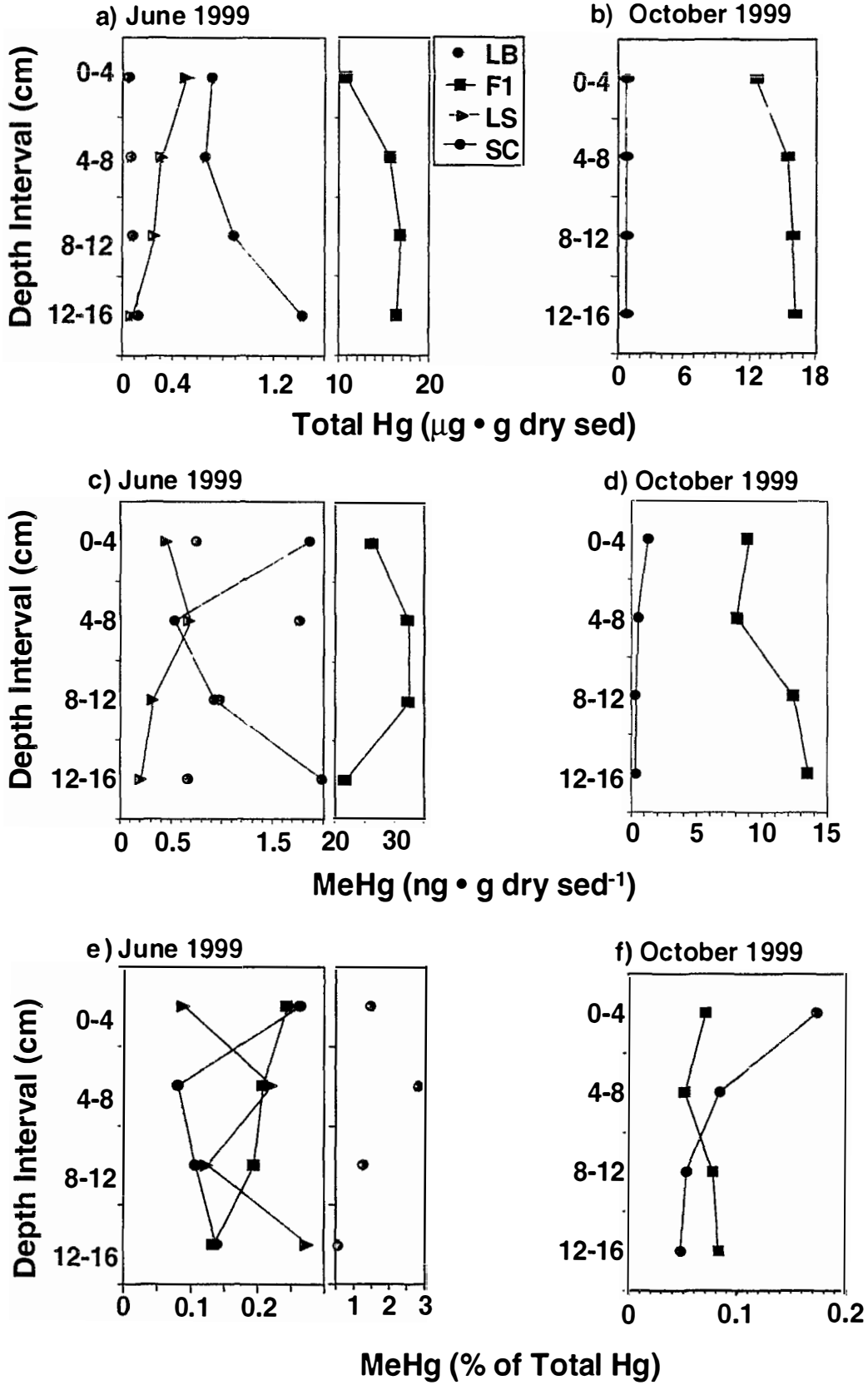

Figure 8. Acid-Extractable "Reactive" Hg(II) Sediment Depth Profiles

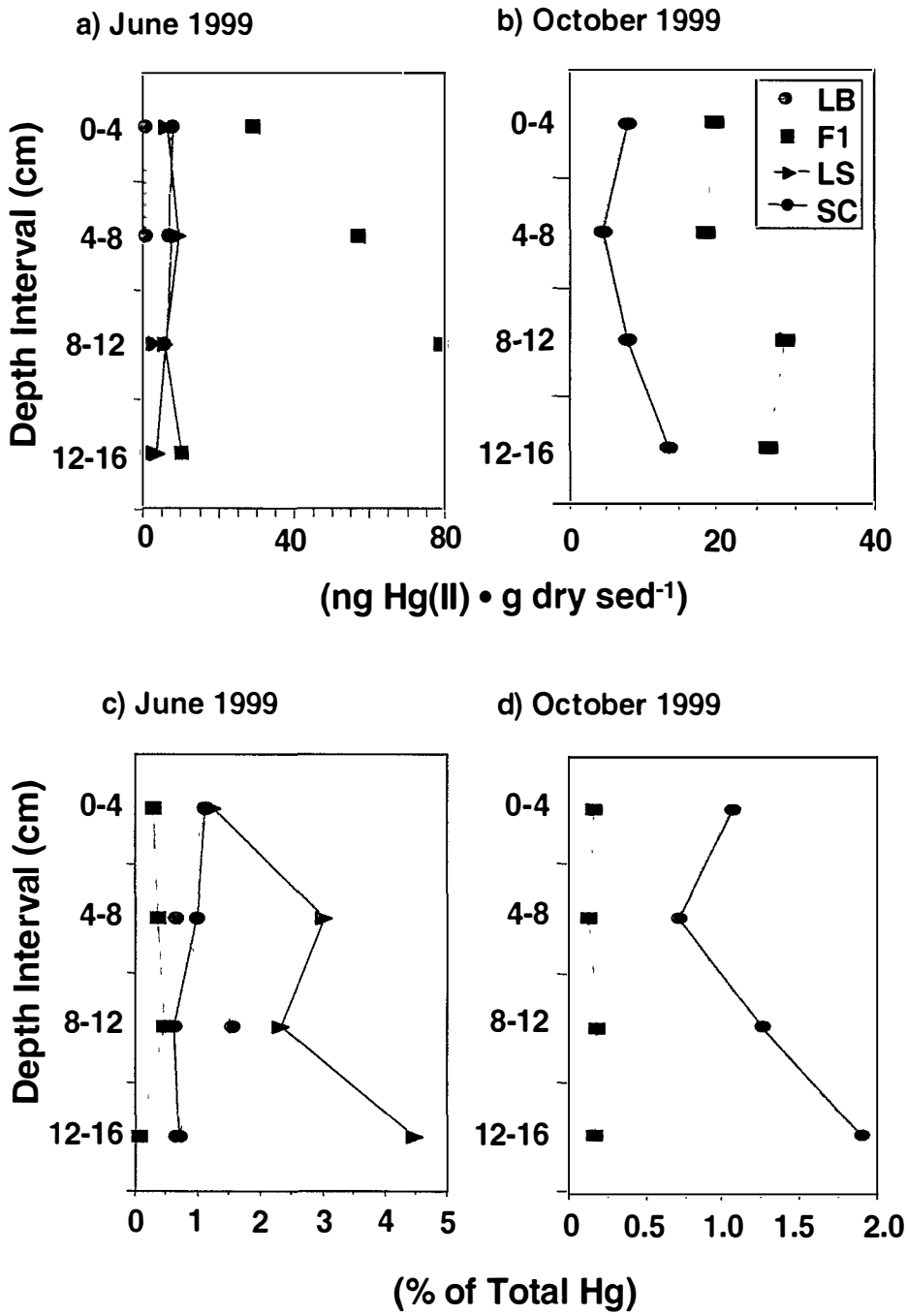

Figure 9. Vertical Bank (Site F3) - Mercury Speciation

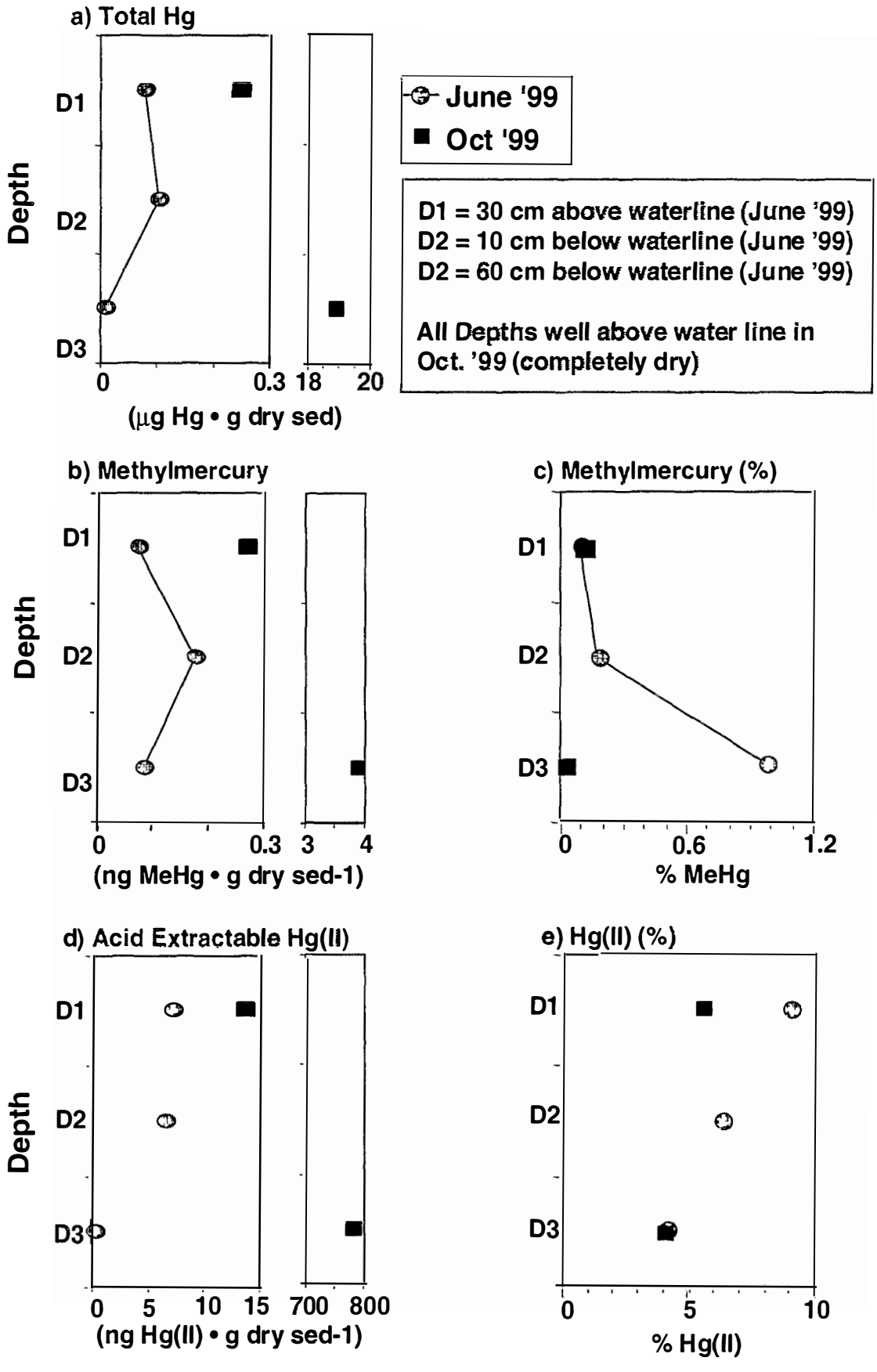

Figure 10. Significant Regressions of Mercury Species

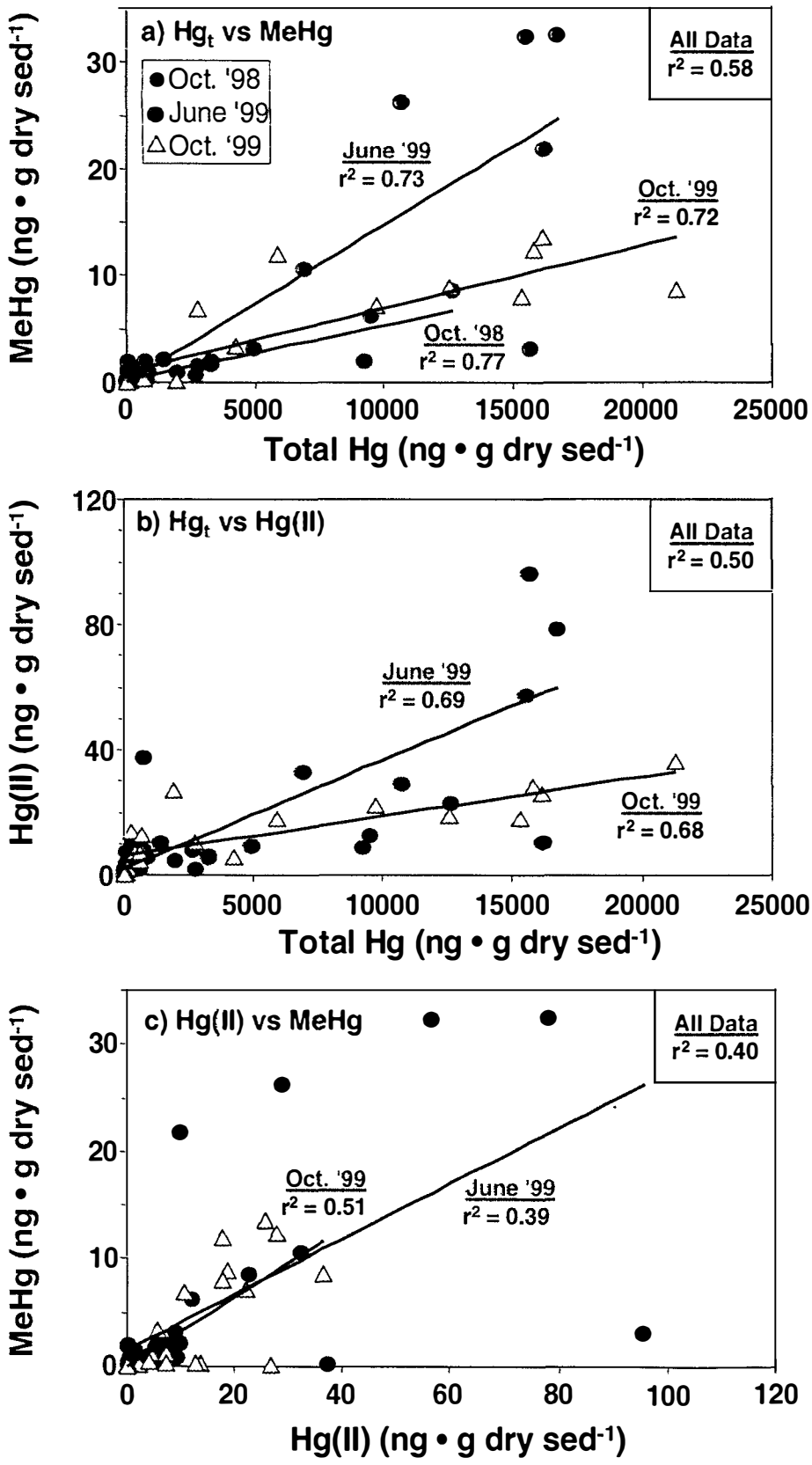

Figure 11. ^{203}Hg-Methylation Rate Constant Surface Sediment (0-4 cm)

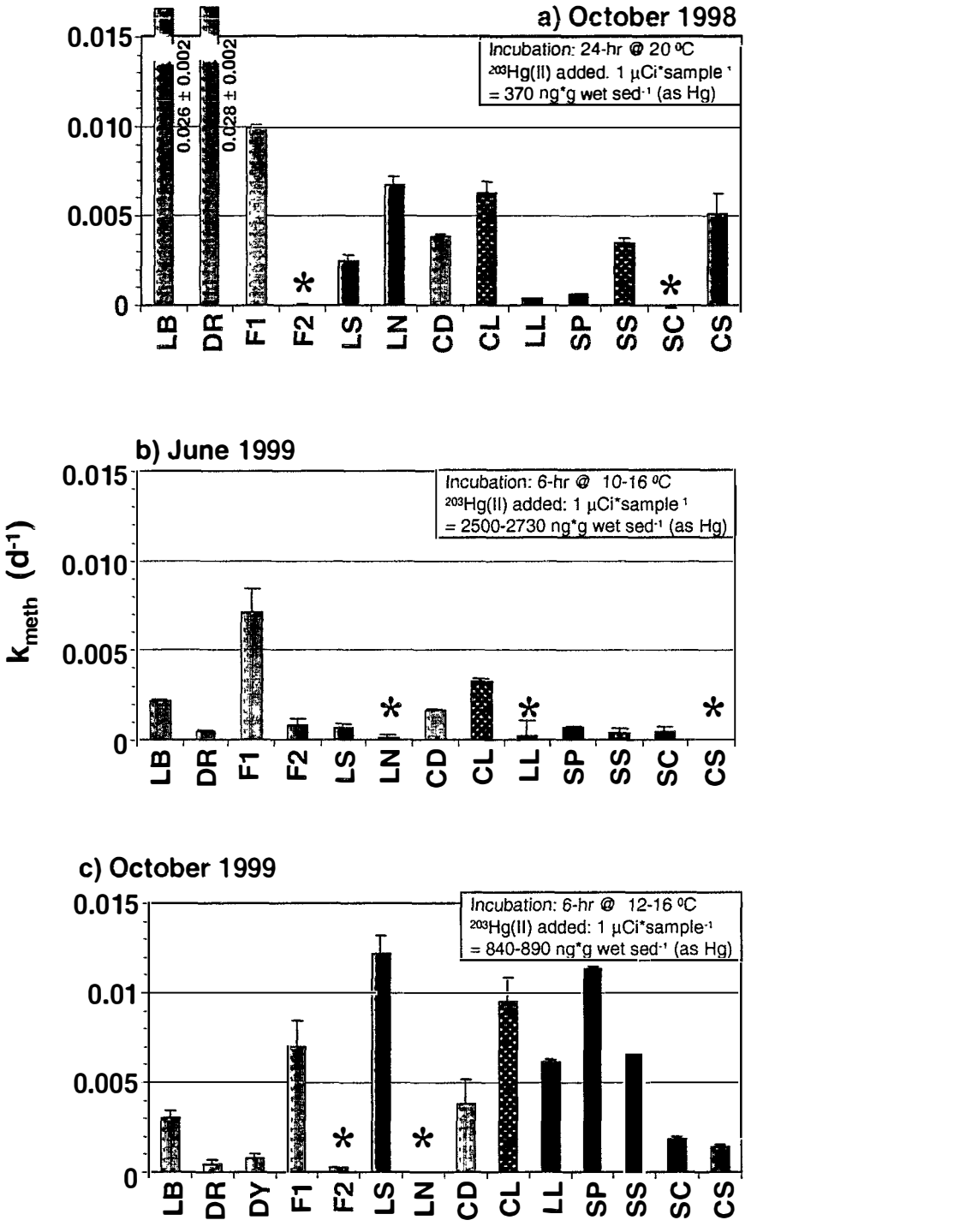

river reservoir wetland wetland / drain playa

* = below detection limit

Figure 12. ^{14}C-MeHg Degradation Rate Constant Surface Sediment (0-4 cm)

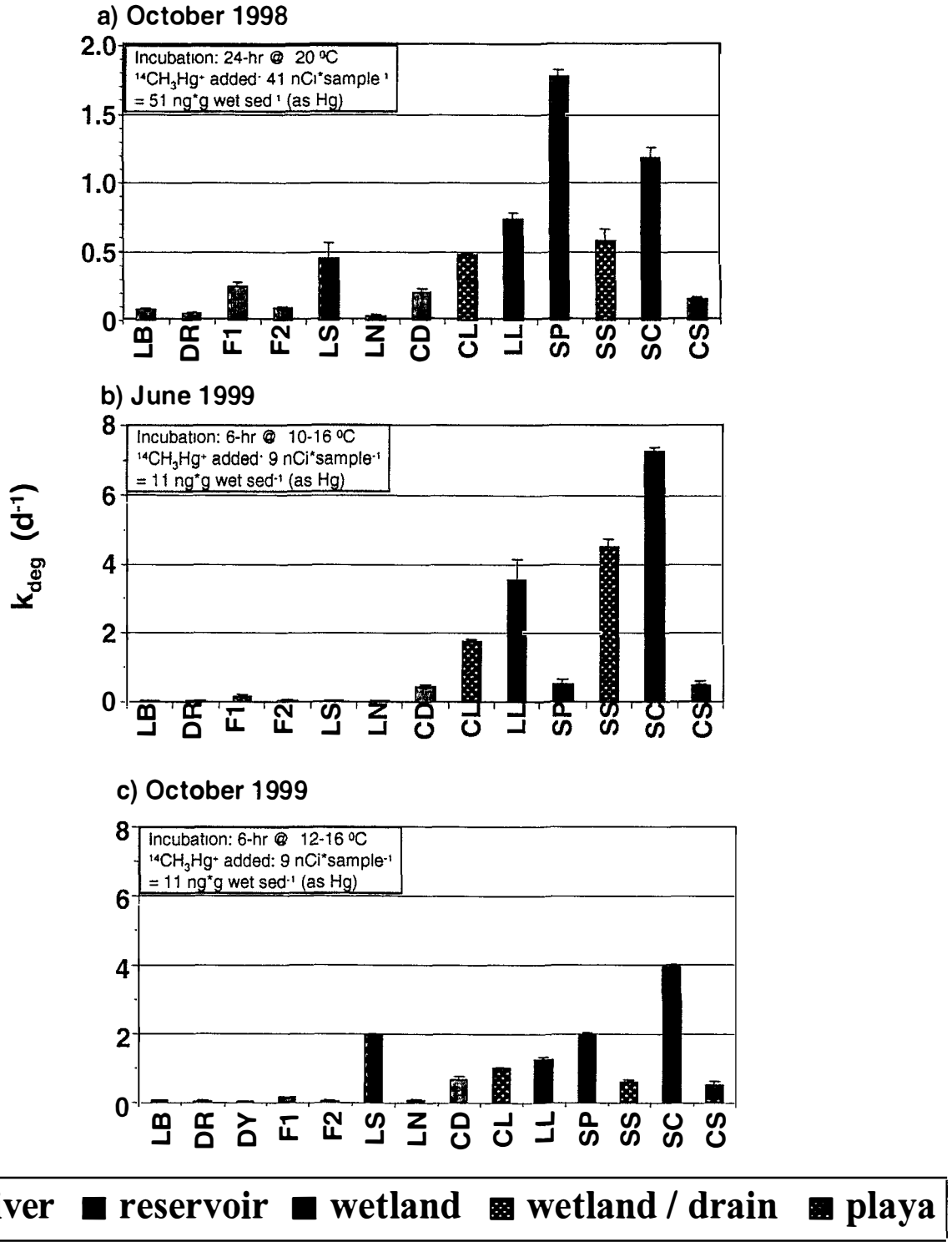

Figure 13. ^{203}Hg-Methylation and ^{14}C-MeHg Degradation Rate Constants Depth Profiles

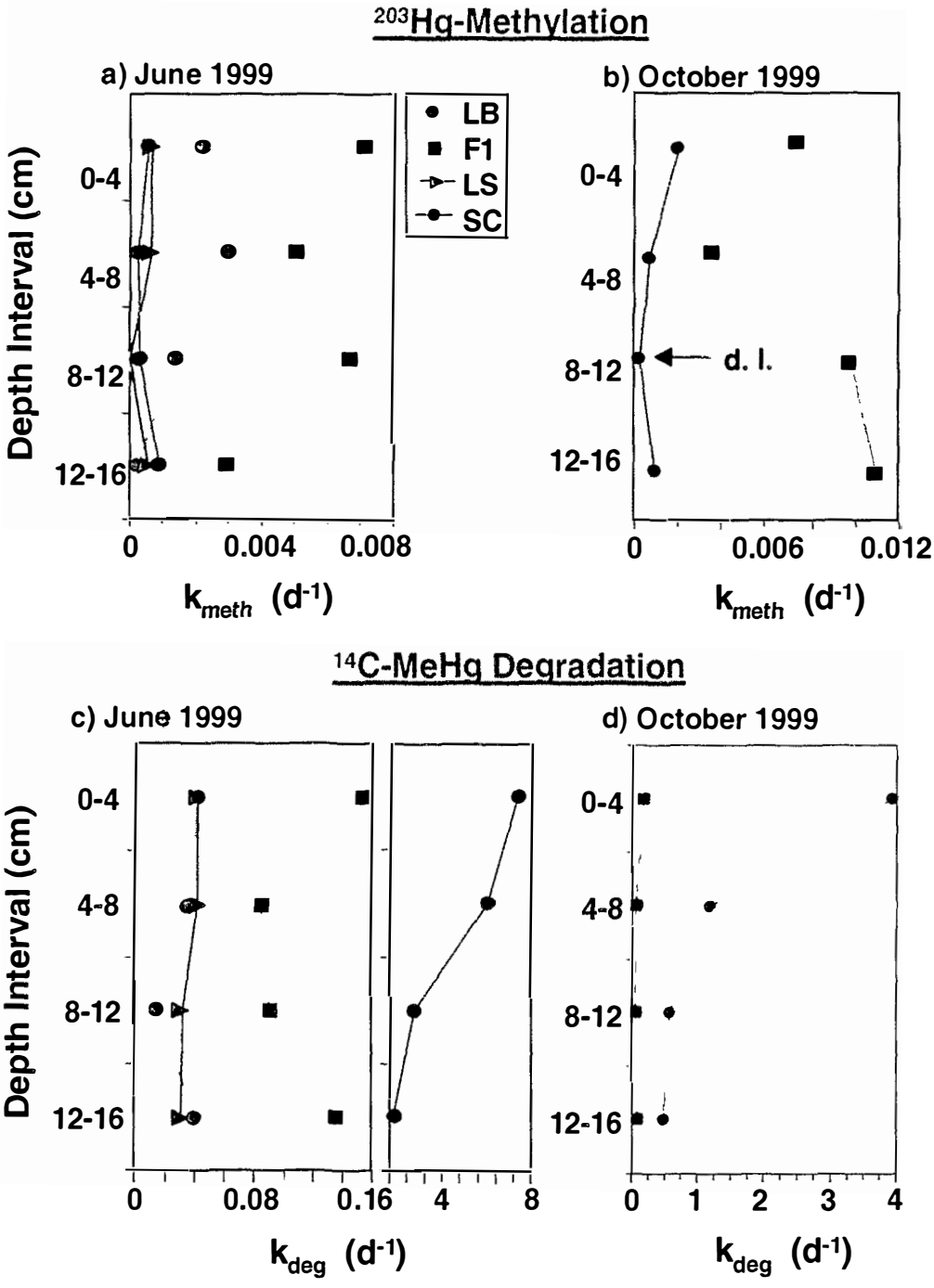

Figure 14. ^{203}Hg-Methylation and ^{14}C-MeHg Degradation Rate Constants Vertical Bank (Site F3)

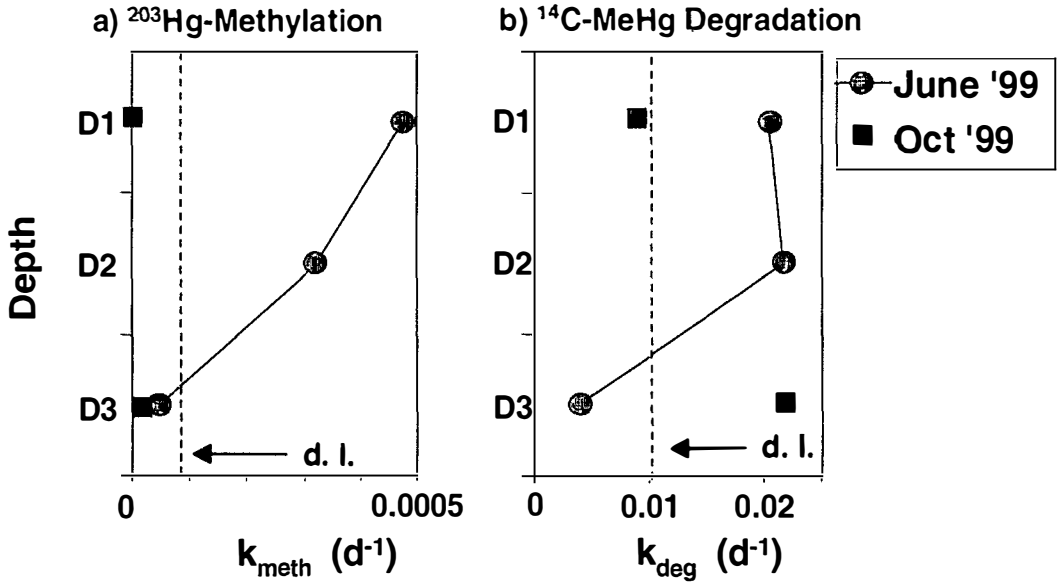

D1 = 30 cm above waterline (June '99)
D2 = 10 cm below waterline (June '99)
D2 = 60 cm below waterline (June '99)

All Depths well above water line in Oct. '99 (completely dry)

Figure 15. Variable $^{203}Hg(II)$ Specific Activity Experiment

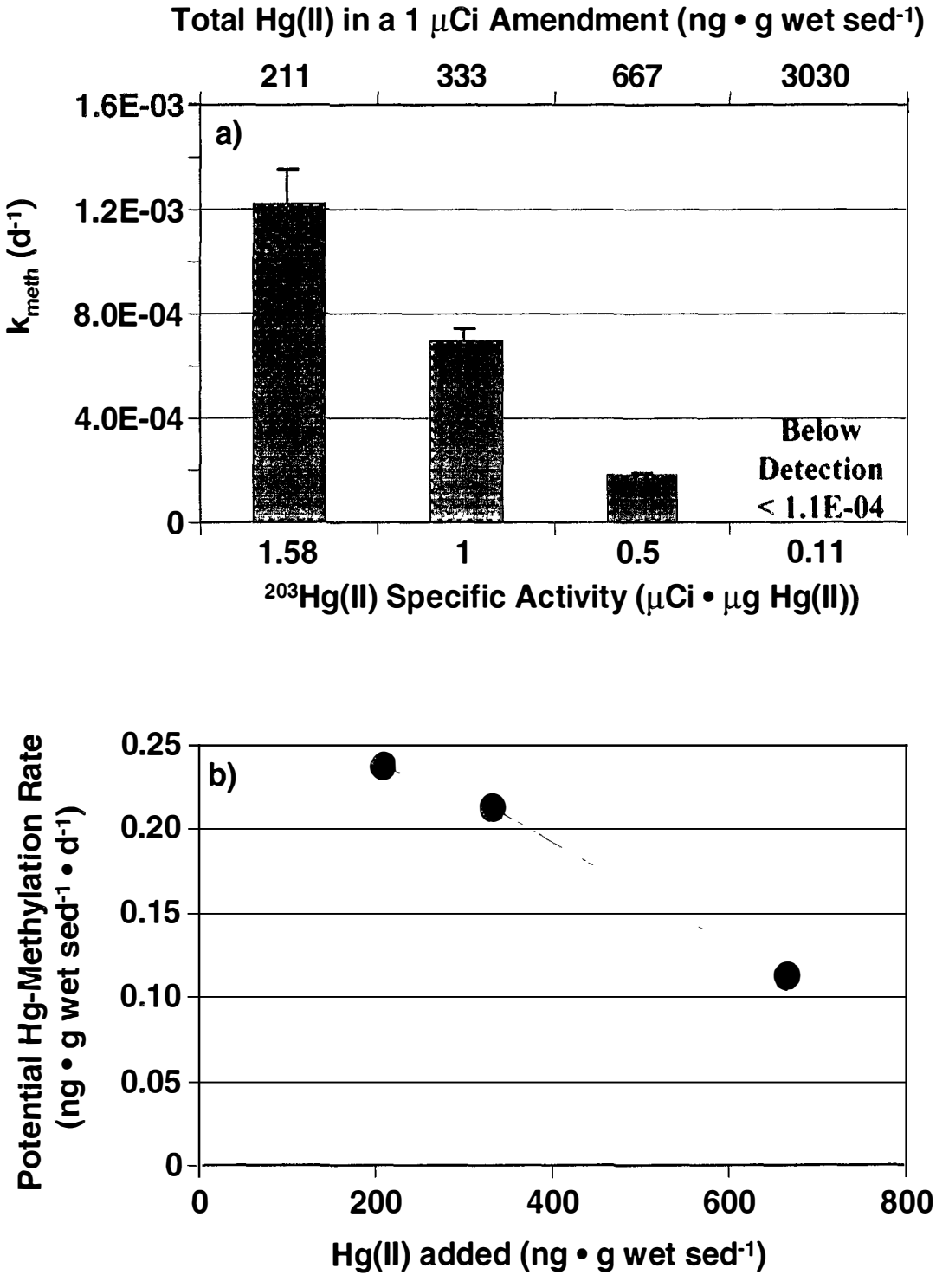

Figure 16. Time Course Incubations - Site F1 (0-4 cm)

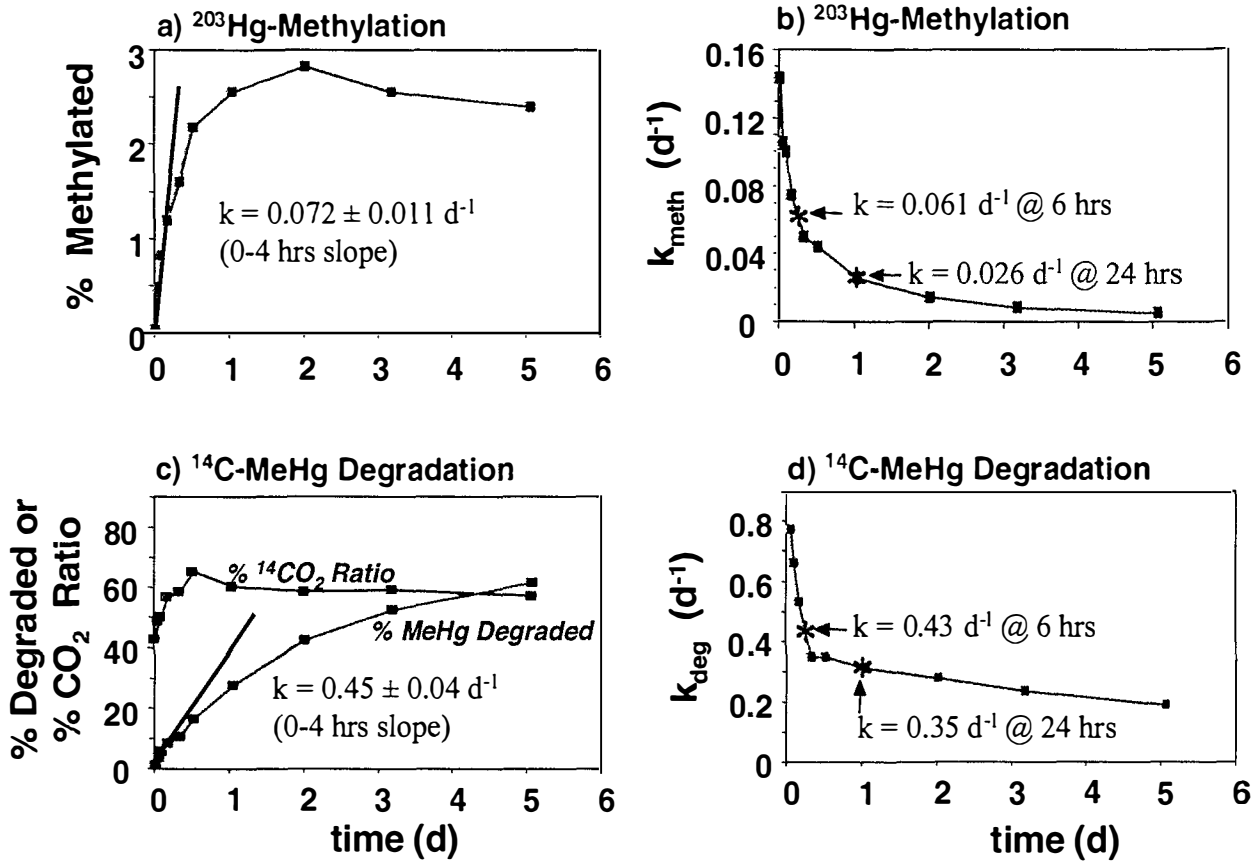

Figure 17. In-Situ MeHg Production Rates - Surface Sediment (0-4 cm)

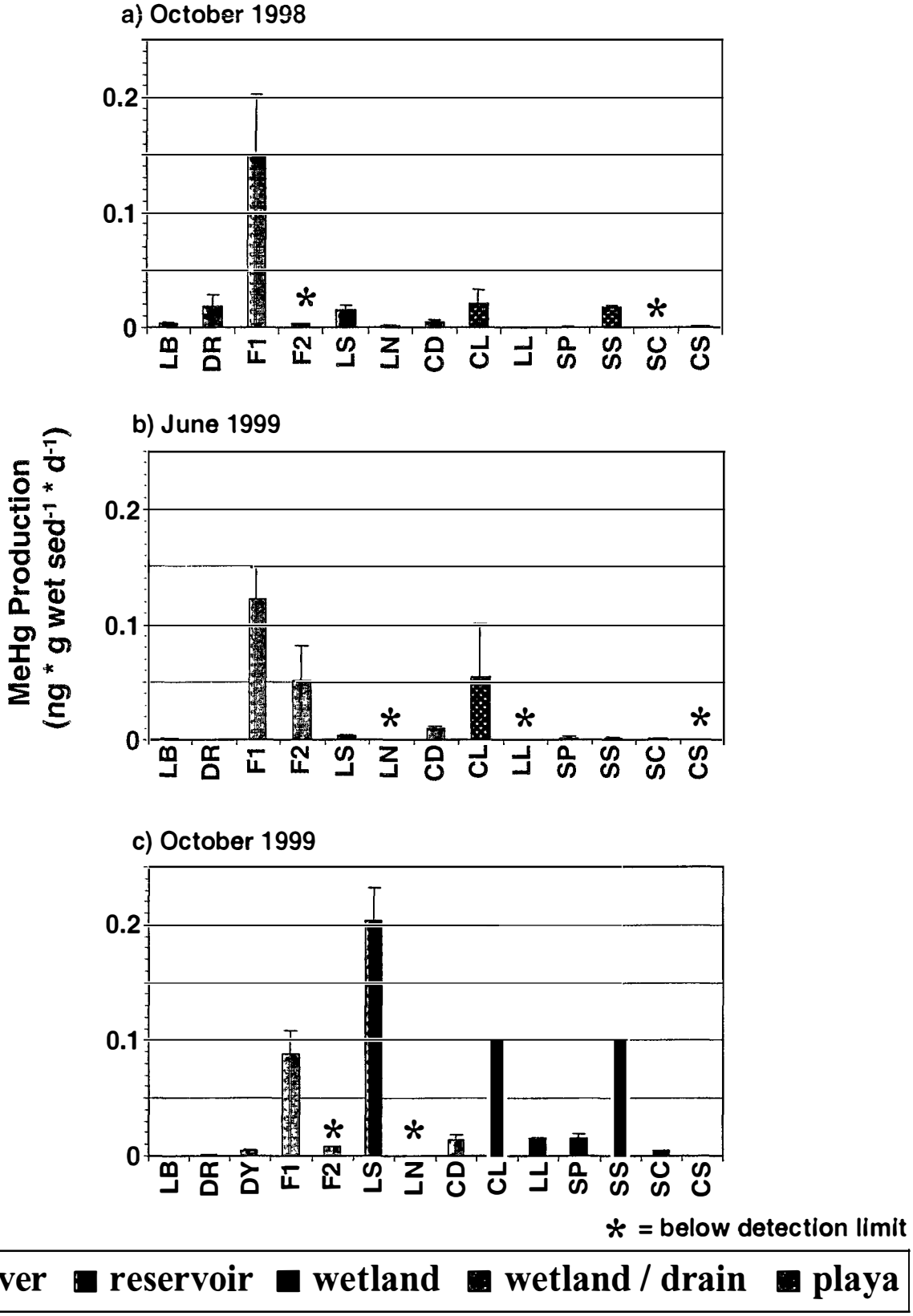

Figure 18. In-Situ MeHg Degradation Rates - Surface Sediment (0-4 cm)

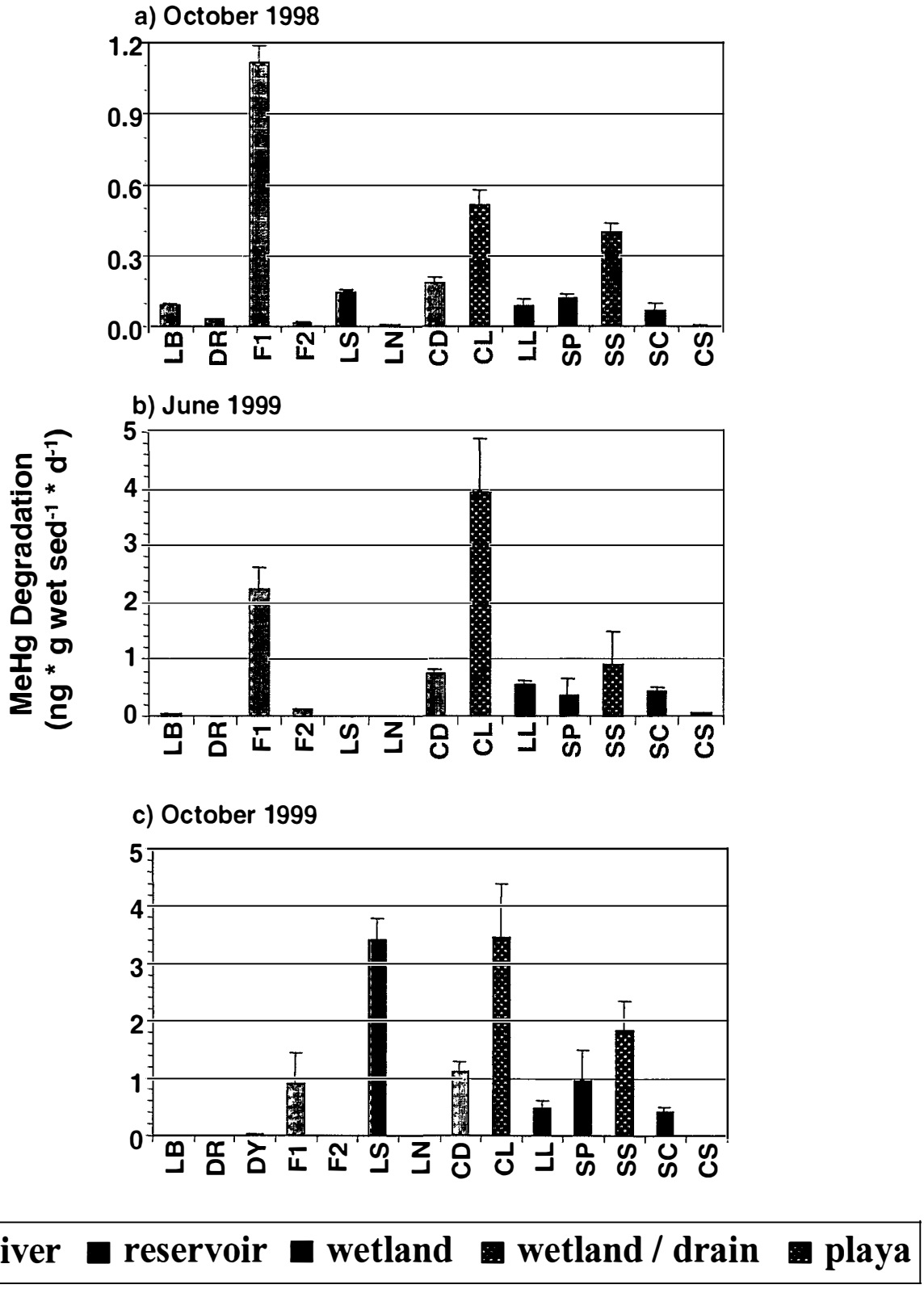

Figure 19. In-Situ MeHg Production and Degradation Rates

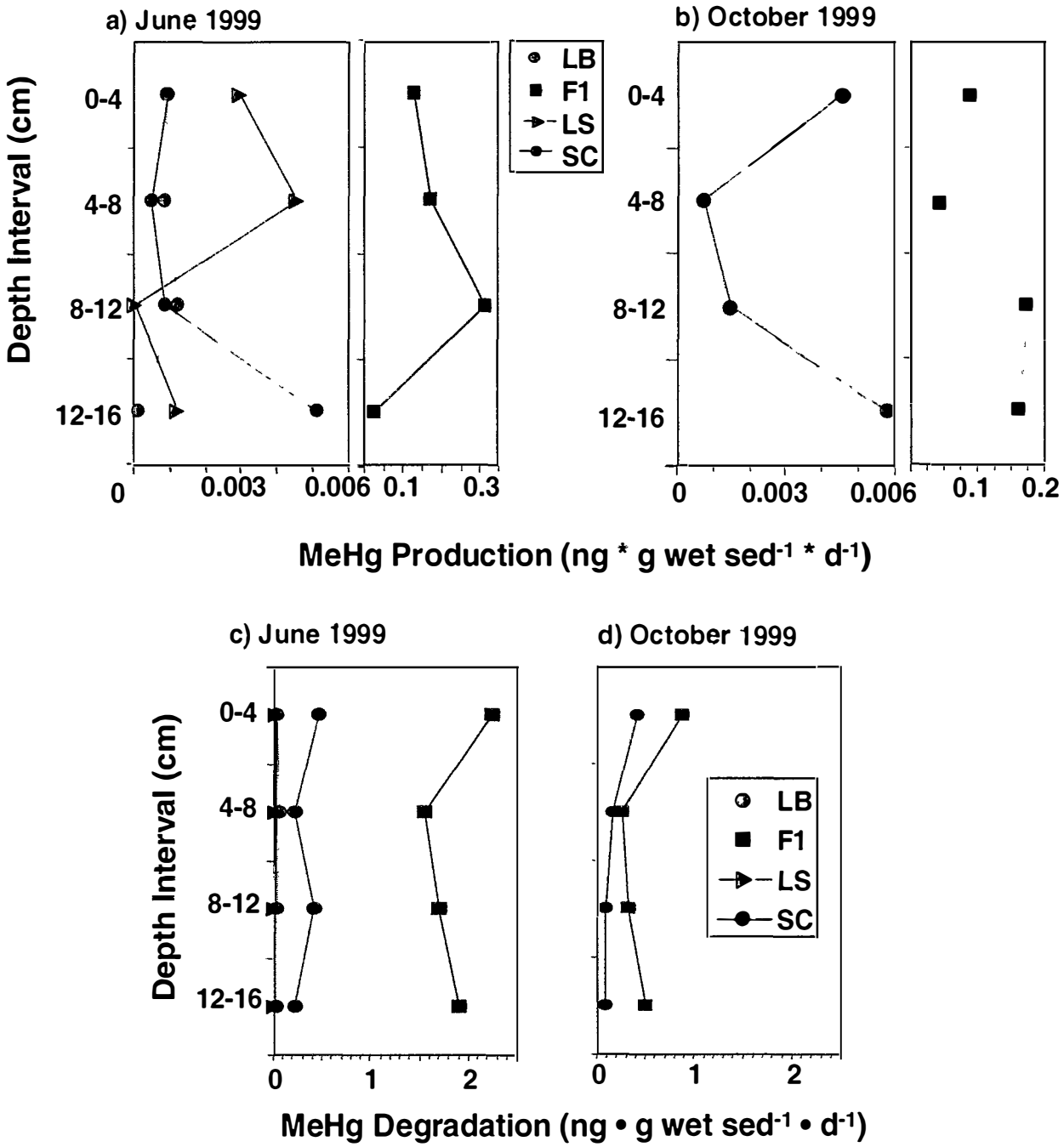

Figure 20. In-Situ MeHg Production and Degradation Rates Vertical Bank (Site F3) – June 1999 only

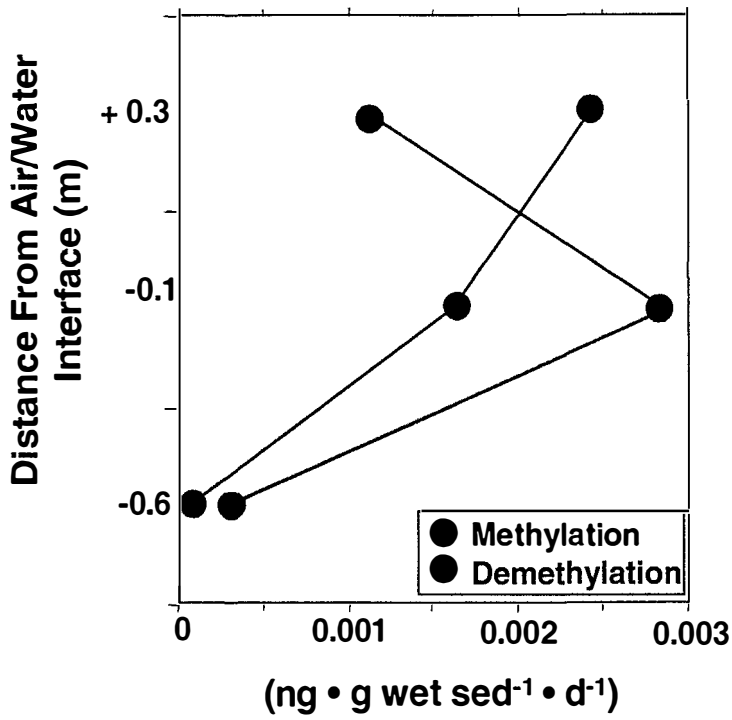

Figure 21. Methylation / Demethylation Ratios (Potential Rates) Surface (0-4) cm Sediment

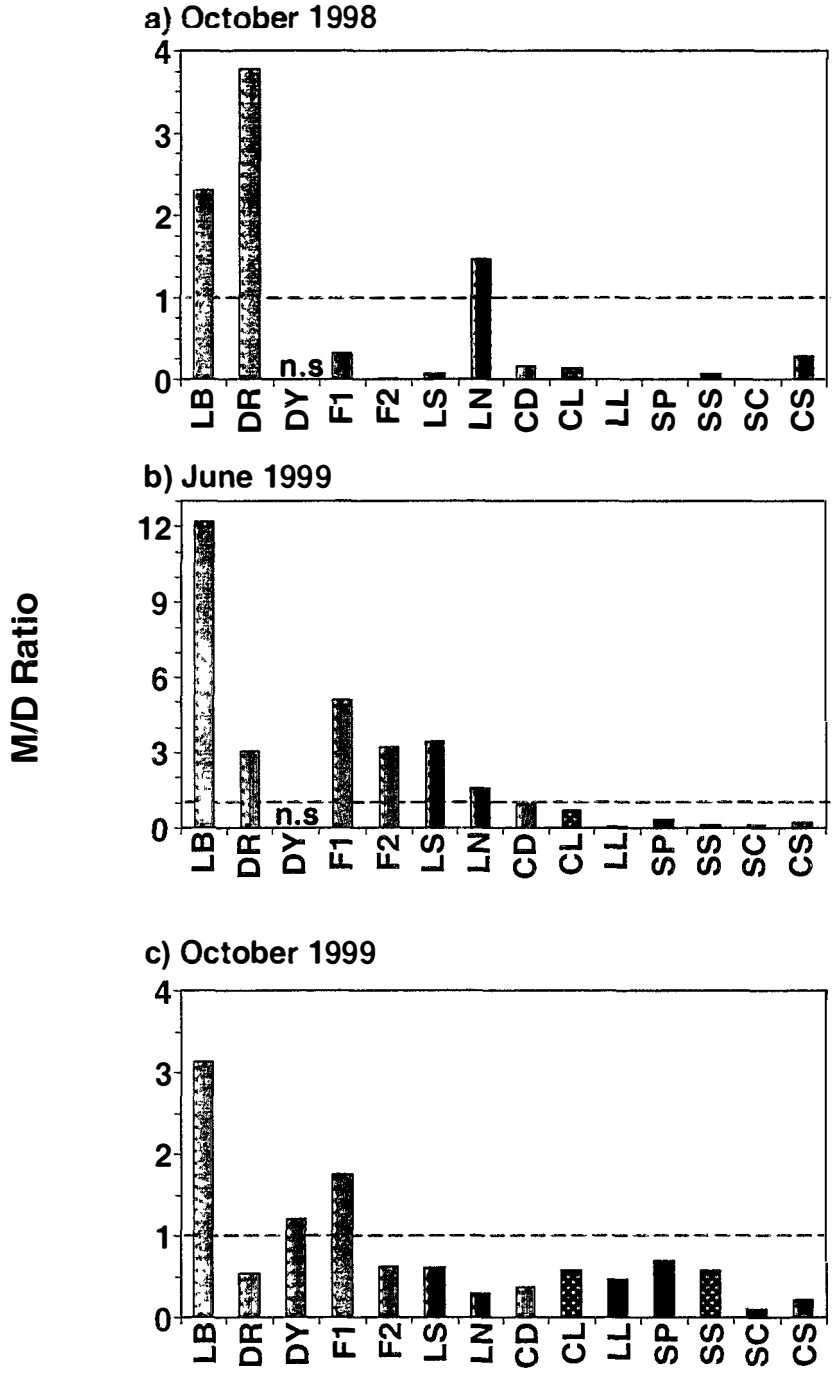

n.s.= not sampled

Figure 22. Methylation / Demethylation Ratios (Potential Rates) Depth Profiles

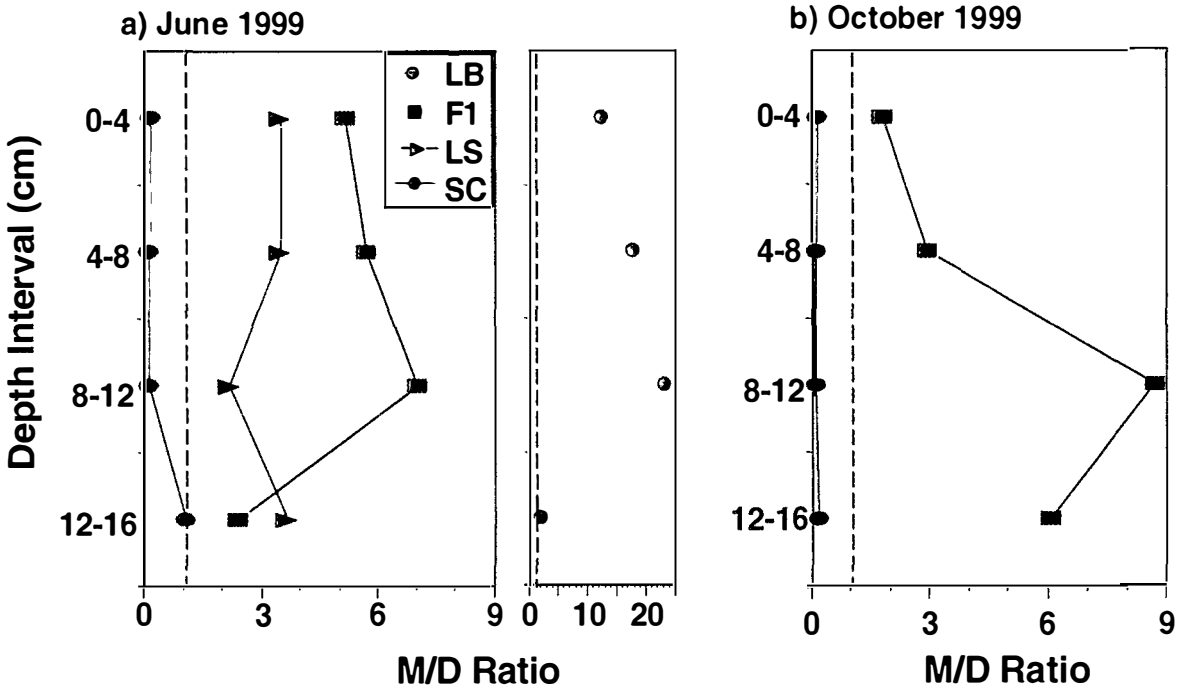

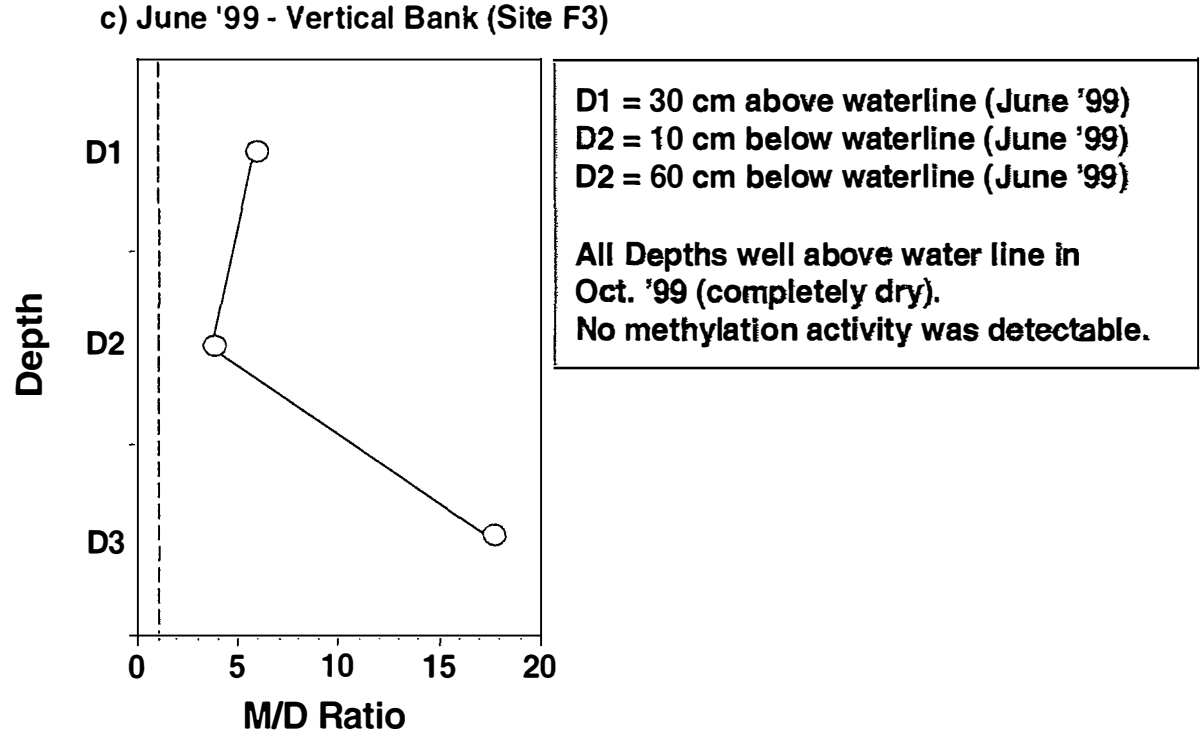

D1 = 30 cm above waterline (June '99)
D2 = 10 cm below waterline (June '99)
D2 = 60 cm below waterline (June '99)

All Depths well above water line in Oct. '99 (completely dry).
No methylation activity was detectable.

Figure 23. In-Situ Acid-Extractable Hg(II) and Total-Hg vs. Hg-Methylation Rate Constant (June & October, 1999)

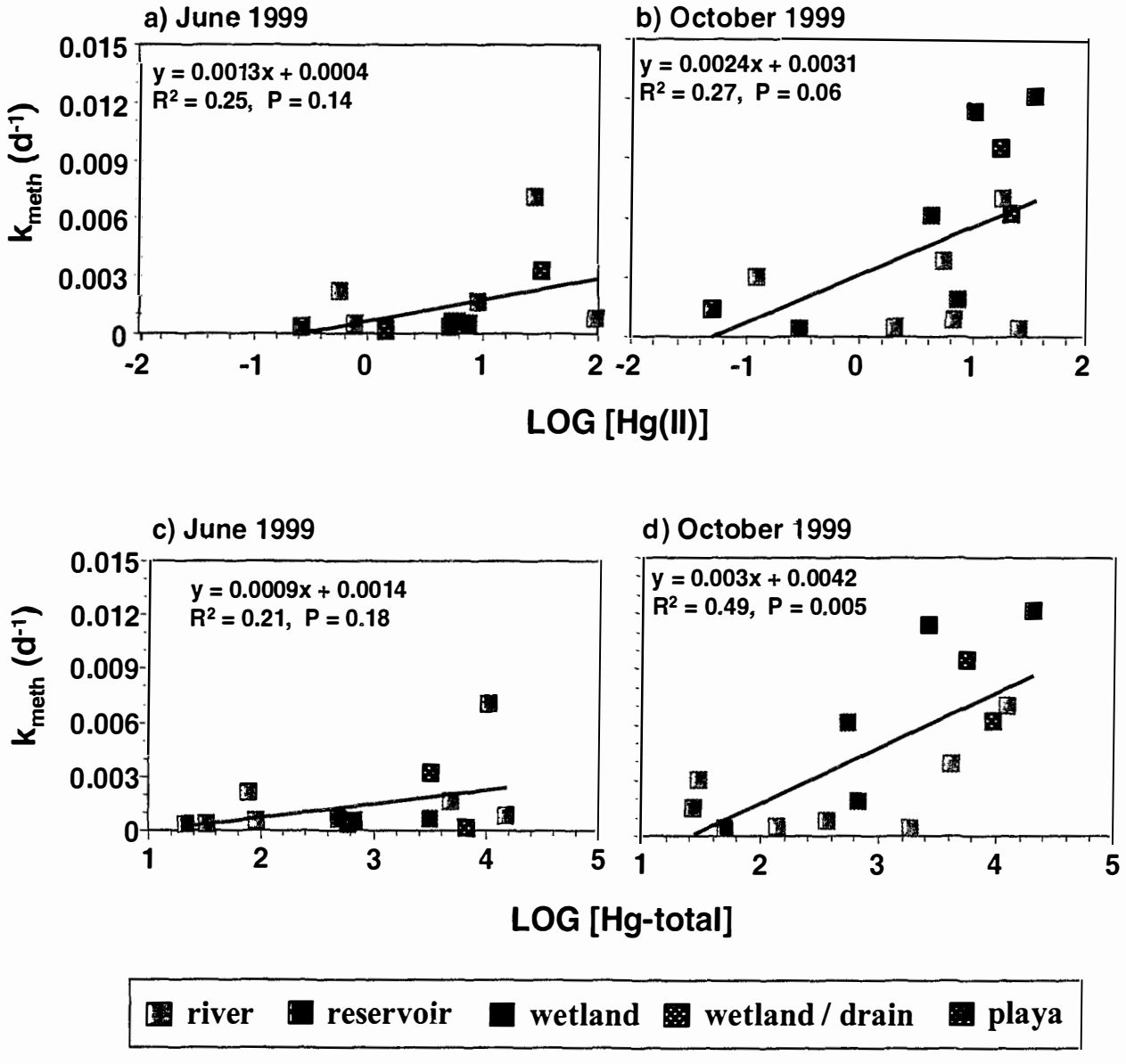

Figure 24. $^{203}Hg(II)$ Extraction Experiment

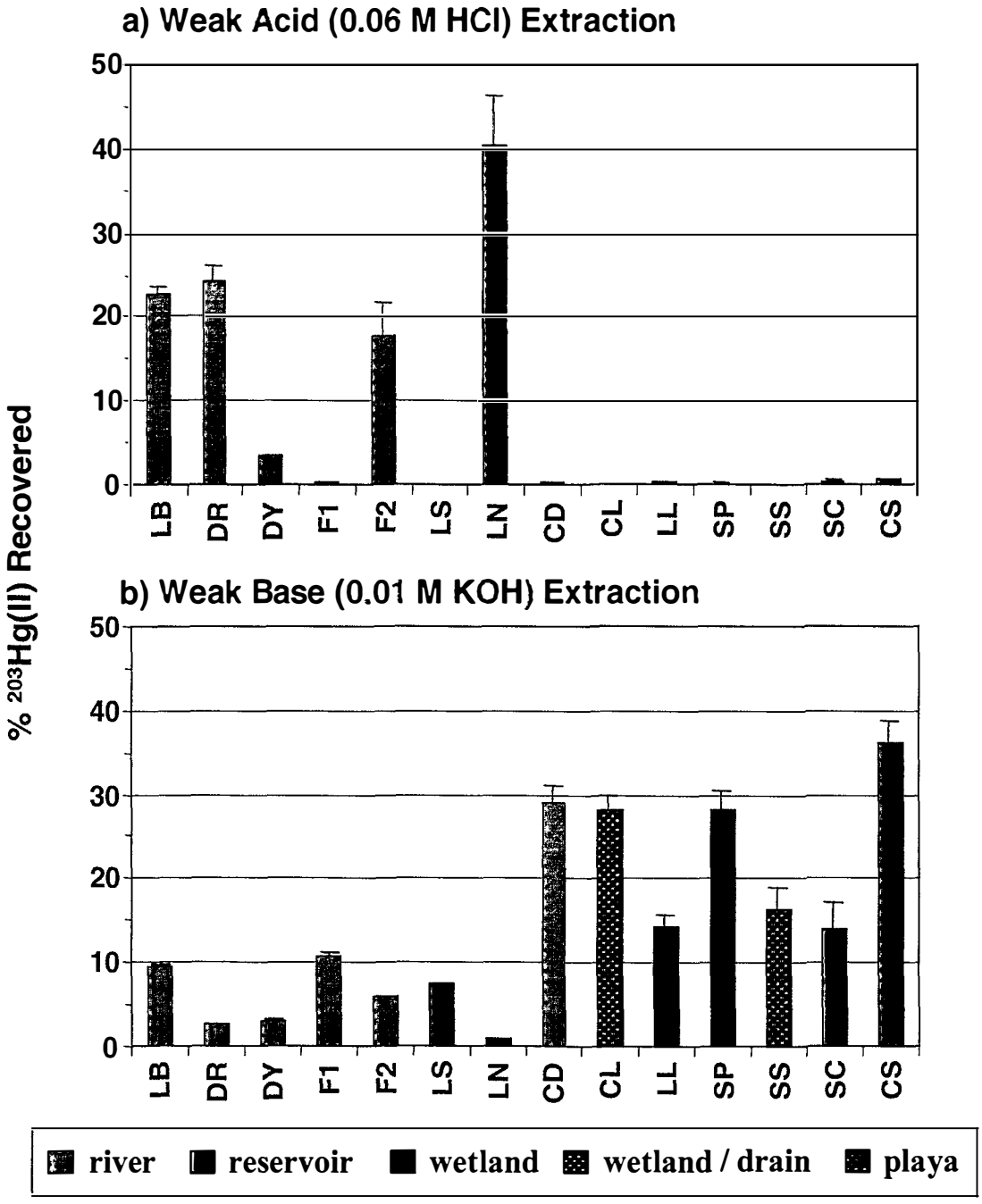

Figure 25. Percent Acid/Base Extractable $^{203}Hg(II)$ versus Sediment Acid Volatile Reduced Sulfur and Organic Content

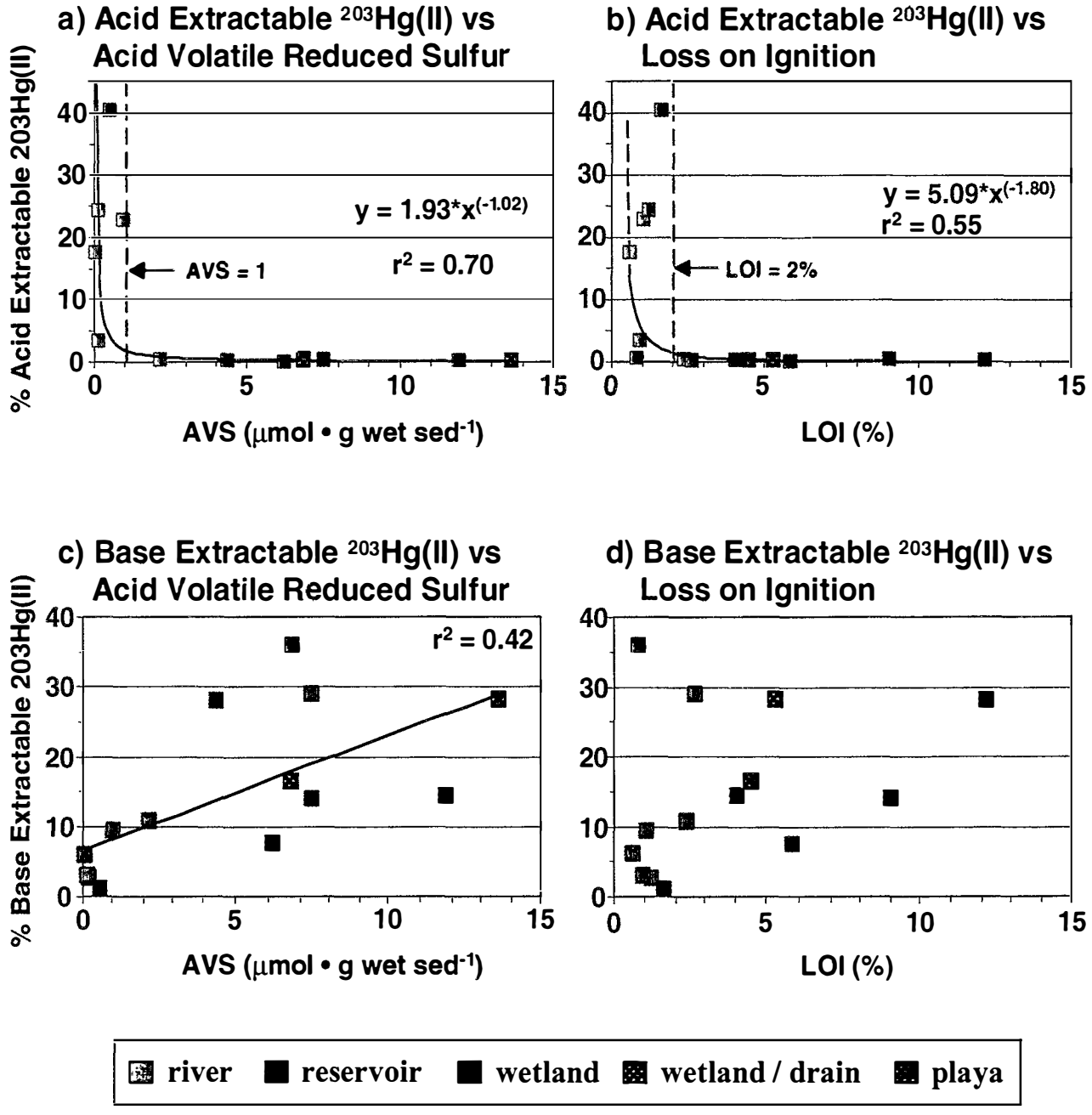

Figure 26. Microbial Sulfate Reduction

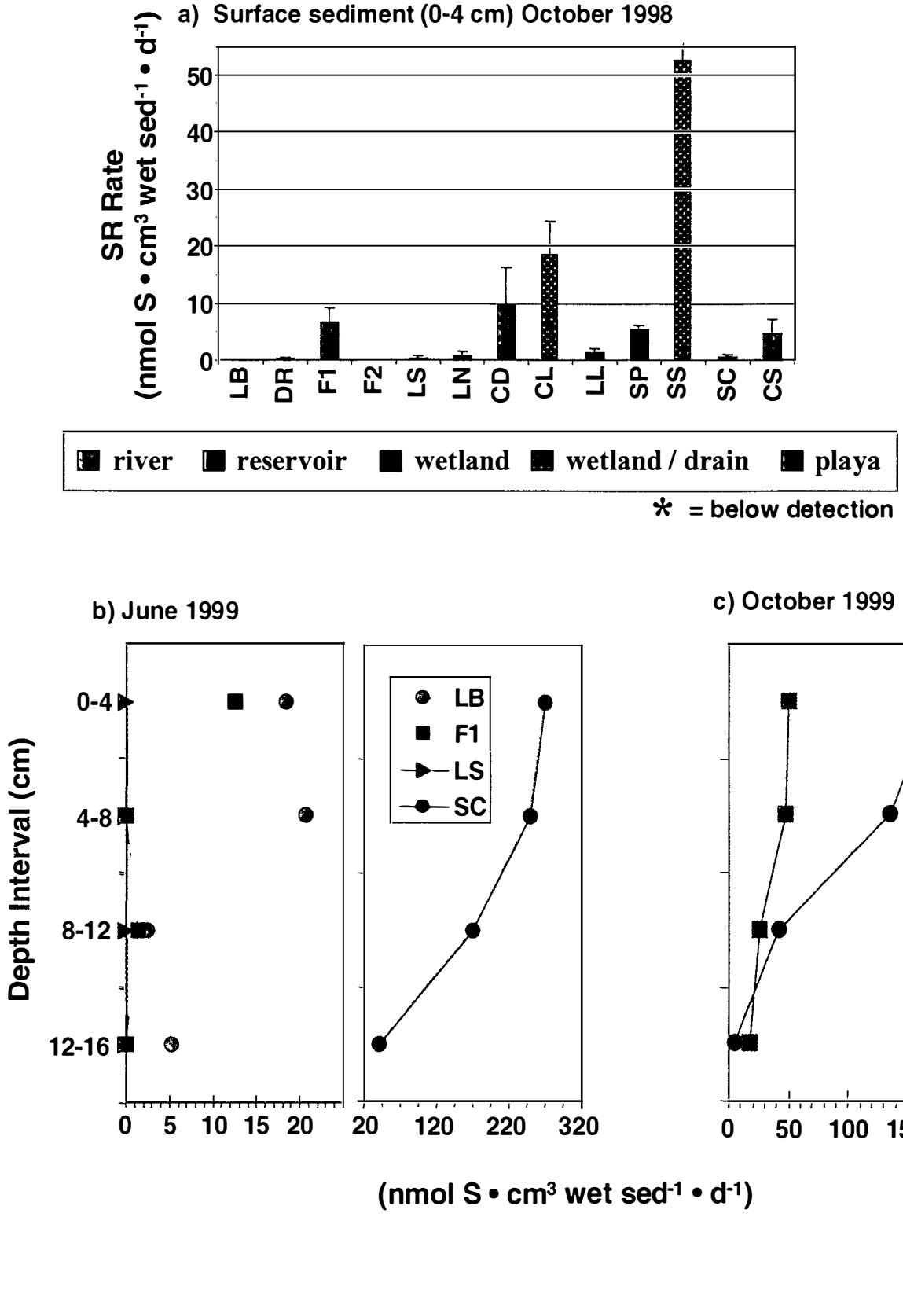

Figure 27. Sediment Acid Volatile Sulfur Surface Sediment (0-4 cm)

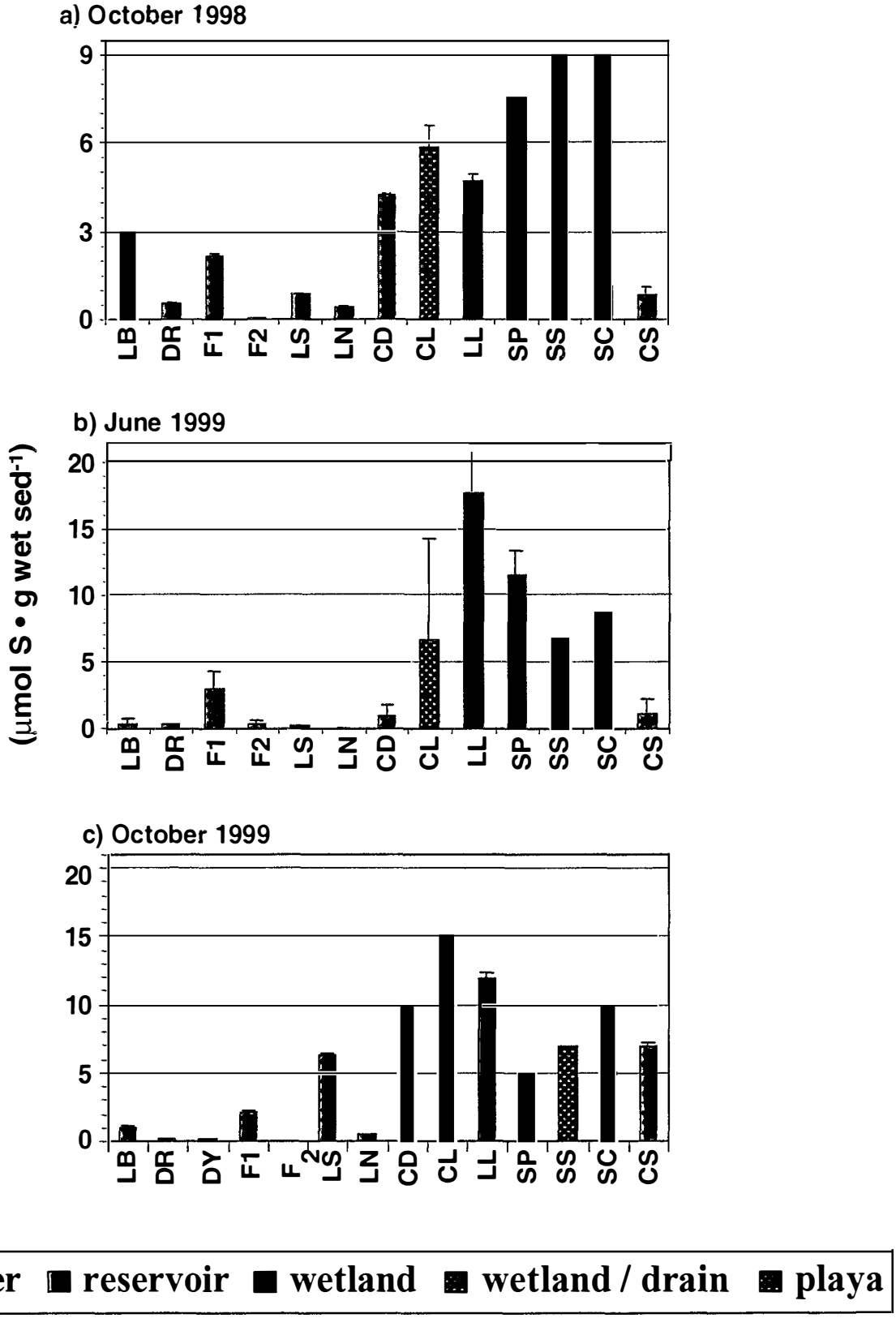

Figure 28. Sediment Acid Volatile Sulfur - Depth Profile

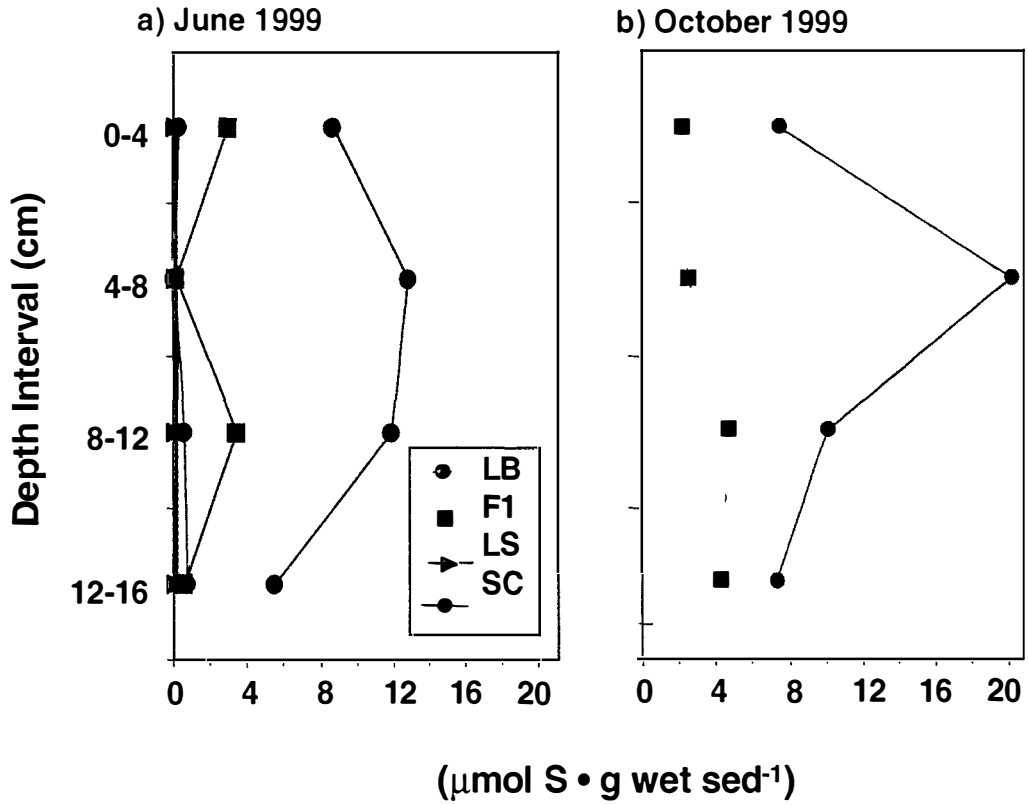

Figure 29. Pore Water Sulfide

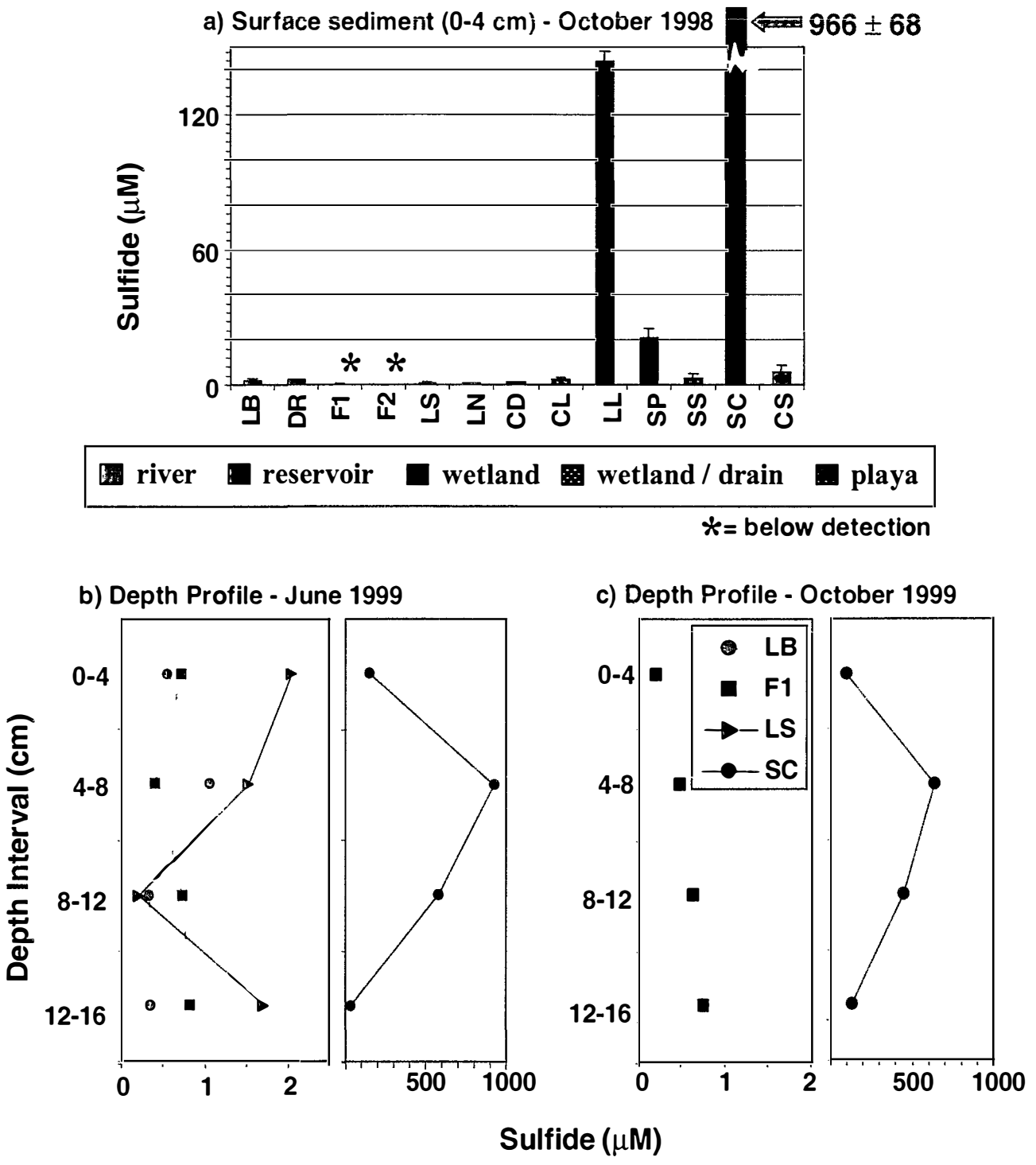

Figure 30. The Influence of Reduced Sulfur on MeHg Production

a) Sites below Lahontan Dam (0-4 cm, Oct. 1998):
Hg-methylation Rate Constant vs Porewater H_2S

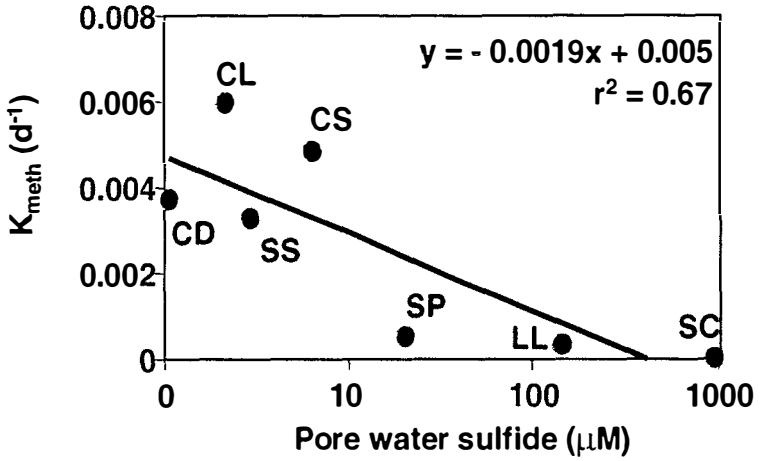

b) Wetland Site SC (all depths):
Hg-methylation Rate Constant vs Porewater H_2S

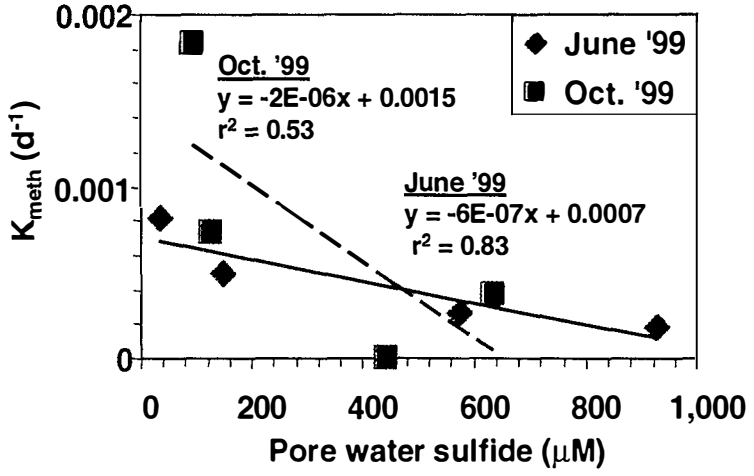

c) All Sites: Sediment AVS vs % Acid-Extractable Hg(II)

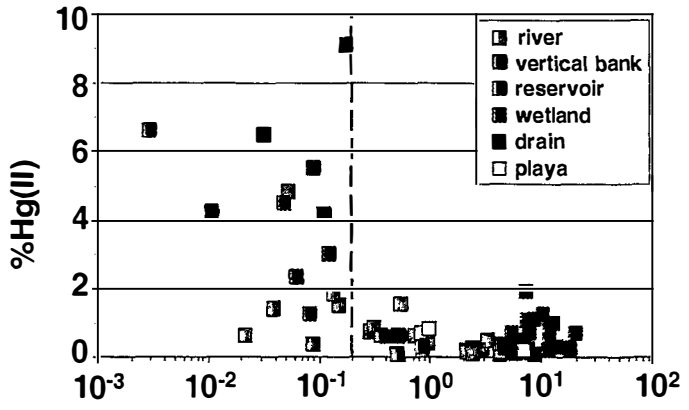

Figure 31. Microbial Methane Production (Methanogenesis)

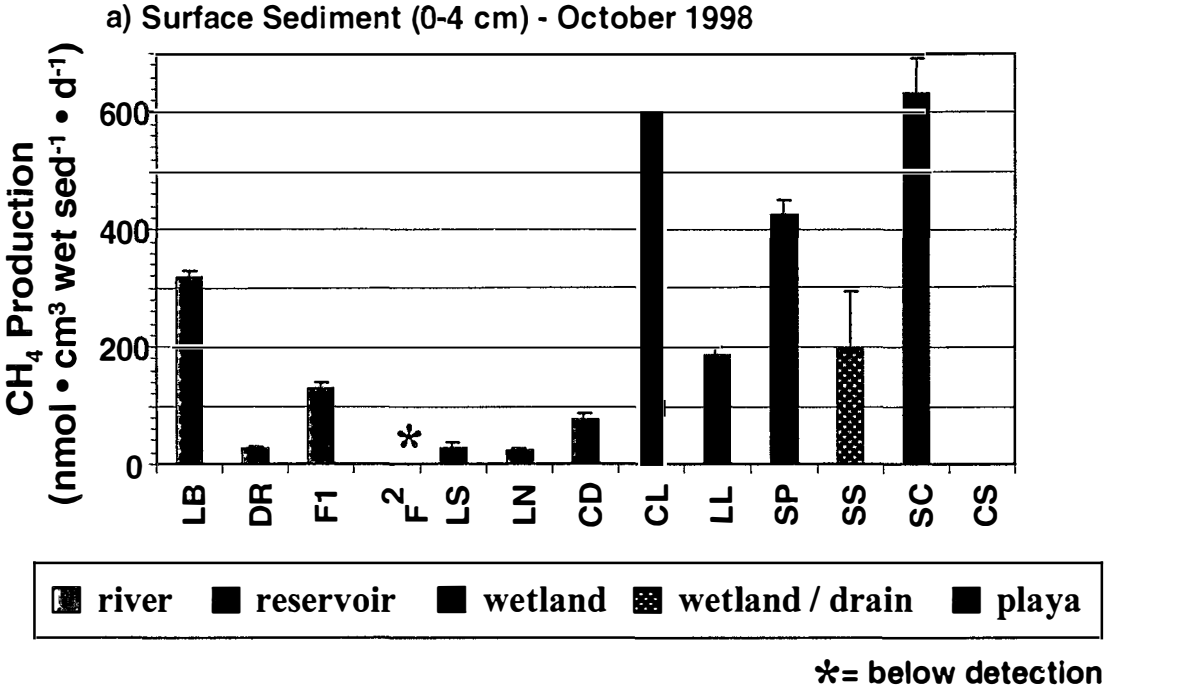

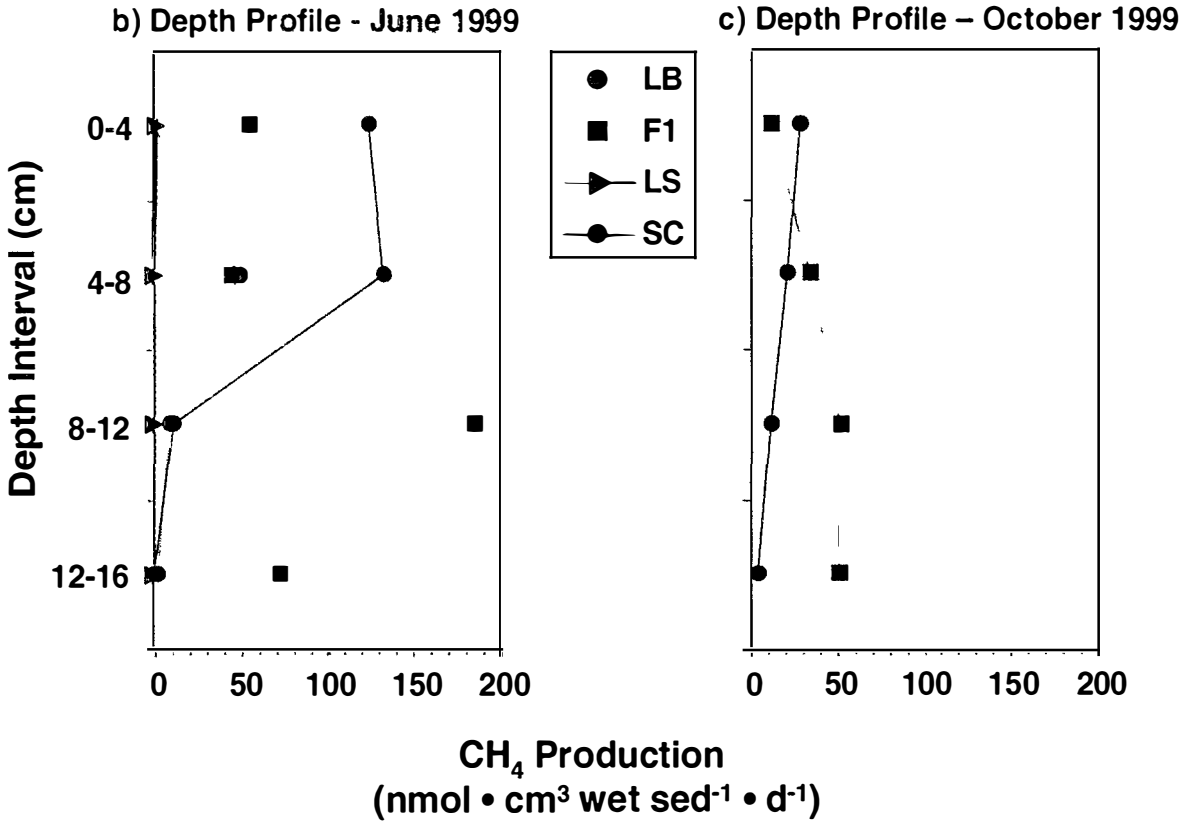

Figure 32. In-Situ Methane Concentration

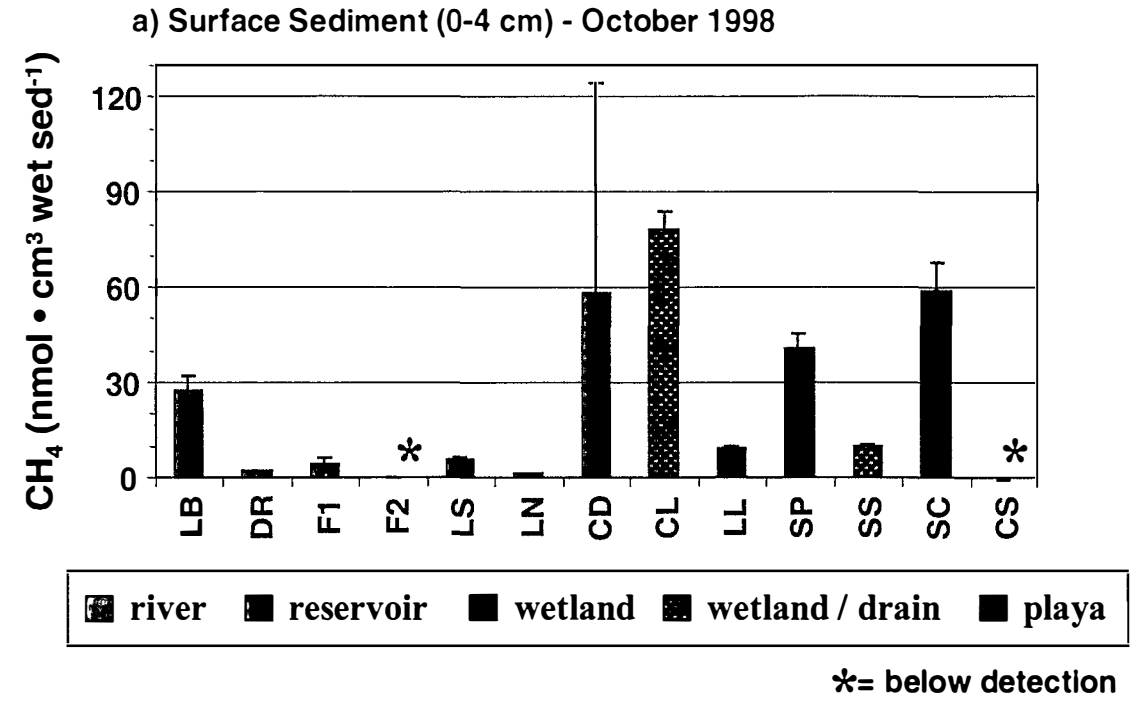

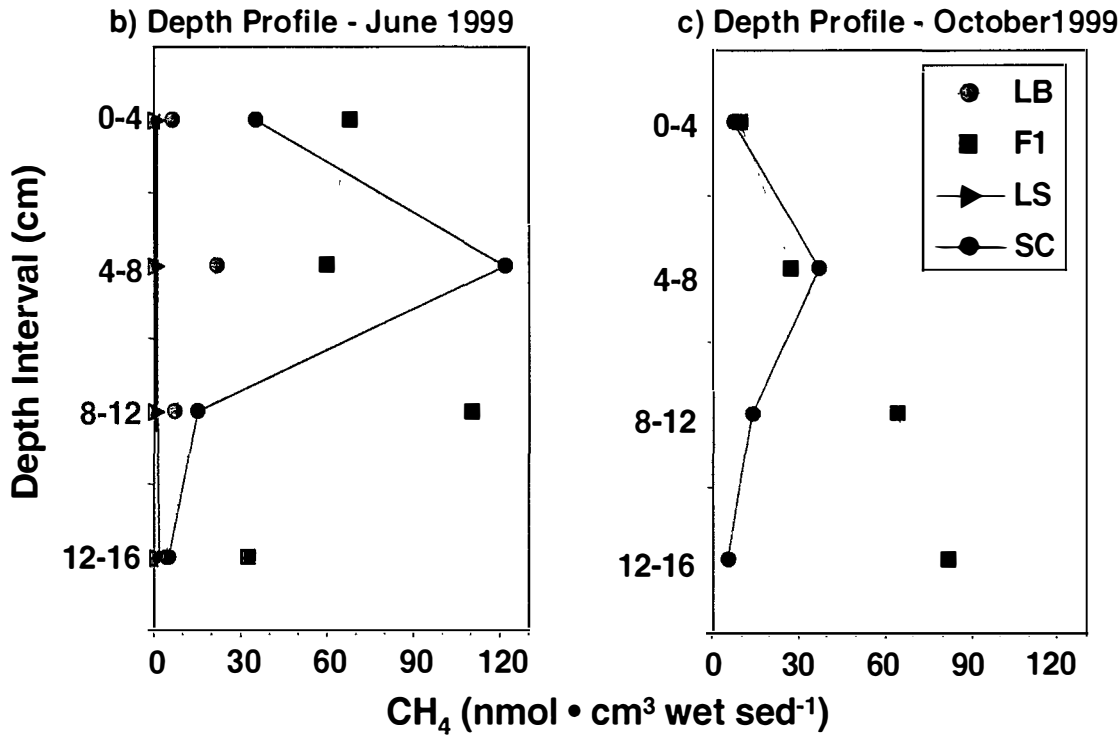

Figure 33. Microbial Iron Reduction – 14 Day Incubation Surface Sediment (0-4 cm) - October 1998

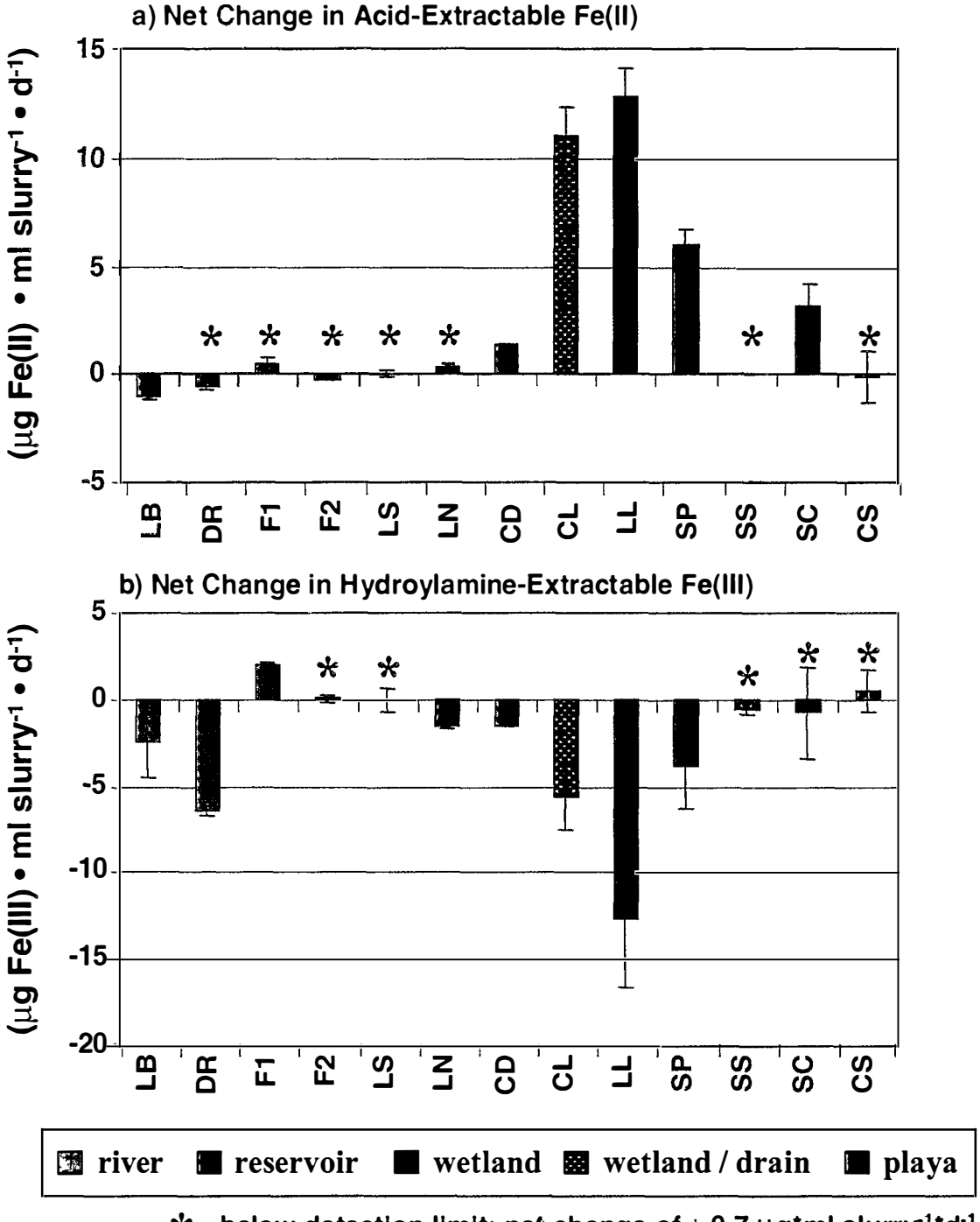

* = below detection limit: net change of ± 0.7 µg*ml slurry^{-1}*d^{-1}

Figure 34. Microbial Iron Reduction

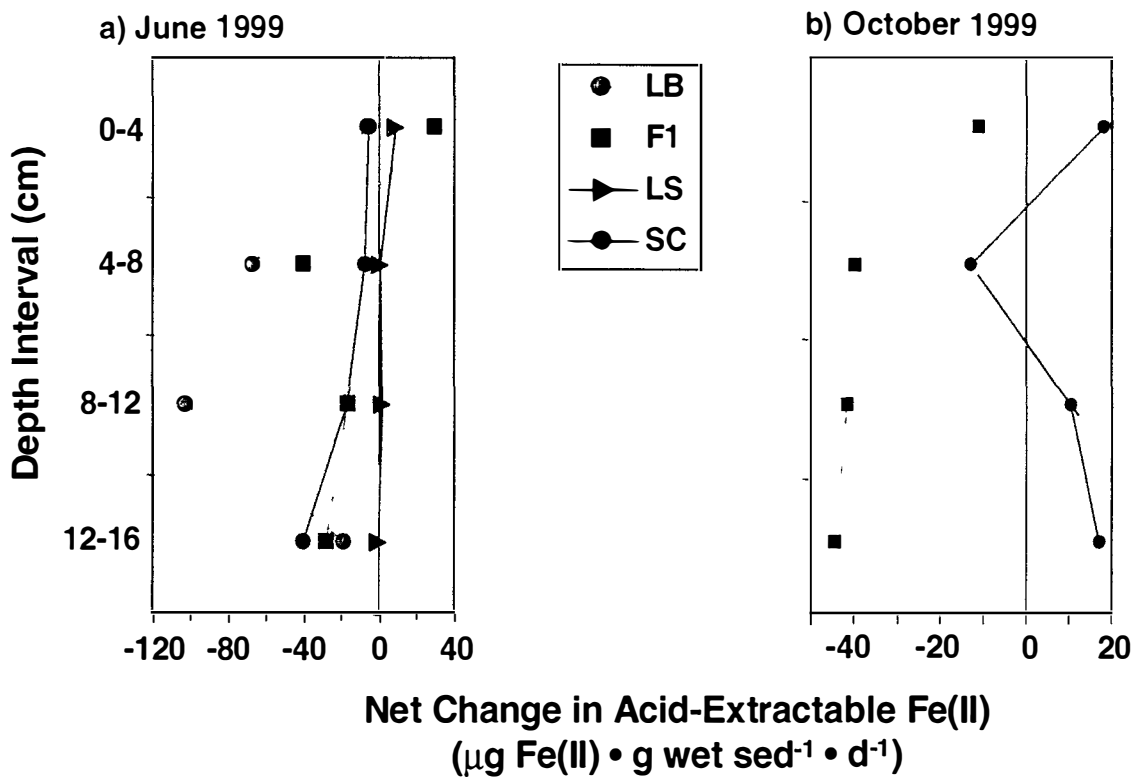

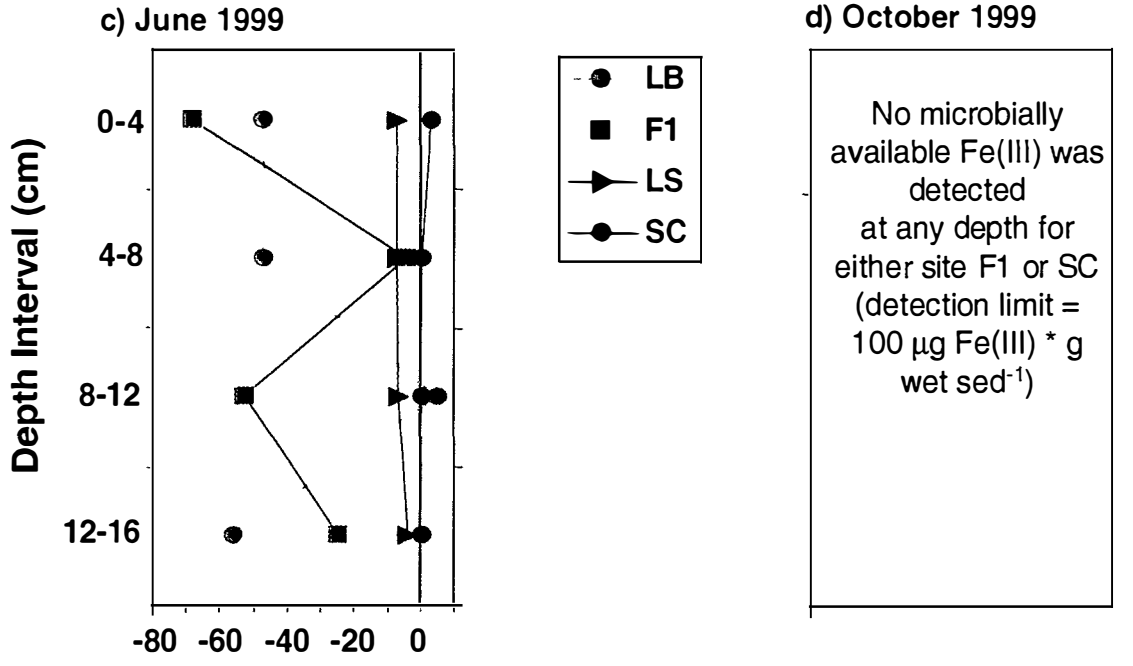

Figure 35. Microbially Available (Hydroxylamine-Extractable) Fe(III)

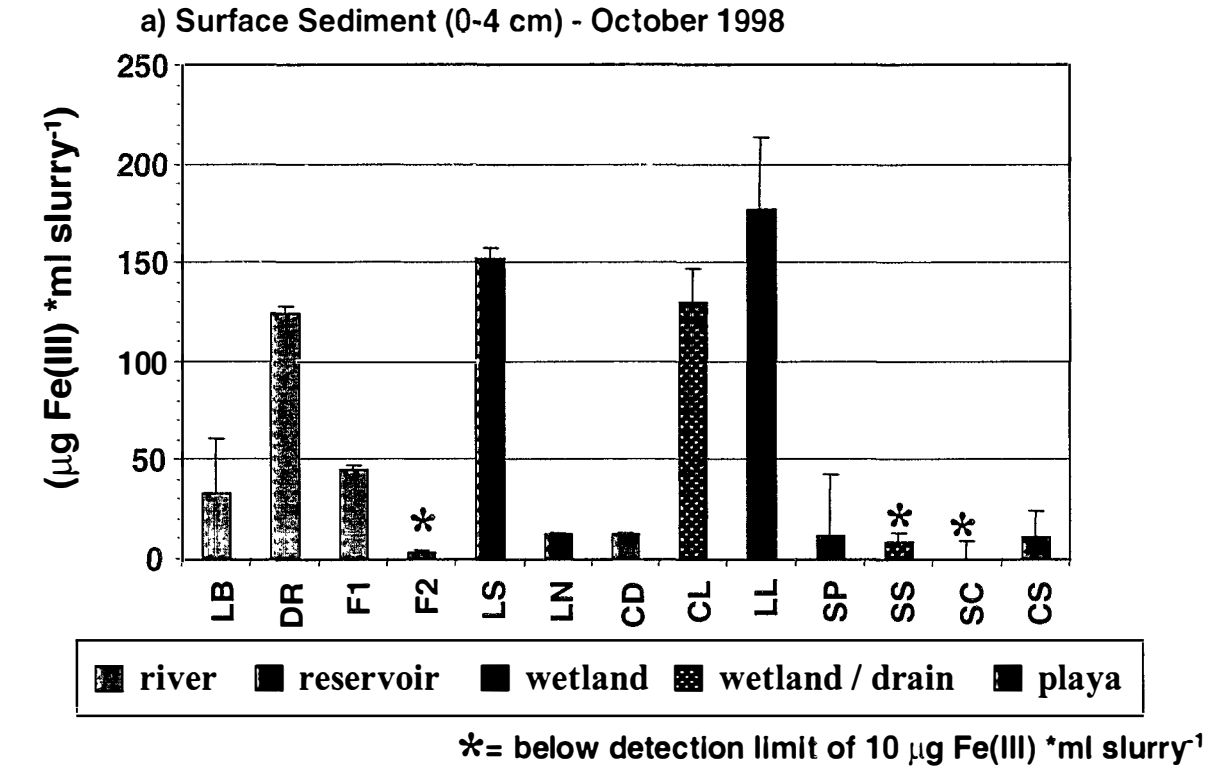

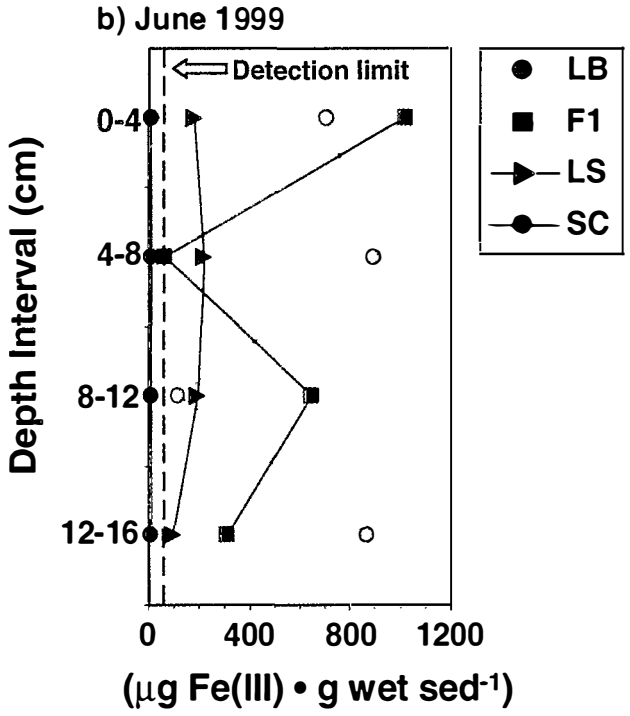

Figure 36. Microbial Manganese Reduction

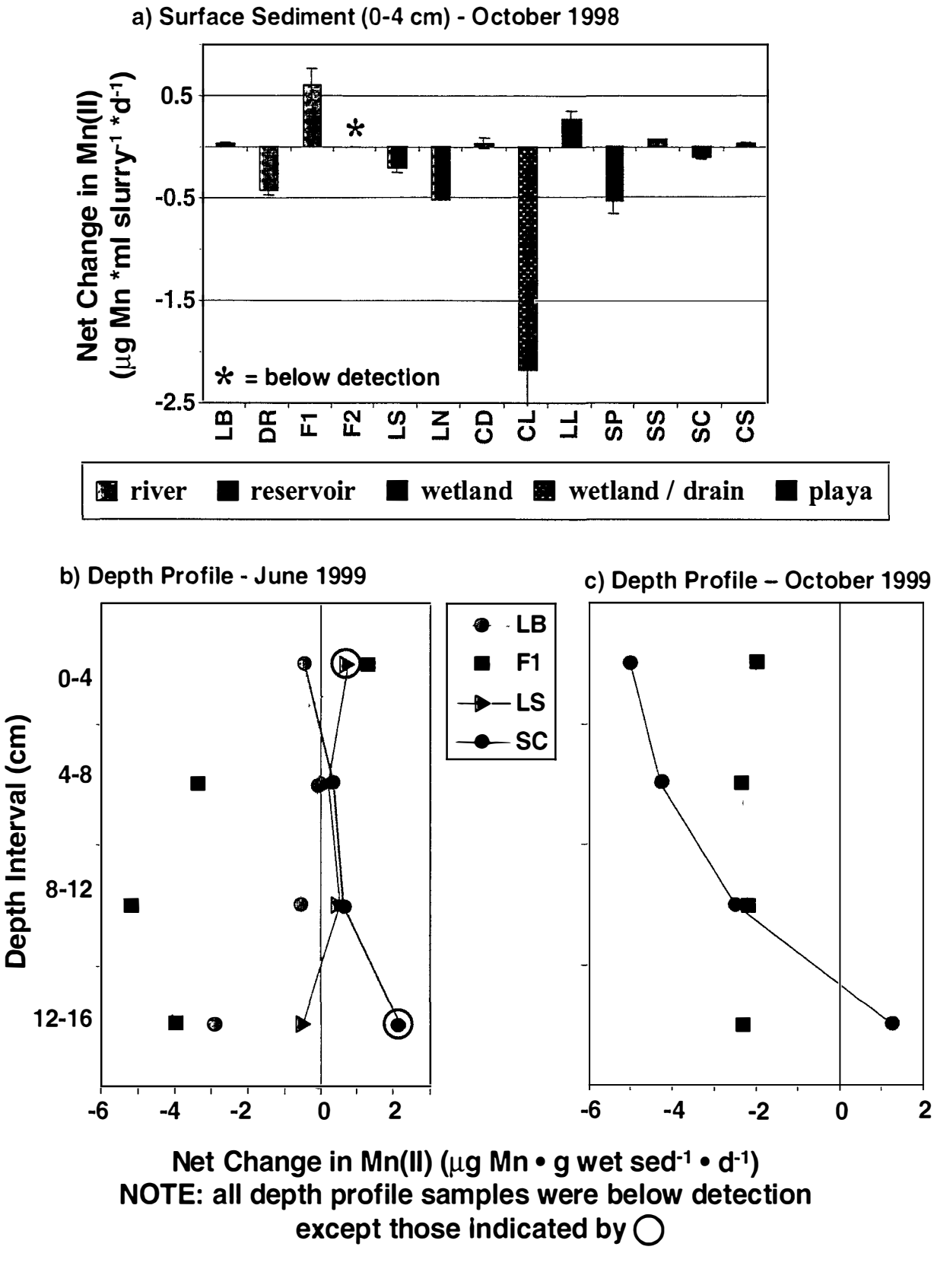

NOTE: all depth profile samples were below detection except those indicated by ◯

Figure 37. Whole Sediment Iron Concentration

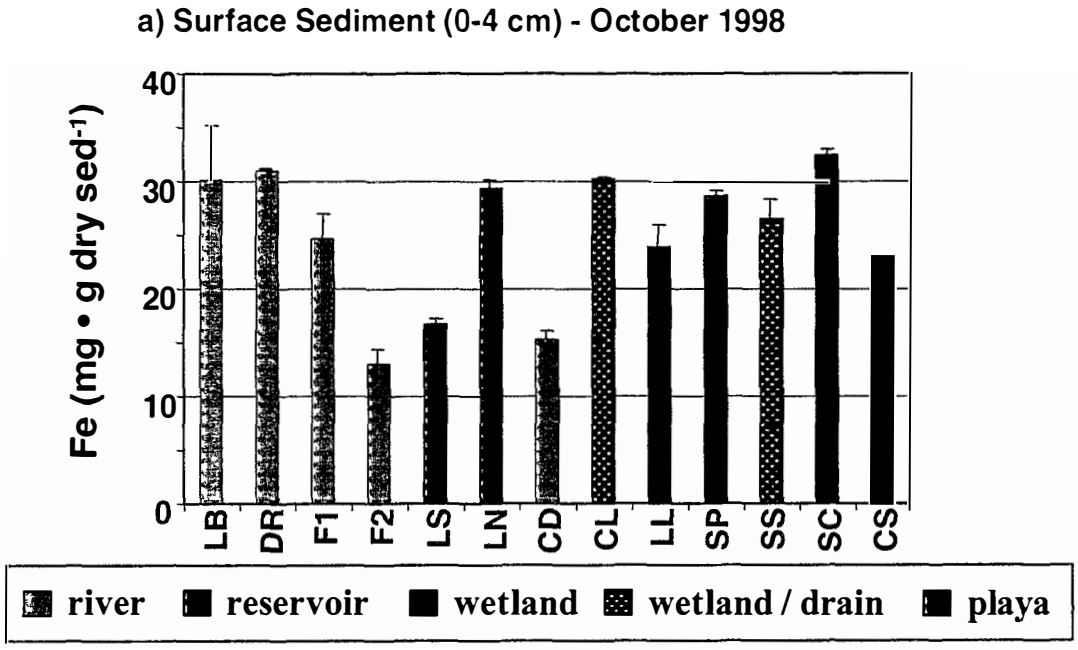

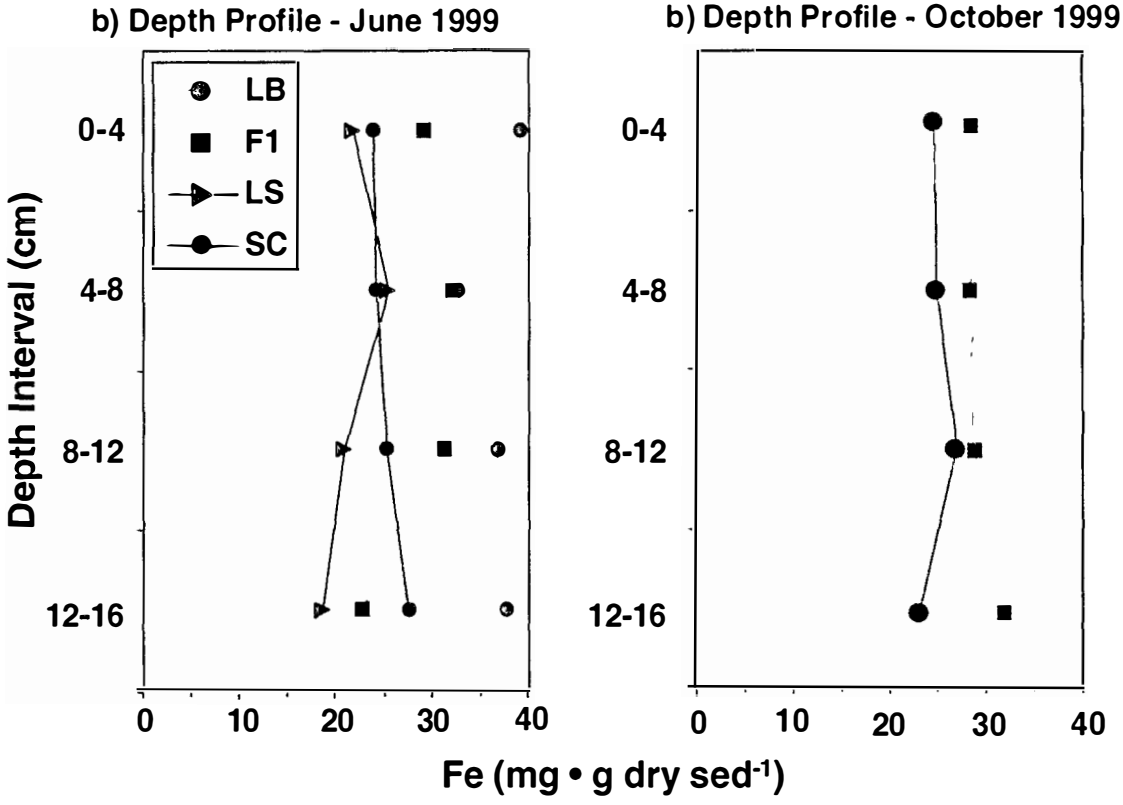

Figure 38. Pore Water Iron Concentration

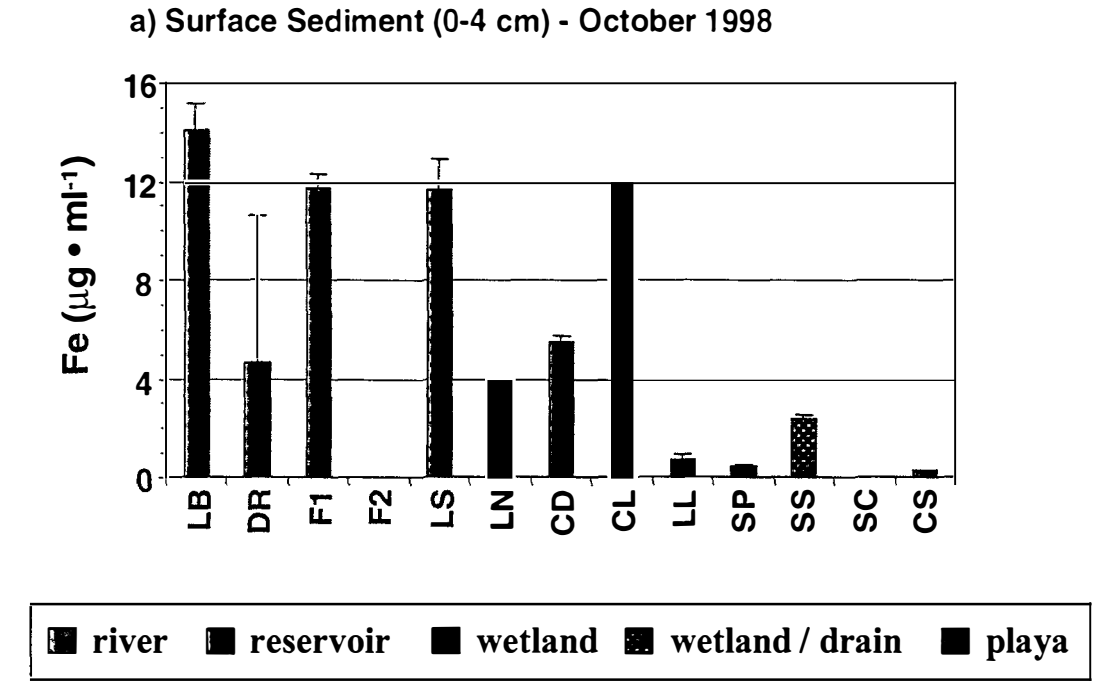

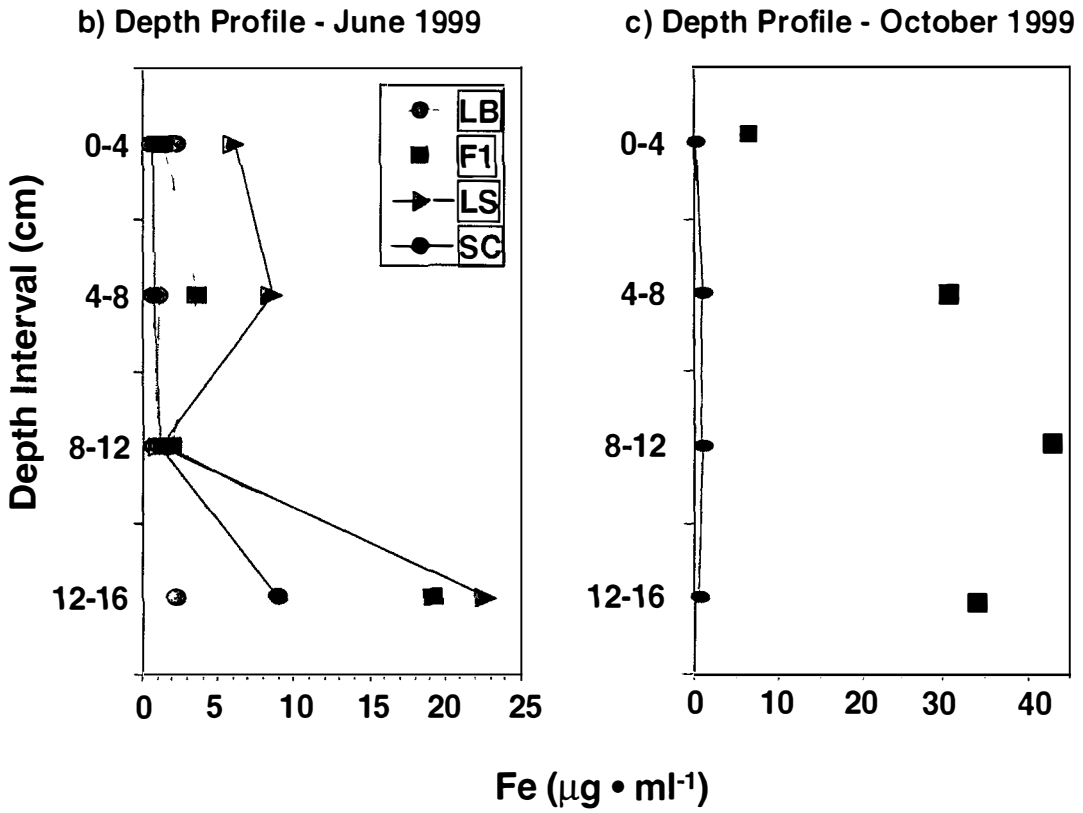

Figure 39. Whole Sediment Manganese Concentration

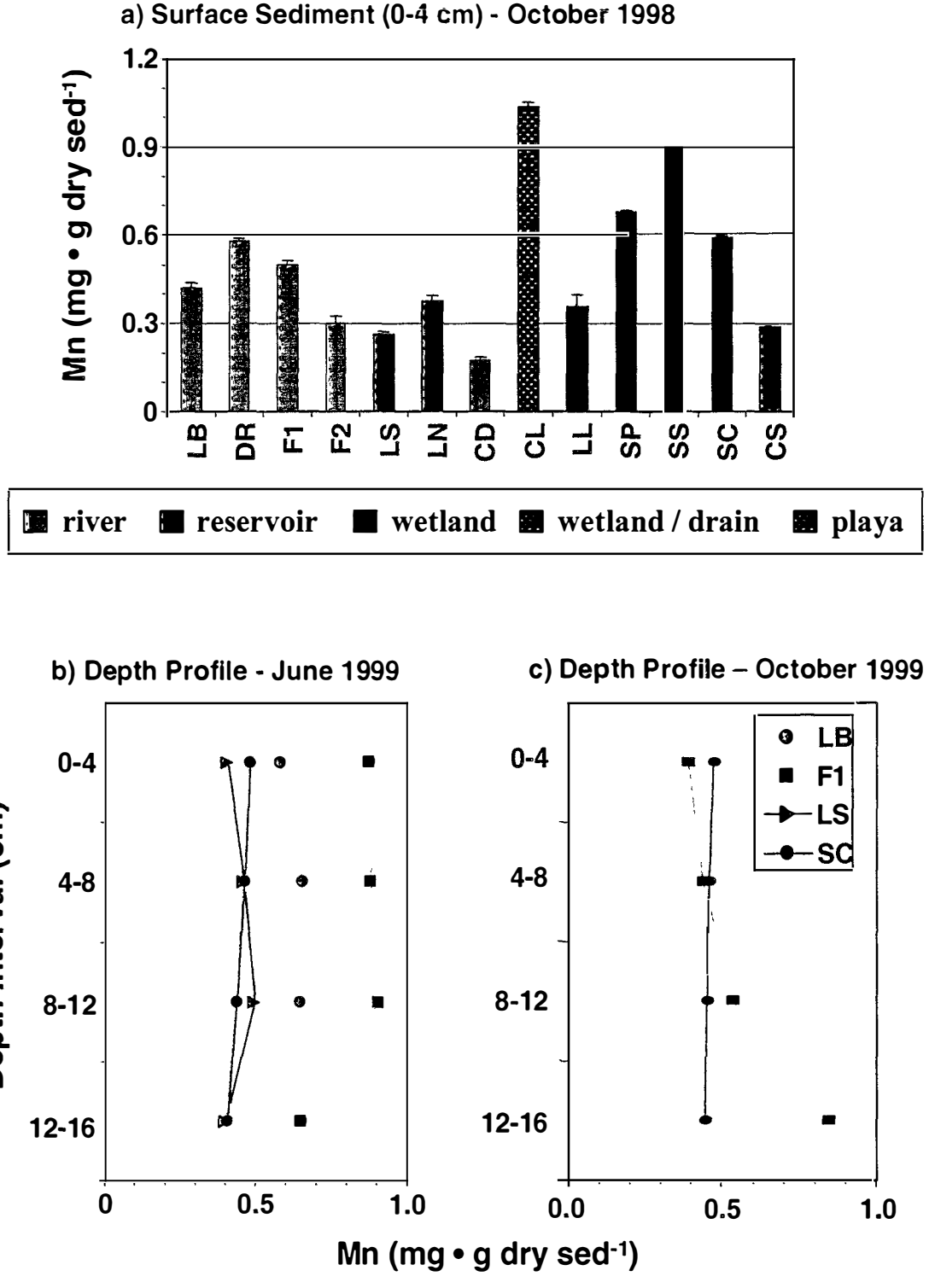

Figure 40. Pore Water Manganese Concentration

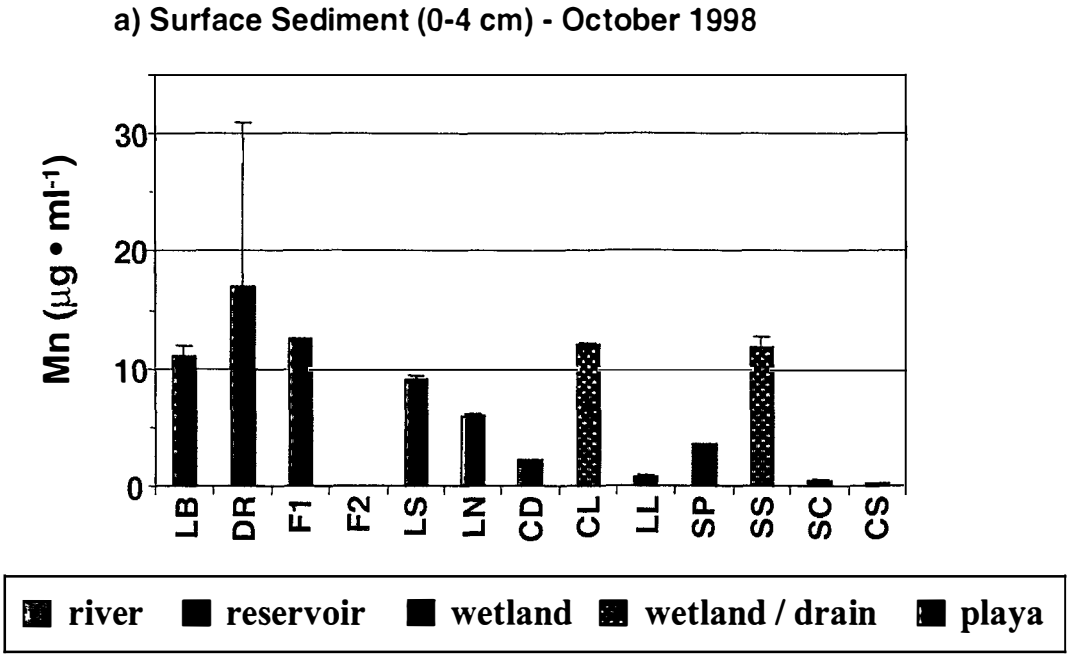

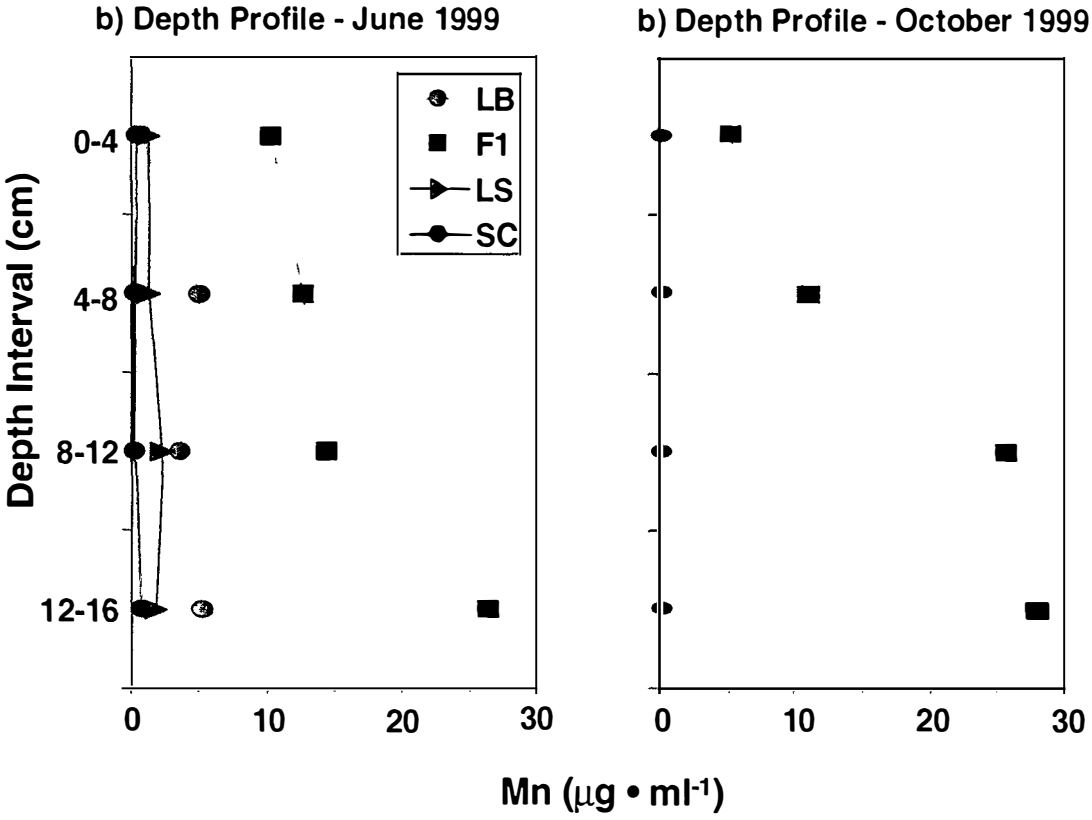

Figure 41. Whole Sediment Iron and Manganese Concentration Vertical Bank (F3) – June 1999 Only

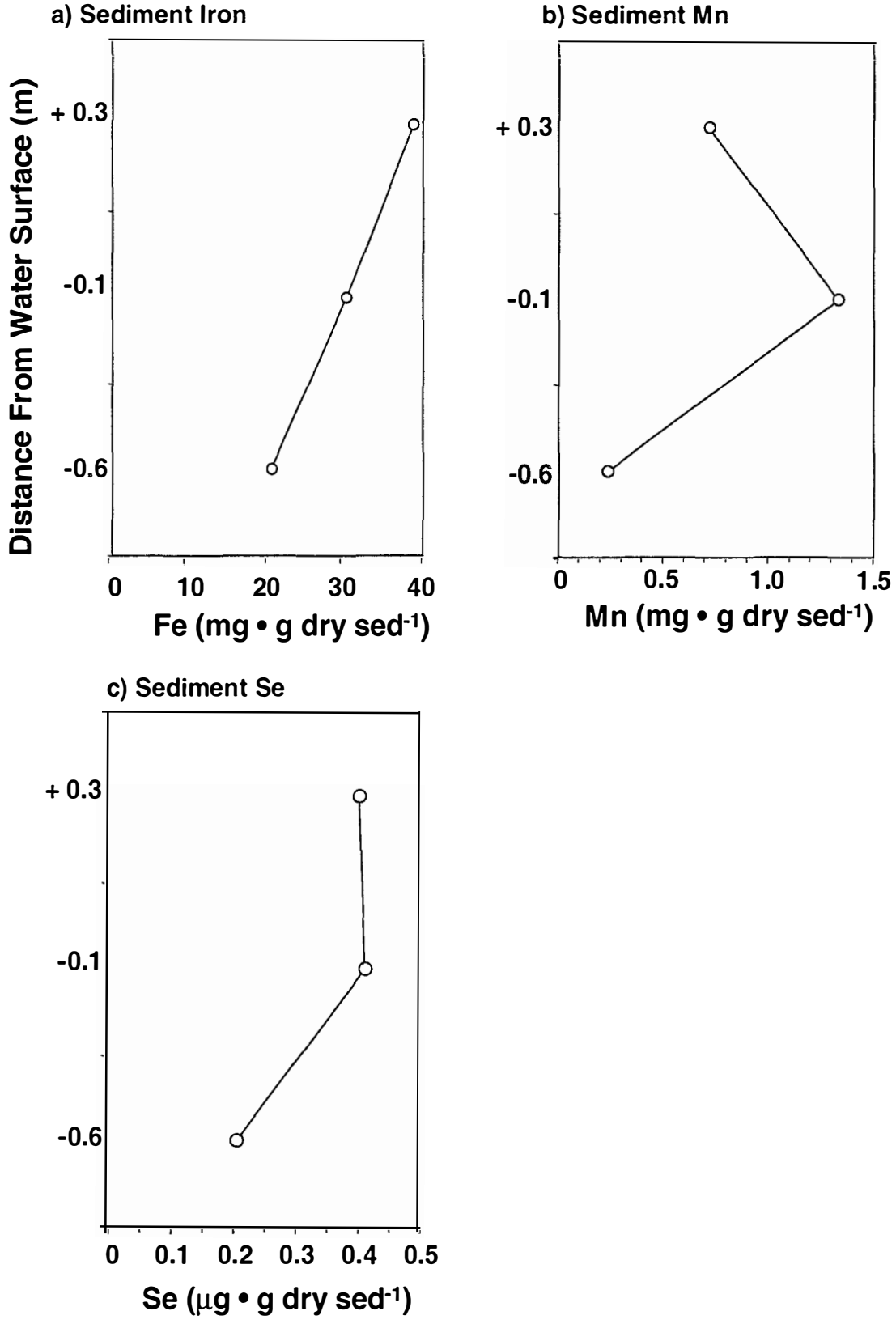

Figure 42. Whole Sediment Selenium Concentration

a) Surface Sediment (0-4 cm) - June 1999

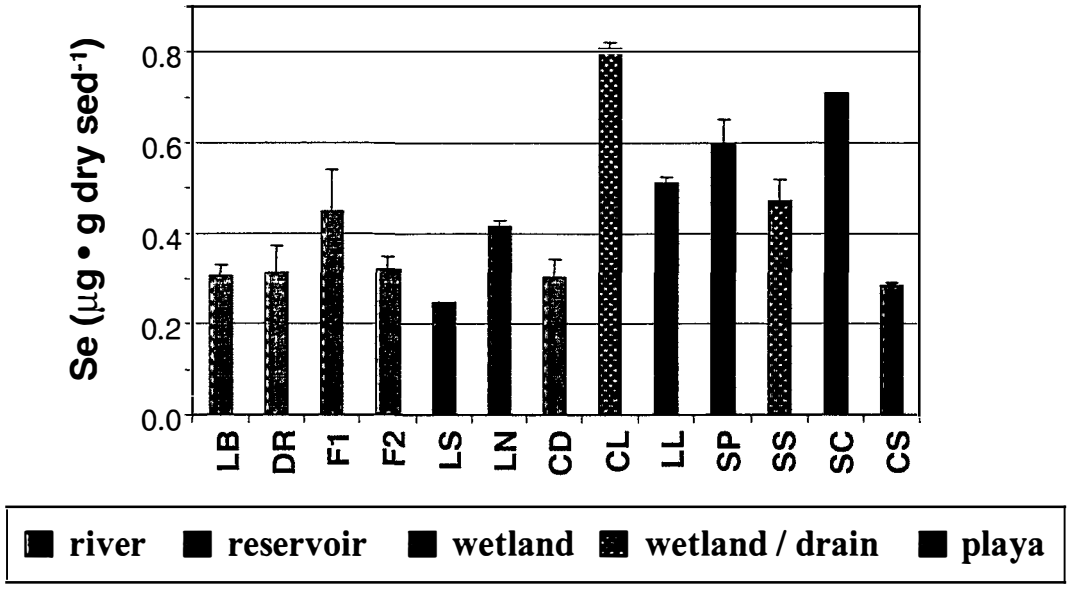

b) Depth Profile - June 1999

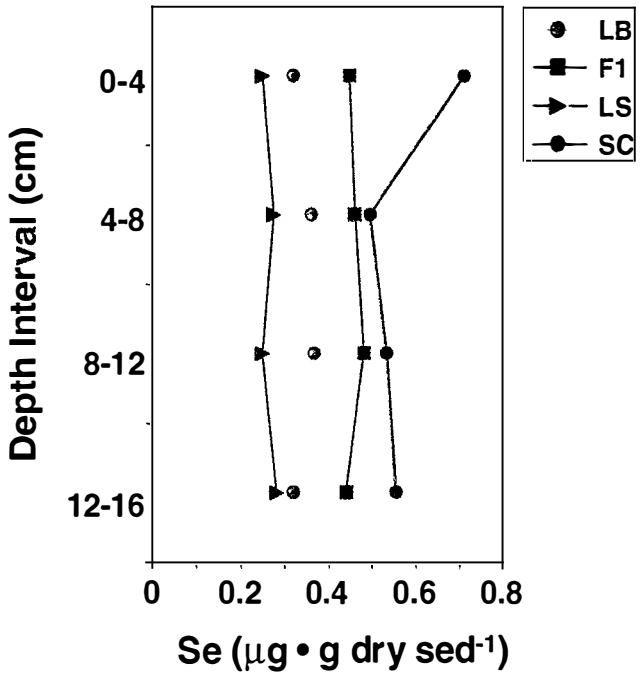

Figure 43. Sediment Grain Size

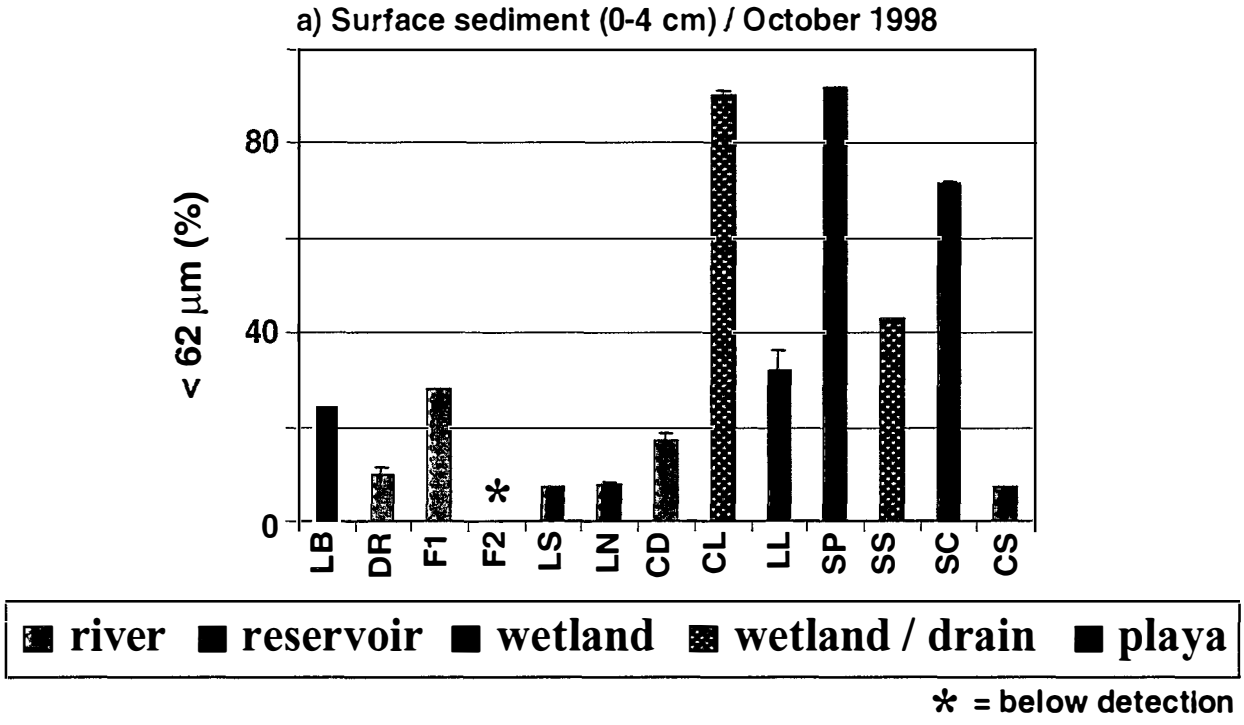

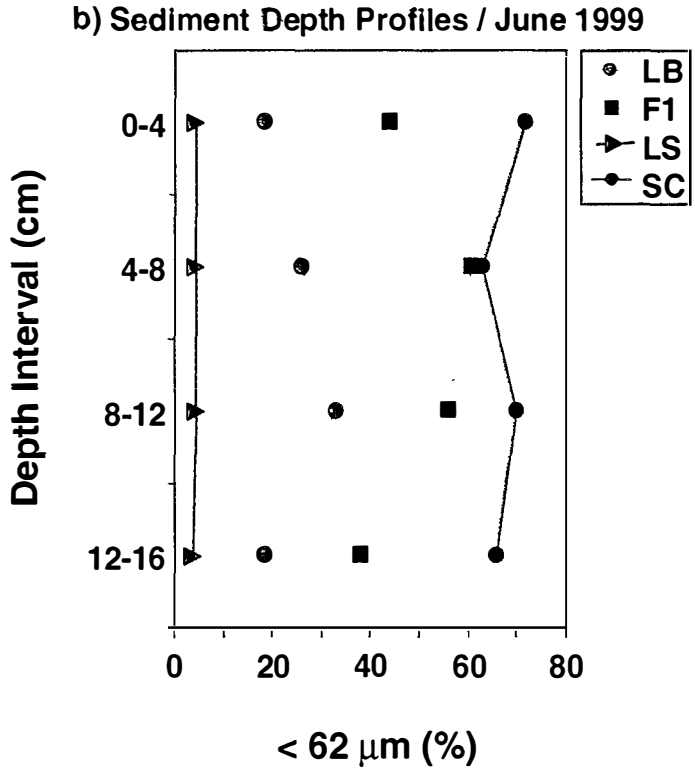

Figure 44. Effect of Grain Size on Hg_t and Hg(II) Concentrations

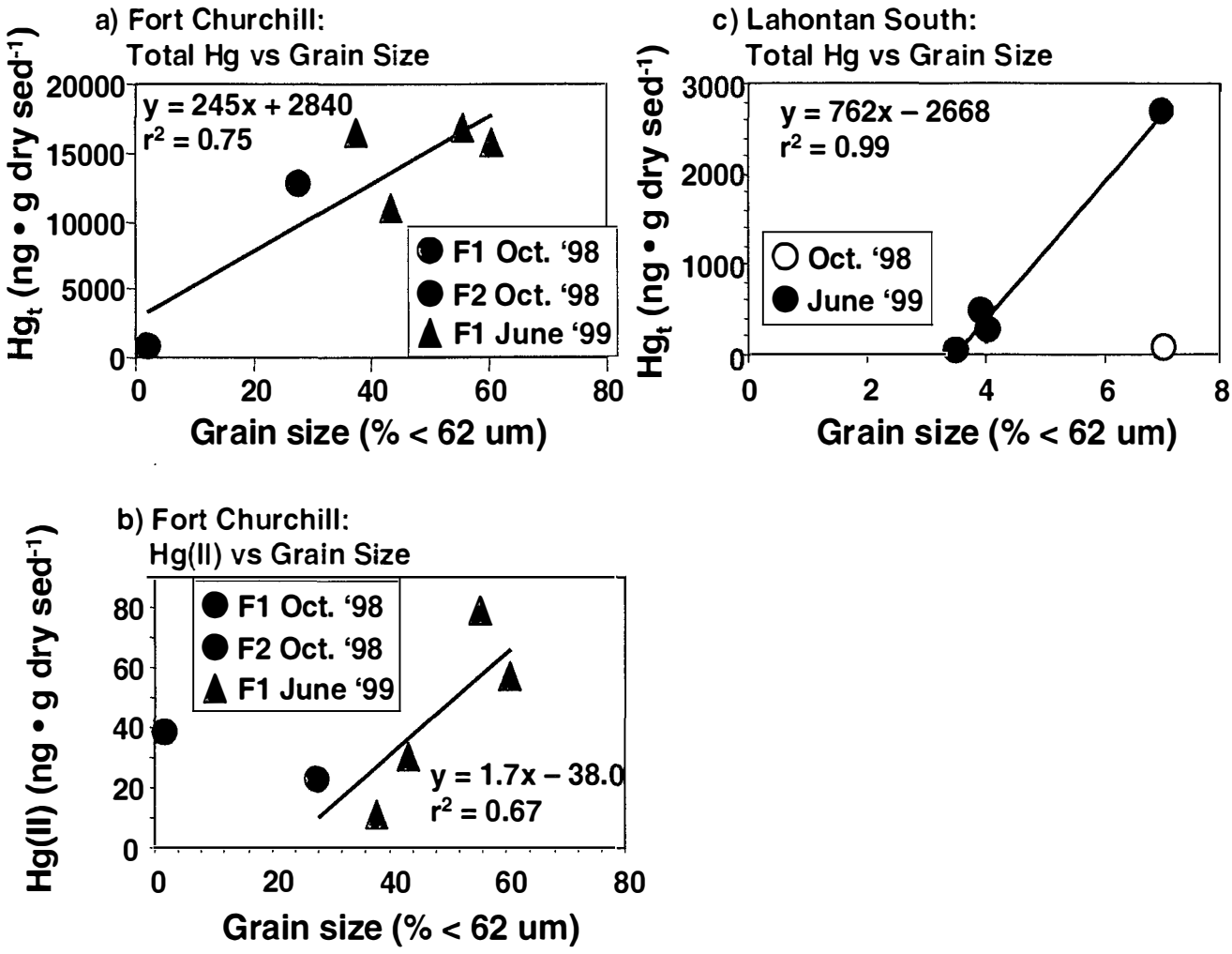

Figure 45. Sediment Percent Water-Surface sediment (0-4 cm)

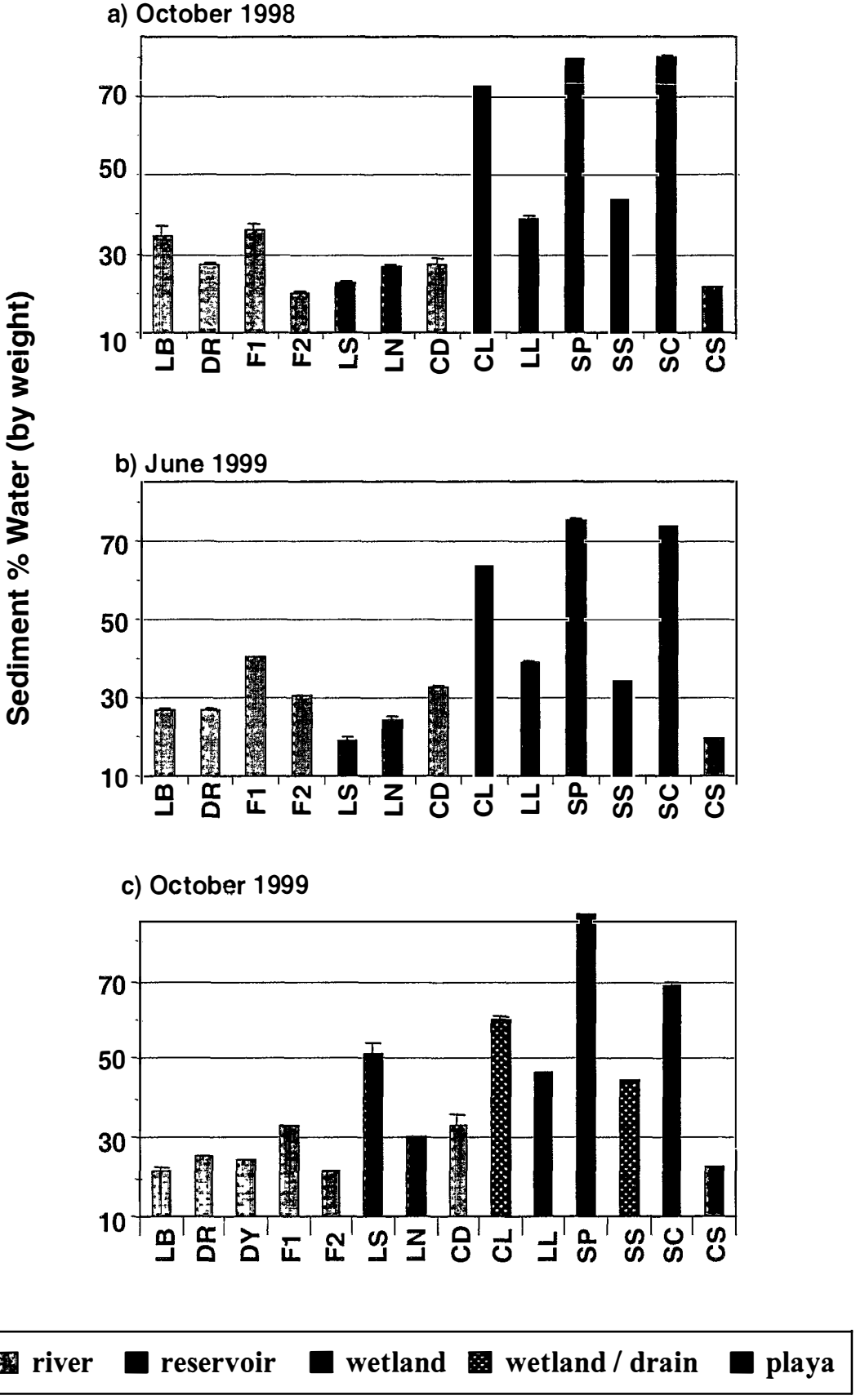

Figure 46. Sediment Percent Water – Depth Profiles

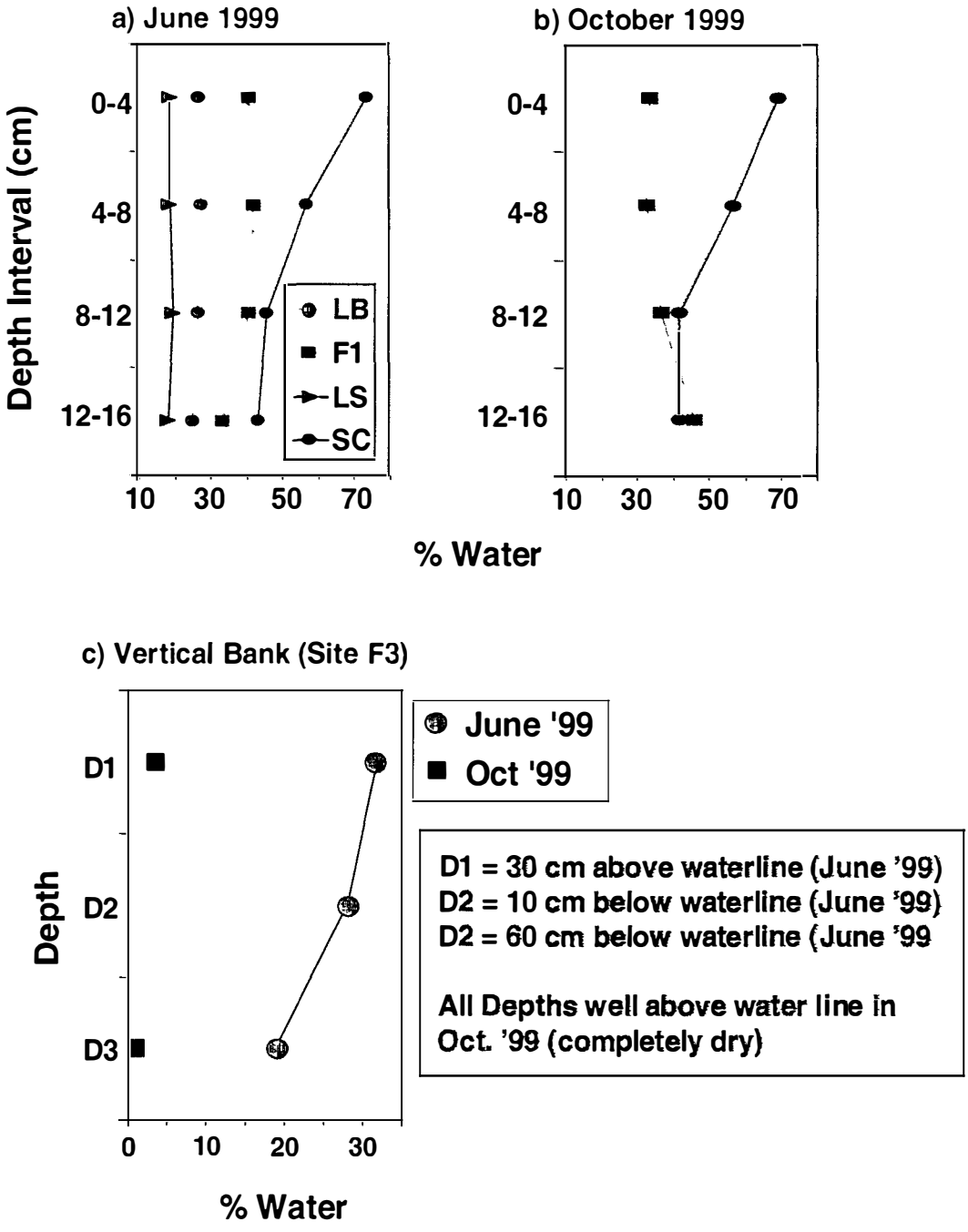

Figure 47. Sediment Redox - Surface sediment (0-4 cm)

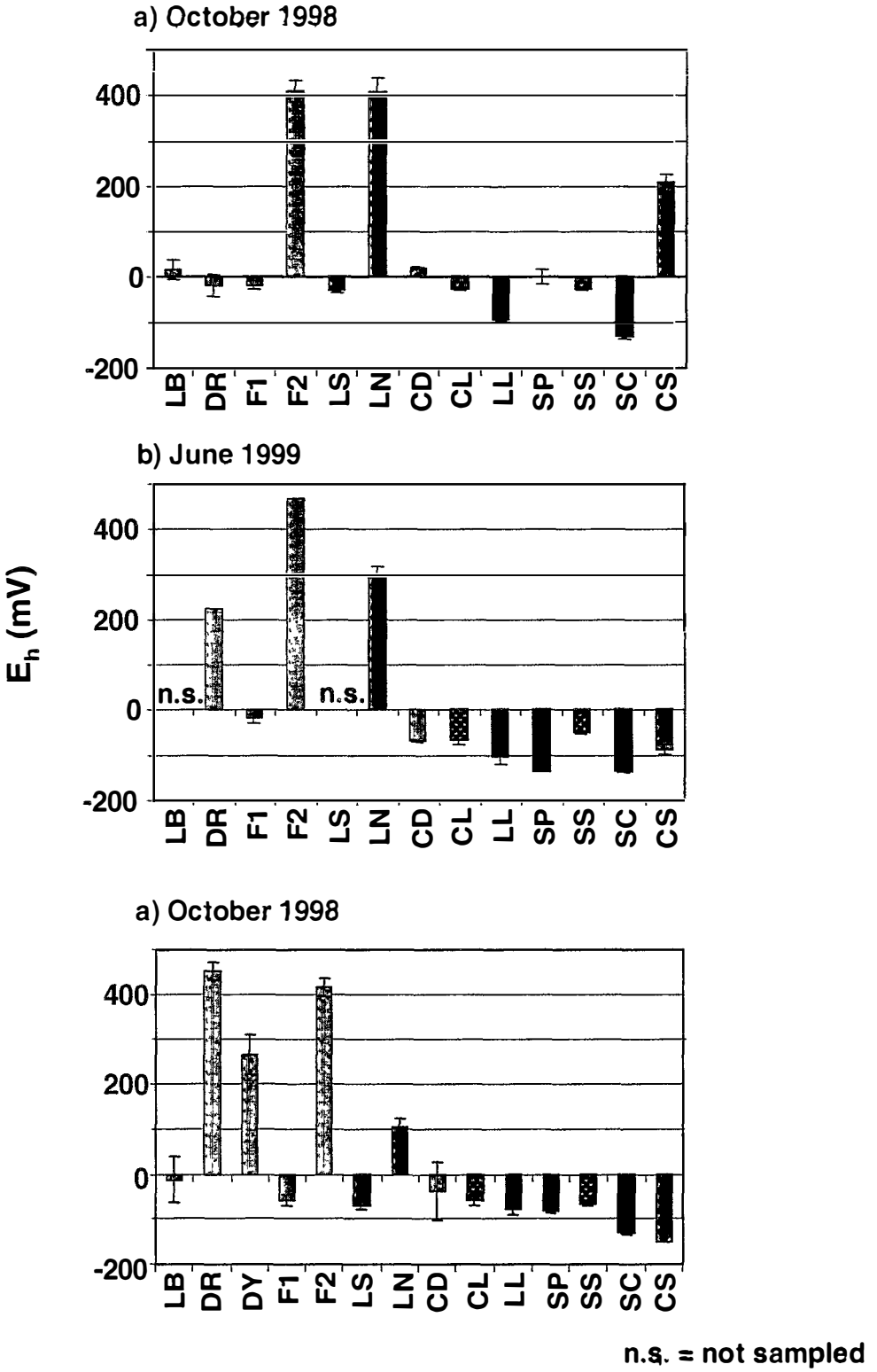

Figure 48. Sediment Redox – Depth Profiles

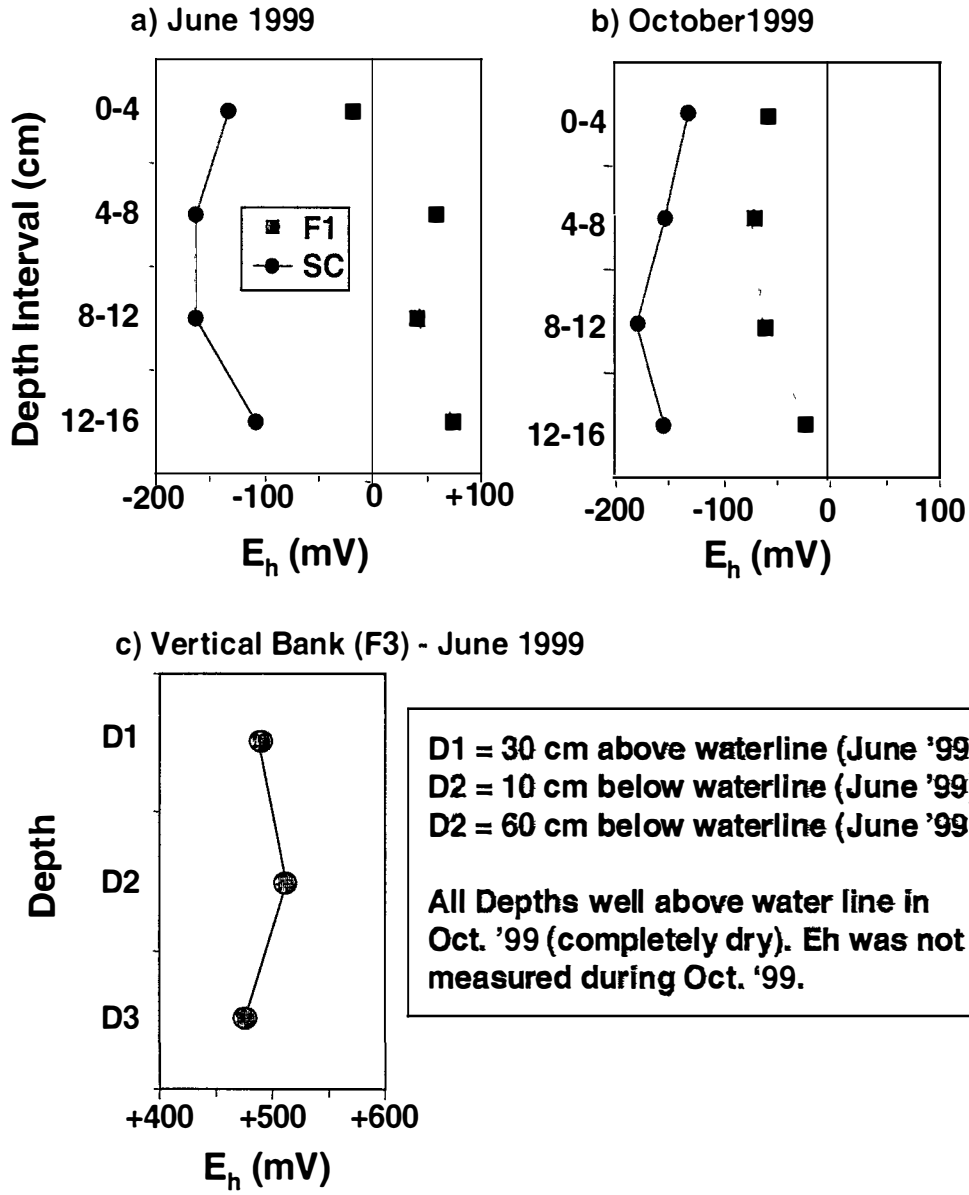

Figure 49. Sediment Redox (0-4 cm only) by Sampling Period (all data)

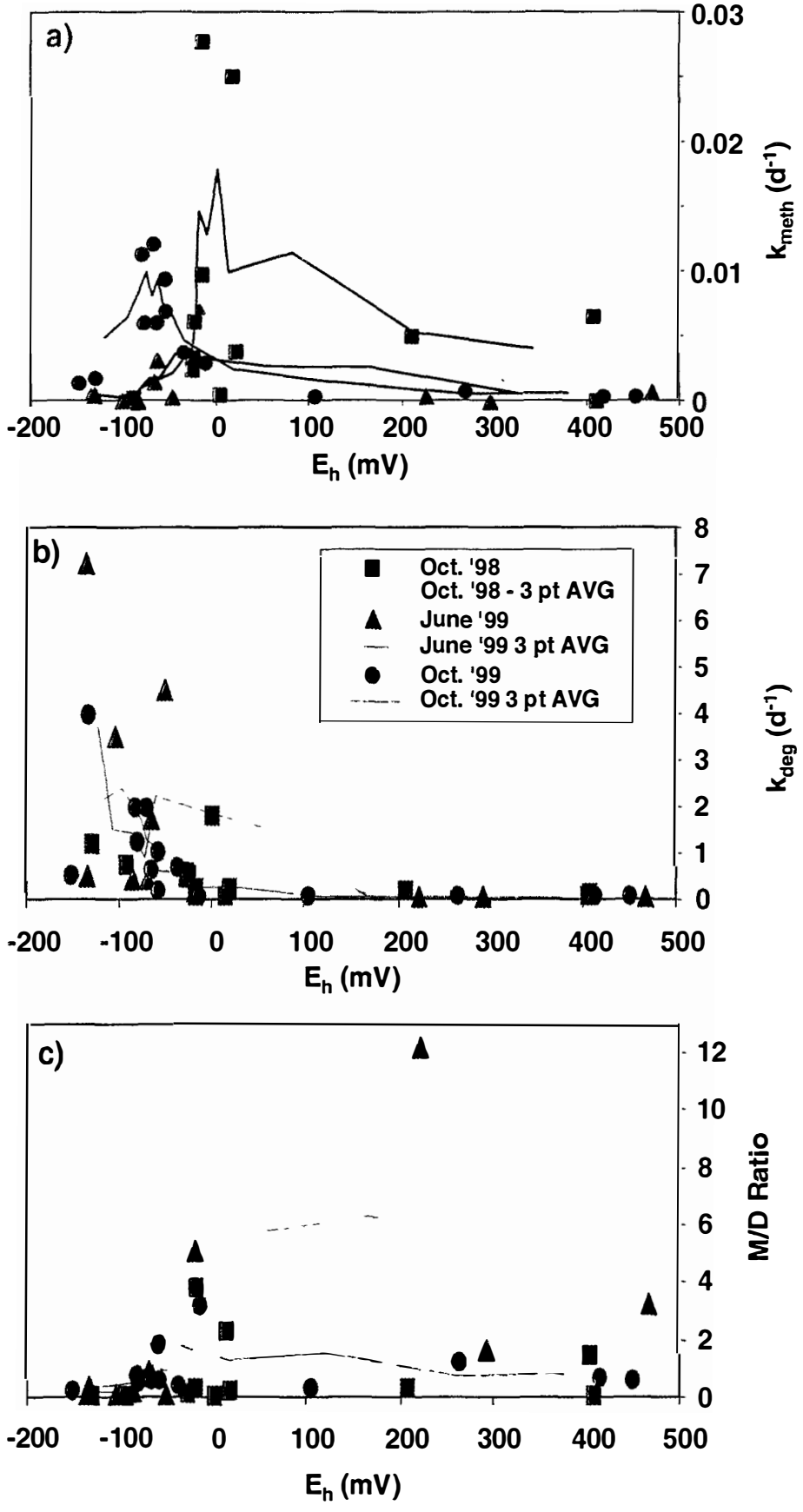

Figure 50. Sediment Redox (0-4 cm only) by Region (all data)

a) Hg-Methylation Rate Constant vs Sediment Redox

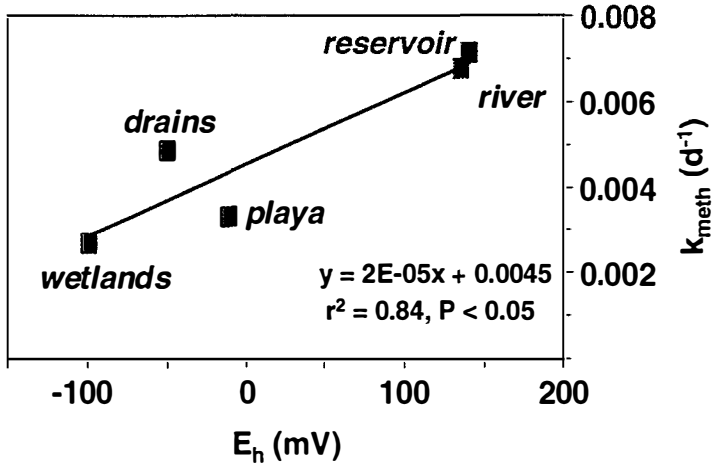

b) MeHg-Degradation Rate Constant vs Sediment Redox

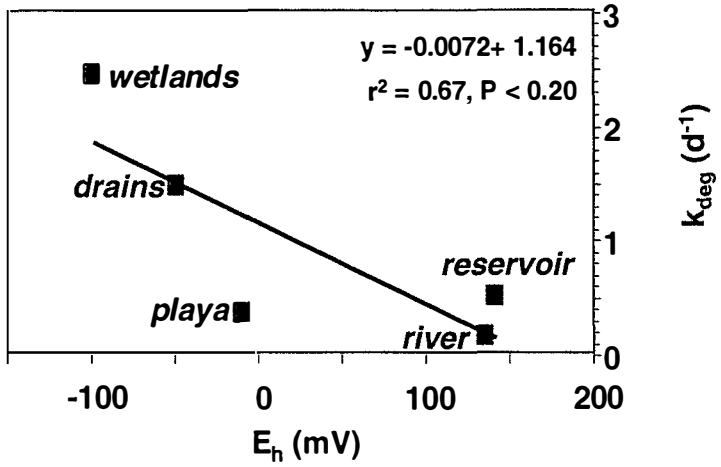

c) Methylation/Degradation Ratio vs Sediment Redox

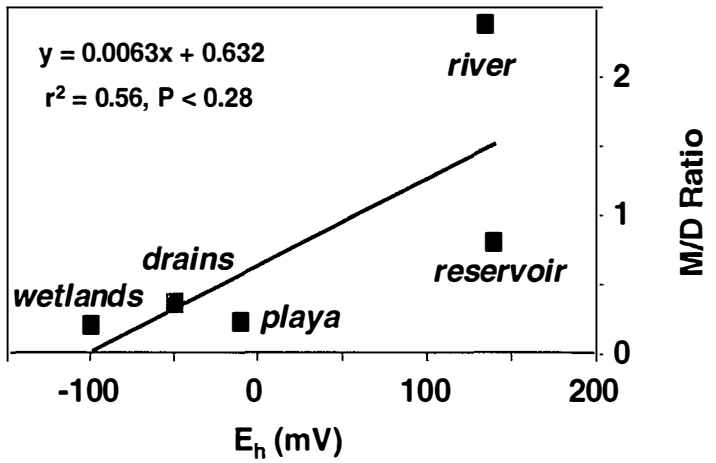

Figure 51. Sediment pH-Surface sediment (0-4 cm)

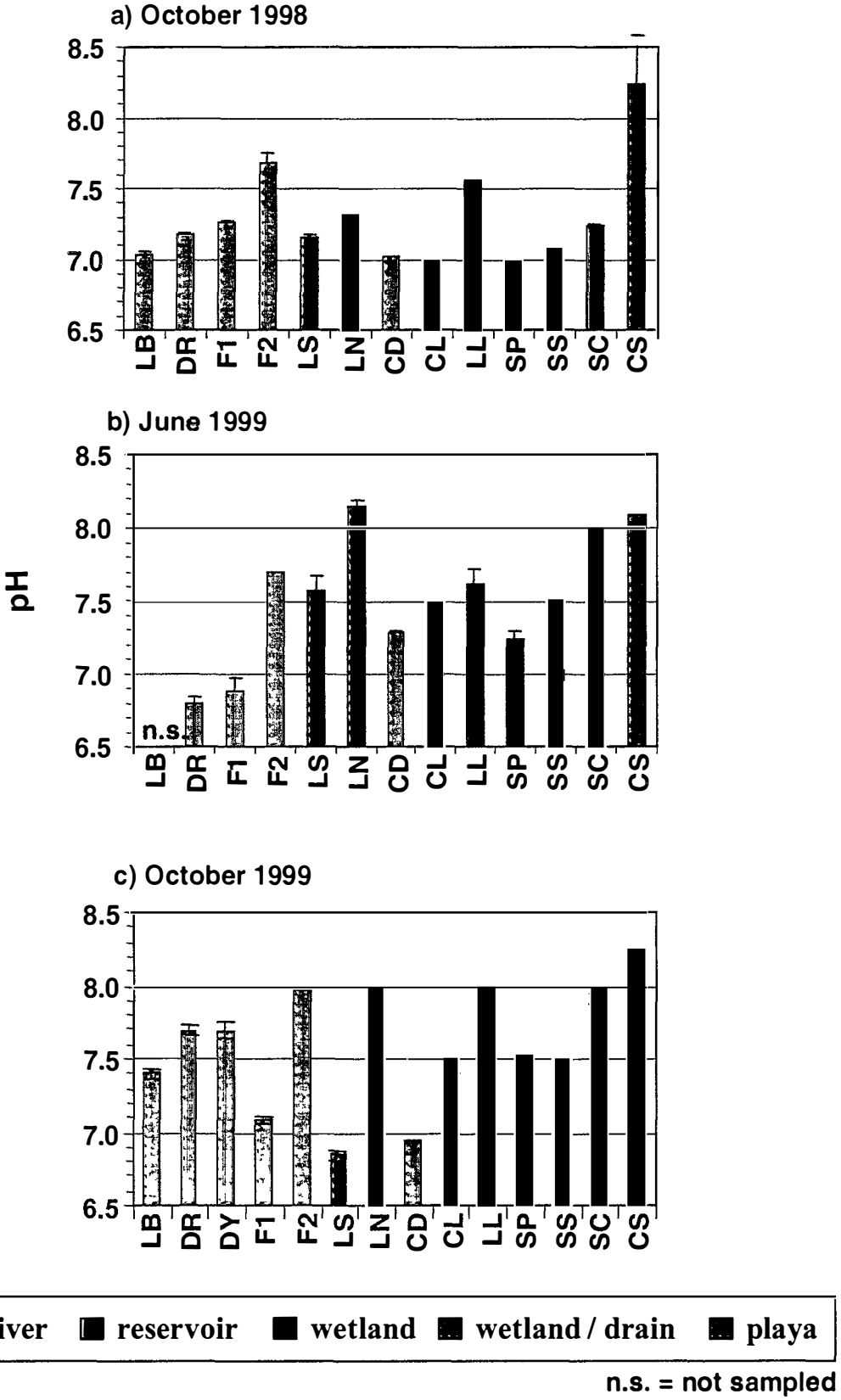

n.s. = not sampled

Figure 52. Sediment pH – Depth Profiles

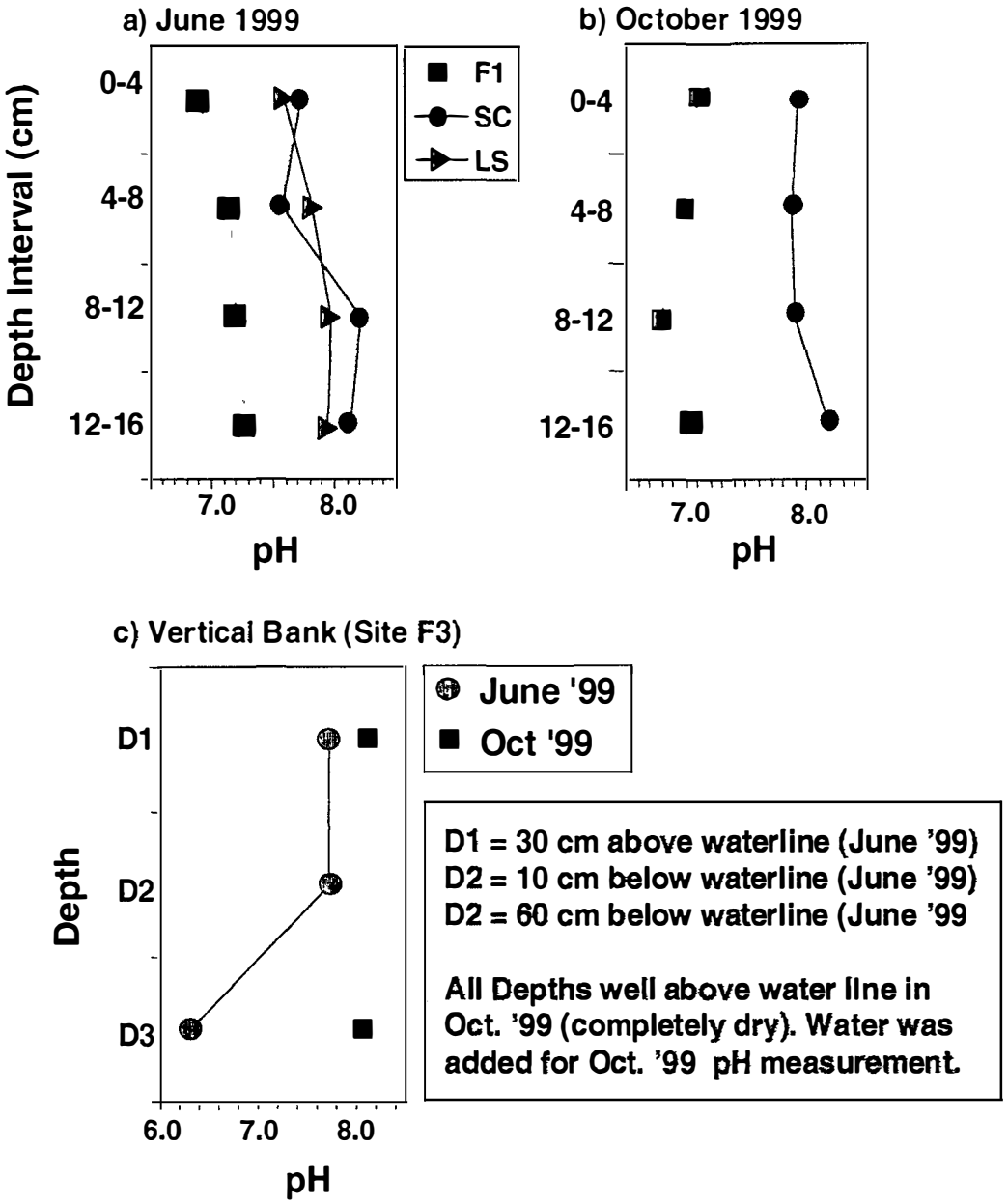

Figure 53. Sediment pH versus Hg-Methylation Rate Constant (0-4 cm data only)

a) pH vs Hg-Methylation Rate Constant by Sampling Period

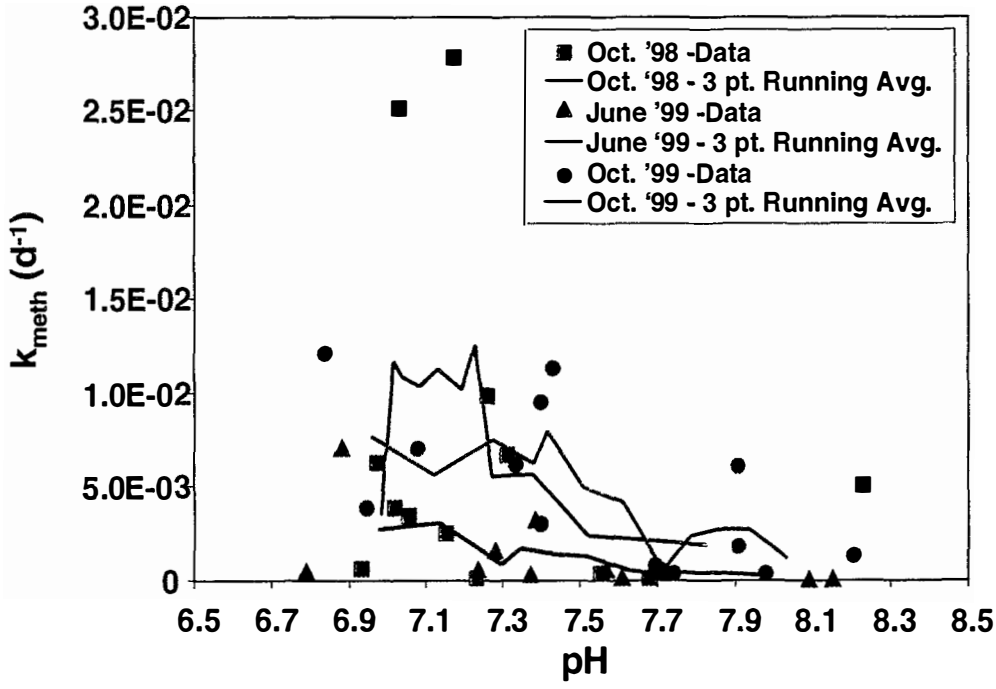

b) pH vs Avg. Hg-Methylation Rate Constant by Region

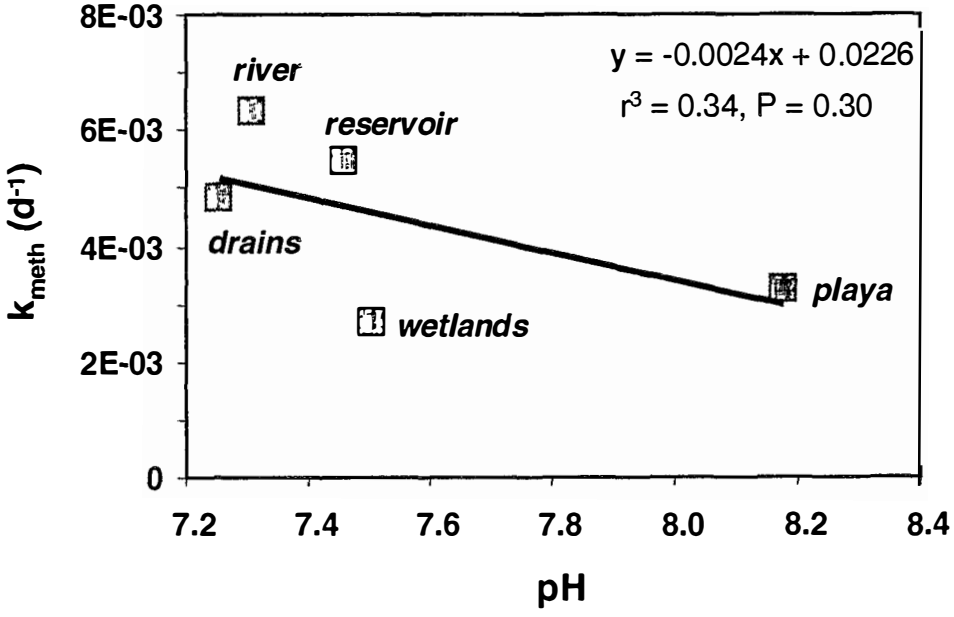

Figure 54. Sediment Percent Carbon

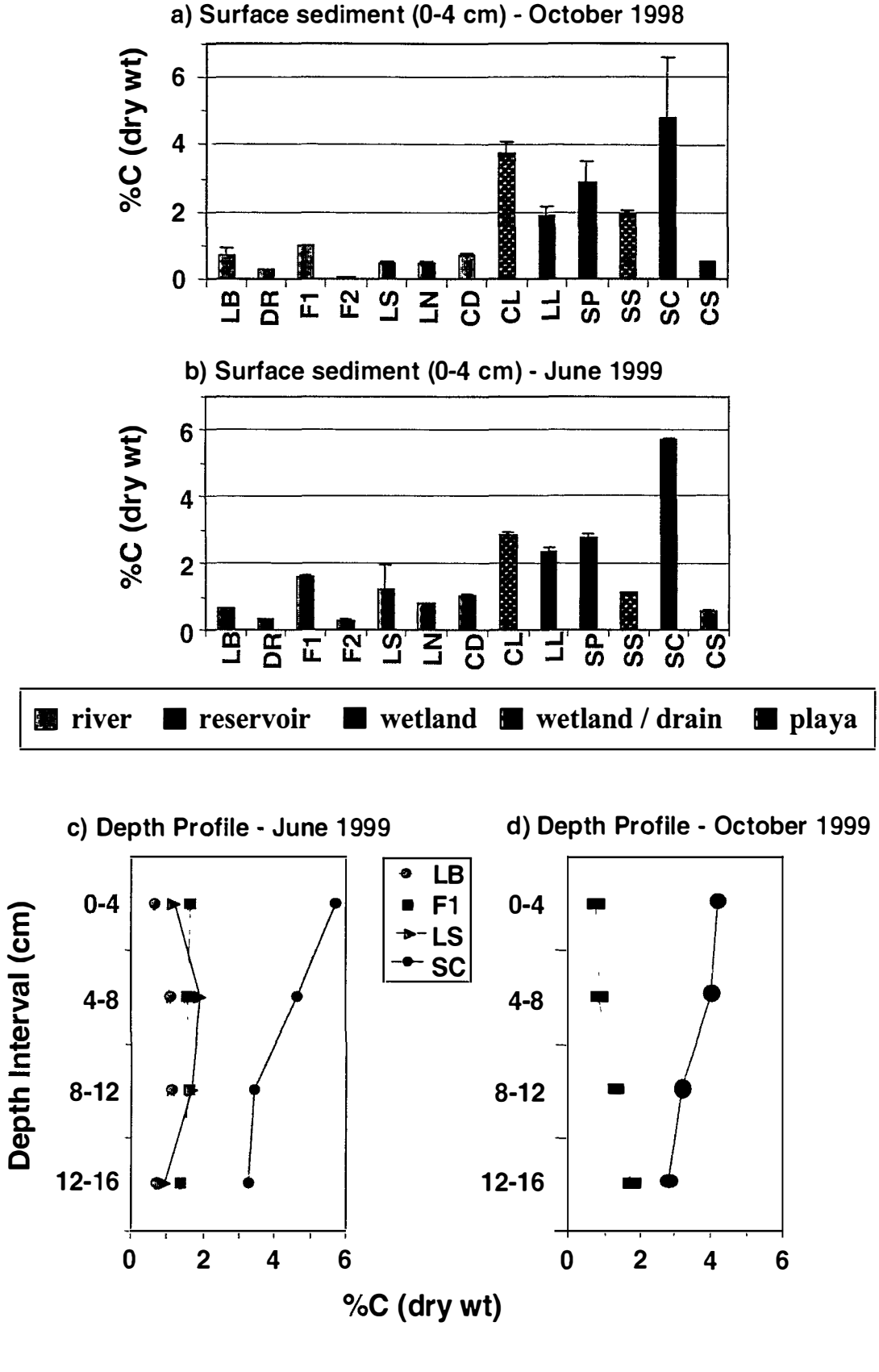

Figure 55. Sediment Percent Weight Loss on Ignition at 500 ^{0}C

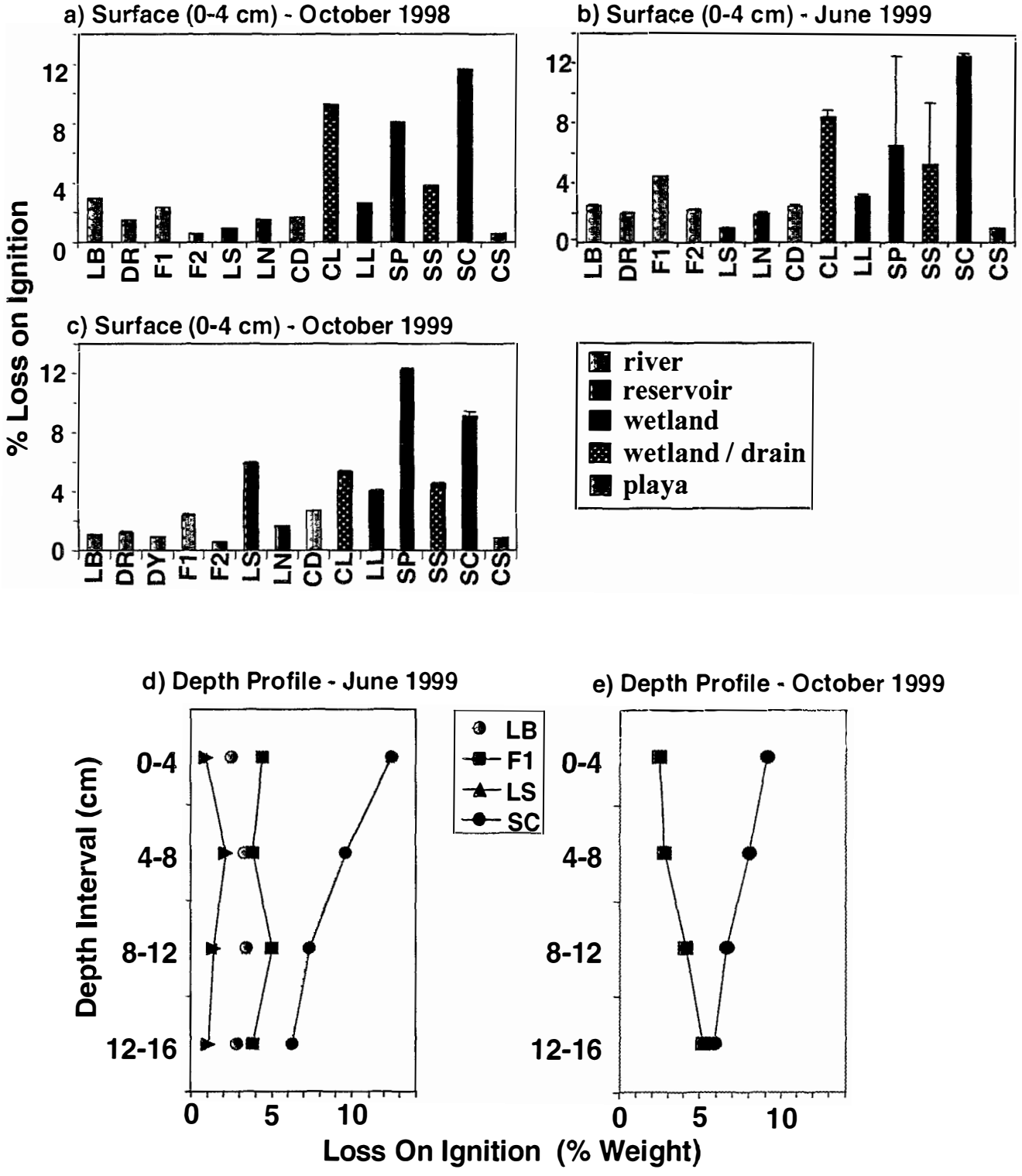

Figure 56. Sediment Particulate Carbon and Loss on Ignition versus MeHg Degradation Rate Constant (0-4 cm data only)

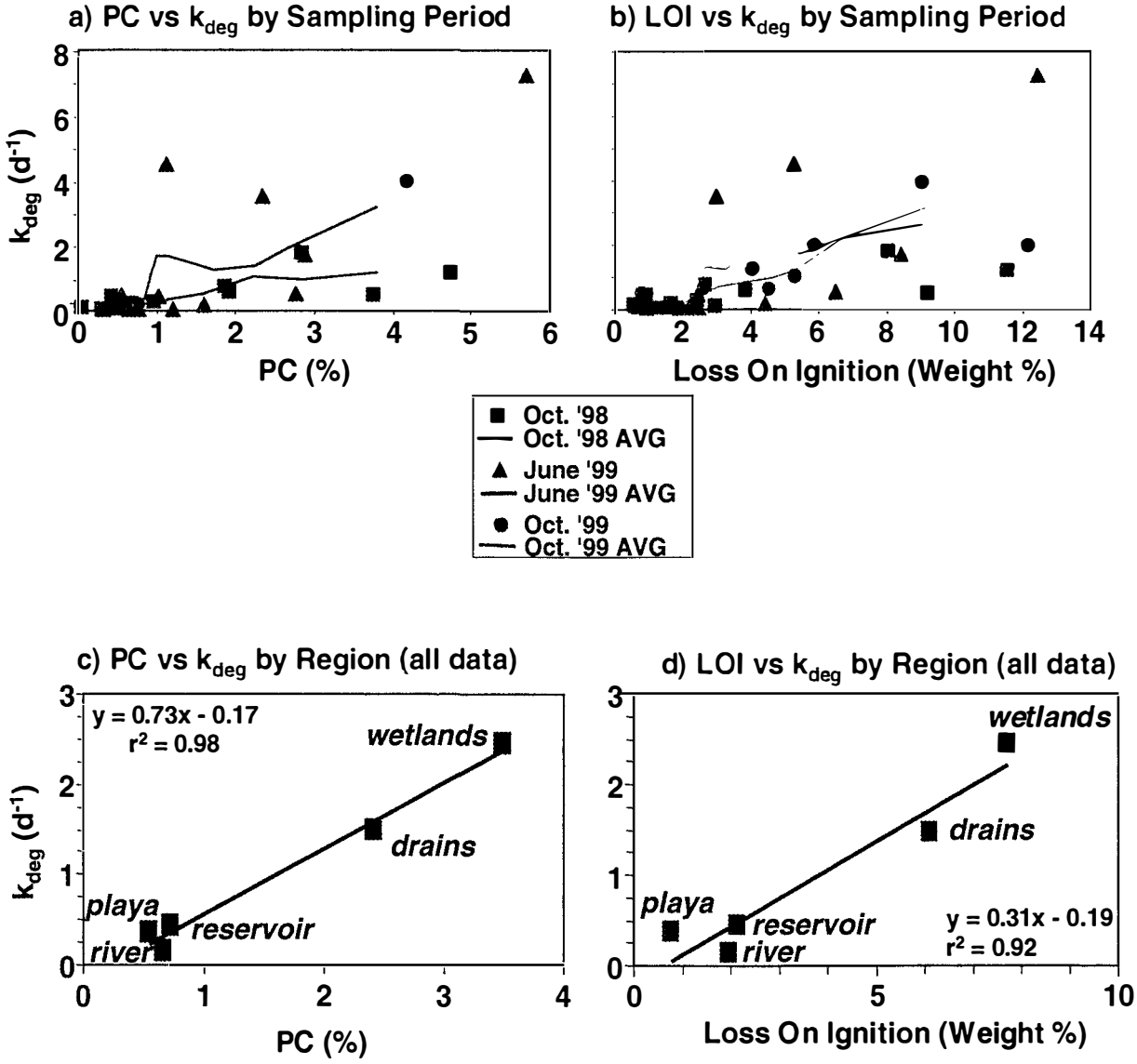

Figure 57. Pore Water Dissolved Organic Carbon

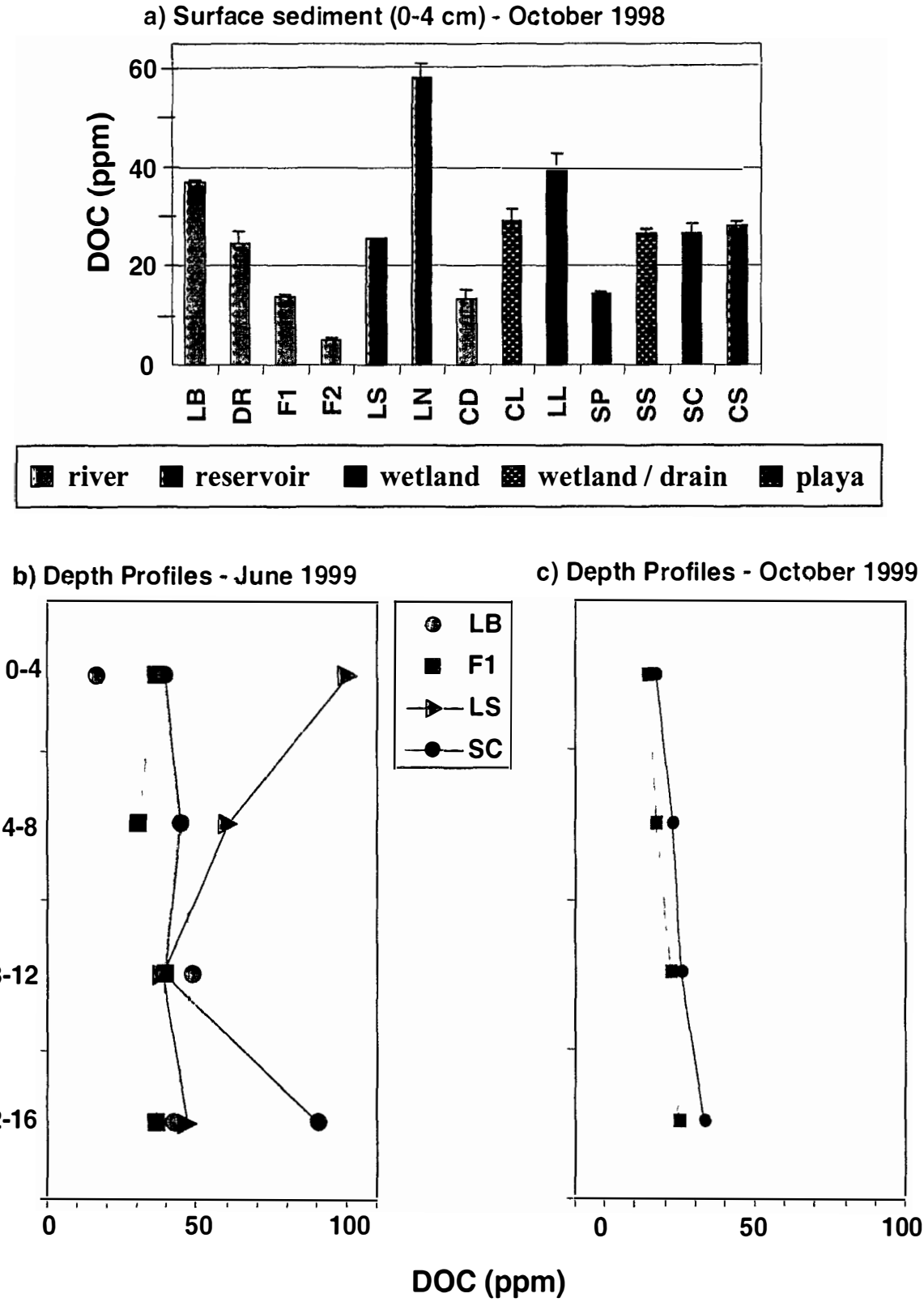

Figure 58. Pore water Dissolved Organic Carbon vs Acid-Extractable Hg(II) / October 1998 (0-4 cm)

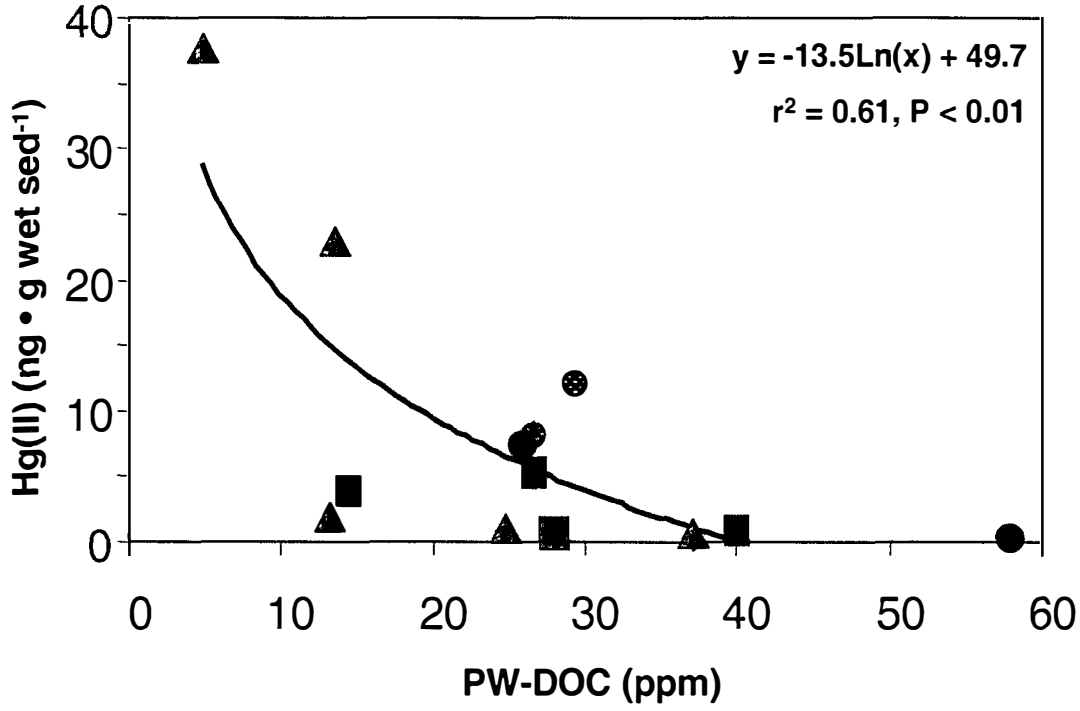

Figure 59. Pore Water Anions – October 1998 (0-4 cm)

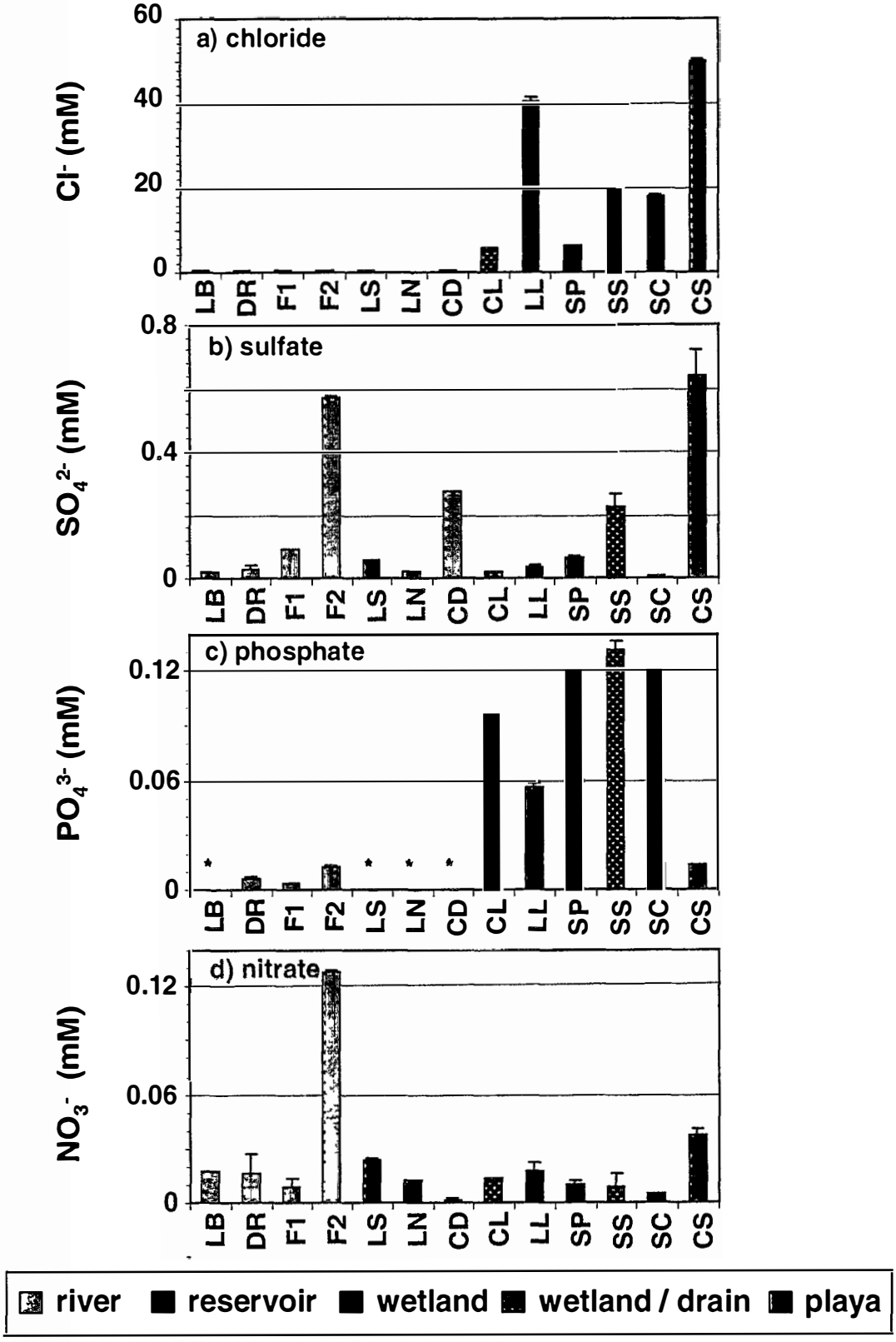

Figure 60. Pore Water Anions – Depth Profiles

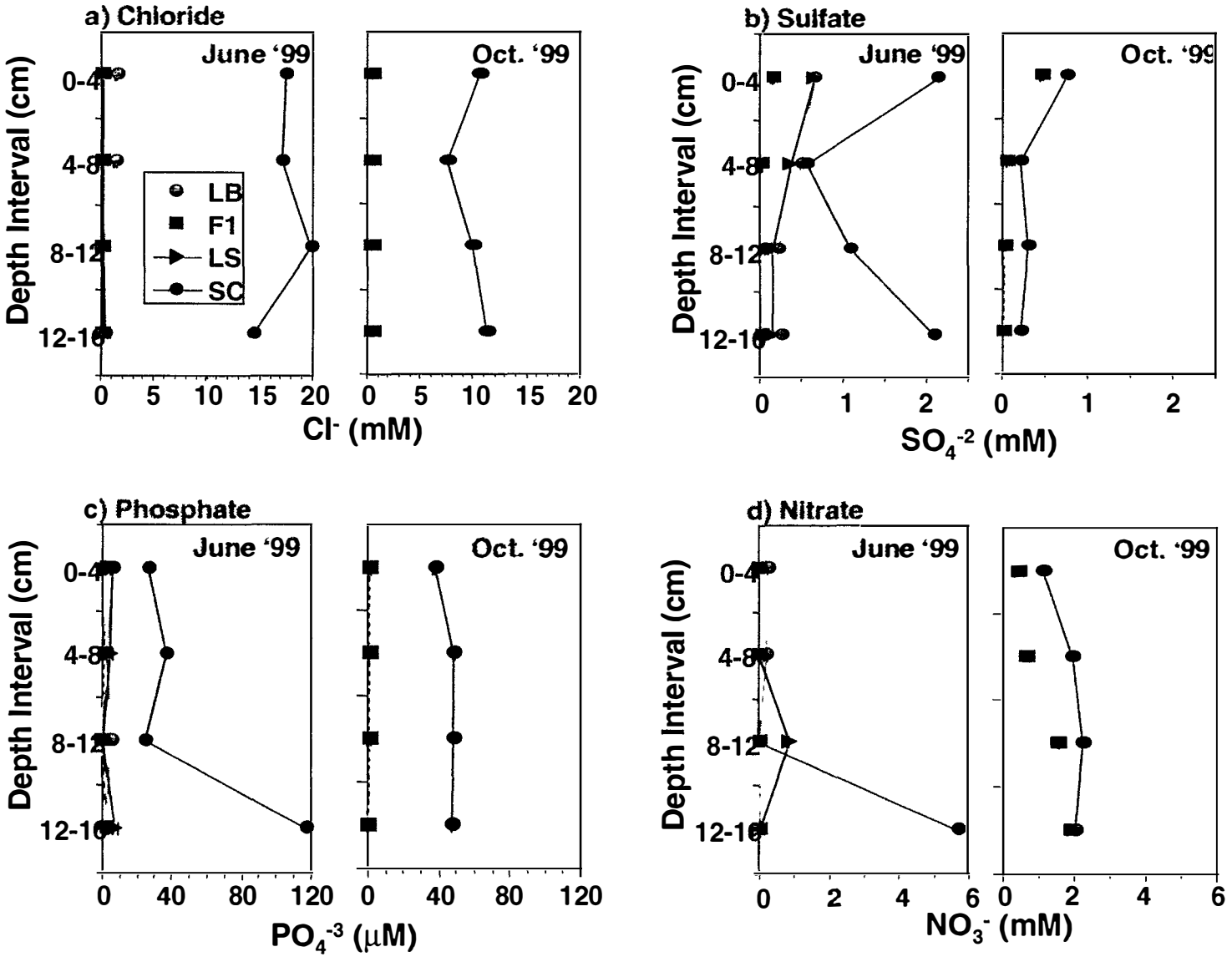

Figure 61. Parameters Correlated with MeHg Degradation Rate Constant (October 1998 data only)

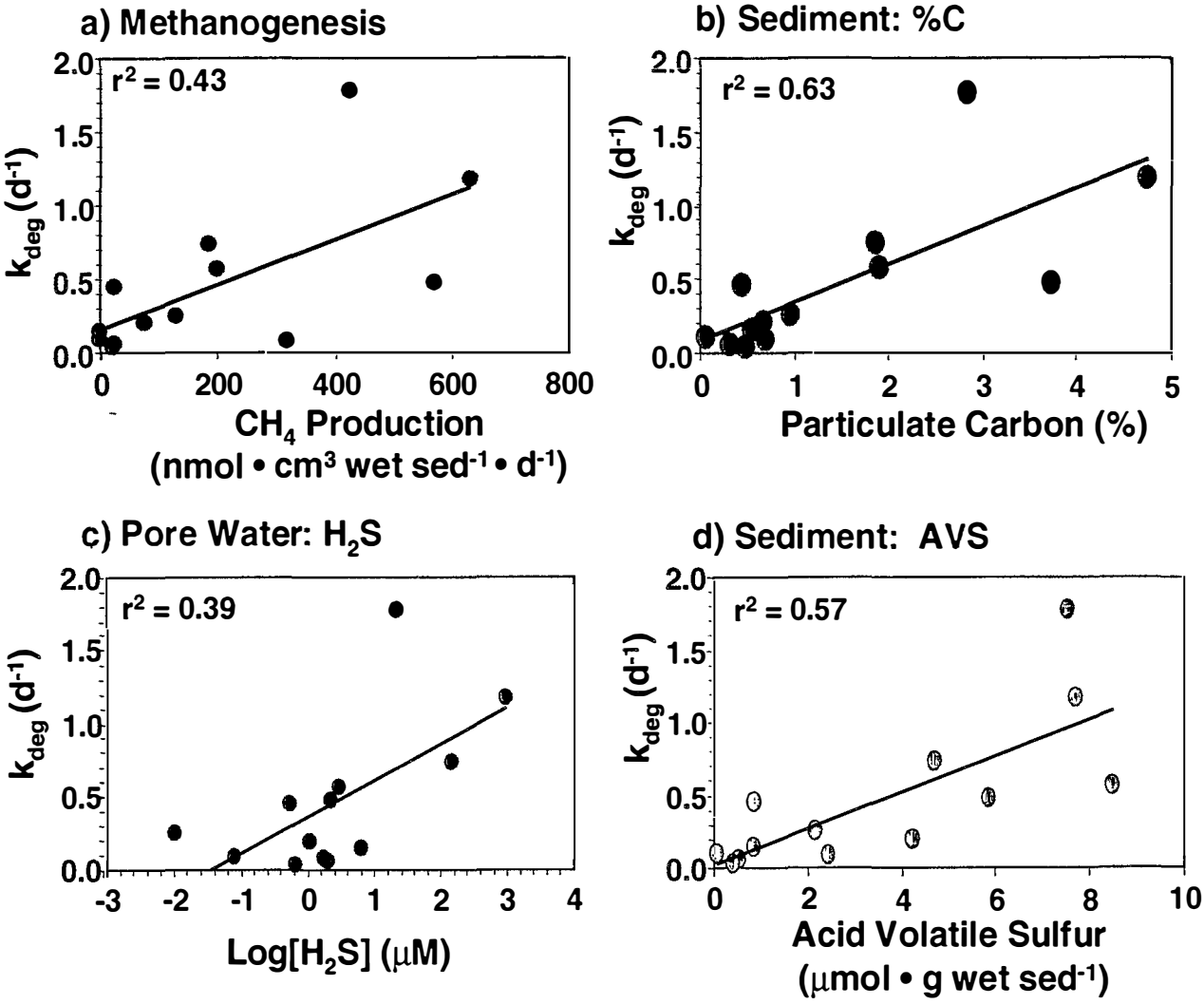

Figure 62. Sediment Manganese and Selenium Concentration vs In-situ MeHg-Degradation Rate (June 1999)

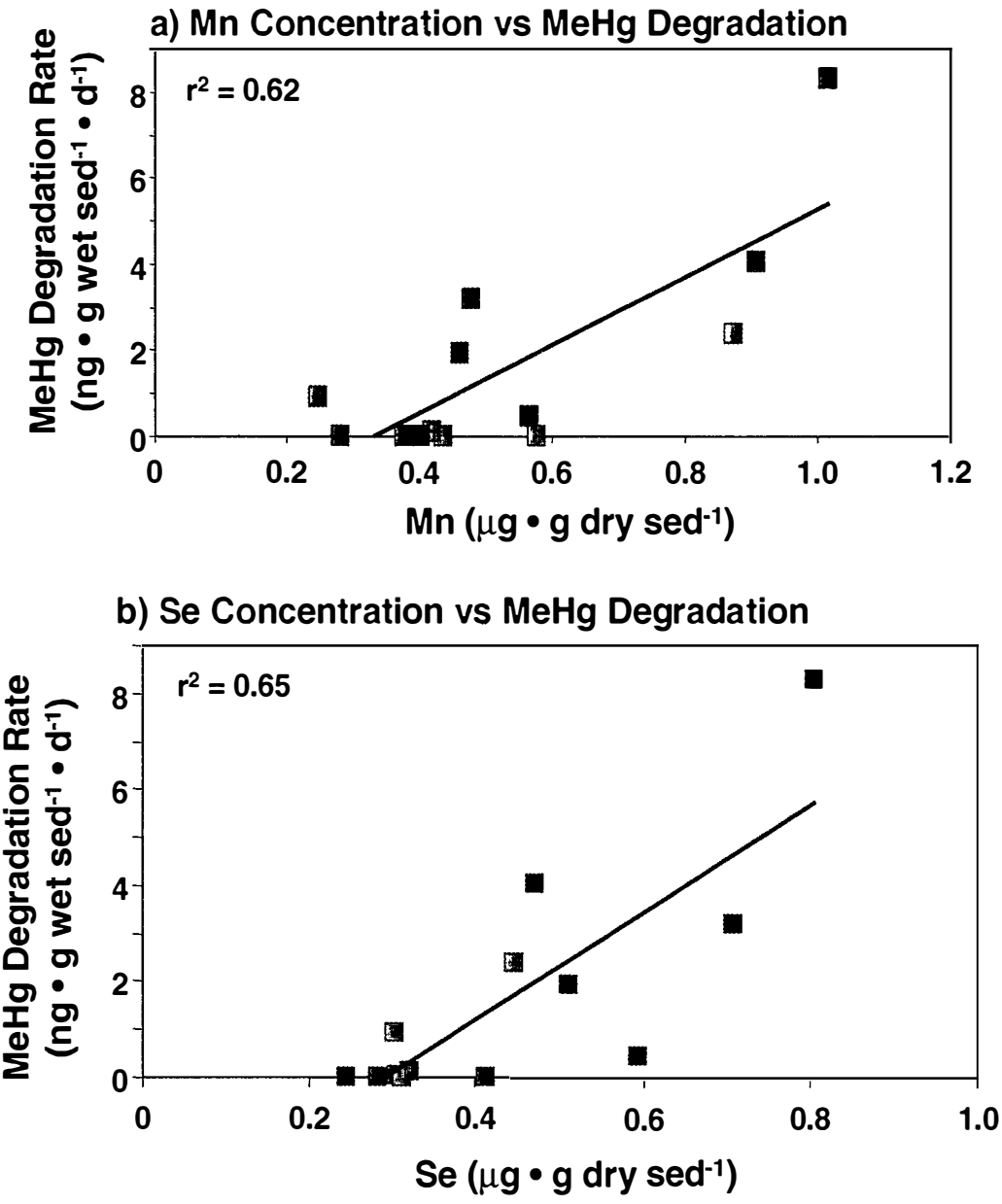

Figure 63. Influence of Hg Contamination on MeHg Degradation

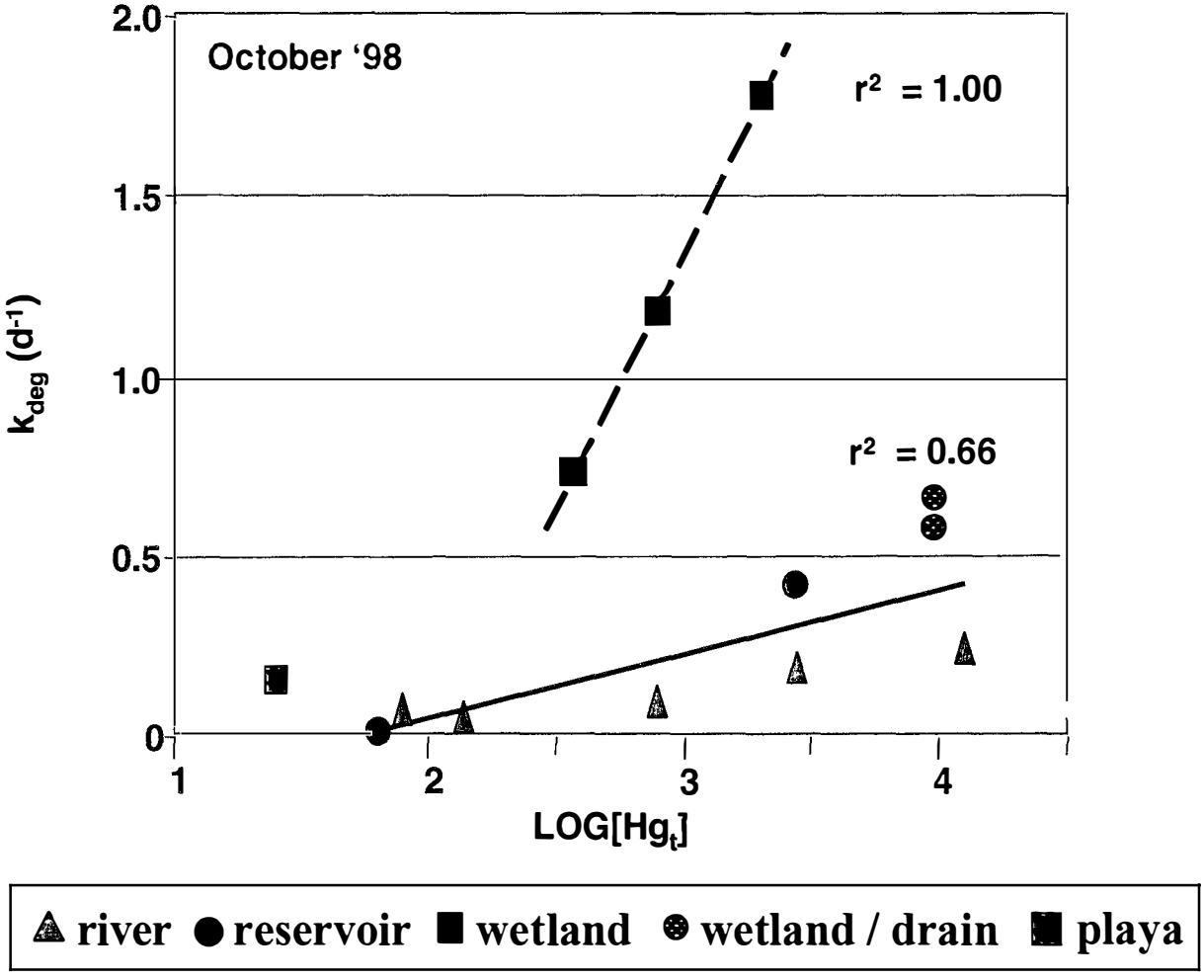

Figure 64. Sequential Extraction of ^{14}C-MeHg

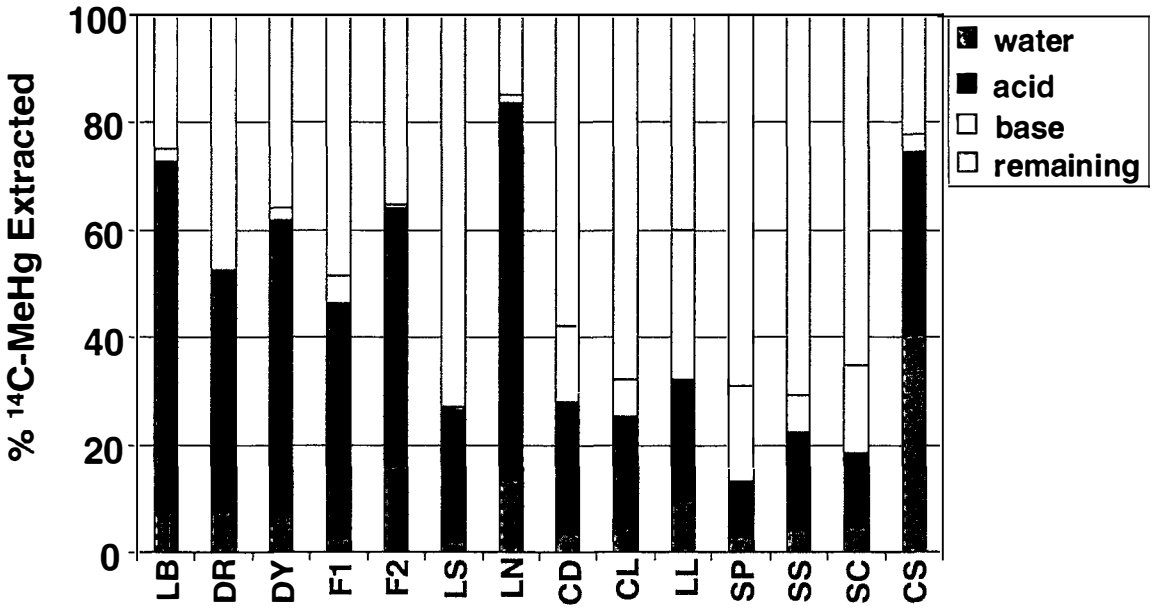

Figure 65. Relationships Between ^{14}C-MeHg Extractable Fractions and Bulk Sediment AVS and LOI Data

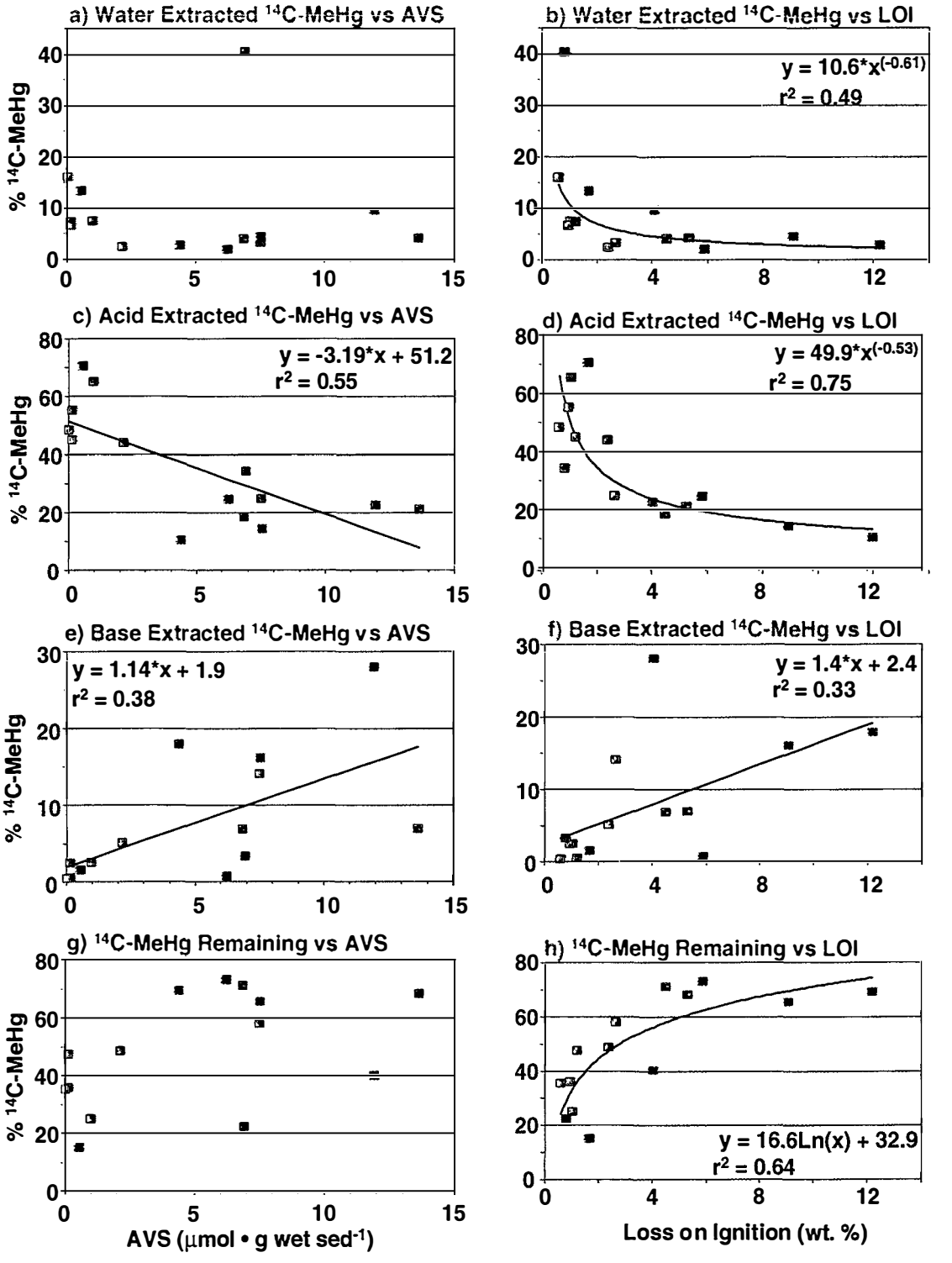

Figure 66. Multiple Factor Experiment: Unamended Sediment Hg-Transformation Rates

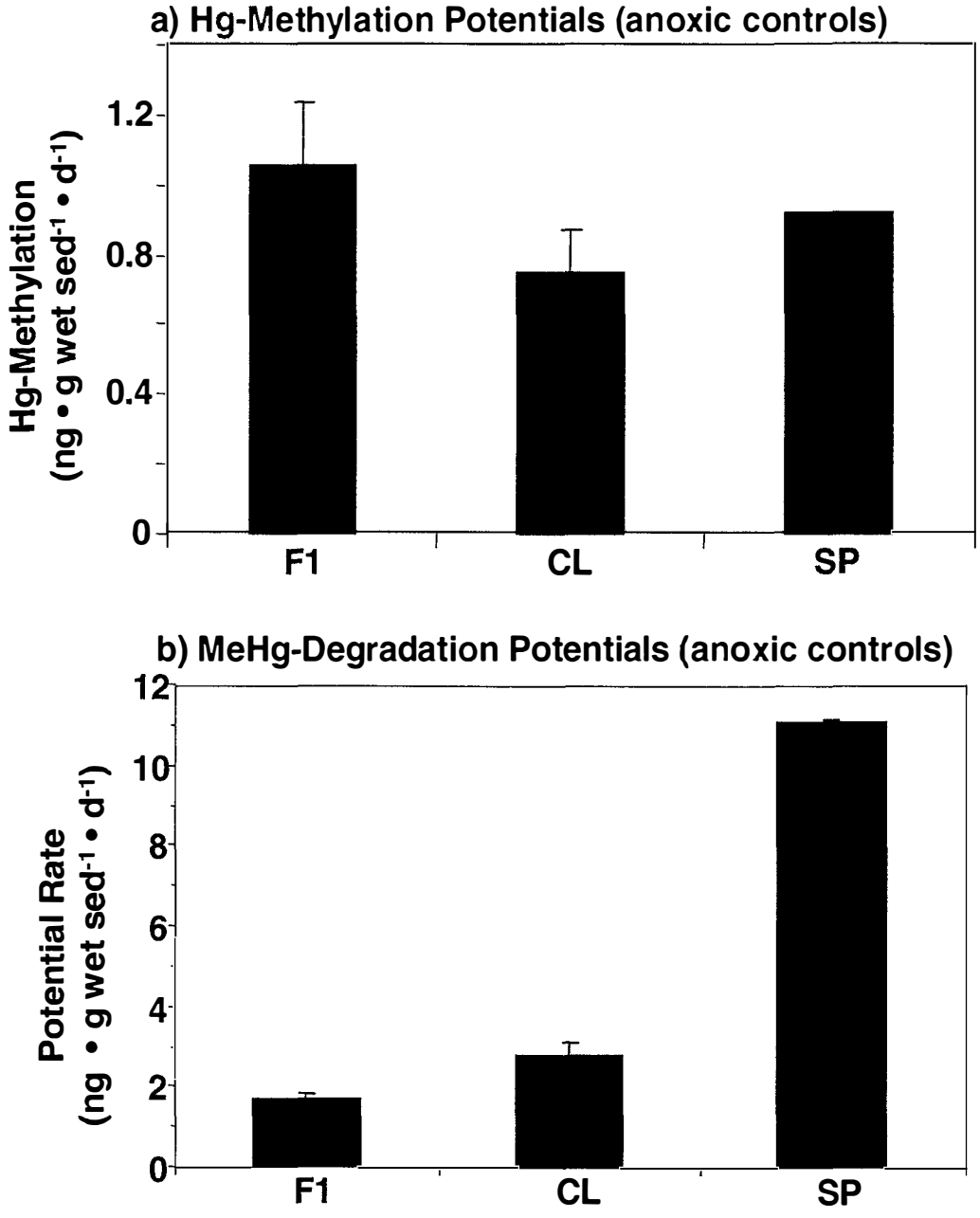

Figure 67. Multiple Factor Experiment: Effects of Key Parameters on MeHg Production and Degradation

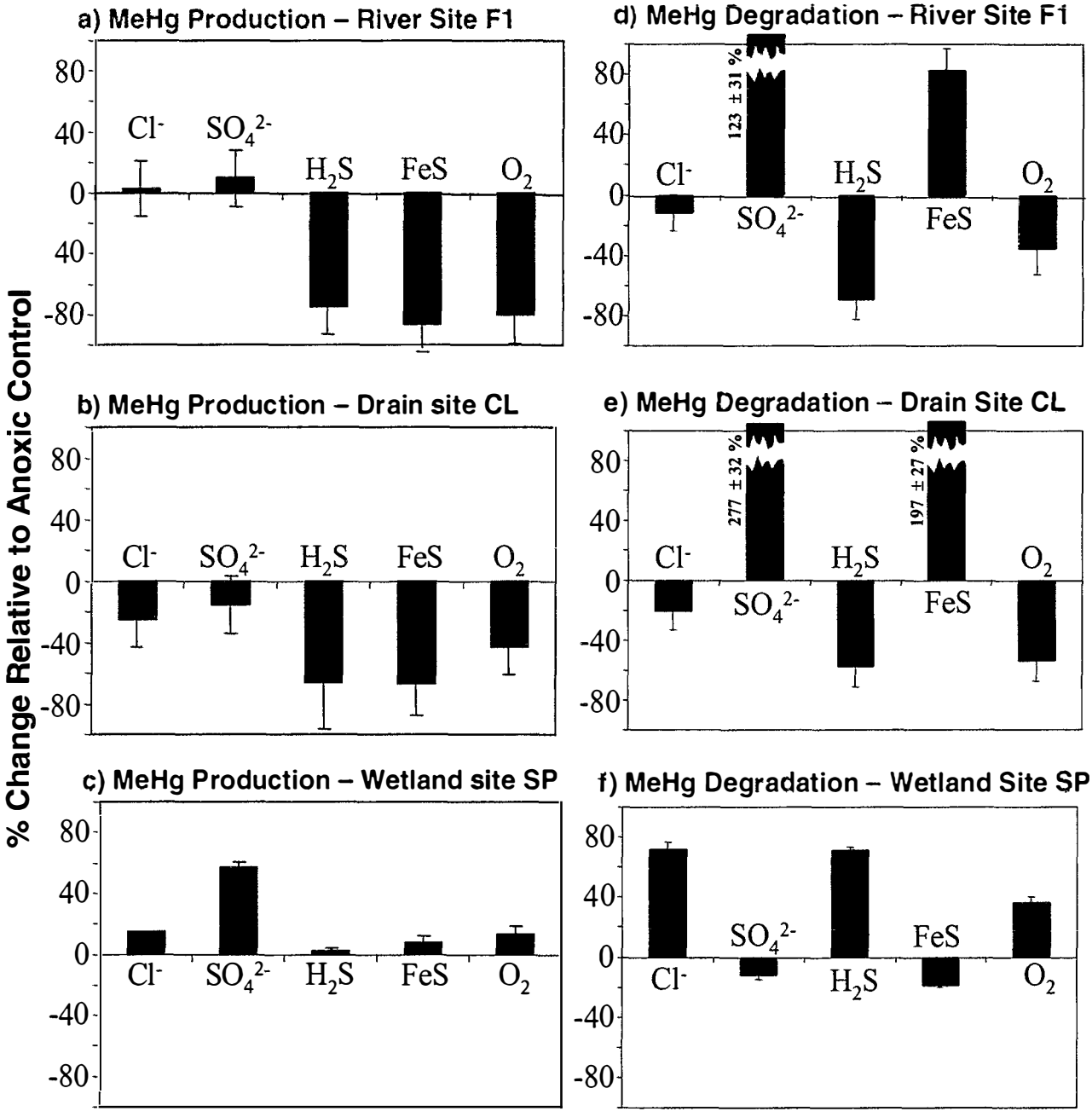

Figure 68. Effects of Temperature on MeHg Production and Degradation

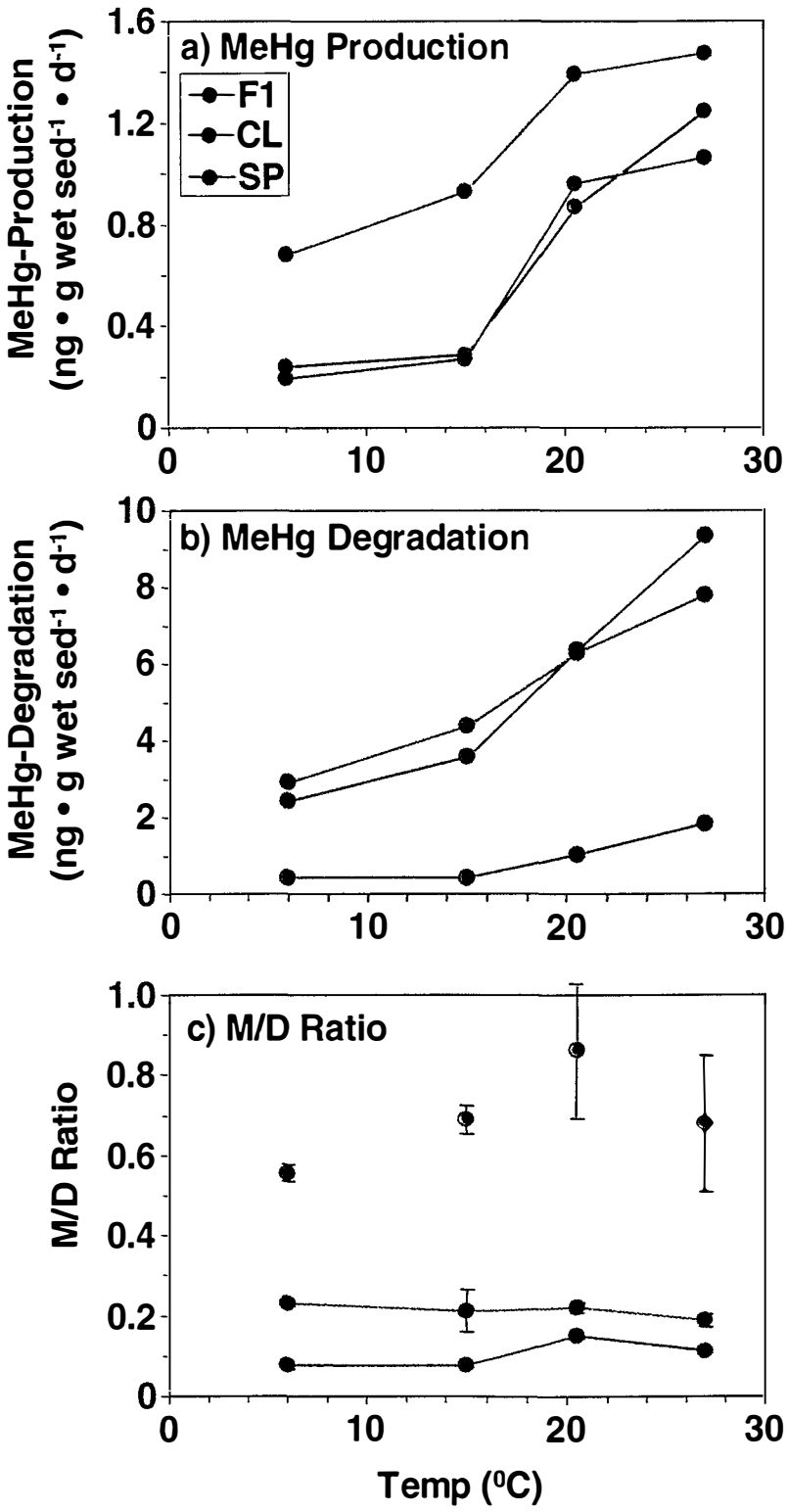

Figure 69. Arrhenius Conversion of Hg-Transformation Rate and Temperature Data.

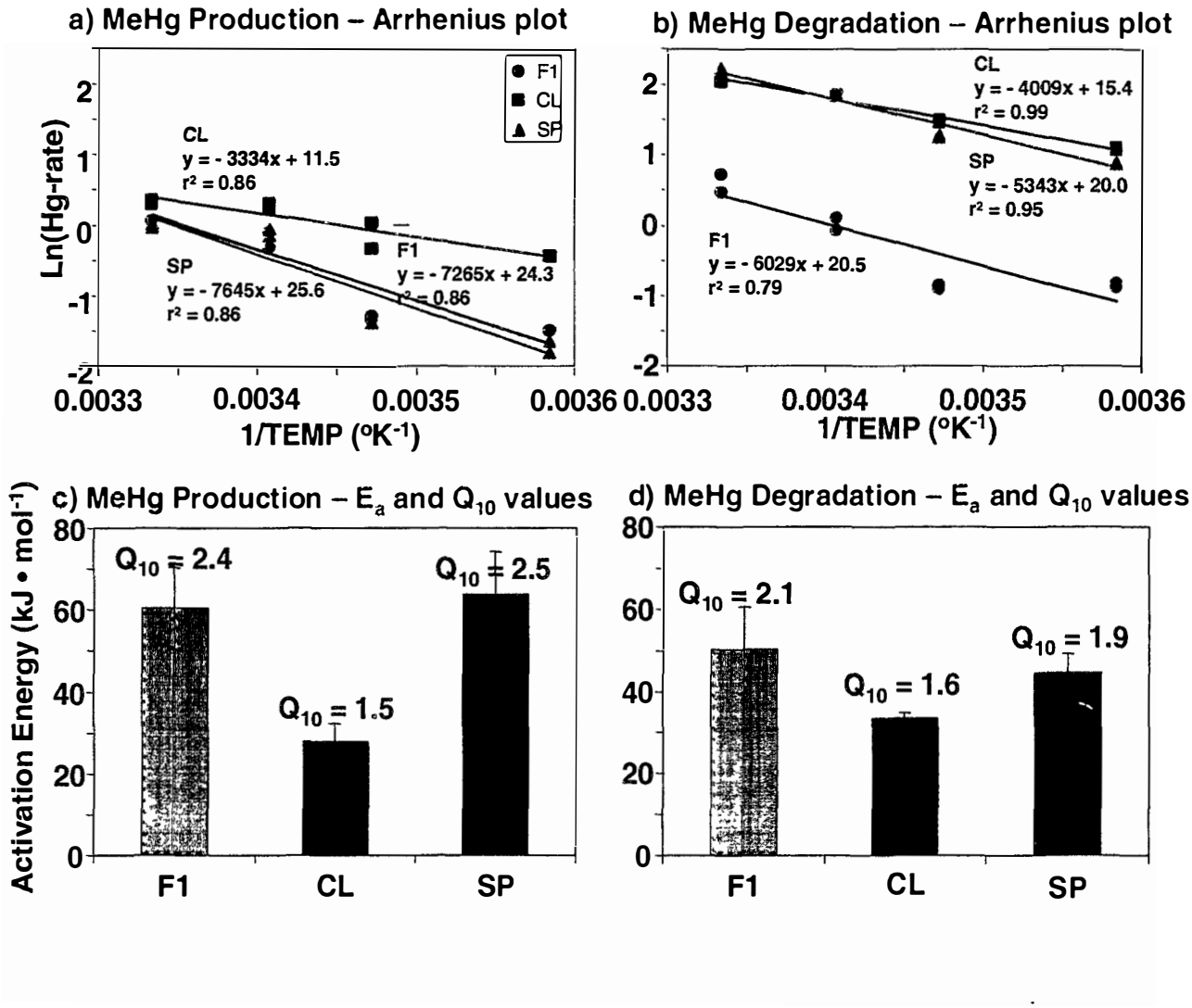

Appendix I – Sample Coding Scheme for the Carson River Mercury Project

General Coding Format: AA-BB-CC-DDDD-EE-FFF

(note: where a particular code does not apply, insert "X's")

1) AA = Site Code:

NAME	CODE	Ecozone Type
Lloyd's Bridge (control site)	**LB**	River
Deer Run Road	**DR**	River
Dayton	**DY**	River
Fort Churchill: Dam Site	**F1**	River
Fort Churchill: Week's Bridge	**F2**	River
Lahontan Reservoir (South)	**LS**	Reservoir
Lahontan Reservoir (North)	**LN**	Reservoir
Carson Diversion Dam	**CD**	River
Carson Lake (Sprig Pond)	**CL**	Agricultural Drain
South Lead Lake	**LL**	Wetland
Stillwater Point Reservoir	**SP**	Wetland
Stillwater Slough Cutoff	**SS**	Agricultural Drain
Swan Check	**SC**	Wetland
Carson Sink	**CS**	Playa

Note: Sites are listed in approximate upstream to downstream order, and in the order typically presented in the Figures.

2) BB = Depth Code:

a) Sediment depth intervals: **D1** = 0-4 cm, **D2** = 4-8 cm, **D3** = 8-12 cm, **D4** = 12-16 cm

b) Site F3 vertical bank sampling height above (+) or below (-) the June '99 water line: **V1** = +30 cm, **V2** = -10 cm, **V3** = -60 cm.

3) CC = Quality Assurance Code:

R1, R2, and **R3** = replicate samples

T1, T2, etc.. = subsequent time points

KC = killed control

RB = reagent blank

EB = equipment "rinsate" blank

MS = matrix spike sample

4) DDDD = Date Code: MMYY

(e.g. 1098 = October 1998 sample collection)

5) EE = Sample Matrix Code:

BS = bulk sediment

PWs = pore-water collected via squeezer method

PWc = pore-water collected via centrifugation

BW = bottom water (above sediment)

Appendix I – (Continued)

6) FFF = Process or Analyte Code:

Process	CODE
MeHg production	**MP**
MeHg degradation	**MD**
Sulfate reduction	**SR**
Methanogenesis	**ME**
Methane oxidation	**MO**
Iron reduction	**IR**
Manganese reduction	**MR**
Total mercury	**Mt**
Methylmercury	**MM**
Reactive (acid-extractabe) Hg(II)	**RM**
Bioavailable Hg(II) (*mer-lux*)	**BM**
Bulk density (sediment)	**BD**
Porosity (sediment)	**POR**
Methane	**CH4**
Grain size	**GS**
pH	**pH**
Sediment Redox	**Eh**
Particulate carbon	**PC**
Particulate nitrogen	**PN**
Loss On Ignition (organic)	**LOI**
Dissolved Organic carbon	**DOC**
Selenium	**Se**
Iron	**Fe**
Manganese	**Mn**
Reduced sulfur	**RS**
Chloride	**Cl**
Sulfate	**SO4**
Nitrate	**NO3**
Nitrite	**NO2**
Phosphate	**PO4**
Sulfide	**SU**
Temperature	**TMP**

Appendix II - Complete Data Set for the Carson River Mercury Project
Note: Bold type indicate value below given detection limit.

A. Microbial Mercury Transformations

A 1a. MeHg Production Rate Constants

A1b. Net MeHg Production Rate

Sample Code	n	Avg.	Std. Dev.	units	Avg.	Std. Dev.	units
LB D1 Rx 1098 BS MP	3	2.5E-02	2.0E-03	d^{-1}	3.6E-03	9.4E-04	ng*g wet sed^{-1}*d^{-1}
DR D1 Rx 1098 BS MP	3	2.8E-02	2.2E-03	d^{-1}	1.8E-02	1.1E-02	ng*g wet sed^{-1}*d^{-1}
F1 D1 Rx 1098 BS MP	3	9.9E-03	1.8E-04	d^{-1}	1.5E-01	5.2E-02	ng*g wet sed^{-1}*d^{-1}
F2 D1 Rx 1098 BS MP	3	**< 9.8E-05**		d^{-1}	**< 3.0E-03**		ng*g wet sed^{-1}*d^{-1}
LS D1 Rx 1098 BS MP	3	2.5E-03	3.2E-04	d^{-1}	1.4E-02	4.9E-03	ng*g wet sed^{-1}*d^{-1}
LN D1 Rx 1098 BS MP	3	6.7E-03	5.0E-04	d^{-1}	1.7E-03	4.2E-04	ng*g wet sed^{-1}*d^{-1}
CD D1 Rx 1098 BS MP	3	3.9E-03	1.1E-04	d^{-1}	4.4E-03	1.8E-03	ng*g wet sed^{-1}*d^{-1}
CL D1 Rx 1098 BS MP	3	6.2E-03	6.7E-04	d^{-1}	2.0E-02	1.3E-02	ng*g wet sed^{-1}*d^{-1}
LL D1 Rx 1098 BS MP	3	3.5E-04	5.3E-05	d^{-1}	2.0E-04	9.2E-05	ng*g wet sed^{-1}*d^{-1}
SP D1 Rx 1098 BS MP	3	5.6E-04	2.7E-05	d^{-1}	5.4E-04	1.8E-04	ng*g wet sed^{-1}*d^{-1}
SS D1 Rx 1098 BS MP	3	3.4E-03	3.0E-04	d^{-1}	1.7E-02	2.5E-03	ng*g wet sed^{-1}*d^{-1}
SC D1 Rx 1098 BS MP	3	**< 8.9E-05**		d^{-1}	**< 8.3E-05**		ng*g wet sed^{-1}*d^{-1}
CS D1 Rx 1098 BS MP	3	5.1E-03	1.2E-03	d^{-1}	6.7E-04	4.0E-04	ng*g wet sed^{-1}*d^{-1}
LB D1 Rx 0699 BS MP	3	2.1E-03	1.3E-04	d^{-1}	8.8E-04	3.9E-04	ng*g wet sed^{-1}*d^{-1}
LB D2 Rx 0699 BS MP	3	2.9E-03	1.3E-03	d^{-1}	8.2E-04	4.8E-04	ng*g wet sed^{-1}*d^{-1}
LB D3 Rx 0699 BS MP	3	1.3E-03	1.8E-03	d^{-1}	1.2E-03	1.6E-03	ng*g wet sed^{-1}*d^{-1}
LB D4 Rx 0699 BS MP	3	**< 2.8E-4**		d^{-1}	**< 1.6E-04**		ng*g wet sed^{-1}*d^{-1}
DR D1 Rx 0699 BS MP	3	4.9E-04	7.7E-05	d^{-1}	2.8E-04	8.1E-05	ng*g wet sed^{-1}*d^{-1}
F1 D1 Rx 0699 BS MP	3	7.1E-03	1.4E-03	d^{-1}	1.2E-01	2.7E-02	ng*g wet sed^{-1}*d^{-1}
F1 D2 Rx 0699 BS MP	3	5.0E-03	6.5E-04	d^{-1}	1.7E-01	3.1E-02	ng*g wet sed^{-1}*d^{-1}
F1 D3 Rx 0699 BS MP	3	6.6E-03	1.2E-03	d^{-1}	3.1E-01	1.8E-01	ng*g wet sed^{-1}*d^{-1}
F1 D4 Rx 0699 BS MP	3	2.8E-03	3.9E-04	d^{-1}	2.0E-02	1.3E-02	ng*g wet sed^{-1}*d^{-1}
F2 D1 Rx 0699 BS MP	3	7.6E-04	4.2E-04	d^{-1}	5.1E-02	3.1E-02	ng*g wet sed^{-1}*d^{-1}
F3 V1 Rx 0699 BS MP	3	4.7E-04	2.2E-04	d^{-1}	2.4E-03	1.2E-03	ng*g wet sed^{-1}*d^{-1}
F3 V2 Rx 0699 BS MP	3	3.2E-04	5.1E-05	d^{-1}	1.6E-03	2.8E-04	ng*g wet sed^{-1}*d^{-1}
F3 V3 Rx 0699 BS MP	3	**< 2.8E-4**		d^{-1}	**< 8.2E-05**		ng*g wet sed^{-1}*d^{-1}
LS D1 Rx 0699 BS MP	3	5.9E-04	3.0E-04	d^{-1}	2.9E-03	1.6E-03	ng*g wet sed^{-1}*d^{-1}
LS D2 Rx 0699 BS MP	3	6.0E-04	6.3E-04	d^{-1}	4.5E-03	4.8E-03	ng*g wet sed^{-1}*d^{-1}
LS D3 Rx 0699 BS MP	3	**< 2.8E-4**		d^{-1}	**< 1.3E-03**		ng*g wet sed^{-1}*d^{-1}
LS D4 Rx 0699 BS MP	3	4.6E-04	3.2E-04	d^{-1}	1.2E-03	1.0E-03	ng*g wet sed^{-1}*d^{-1}
LN D1 Rx 0699 BS MP	3	**< 2.8E-4**		d^{-1}	**< 3.1E-04**		ng*g wet sed^{-1}*d^{-1}
CD D1 Rx 0699 BS MP	3	1.6E-03	1.4E-04	d^{-1}	9.9E-03	1.2E-03	ng*g wet sed^{-1}*d^{-1}
CL D1 Rx 0699 BS MP	3	3.2E-03	1.9E-04	d^{-1}	5.4E-02	4.7E-02	ng*g wet sed^{-1}*d^{-1}
LL D1 Rx 0699 BS MP	3	**< 2.8E-4**		d^{-1}	**< 2.6E-04**		ng*g wet sed^{-1}*d^{-1}
SP D1 Rx 0699 BS MP	3	5.9E-04	1.0E-04	d^{-1}	1.6E-03	1.4E-03	ng*g wet sed^{-1}*d^{-1}
SS D1 Rx 0699 BS MP	3	3.7E-04	2.5E-04	d^{-1}	1.1E-03	1.2E-03	ng*g wet sed^{-1}*d^{-1}
SC D1 Rx 0699 BS MP	3	4.9E-04	1.9E-04	d^{-1}	9.0E-04	3.5E-04	ng*g wet sed^{-1}*d^{-1}
SC D2 Rx 0699 BS MP	3	**< 2.8E-4**		d^{-1}	**< 7.4E-04**		ng*g wet sed^{-1}*d^{-1}
SC D3 Rx 0699 BS MP	3	**< 2.8E-4**		d^{-1}	**< 8.8E-04**		ng*g wet sed^{-1}*d^{-1}
SC D4 Rx 0699 BS MP	3	8.2E-04	1.5E-04	d^{-1}	5.1E-03	1.5E-03	ng*g wet sed^{-1}*d^{-1}
CS D1 Rx 0699 BS MP	3	**< 2.8E-4**		d^{-1}	**< 5.9E-05**		ng*g wet sed^{-1}*d^{-1}
LB D1 Rx 1099 BS MP	3	3.0E-03	4.6E-04	d^{-1}	3.0E-04	4.9E-05	ng*g wet sed^{-1}*d^{-1}
DR D1 Rx 1099 BS MP	3	4.3E-04	2.3E-04	d^{-1}	6.7E-04	4.0E-04	ng*g wet sed^{-1}*d^{-1}
DY D1 Rx 1099 BS MP	3	8.0E-04	2.2E-04	d^{-1}	4.3E-03	1.7E-03	ng*g wet sed^{-1}*d^{-1}
F1 D1 Rx 1099 BS MP	3	7.0E-03	1.5E-03	d^{-1}	8.8E-02	2.5E-02	ng*g wet sed^{-1}*d^{-1}
F1 D2 Rx 1099 BS MP	3	3.2E-03	3.1E-04	d^{-1}	3.9E-02	7.2E-03	ng*g wet sed^{-1}*d^{-1}

Sample Code						n	Avg.	Std. Dev	Units	Avg.	Std. Dev	Units
F1	D3	Rx	1099	BS	MP	3	9.7E-03	3.8E-03	d^{-1}	1.7E-01	6.7E-02	ng*g wet sed^{-1}*d^{-1}
F1	D4	Rx	1099	BS	MP	3	1.1E-02	1.8E-03	d^{-1}	1.6E-01	3.1E-02	ng*g wet sed^{-1}*d^{-1}
F2	D1	Rx	1099	BS	MP	3	**< 3.6E-4**		d^{-1}	**< 7.6E-03**		ng*g wet sed^{-1}*d^{-1}
F3	V1	Rx	1099	BS	MP	3	**< 3.6E-4**		d^{-1}	**< 4.8E-03**		ng*g wet sed^{-1}*d^{-1}
F3	V3	Rx	1099	BS	MP	3	**< 3.6E-4**		d^{-1}	**< 2.8E-01**		ng*g wet sed^{-1}*d^{-1}
LS	D1	Rx	1099	BS	MP	3	1.2E-02	1.1E-03	d^{-1}	2.0E-01	3.3E-02	ng*g wet sed^{-1}*d^{-1}
LN	D1	Rx	1099	BS	MP	3	**< 3.6E-4**		d^{-1}	**< 8.0E-05**		ng*g wet sed^{-1}*d^{-1}
CD	D1	Rx	1099	BS	MP	3	3.8E-03	1.4E-03	d^{-1}	1.4E-02	5.1E-03	ng*g wet sed^{-1}*d^{-1}
CL	D1	Rx	1099	BS	MP	3	9.5E-03	1.2E-03	d^{-1}	7.7E-02	1.1E-02	ng*g wet sed^{-1}*d^{-1}
LL	D1	Rx	1099	BS	MP	3	6.1E-03	2.1E-04	d^{-1}	1.5E-02	1.4E-03	ng*g wet sed^{-1}*d^{-1}
SP	D1	Rx	1099	BS	MP	3	1.1E-02	1.3E-04	d^{-1}	1.5E-02	3.3E-03	ng*g wet sed^{-1}*d^{-1}
SS	D1	Rx	1099	BS	MP	3	6.1E-03	4.0E-04	d^{-1}	7.6E-02	1.1E-02	ng*g wet sed^{-1}*d^{-1}
SC	D1	Rx	1099	BS	MP	3	1.8E-03	1.8E-04	d^{-1}	4.5E-03	7.2E-04	ng*g wet sed^{-1}*d^{-1}
SC	D2	Rx	1099	BS	MP	3	3.7E-04	3.8E-04	d^{-1}	6.6E-04	6.8E-04	ng*g wet sed^{-1}*d^{-1}
SC	D3	Rx	1099	BS	MP	3	**< 3.6E-4**		d^{-1}	**< 1.4E-03**		ng*g wet sed^{-1}*d^{-1}
SC	D4	Rx	1099	BS	MP	3	7.3E-04	5.4E-05	d^{-1}	5.7E-03	4.2E-04	ng*g wet sed^{-1}*d^{-1}
CS	D1	Rx	1099	BS	MP	3	1.4E-03	1.4E-04	d^{-1}	5.5E-05	3.8E-05	ng*g wet sed^{-1}*d^{-1}

A2a. MeHg Degradation Rate Constants | *A2b. Gross MeHg Degradation Rate*

LB	D1	Rx	1098	BS	MD	4	7.9E-02	1.3E-02	d^{-1}	9.7E-02	1.8E-02	ng*g wet sed^{-1}*d^{-1}
DR	D1	Rx	1098	BS	MD	4	5.3E-02	7.6E-03	d^{-1}	3.4E-02	5.0E-03	ng*g wet sed^{-1}*d^{-1}
F1	D1	Rx	1098	BS	MD	4	2.5E-01	2.7E-02	d^{-1}	1.2E+00	1.6E-01	ng*g wet sed^{-1}*d^{-1}
F2	D1	Rx	1098	BS	MD	4	9.3E-02	7.9E-03	d^{-1}	1.3E-02	1.1E-02	ng*g wet sed^{-1}*d^{-1}
LS	D1	Rx	1098	BS	MD	4	4.5E-01	1.1E-01	d^{-1}	1.7E-01	4.5E-02	ng*g wet sed^{-1}*d^{-1}
LN	D1	Rx	1098	BS	MD	4	3.3E-02	8.0E-03	d^{-1}	6.1E-03	3.1E-03	ng*g wet sed^{-1}*d^{-1}
CD	D1	Rx	1098	BS	MD	4	1.9E-01	3.6E-02	d^{-1}	2.0E-01	4.8E-02	ng*g wet sed^{-1}*d^{-1}
CL	D1	Rx	1098	BS	MD	4	4.8E-01	1.1E-02	d^{-1}	6.2E-01	8.0E-02	ng*g wet sed^{-1}*d^{-1}
LL	D1	Rx	1098	BS	MD	4	7.3E-01	5.2E-02	d^{-1}	1.1E-01	3.8E-02	ng*g wet sed^{-1}*d^{-1}
SP	D1	Rx	1098	BS	MD	4	1.8E+00	4.4E-02	d^{-1}	1.7E-01	2.8E-02	ng*g wet sed^{-1}*d^{-1}
SS	D1	Rx	1098	BS	MD	4	5.7E-01	8.9E-02	d^{-1}	4.8E-01	9.1E-02	ng*g wet sed^{-1}*d^{-1}
SC	D1	Rx	1098	BS	MD	4	1.2E+00	8.4E-02	d^{-1}	8.5E-02	4.7E-02	ng*g wet sed^{-1}*d^{-1}
CS	D1	Rx	1098	BS	MD	4	1.5E-01	2.8E-02	d^{-1}	1.9E-03	2.1E-03	ng*g wet sed^{-1}*d^{-1}
LB	D1	Rx	0699	BS	MD	3	4.2E-02	1.3E-02	d^{-1}	2.2E-02	7.8E-03	ng*g wet sed^{-1}*d^{-1}
LB	D2	Rx	0699	BS	MD	3	3.8E-02	7.0E-03	d^{-1}	4.7E-02	1.3E-02	ng*g wet sed^{-1}*d^{-1}
LB	D3	Rx	0699	BS	MD	3	1.4E-02	1.2E-02	d^{-1}	9.7E-03	8.6E-03	ng*g wet sed^{-1}*d^{-1}
LB	D4	Rx	0699	BS	MD	3	4.0E-02	5.6E-03	d^{-1}	1.9E-02	2.8E-03	ng*g wet sed^{-1}*d^{-1}
DR	D1	Rx	0699	BS	MD	3	4.0E-02	6.1E-03	d^{-1}	7.8E-03	1.3E-03	ng*g wet sed^{-1}*d^{-1}
F1	D1	Rx	0699	BS	MD	3	1.5E-01	2.6E-02	d^{-1}	2.2E+00	3.8E-01	ng*g wet sed^{-1}*d^{-1}
F1	D2	Rx	0699	BS	MD	3	8.4E-02	8.2E-02	d^{-1}	1.5E+00	1.5E+00	ng*g wet sed^{-1}*d^{-1}
F1	D3	Rx	0699	BS	MD	3	9.1E-02	3.2E-02	d^{-1}	1.7E+00	7.1E-01	ng*g wet sed^{-1}*d^{-1}
F1	D4	Rx	0699	BS	MD	3	1.3E-01	7.3E-02	d^{-1}	1.9E+00	1.0E+00	ng*g wet sed^{-1}*d^{-1}
F2	D1	Rx	0699	BS	MD	3	5.1E-02	1.1E-02	d^{-1}	1.1E-01	2.2E-02	ng*g wet sed^{-1}*d^{-1}
F3	V1	Rx	0699	BS	MD	3	2.0E-02	2.4E-03	d^{-1}	1.1E-03	6.3E-04	ng*g wet sed^{-1}*d^{-1}
F3	V2	Rx	0699	BS	MD	3	2.2E-02	1.0E-02	d^{-1}	2.8E-03	2.4E-03	ng*g wet sed^{-1}*d^{-1}
F3	V3	Rx	0699	BS	MD	3	3.9E-03	1.1E-03	d^{-1}	2.7E-04	1.6E-04	ng*g wet sed^{-1}*d^{-1}
LS	D1	Rx	0699	BS	MD	3	4.2E-02	6.4E-03	d^{-1}	1.5E-02	2.4E-03	ng*g wet sed^{-1}*d^{-1}
LS	D2	Rx	0699	BS	MD	3	4.2E-02	1.3E-02	d^{-1}	2.2E-02	9.0E-03	ng*g wet sed^{-1}*d^{-1}
LS	D3	Rx	0699	BS	MD	3	3.2E-02	2.8E-03	d^{-1}	7.7E-03	6.6E-04	ng*g wet sed^{-1}*d^{-1}
LS	D4	Rx	0699	BS	MD	3	3.1E-02	5.5E-03	d^{-1}	4.9E-03	1.0E-03	ng*g wet sed^{-1}*d^{-1}
LN	D1	Rx	0699	BS	MD	3	4.4E-02	3.7E-03	d^{-1}	**< 5.2E-03**		ng*g wet sed^{-1}*d^{-1}
CD	D1	Rx	0699	BS	MD	3	4.4E-01	4.9E-02	d^{-1}	7.5E-01	8.4E-02	ng*g wet sed^{-1}*d^{-1}
CL	D1	Rx	0699	BS	MD	3	1.7E+00	3.2E-02	d^{-1}	4.0E+00	9.1E-01	ng*g wet sed^{-1}*d^{-1}
LL	D1	Rx	0699	BS	MD	3	3.5E+00	6.4E-01	d^{-1}	5.4E-01	9.9E-02	ng*g wet sed^{-1}*d^{-1}
SP	D1	Rx	0699	BS	MD	3	5.1E-01	1.5E-01	d^{-1}	3.6E-01	3.2E-01	ng*g wet sed^{-1}*d^{-1}

Sample Code						n	Avg.	Std. Dev	Units	Avg.	Std. Dev	Units
SS	D1	Rx	0699	BS	MD	3	4.5E+00	2.1E-01	d^{-1}	8.9E-01	5.9E-01	$ng*g\ wet\ sed^{-1}*d^{-1}$
SC	D1	Rx	0699	BS	MD	3	7.2E+00	1.1E-01	d^{-1}	4.4E-01	5.6E-02	$ng*g\ wet\ sed^{-1}*d^{-1}$
SC	D2	Rx	0699	BS	MD	3	5.5E+00	3.7E-01	d^{-1}	2.1E-01	2.6E-02	$ng*g\ wet\ sed^{-1}*d^{-1}$
SC	D3	Rx	0699	BS	MD	3	1.4E+00	5.2E-02	d^{-1}	4.0E-01	1.7E-02	$ng*g\ wet\ sed^{-1}*d^{-1}$
SC	D4	Rx	0699	BS	MD	3	1.9E-01	4.4E-02	d^{-1}	2.2E-01	5.0E-02	$ng*g\ wet\ sed^{-1}*d^{-1}$
CS	D1	Rx	0699	BS	MD	3	4.5E-01	6.2E-02	d^{-1}	**< 2.3E-02**		$ng*g\ wet\ sed^{-1}*d^{-1}$
LB	D1	Rx	1099	BS	MD	3	5.6E-02	1.7E-02	d^{-1}	1.7E-01	3.4E-02	$ng*g\ wet\ sed^{-1}*d^{-1}$
DR	D1	Rx	1099	BS	MD	3	4.6E-02	1.9E-02	d^{-1}	3.5E-03	2.1E-04	$ng*g\ wet\ sed^{-1}*d^{-1}$
DY	D1	Rx	1099	BS	MD	3	3.7E-02	1.1E-02	d^{-1}	2.8E-02	3.5E-03	$ng*g\ wet\ sed^{-1}*d^{-1}$
F1	D1	Rx	1099	BS	MD	3	1.6E-01	1.4E-02	d^{-1}	8.7E-01	5.1E-01	$ng*g\ wet\ sed^{-1}*d^{-1}$
F1	D2	Rx	1099	BS	MD	3	4.5E-02	1.8E-02	d^{-1}	2.4E-01	1.2E-02	$ng*g\ wet\ sed^{-1}*d^{-1}$
F1	D3	Rx	1099	BS	MD	3	3.9E-02	8.5E-03	d^{-1}	3.0E-01	6.1E-02	$ng*g\ wet\ sed^{-1}*d^{-1}$
F1	D4	Rx	1099	BS	MD	3	6.3E-02	1.3E-02	d^{-1}	4.8E-01	5.8E-02	$ng*g\ wet\ sed^{-1}*d^{-1}$
F2	D1	Rx	1099	BS	MD	3	3.4E-02	1.9E-02	d^{-1}	3.9E-03	2.7E-04	$ng*g\ wet\ sed^{-1}*d^{-1}$
F3	V1	Rx	1099	BS	MD	3	**< 1.0E-02**		d^{-1}	**< 2.6E-03**		$ng*g\ wet\ sed^{-1}*d^{-1}$
F3	V3	Rx	1099	BS	MD	3	2.2E-02	5.8E-03	d^{-1}	8.3E-02	1.8E-02	$ng*g\ wet\ sed^{-1}*d^{-1}$
LS	D1	Rx	1099	BS	MD	3	2.0E+00	5.1E-02	d^{-1}	3.4E+00	4.0E-01	$ng*g\ wet\ sed^{-1}*d^{-1}$
LN	D1	Rx	1099	BS	MD	3	7.6E-02	1.9E-02	d^{-1}	5.5E-03	1.1E-03	$ng*g\ wet\ sed^{-1}*d^{-1}$
CD	D1	Rx	1099	BS	MD	3	6.7E-01	8.7E-02	d^{-1}	1.1E+00	1.9E-01	$ng*g\ wet\ sed^{-1}*d^{-1}$
CL	D1	Rx	1099	BS	MD	3	1.0E+00	4.6E-02	d^{-1}	3.5E+00	9.3E-01	$ng*g\ wet\ sed^{-1}*d^{-1}$
LL	D1	Rx	1099	BS	MD	3	1.2E+00	7.5E-02	d^{-1}	4.8E-01	1.2E-01	$ng*g\ wet\ sed^{-1}*d^{-1}$
SP	D1	Rx	1099	BS	MD	3	1.9E+00	6.5E-02	d^{-1}	9.5E-01	5.4E-01	$ng*g\ wet\ sed^{-1}*d^{-1}$
SS	D1	Rx	1099	BS	MD	3	6.1E-01	5.2E-02	d^{-1}	1.8E+00	5.1E-01	$ng*g\ wet\ sed^{-1}*d^{-1}$
SC	D1	Rx	1099	BS	MD	3	3.9E+00	9.7E-02	d^{-1}	4.0E-01	8.9E-02	$ng*g\ wet\ sed^{-1}*d^{-1}$
SC	D2	Rx	1099	BS	MD	3	1.2E+00	1.8E-01	d^{-1}	1.4E-01	4.1E-02	$ng*g\ wet\ sed^{-1}*d^{-1}$
SC	D3	Rx	1099	BS	MD	3	5.6E-01	8.9E-02	d^{-1}	7.5E-02	4.3E-02	$ng*g\ wet\ sed^{-1}*d^{-1}$
SC	D4	Rx	1099	BS	MD	3	4.7E-01	7.8E-02	d^{-1}	7.5E-02	8.4E-02	$ng*g\ wet\ sed^{-1}*d^{-1}$
CS	D1	Rx	1099	BS	MD	3	5.0E-01	1.2E-01	d^{-1}	4.4E-03	3.0E-03	$ng*g\ wet\ sed^{-1}*d^{-1}$

B. Ancillary Microbial Processes

B1a. Sulfate Reduction Rate Constant

B1b. Sulfate Reduction Rate

LB	D1	Rx	1098	BS	SR	2	8.8E-03	7.5E-04	d^{-1}	9.4E-02	1.9E-02	$nmol*cc\ wet\ sed^{-1}*d^{-1}$
DR	D1	Rx	1098	BS	SR	2	2.6E-02	4.5E-03	d^{-1}	3.4E-01	2.1E-01	$nmol*cc\ wet\ sed^{-1}*d^{-1}$
F1	D1	Rx	1098	BS	SR	2	1.2E-01	4.6E-02	d^{-1}	6.6E+00	2.6E+00	$nmol*cc\ wet\ sed^{-1}*d^{-1}$
F2	D1	Rx	1098	BS	SR	1	**<3.2E-04**		d^{-1}	**< 0.1**		$nmol*cc\ wet\ sed^{-1}*d^{-1}$
LS	D1	Rx	1098	BS	SR	2	1.6E-02	1.6E-02	d^{-1}	3.8E-01	3.7E-01	$nmol*cc\ wet\ sed^{-1}*d^{-1}$
LN	D1	Rx	1098	BS	SR	2	9.5E-02	7.3E-02	d^{-1}	8.1E-01	6.2E-01	$nmol*cc\ wet\ sed^{-1}*d^{-1}$
CD	D1	Rx	1098	BS	SR	2	7.6E-02	5.0E-02	d^{-1}	9.8E+00	6.5E+00	$nmol*cc\ wet\ sed^{-1}*d^{-1}$
CL	D1	Rx	1098	BS	SR	2	1.2E+00	5.9E-01	d^{-1}	1.8E+01	9.2E+00	$nmol*cc\ wet\ sed^{-1}*d^{-1}$
LL	D1	Rx	1098	BS	SR	2	6.5E-02	3.8E-02	d^{-1}	1.3E+00	7.9E-01	$nmol*cc\ wet\ sed^{-1}*d^{-1}$
SP	D1	Rx	1098	BS	SR	2	9.6E-02	9.7E-03	d^{-1}	5.4E+00	8.4E-01	$nmol*cc\ wet\ sed^{-1}*d^{-1}$
SS	D1	Rx	1098	BS	SR	2	3.9E-01	2.3E-01	d^{-1}	5.2E+01	3.2E+01	$nmol*cc\ wet\ sed^{-1}*d^{-1}$
SC	D1	Rx	1098	BS	SR	3	1.3E-01	2.3E-02	d^{-1}	6.4E-01	2.8E-01	$nmol*cc\ wet\ sed^{-1}*d^{-1}$
CS	D1	Rx	1098	BS	SR	2	1.8E-02	1.0E-02	d^{-1}	4.5E+00	2.6E+00	$nmol*cc\ wet\ sed^{-1}*d^{-1}$
LB	D1	Rx	0699	BS	SR	3	5.9E-02	5.0E-02	d^{-1}	1.8E+01	1.6E+01	$nmol*cc\ wet\ sed^{-1}*d^{-1}$
LB	D2	Rx	0699	BS	SR	2	8.4E-02	4.9E-02	d^{-1}	2.1E+01	1.2E+01	$nmol*cc\ wet\ sed^{-1}*d^{-1}$
LB	D3	Rx	0699	BS	SR	2	2.3E-02	9.8E-03	d^{-1}	2.4E+00	1.7E+00	$nmol*cc\ wet\ sed^{-1}*d^{-1}$
LB	D4	Rx	0699	BS	SR	2	4.7E-02	2.7E-02	d^{-1}	5.2E+00	3.0E+00	$nmol*cc\ wet\ sed^{-1}*d^{-1}$
F1	D1	Rx	0699	BS	SR	2	1.4E-01	9.1E-02	d^{-1}	1.3E+01	8.4E+00	$nmol*cc\ wet\ sed^{-1}*d^{-1}$
F1	D2	Rx	0699	BS	SR	2	6.1E-04	1.5E-04	d^{-1}	1.2E-02	3.1E-03	$nmol*cc\ wet\ sed^{-1}*d^{-1}$
F1	D3	Rx	0699	BS	SR	2	3.5E-02	2.4E-02	d^{-1}	1.4E+00	1.3E+00	$nmol*cc\ wet\ sed^{-1}*d^{-1}$
F1	D4	Rx	0699	BS	SR	2	1.0E-03	5.1E-04	d^{-1}	8.4E-03	4.9E-03	$nmol*cc\ wet\ sed^{-1}*d^{-1}$
LS	D1	Rx	0699	BS	SR	2	**< 1.6E-04**		d^{-1}	**< 3.3E-02**		$nmol*cc\ wet\ sed^{-1}*d^{-1}$
LS	D2	Rx	0699	BS	SR	2	**< 1.6E-04**		d^{-1}	**< 1.9E-02**		$nmol*cc\ wet\ sed^{-1}*d^{-1}$
LS	D3	Rx	0699	BS	SR	2	6.3E-04	1.1E-04	d^{-1}	3.4E-02	6.5E-03	$nmol*cc\ wet\ sed^{-1}*d^{-1}$
LS	D4	Rx	0699	BS	SR	2	5.4E-04	3.3E-04	d^{-1}	2.5E-02	1.6E-02	$nmol*cc\ wet\ sed^{-1}*d^{-1}$

Sample Code						n	Avg.	Std. Dev	Units	Avg.	Std. Dev	Units
SC	D1	Rx	0699	BS	SR	2	2.4E-01	2.3E-02	d^{-1}	2.7E+02	2.9E+01	nmol*cc wet sed^{-1}*d^{-1}
SC	D2	Rx	0699	BS	SR	2	1.2E+00	9.7E-02	d^{-1}	2.5E+02	7.0E+01	nmol*cc wet sed^{-1}*d^{-1}
SC	D3	Rx	0699	BS	SR	2	2.4E-01	6.5E-02	d^{-1}	1.7E+02	4.7E+01	nmol*cc wet sed^{-1}*d^{-1}
SC	D4	Rx	0699	BS	SR	2	3.0E-02	2.9E-03	d^{-1}	3.9E+01	6.7E+00	nmol*cc wet sed^{-1}*d^{-1}
F1	D1	Rx	1099	BS	SR	2	3.8E-01	2.3E-01	d^{-1}	4.8E+01	3.0E+01	nmol*cc wet sed^{-1}*d^{-1}
F1	D2	Rx	1099	BS	SR	2	3.7E+00	2.1E+00	d^{-1}	4.6E+01	2.7E+01	nmol*cc wet sed^{-1}*d^{-1}
F1	D3	Rx	1099	BS	SR	2	3.4E+00	2.0E+00	d^{-1}	2.5E+01	1.4E+01	nmol*cc wet sed^{-1}*d^{-1}
F1	D4	Rx	1099	BS	SR	2	4.3E+00	2.5E+00	d^{-1}	1.6E+01	9.3E+00	nmol*cc wet sed^{-1}*d^{-1}
SC	D1	Rx	1099	BS	SR	2	5.5E-01	3.5E-01	d^{-1}	1.7E+02	1.1E+02	nmol*cc wet sed^{-1}*d^{-1}
SC	D2	Rx	1099	BS	SR	2	1.9E+00	1.1E+00	d^{-1}	1.3E+02	1.1E+02	nmol*cc wet sed^{-1}*d^{-1}
SC	D3	Rx	1099	BS	SR	2	4.6E-01	2.7E-01	d^{-1}	4.1E+01	2.5E+01	nmol*cc wet sed^{-1}*d^{-1}
SC	D4	Rx	1099	BS	SR	2	7.2E-02	4.3E-02	d^{-1}	4.5E+00	2.7E+00	nmol*cc wet sed^{-1}*d^{-1}

B2. Methanogenesis

LB	D1	Rx	1098	BS	ME	2	317.1	10.7	nmol*cc wet sed^{-1}*d^{-1}
DR	D1	Rx	1098	BS	ME	2	26.1	3.0	nmol*cc wet sed^{-1}*d^{-1}
F1	D1	Rx	1098	BS	ME	2	128.3	10.1	nmol*cc wet sed^{-1}*d^{-1}
F2	D1	Rx	1098	BS	ME	2	**< 0.14**		nmol*cc wet sed^{-1}*d^{-1}
LS	D1	Rx	1098	BS	ME	2	24.9	12.6	nmol*cc wet sed^{-1}*d^{-1}
LN	D1	Rx	1098	BS	ME	2	21.3	3.8	nmol*cc wet sed^{-1}*d^{-1}
CD	D1	Rx	1098	BS	ME	2	76.6	10.6	nmol*cc wet sed^{-1}*d^{-1}
CL	D1	Rx	1098	BS	ME	2	568.6	6.5	nmol*cc wet sed^{-1}*d^{-1}
LL	D1	Rx	1098	BS	ME	2	185.6	16.8	nmol*cc wet sed^{-1}*d^{-1}
SP	D1	Rx	1098	BS	ME	2	423.3	26.9	nmol*cc wet sed^{-1}*d^{-1}
SS	D1	Rx	1098	BS	ME	2	198.4	97.9	nmol*cc wet sed^{-1}*d^{-1}
SC	D1	Rx	1098	BS	ME	3	631.8	60.6	nmol*cc wet sed^{-1}*d^{-1}
CS	D1	Rx	1098	BS	ME	2	0.7	0.3	nmol*cc wet sed^{-1}*d^{-1}
LB	D1	Rx	0699	BS	ME	3	**< 1.7**		nmol*cc wet sed^{-1}*d^{-1}
LB	D2	Rx	0699	BS	ME	2	49.5	3.7	nmol*cc wet sed^{-1}*d^{-1}
LB	D3	Rx	0699	BS	ME	2	8.9	9.0	nmol*cc wet sed^{-1}*d^{-1}
LB	D4	Rx	0699	BS	ME	2	**< 1.7**		nmol*cc wet sed^{-1}*d^{-1}
F1	D1	Rx	0699	BS	ME	2	54.3	14.2	nmol*cc wet sed^{-1}*d^{-1}
F1	D2	Rx	0699	BS	ME	2	45.0	7.9	nmol*cc wet sed^{-1}*d^{-1}
F1	D3	Rx	0699	BS	ME	2	185.2	39.3	nmol*cc wet sed^{-1}*d^{-1}
F1	D4	Rx	0699	BS	ME	2	72.7	6.2	nmol*cc wet sed^{-1}*d^{-1}
LS	D1	Rx	0699	BS	ME	2	0.8	1.1	nmol*cc wet sed^{-1}*d^{-1}
LS	D2	Rx	0699	BS	ME	2	**< 0.2**		nmol*cc wet sed^{-1}*d^{-1}
LS	D3	Rx	0699	BS	ME	2	**< 0.2**		nmol*cc wet sed^{-1}*d^{-1}
LS	D4	Rx	0699	BS	ME	2	**< 0.2**		nmol*cc wet sed^{-1}*d^{-1}
SC	D1	Rx	0699	BS	ME	2	124.3	34.6	nmol*cc wet sed^{-1}*d^{-1}
SC	D2	Rx	0699	BS	ME	2	132.9	5.0	nmol*cc wet sed^{-1}*d^{-1}
SC	D3	Rx	0699	BS	ME	2	10.9	14.6	nmol*cc wet sed^{-1}*d^{-1}
SC	D4	Rx	0699	BS	ME	2	0.4	0.1	nmol*cc wet sed^{-1}*d^{-1}
F1	D1	Rx	1099	BS	ME	2	21.3	2.1	nmol*cc wet sed^{-1}*d^{-1}
F1	D2	Rx	1099	BS	ME	2	68.9	1.6	nmol*cc wet sed^{-1}*d^{-1}
F1	D3	Rx	1099	BS	ME	2	104.4	2.4	nmol*cc wet sed^{-1}*d^{-1}
F1	D4	Rx	1099	BS	ME	2	102.5	2.0	nmol*cc wet sed^{-1}*d^{-1}
SC	D1	Rx	1099	BS	ME	3	54.3	3.7	nmol*cc wet sed^{-1}*d^{-1}
SC	D2	Rx	1099	BS	ME	2	40.6	1.5	nmol*cc wet sed^{-1}*d^{-1}
SC	D3	Rx	1099	BS	ME	2	21.6	0.2	nmol*cc wet sed^{-1}*d^{-1}
SC	D4	Rx	1099	BS	ME	2	8.0	0.2	nmol*cc wet sed^{-1}*d^{-1}

B3. Methane Oxidation Rate Constant

LB	D1	Rx	1098	BS	MO	2	**< 8.2E-04**	d^{-1}
DR	D1	Rx	1098	BS	MO	2	**< 8.2E-04**	d^{-1}
F1	D1	Rx	1098	BS	MO	2	**< 8.2E-04**	d^{-1}
F2	D1	Rx	1098	BS	MO	2	**< 8.2E-04**	d^{-1}
LS	D1	Rx	1098	BS	MO	2	**< 8.2E-04**	d^{-1}

Sample Code						n	Avg.	Std. Dev	Units	Avg.	Std. Dev	Units
LN	D1	Rx	1098	BS	MO	2	< 8.2E-04		d^{-1}			
CD	D1	Rx	1098	BS	MO	2	< 8.2E-04		d^{-1}			
CL	D1	Rx	1098	BS	MO	2	< 8.2E-04		d^{-1}			
LL	D1	Rx	1098	BS	MO	2	< 8.2E-04		d^{-1}			
SP	D1	Rx	1098	BS	MO	2	< 9.2E-04	< 1.5E-04	d^{-1}			
SS	D1	Rx	1098	BS	MO	2	< 8.2E-04		d^{-1}			
SC	D1	Rx	1098	BS	MO	3	< 8.2E-04		d^{-1}			
CS	D1	Rx	1098	BS	MO	2	< 8.2E-04		d^{-1}			

B4a. Iron Reduction Rate

LB	D1	Rx	1098	BS	IR	2	< 0.7		ug*ml slurry^{-1}*d^{-1}			
DR	D1	Rx	1098	BS	IR	2	< 0.7		ug*ml slurry^{-1}*d^{-1}			
F1	D1	Rx	1098	BS	IR	2	< 0.7		ug*ml slurry^{-1}*d^{-1}			
F2	D1	Rx	1098	BS	IR	2	< 0.7		ug*ml slurry^{-1}*d^{-1}			
LS	D1	Rx	1098	BS	IR	2	< 0.7		ug*ml slurry^{-1}*d^{-1}			
LN	D1	Rx	1098	BS	IR	2	< 0.7		ug*ml slurry^{-1}*d^{-1}			
CD	D1	Rx	1098	BS	IR	2	1.3	0.0	ug*ml slurry^{-1}*d^{-1}			
CL	D1	Rx	1098	BS	IR	2	11.1	1.2	ug*ml slurry^{-1}*d^{-1}			
LL	D1	Rx	1098	BS	IR	2	12.8	1.4	ug*ml slurry^{-1}*d^{-1}			
SP	D1	Rx	1098	BS	IR	2	6.0	0.7	ug*ml slurry^{-1}*d^{-1}			
SS	D1	Rx	1098	BS	IR	2	< 0.7		ug*ml slurry^{-1}*d^{-1}			
SC	D1	Rx	1098	BS	IR	3	3.1	1.1	ug*ml slurry^{-1}*d^{-1}			
CS	D1	Rx	1098	BS	IR	2	< 0.7		ug*ml slurry^{-1}*d^{-1}			

LB	D1	Rx	0699	BS	IR	2	< 3.1		ug*g wet sed^{-1}*d^{-1}			
LB	D2	Rx	0699	BS	IR	2	< 3.1		ug*g wet sed^{-1}*d^{-1}			
LB	D3	Rx	0699	BS	IR	2	< 3.1		ug*g wet sed^{-1}*d^{-1}			
LB	D4	Rx	0699	BS	IR	2	< 3.1		ug*g wet sed^{-1}*d^{-1}			
F1	D1	Rx	0699	BS	IR	2	29.0	12.3	ug*g wet sed^{-1}*d^{-1}			
F1	D2	Rx	0699	BS	IR	2	< 3.1		ug*g wet sed^{-1}*d^{-1}			
F1	D3	Rx	0699	BS	IR	2	< 3.1		ug*g wet sed^{-1}*d^{-1}			
F1	D4	Rx	0699	BS	IR	2	< 3.1		ug*g wet sed^{-1}*d^{-1}			
LS	D1	Rx	0699	BS	IR	2	7.8	2.9	ug*g wet sed^{-1}*d^{-1}			
LS	D2	Rx	0699	BS	IR	2	< 3.1		ug*g wet sed^{-1}*d^{-1}			
LS	D3	Rx	0699	BS	IR	2	< 3.1		ug*g wet sed^{-1}*d^{-1}			
LS	D4	Rx	0699	BS	IR	2	< 3.1		ug*g wet sed^{-1}*d^{-1}			
SC	D1	Rx	0699	BS	IR	2	< 3.1		ug*g wet sed^{-1}*d^{-1}			
SC	D2	Rx	0699	BS	IR	2	< 3.1		ug*g wet sed^{-1}*d^{-1}			
SC	D3	Rx	0699	BS	IR	2	< 3.1		ug*g wet sed^{-1}*d^{-1}			
SC	D4	Rx	0699	BS	IR	2	< 3.1		ug*g wet sed^{-1}*d^{-1}			

F1	D1	Rx	1099	BS	IR	2	< 3.6		ug*g wet sed^{-1}*d^{-1}			
F1	D2	Rx	1099	BS	IR	2	< 3.6		ug*g wet sed^{-1}*d^{-1}			
F1	D3	Rx	1099	BS	IR	2	< 3.6		ug*g wet sed^{-1}*d^{-1}			
F1	D4	Rx	1099	BS	IR	2	< 3.6		ug*g wet sed^{-1}*d^{-1}			
SC	D1	Rx	1099	BS	IR	2	17.5	11.2	ug*g wet sed^{-1}*d^{-1}			
SC	D2	Rx	1099	BS	IR	2	< 3.6		ug*g wet sed^{-1}*d^{-1}			
SC	D3	Rx	1099	BS	IR	2	10.2	10.6	ug*g wet sed^{-1}*d^{-1}			
SC	D4	Rx	1099	BS	IR	2	16.7	5.0	ug*g wet sed^{-1}*d^{-1}			

B5. Manganese Reduction Rate

LB	D1	Rx	1098	BS	MR	2	0.03	0.02	ug*ml slurry^{-1}*d^{-1}			
DR	D1	Rx	1098	BS	MR	2	< 0.01		ug*ml slurry^{-1}*d^{-1}			
F1	D1	Rx	1098	BS	MR	2	0.61	0.20	ug*ml slurry^{-1}*d^{-1}			
F2	D1	Rx	1098	BS	MR	2	< 0.01		ug*ml slurry^{-1}*d^{-1}			
LS	D1	Rx	1098	BS	MR	2	< 0.01		ug*ml slurry^{-1}*d^{-1}			
LN	D1	Rx	1098	BS	MR	1	< 0.01		ug*ml slurry^{-1}*d^{-1}			
CD	D1	Rx	1098	BS	MR	2	0.03	0.07	ug*ml slurry^{-1}*d^{-1}			
CL	D1	Rx	1098	BS	MR	2	< 0.01		ug*ml slurry^{-1}*d^{-1}			
LL	D1	Rx	1098	BS	MR	2	0.26	0.33	ug*ml slurry^{-1}*d^{-1}			
SP	D1	Rx	1098	BS	MR	2	< 0.01		ug*ml slurry^{-1}*d^{-1}			

Sample Code						n	Avg.	Std. Dev	Units	Avg.	Std. Dev	Units
SS	D1	Rx	1098	BS	MR	2	0.07		ug*ml slurry^{-1}*d^{-1}			
SC	D1	Rx	1098	BS	MR	3	< 0.01		ug*ml slurry^{-1}*d^{-1}			
CS	D1	Rx	1098	BS	MR	2	0.04	0.07	ug*ml slurry^{-1}*d^{-1}			
LB	D1	Rx	0699	BS	MR	2	< 2.1		ug*g wet sed^{-1}*d^{-1}			
LB	D2	Rx	0699	BS	MR	2	< 2.1		ug*g wet sed^{-1}*d^{-1}			
LB	D3	Rx	0699	BS	MR	2	< 2.1		ug*g wet sed^{-1}*d^{-1}			
LB	D4	Rx	0699	BS	MR	2	< 2.1		ug*g wet sed^{-1}*d^{-1}			
F1	D1	Rx	0699	BS	MR	2	< 10.3		ug*g wet sed^{-1}*d^{-1}			
F1	D2	Rx	0699	BS	MR	2	< 10.3		ug*g wet sed^{-1}*d^{-1}			
F1	D3	Rx	0699	BS	MR	2	< 10.3		ug*g wet sed^{-1}*d^{-1}			
F1	D4	Rx	0699	BS	MR	2	< 10.3		ug*g wet sed^{-1}*d^{-1}			
LS	D1	Rx	0699	BS	MR	2	0.7	0.0	ug*g wet sed^{-1}*d^{-1}			
LS	D2	Rx	0699	BS	MR	2	< 0.4		ug*g wet sed^{-1}*d^{-1}			
LS	D3	Rx	0699	BS	MR	2	< 1.0		ug*g wet sed^{-1}*d^{-1}			
LS	D4	Rx	0699	BS	MR	2	< 1.0		ug*g wet sed^{-1}*d^{-1}			
SC	D1	Rx	0699	BS	MR	2	< 2.1		ug*g wet sed^{-1}*d^{-1}			
SC	D2	Rx	0699	BS	MR	2	< 2.1		ug*g wet sed^{-1}*d^{-1}			
SC	D3	Rx	0699	BS	MR	2	< 2.1		ug*g wet sed^{-1}*d^{-1}			
SC	D4	Rx	0699	BS	MR	2	2.2	1.2	ug*g wet sed^{-1}*d^{-1}			
F1	D1	Rx	1099	BS	MR	2	< 0.4		ug*g wet sed^{-1}*d^{-1}			
F1	D2	Rx	1099	BS	MR	2	< 0.4		ug*g wet sed^{-1}*d^{-1}			
F1	D3	Rx	1099	BS	MR	2	< 0.9		ug*g wet sed^{-1}*d^{-1}			
F1	D4	Rx	1099	BS	MR	2	< 0.9		ug*g wet sed^{-1}*d^{-1}			
SC	D1	Rx	1099	BS	MR	2	< 0.9		ug*g wet sed^{-1}*d^{-1}			
SC	D2	Rx	1099	BS	MR	2	< 1.3		ug*g wet sed^{-1}*d^{-1}			
SC	D3	Rx	1099	BS	MR	2	< 1.3		ug*g wet sed^{-1}*d^{-1}			
SC	D4	Rx	1099	BS	MR	2	< 1.3		ug*g wet sed^{-1}*d^{-1}			

C. Whole Sediment Parameters

C1a. Total Mercury (wet sediment)

C1b. Total Mercury (dry sediment)

LB	D1	Rx	1098	BS	Mt	2	54	2	ng*g wet sed^{-1}	79	7	ng*g dry sed^{-1}
DR	D1	Rx	1098	BS	Mt	2	99	24	ng*g wet sed^{-1}	137	32	ng*g dry sed^{-1}
F1	D1	Rx	1098	BS	Mt	2	8574	277	ng*g wet sed^{-1}	12691	224	ng*g dry sed^{-1}
F2	D1	Rx	1098	BS	Mt	2	639	43	ng*g wet sed^{-1}	777	43	ng*g dry sed^{-1}
LS	D1	Rx	1098	BS	Mt	2	2049	76	ng*g wet sed^{-1}	2679	111	ng*g dry sed^{-1}
LN	D1	Rx	1098	BS	Mt	2	44	1	ng*g wet sed^{-1}	61	1	ng*g dry sed^{-1}
CD	D1	Rx	1098	BS	Mt	2	2050	69	ng*g wet sed^{-1}	2810	86	ng*g dry sed^{-1}
CL	D1	Rx	1098	BS	Mt	2	2560	119	ng*g wet sed^{-1}	9507	566	ng*g dry sed^{-1}
LL	D1	Rx	1098	BS	Mt	2	231	10	ng*g wet sed^{-1}	357	26	ng*g dry sed^{-1}
SP	D1	Rx	1098	BS	Mt	2	472	41	ng*g wet sed^{-1}	1999	202	ng*g dry sed^{-1}
SS	D1	Rx	1098	BS	Mt	2	5371	494	ng*g wet sed^{-1}	9254	719	ng*g dry sed^{-1}
SC	D1	Rx	1098	BS	Mt	2	137	21	ng*g wet sed^{-1}	760	148	ng*g dry sed^{-1}
CS	D1	Rx	1098	BS	Mt	2	19	2	ng*g wet sed^{-1}	25	3	ng*g dry sed^{-1}
LB	D1	Rx	0699	BS	Mt	3	55	38	ng*g wet sed^{-1}	76	51	ng*g dry sed^{-1}
LB	D2	Rx	0699	BS	Mt	2	45	7	ng*g wet sed^{-1}	62	9	ng*g dry sed^{-1}
LB	D3	Rx	0699	BS	Mt	2	57	7	ng*g wet sed^{-1}	78	10	ng*g dry sed^{-1}
LB	D4	Rx	0699	BS	Mt	2	89	60	ng*g wet sed^{-1}	120	82	ng*g dry sed^{-1}
DR	D1	Rx	0699	BS	Mt	2	68	25	ng*g wet sed^{-1}	93	34	ng*g dry sed^{-1}
F1	D1	Rx	0699	BS	Mt	2	6423	356	ng*g wet sed^{-1}	10726	699	ng*g dry sed^{-1}
F1	D2	Rx	0699	BS	Mt	2	9262	319	ng*g wet sed^{-1}	15561	725	ng*g dry sed^{-1}
F1	D3	Rx	0699	BS	Mt	2	9939	1240	ng*g wet sed^{-1}	16705	2256	ng*g dry sed^{-1}
F1	D4	Rx	0699	BS	Mt	2	11193	957	ng*g wet sed^{-1}	16225	1699	ng*g dry sed^{-1}
F2	D1	Rx	0699	BS	Mt	2	10869	24	ng*g wet sed^{-1}	15666	7	ng*g dry sed^{-1}
F3	V1	Rx	0699	BS	Mt	2	57	1	ng*g wet sed^{-1}	78	6	ng*g dry sed^{-1}
F3	V2	Rx	0699	BS	Mt	2	81	26	ng*g wet sed^{-1}	102	25	ng*g dry sed^{-1}
F3	V3	Rx	0699	BS	Mt	2	7	0	ng*g wet sed^{-1}	8	0	ng*g dry sed^{-1}
LS	D1	Rx	0699	BS	Mt	2	404	55	ng*g wet sed^{-1}	496	69	ng*g dry sed^{-1}
LS	D2	Rx	0699	BS	Mt	2	248	4	ng*g wet sed^{-1}	307	8	ng*g dry sed^{-1}

Sample Code						n	Avg.	Std. Dev	Units	Avg.	Std. Dev	Units
LS	D3	Rx	0699	BS	Mt	2	197	18	ng*g wet sed^{-1}	252	22	ng*g dry sed^{-1}
LS	D4	Rx	0699	BS	Mt	2	58	9	ng*g wet sed^{-1}	72	11	ng*g dry sed^{-1}
LN	D1	Rx	0699	BS	Mt	2	17	0	ng*g wet sed^{-1}	22	0	ng*g dry sed^{-1}
CD	D1	Rx	0699	BS	Mt	2	3385	279	ng*g wet sed^{-1}	4931	394	ng*g dry sed^{-1}
CL	D1	Rx	0699	BS	Mt	2	3184	915	ng*g wet sed^{-1}	6934	574	ng*g dry sed^{-1}
LL	D1	Rx	0699	BS	Mt	2	369	3	ng*g wet sed^{-1}	597	6	ng*g dry sed^{-1}
SP	D1	Rx	0699	BS	Mt	2	1776	1884	ng*g wet sed^{-1}	3285	1981	ng*g dry sed^{-1}
SS	D1	Rx	0699	BS	Mt	2	1891	1706	ng*g wet sed^{-1}	3298	1932	ng*g dry sed^{-1}
SC	D1	Rx	0699	BS	Mt	2	167	6	ng*g wet sed^{-1}	700	23	ng*g dry sed^{-1}
SC	D2	Rx	0699	BS	Mt	2	266	3	ng*g wet sed^{-1}	653	19	ng*g dry sed^{-1}
SC	D3	Rx	0699	BS	Mt	2	505	21	ng*g wet sed^{-1}	870	24	ng*g dry sed^{-1}
SC	D4	Rx	0699	BS	Mt	2	893	4	ng*g wet sed^{-1}	1423	12	ng*g dry sed^{-1}
CS	D1	Rx	0699	BS	Mt	2	26	4	ng*g wet sed^{-1}	33	5	ng*g dry sed^{-1}
LB	D1	Rx	1099	BS	Mt	2	24	3	ng*g wet sed^{-1}	30	3	ng*g dry sed^{-1}
DR	D1	Rx	1099	BS	Mt	2	103	1	ng*g wet sed^{-1}	139	0	ng*g dry sed^{-1}
DY	D1	Rx	1099	BS	Mt	2	291	70	ng*g wet sed^{-1}	378	95	ng*g dry sed^{-1}
F1	D1	Rx	1099	BS	Mt	2	8518	381	ng*g wet sed^{-1}	12577	579	ng*g dry sed^{-1}
F1	D2	Rx	1099	BS	Mt	2	10500	1246	ng*g wet sed^{-1}	15332	1869	ng*g dry sed^{-1}
F1	D3	Rx	1099	BS	Mt	2	9983	2436	ng*g wet sed^{-1}	15810	4005	ng*g dry sed^{-1}
F1	D4	Rx	1099	BS	Mt	2	9395	1120	ng*g wet sed^{-1}	16105	1869	ng*g dry sed^{-1}
F2	D1	Rx	1099	BS	Mt	2	1518	137	ng*g wet sed^{-1}	1905	150	ng*g dry sed^{-1}
F3	V1	Rx	1099	BS	Mt	2	244	67	ng*g wet sed^{-1}	249	69	ng*g dry sed^{-1}
F3	V3	Rx	1099	BS	Mt	2	18762	47	ng*g wet sed^{-1}	18879	52	ng*g dry sed^{-1}
LS	D1	Rx	1099	BS	Mt	2	9822	427	ng*g wet sed^{-1}	21286	1088	ng*g dry sed^{-1}
LN	D1	Rx	1099	BS	Mt	2	37	3	ng*g wet sed^{-1}	51	4	ng*g dry sed^{-1}
CD	D1	Rx	1099	BS	Mt	2	2812	52	ng*g wet sed^{-1}	4260	118	ng*g dry sed^{-1}
CL	D1	Rx	1099	BS	Mt	2	2712	106	ng*g wet sed^{-1}	5912	178	ng*g dry sed^{-1}
LL	D1	Rx	1099	BS	Mt	2	303	22	ng*g wet sed^{-1}	555	38	ng*g dry sed^{-1}
SP	D1	Rx	1099	BS	Mt	2	407	1	ng*g wet sed^{-1}	2760	869	ng*g dry sed^{-1}
SS	D1	Rx	1099	BS	Mt	2	5475	309	ng*g wet sed^{-1}	9717	576	ng*g dry sed^{-1}
SC	D1	Rx	1099	BS	Mt	2	234	9	ng*g wet sed^{-1}	690	56	ng*g dry sed^{-1}
SC	D2	Rx	1099	BS	Mt	2	249	2	ng*g wet sed^{-1}	567	33	ng*g dry sed^{-1}
SC	D3	Rx	1099	BS	Mt	2	322	1	ng*g wet sed^{-1}	574	10	ng*g dry sed^{-1}
SC	D4	Rx	1099	BS	Mt	2	415	21	ng*g wet sed^{-1}	676	31	ng*g dry sed^{-1}
CS	D1	Rx	1099	BS	Mt	2	21	4	ng*g wet sed^{-1}	27	.5	ng*g dry sed^{-1}

C2a.Methylmercury (wet sediment) *C2b.Methylmercury (dry sediment)*

LB	D1	Rx	1098	BS	MM	2	1.28	0.09	ng*g wet sed^{-1}	1.87	0.03	ng*g dry sed^{-1}
DR	D1	Rx	1098	BS	MM	2	0.66	0.02	ng*g wet sed^{-1}	0.91	0.03	ng*g dry sed^{-1}
F1	D1	Rx	1098	BS	MM	2	5.68	0.36	ng*g wet sed^{-1}	8.40	0.40	ng*g dry sed^{-1}
F2	D1	Rx	1098	BS	MM	2	0.14	0.13	ng*g wet sed^{-1}	0.17	0.15	ng*g dry sed^{-1}
LS	D1	Rx	1098	BS	MM	2	0.48	0.03	ng*g wet sed^{-1}	0.62	0.04	ng*g dry sed^{-1}
LN	D1	Rx	1098	BS	MM	2	0.19	0.08	ng*g wet sed^{-1}	0.26	0.12	ng*g dry sed^{-1}
CD	D1	Rx	1098	BS	MM	2	1.11	0.18	ng*g wet sed^{-1}	1.53	0.25	ng*g dry sed^{-1}
CL	D1	Rx	1098	BS	MM	2	1.63	0.21	ng*g wet sed^{-1}	6.06	0.85	ng*g dry sed^{-1}
LL	D1	Rx	1098	BS	MM	2	0.21	0.07	ng*g wet sed^{-1}	0.33	0.10	ng*g dry sed^{-1}
SP	D1	Rx	1098	BS	MM	2	0.21	0.03	ng*g wet sed^{-1}	0.88	0.16	ng*g dry sed^{-1}
SS	D1	Rx	1098	BS	MM	2	1.12	0.12	ng*g wet sed^{-1}	1.92	0.17	ng*g dry sed^{-1}
SC	D1	Rx	1098	BS	MM	2	0.12	0.07	ng*g wet sed^{-1}	0.69	0.40	ng*g dry sed^{-1}
CS	D1	Rx	1098	BS	MM	2	0.01	0.02	ng*g wet sed^{-1}	0.02	0.02	ng*g dry sed^{-1}
LB	D1	Rx	0699	BS	MM	3	0.53	0.10	ng*g wet sed^{-1}	0.74	0.14	ng*g dry sed^{-1}
LB	D2	Rx	0699	BS	MM	2	1.26	0.25	ng*g wet sed^{-1}	1.76	0.34	ng*g dry sed^{-1}
LB	D3	Rx	0699	BS	MM	2	0.72	0.13	ng*g wet sed^{-1}	0.97	0.17	ng*g dry sed^{-1}
LB	D4	Rx	0699	BS	MM	2	0.48	0.02	ng*g wet sed^{-1}	0.65	0.03	ng*g dry sed^{-1}
DR	D1	Rx	0699	BS	MM	2	0.20	0.01	ng*g wet sed^{-1}	0.28	0.02	ng*g dry sed^{-1}
F1	D1	Rx	0699	BS	MM	2	15.65	0.17	ng*g wet sed^{-1}	26.12	0.03	ng*g dry sed^{-1}
F1	D2	Rx	0699	BS	MM	2	19.15	0.01	ng*g wet sed^{-1}	32.16	0.38	ng*g dry sed^{-1}
F1	D3	Rx	0699	BS	MM	2	19.30	4.59	ng*g wet sed^{-1}	32.38	7.37	ng*g dry sed^{-1}
F1	D4	Rx	0699	BS	MM	2	15.04	1.07	ng*g wet sed^{-1}	21.76	1.13	ng*g dry sed^{-1}

Sample Code						n	Avg.	Std. Dev	Units	Avg.	Std. Dev	Units
F2	D1	Rx	0699	BS	MM	2	2.10	0.03	ng*g wet sed^{-1}	3.03	0.05	ng*g dry sed^{-1}
F3	V1	Rx	0699	BS	MM	2	0.05	0.03	ng*g wet sed^{-1}	0.07	0.04	ng*g dry sed^{-1}
F3	V2	Rx	0699	BS	MM	2	0.13	0.10	ng*g wet sed^{-1}	0.18	0.13	ng*g dry sed^{-1}
F3	V3	Rx	0699	BS	MM	2	0.07	0.04	ng*g wet sed^{-1}	0.08	0.04	ng*g dry sed^{-1}
LS	D1	Rx	0699	BS	MM	2	0.36	0.02	ng*g wet sed^{-1}	0.44	0.03	ng*g dry sed^{-1}
LS	D2	Rx	0699	BS	MM	2	0.54	0.14	ng*g wet sed^{-1}	0.68	0.18	ng*g dry sed^{-1}
LS	D3	Rx	0699	BS	MM	2	0.24	0.00	ng*g wet sed^{-1}	0.31	0.00	ng*g dry sed^{-1}
LS	D4	Rx	0699	BS	MM	2	0.16	0.02	ng*g wet sed^{-1}	0.20	0.02	ng*g dry sed^{-1}
LN	D1	Rx	0699	BS	MM	2	< 0.02		ng*g wet sed^{-1}	< 0.12		ng*g dry sed^{-1}
CD	D1	Rx	0699	BS	MM	2	2.10	0.04	ng*g wet sed^{-1}	3.06	0.08	ng*g dry sed^{-1}
CL	D1	Rx	0699	BS	MM	2	4.82	1.11	ng*g wet sed^{-1}	10.55	0.25	ng*g dry sed^{-1}
LL	D1	Rx	0699	BS	MM	2	0.56	0.01	ng*g wet sed^{-1}	0.90	0.02	ng*g dry sed^{-1}
SP	D1	Rx	0699	BS	MM	2	0.91	0.76	ng*g wet sed^{-1}	1.89	0.41	ng*g dry sed^{-1}
SS	D1	Rx	0699	BS	MM	2	0.90	0.60	ng*g wet sed^{-1}	1.68	0.46	ng*g dry sed^{-1}
SC	D1	Rx	0699	BS	MM	2	0.44	0.06	ng*g wet sed^{-1}	1.85	0.24	ng*g dry sed^{-1}
SC	D2	Rx	0699	BS	MM	2	0.21	0.02	ng*g wet sed^{-1}	0.52	0.05	ng*g dry sed^{-1}
SC	D3	Rx	0699	BS	MM	2	0.53	0.01	ng*g wet sed^{-1}	0.92	0.03	ng*g dry sed^{-1}
SC	D4	Rx	0699	BS	MM	2	1.24	0.02	ng*g wet sed^{-1}	1.98	0.05	ng*g dry sed^{-1}
CS	D1	Rx	0699	BS	MM	2	< 0.01		ng*g wet sed^{-1}	< 0.06		ng*g dry sed^{-1}
LB	D1	Rx	1099	BS	MM	3	0.17	0.03	ng*g wet sed^{-1}	0.21	0.04	ng*g dry sed^{-1}
DR	D1	Rx	1099	BS	MM	2	0.08	0.00	ng*g wet sed^{-1}	0.11	0.01	ng*g dry sed^{-1}
DY	D1	Rx	1099	BS	MM	3	0.78	0.10	ng*g wet sed^{-1}	1.02	0.12	ng*g dry sed^{-1}
F1	D1	Rx	1099	BS	MM	3	6.05	3.54	ng*g wet sed^{-1}	8.95	5.24	ng*g dry sed^{-1}
F1	D2	Rx	1099	BS	MM	3	5.48	0.28	ng*g wet sed^{-1}	7.99	0.40	ng*g dry sed^{-1}
F1	D3	Rx	1099	BS	MM	3	7.78	1.60	ng*g wet sed^{-1}	12.35	2.60	ng*g dry sed^{-1}
F1	D4	Rx	1099	BS	MM	3	7.89	0.95	ng*g wet sed^{-1}	13.51	1.62	ng*g dry sed^{-1}
F2	D1	Rx	1099	BS	MM	3	0.12	0.01	ng*g wet sed^{-1}	0.15	0.01	ng*g dry sed^{-1}
F3	V1	Rx	1099	BS	MM	3	0.26	0.13	ng*g wet sed^{-1}	0.27	0.13	ng*g dry sed^{-1}
F3	V3	Rx	1099	BS	MM	3	3.86	0.85	ng*g wet sed^{-1}	3.88	0.86	ng*g dry sed^{-1}
LS	D1	Rx	1099	BS	MM	2	3.96	0.46	ng*g wet sed^{-1}	8.53	1.06	ng*g dry sed^{-1}
LN	D1	Rx	1099	BS	MM	3	0.08	0.02	ng*g wet sed^{-1}	0.10	0.02	ng*g dry sed^{-1}
CD	D1	Rx	1099	BS	MM	3	2.26	0.39	ng*g wet sed^{-1}	3.42	0.57	ng*g dry sed^{-1}
CL	D1	Rx	1099	BS	MM	2	5.47	1.48	ng*g wet sed^{-1}	11.92	3.12	ng*g dry sed^{-1}
LL	D1	Rx	1099	BS	MM	3	0.67	0.17	ng*g wet sed^{-1}	1.23	0.31	ng*g dry sed^{-1}
SP	D1	Rx	1099	BS	MM	2	1.11	0.62	ng*g wet sed^{-1}	6.87	1.88	ng*g dry sed^{-1}
SS	D1	Rx	1099	BS	MM	2	4.00	1.11	ng*g wet sed^{-1}	7.08	2.00	ng*g dry sed^{-1}
SC	D1	Rx	1099	BS	MM	3	0.41	0.09	ng*g wet sed^{-1}	1.20	0.30	ng*g dry sed^{-1}
SC	D2	Rx	1099	BS	MM	2	0.21	0.06	ng*g wet sed^{-1}	0.48	0.16	ng*g dry sed^{-1}
SC	D3	Rx	1099	BS	MM	2	0.17	0.10	ng*g wet sed^{-1}	0.31	0.17	ng*g dry sed^{-1}
SC	D4	Rx	1099	BS	MM	2	0.20	0.23	ng*g wet sed^{-1}	0.33	0.37	ng*g dry sed^{-1}
CS	D1	Rx	1099	BS	MM	2	0.01	0.01	ng*g wet sed^{-1}	0.01	0.01	ng*g dry sed^{-1}

C3a.Acid-Labile Hg(II) (wet sediment)

C3b.Acid-Labile Hg(II) (dry sediment)

LB	D1	Rx	1098	BS	RM	2	0.14	0.04	ng*g wet sed^{-1}	0.21	0.04	ng*g dry sed^{-1}
DR	D1	Rx	1098	BS	RM	2	0.63	0.39	ng*g wet sed^{-1}	0.87	0.53	ng*g dry sed^{-1}
F1	D1	Rx	1098	BS	RM	2	15.28	5.26	ng*g wet sed^{-1}	22.68	8.13	ng*g dry sed^{-1}
F2	D1	Rx	1098	BS	RM	2	30.67	4.09	ng*g wet sed^{-1}	37.35	5.43	ng*g dry sed^{-1}
LS	D1	Rx	1098	BS	RM	2	5.80	1.84	ng*g wet sed^{-1}	7.57	2.38	ng*g dry sed^{-1}
LN	D1	Rx	1098	BS	RM	2	0.25	0.06	ng*g wet sed^{-1}	0.35	0.08	ng*g dry sed^{-1}
CD	D1	Rx	1098	BS	RM	2	1.15	0.47	ng*g wet sed^{-1}	1.58	0.64	ng*g dry sed^{-1}
CL	D1	Rx	1098	BS	RM	2	3.25	2.09	ng*g wet sed^{-1}	12.13	7.91	ng*g dry sed^{-1}
LL	D1	Rx	1098	BS	RM	2	0.56	0.25	ng*g wet sed^{-1}	0.86	0.36	ng*g dry sed^{-1}
SP	D1	Rx	1098	BS	RM	2	0.97	0.32	ng*g wet sed^{-1}	4.11	1.41	ng*g dry sed^{-1}
SS	D1	Rx	1098	BS	RM	2	4.85	0.60	ng*g wet sed^{-1}	8.37	1.15	ng*g dry sed^{-1}
SC	D1	Rx	1098	BS	RM	2	0.93	0.00	ng*g wet sed^{-1}	5.18	0.25	ng*g dry sed^{-1}
CS	D1	Rx	1098	BS	RM	2	0.13	0.07	ng*g wet sed^{-1}	0.17	0.09	ng*g dry sed^{-1}

Sample Code						n	Avg.	Std. Dev	Units	Avg.	Std. Dev	Units
LB	D1	Rx	0699	BS	RM	3	0.4	0.2	ng*g wet sed^{-1}	0.57	0.24	ng*g dry sed^{-1}
LB	D2	Rx	0699	BS	RM	2	0.3	0.1	ng*g wet sed^{-1}	0.4	0.1	ng*g dry sed^{-1}
LB	D3	Rx	0699	BS	RM	2	0.9	0.0	ng*g wet sed^{-1}	1.2	0.1	ng*g dry sed^{-1}
LB	D4	Rx	0699	BS	RM	2	0.6	0.0	ng*g wet sed^{-1}	0.8	0.0	ng*g dry sed^{-1}
DR	D1	Rx	0699	BS	RM	2	0.6	0.1	ng*g wet sed^{-1}	0.79	0.19	ng*g dry sed^{-1}
F1	D1	Rx	0699	BS	RM	2	17.3	1.7	ng*g wet sed^{-1}	28.94	2.55	ng*g dry sed^{-1}
F1	D2	Rx	0699	BS	RM	2	33.9	4.3	ng*g wet sed^{-1}	56 9	6.6	ng*g dry sed^{-1}
F1	D3	Rx	0699	BS	RM	2	46.8	26.4	ng*g wet sed^{-1}	78.3	43.5	ng*g dry sed^{-1}
F1	D4	Rx	0699	BS	RM	2	6.9	4.6	ng*g wet sed^{-1}	10.0	6.5	ng*g dry sed^{-1}
F2	D1	Rx	0699	BS	RM	2	66.5	18.2	ng*g wet sed^{-1}	95.84	26.51	ng*g dry sed^{-1}
F3	V1	Rx	0699	BS	RM	2	5.1	0.8	ng*g wet sed^{-1}	7.1	1.7	ng*g dry sed^{-1}
F3	V2	Rx	0699	BS	RM	2	5.0	0.3	ng*g wet sed^{-1}	6.6	0.5	ng*g dry sed^{-1}
F3	V3	Rx	0699	BS	RM	2	0.3	0.0	ng*g wet sed^{-1}	0.3	0.0	ng*g dry sed^{-1}
LS	D1	Rx	0699	BS	RM	2	5.0	0.7	ng*g wet sed^{-1}	6.14	0.87	ng*g dry sed^{-1}
LS	D2	Rx	0699	BS	RM	2	7.5	1.4	ng*g wet sed^{-1}	9.3	1.7	ng*g dry sed^{-1}
LS	D3	Rx	0699	BS	RM	2	4.5	0.4	ng*g wet sed^{-1}	5.8	0.5	ng*g dry sed^{-1}
LS	D4	Rx	0699	BS	RM	2	2.6	1.3	ng*g wet sed^{-1}	3.2	1.6	ng*g dry sed^{-1}
LN	D1	Rx	0699	BS	RM	2	1.1	0.3	ng*g wet sed^{-1}	1.44	0.35	ng*g dry sed^{-1}
CD	D1	Rx	0699	BS	RM	2	6.2	0.5	ng*g wet sed^{-1}	9.09	0.68	ng*g dry sed^{-1}
CL	D1	Rx	0699	BS	RM	2	16.6	14.5	ng*g wet sed^{-1}	32.56	27.14	ng*g dry sed^{-1}
LL	D1	Rx	0699	BS	RM	2	0.9	0.1	ng*g wet sed^{-1}	1.49	0.12	ng*g dry sed^{-1}
SP	D1	Rx	0699	BS	RM	2	2.7	2.3	ng*g wet sed^{-1}	5.47	1.48	ng*g dry sed^{-1}
SS	D1	Rx	0699	BS	RM	2	3.0	2.5	ng*g wet sed^{-1}	5.25	2.65	ng*g dry sed^{-1}
SC	D1	Rx	0699	BS	RM	2	1.8	0.1	ng*g wet sed^{-1}	7.64	0.60	ng*g dry sed^{-1}
SC	D2	Rx	0699	BS	RM	2	2.6	0.5	ng*g wet sed^{-1}	6.4	1.2	ng*g dry sed^{-1}
SC	D3	Rx	0699	BS	RM	2	3.1	0.5	ng*g wet sed^{-1}	5.4	0.9	ng*g dry sed^{-1}
SC	D4	Rx	0699	BS	RM	2	6.2	1.4	ng*g wet sed^{-1}	9.9	2.1	ng*g dry sed^{-1}
CS	D1	Rx	0699	BS	RM	2	0.2	0.0	ng*g wet sed^{-1}	0.27	0.04	ng*g dry sed^{-1}
LB	D1	Rx	1099	BS	RM	2	0.1	0.0	ng*g wet sed^{-1}	0.1	0.0	ng*g dry sed^{-1}
DR	D1	Rx	1099	BS	RM	2	1.5	0.4	ng*g wet sed^{-1}	2.1	0.5	ng*g dry sed^{-1}
DY	D1	Rx	1099	BS	RM	2	5.4	1.5	ng*g wet sed^{-1}	6.9	2.0	ng*g dry sed^{-1}
F1	D1	Rx	1099	BS	RM	2	12.6	2.3	ng*g wet sed^{-1}	18.6	3.3	ng*g dry sed^{-1}
F1	D2	Rx	1099	BS	RM	2	12.1	1.9	ng*g wet sed^{-1}	17.7	2.8	ng*g dry sed^{-1}
F1	D3	Rx	1099	BS	RM	2	17.8	0.1	ng*g wet sed^{-1}	28.1	0.4	ng*g dry sed^{-1}
F1	D4	Rx	1099	BS	RM	2	15.1	1.6	ng*g wet sed^{-1}	25.8	2.6	ng*g dry sed^{-1}
F2	D1	Rx	1099	BS	RM	2	21.3	1.7	ng*g wet sed^{-1}	26.7	1.8	ng*g dry sed^{-1}
F3	V1	Rx	1099	BS	RM	2	13.4	2.8	ng*g wet sed^{-1}	13.6	2.8	ng*g dry sed^{-1}
F3	V3	Rx	1099	BS	RM	2	776.5	32.5	ng*g wet sed^{-1}	781.3	32.9	ng*g dry sed^{-1}
LS	D1	Rx	1099	BS	RM	2	16.9	2.3	ng*g wet sed^{-1}	36.4	5.2	ng*g dry sed^{-1}
LN	D1	Rx	1099	BS	RM	2	0.2	0.0	ng*g wet sed^{-1}	0.3	0.0	ng*g dry sed^{-1}
CD	D1	Rx	1099	BS	RM	2	3.6	0.3	ng*g wet sed^{-1}	5.5	0.5	ng*g dry sed^{-1}
CL	D1	Rx	1099	BS	RM	2	8.2	0.5	ng*g wet sed^{-1}	17.8	1.0	ng*g dry sed^{-1}
LL	D1	Rx	1099	BS	RM	2	2.4	0.2	ng*g wet sed^{-1}	4.4	0.4	ng*g dry sed^{-1}
SP	D1	Rx	1099	BS	RM	2	1.4	0.3	ng*g wet sed^{-1}	10.6	3.8	ng*g dry sed^{-1}
SS	D1	Rx	1099	BS	RM	2	12.5	1.6	ng*g wet sed^{-1}	22.2	2.9	ng*g dry sed^{-1}
SC	D1	Rx	1099	BS	RM	2	2.5	0.3	ng*g wet sed^{-1}	7.3	1.1	ng*g dry sed^{-1}
SC	D2	Rx	1099	BS	RM	2	1.8	0.2	ng*g wet sed^{-1}	4.0	0.3	ng*g dry sed^{-1}
SC	D3	Rx	1099	BS	RM	2	4.0	0.6	ng*g wet sed^{-1}	7.1	1.1	ng*g dry sed^{-1}
SC	D4	Rx	1099	BS	RM	2	7.8	0.1	ng*g wet sed^{-1}	12.7	0.2	ng*g dry sed^{-1}
CS	D1	Rx	1099	BS	RM	2	0.0	0.0	ng*g wet sed^{-1}	0.1	0.0	ng*g dry sed^{-1}

C4.Sediment Bulk Density

LB	D1	Rx	1098	BS	BD	3	1.76	0.02	g*cc wet sed^{-1}
DR	D1	Rx	1098	BS	BD	3	1.72	0.02	g*cc wet sed^{-1}
F1	D1	Rx	1098	BS	BD	3	1.68	0.02	g*cc wet sed^{-1}
F2	D1	Rx	1098	BS	BD	3	1.44	0.01	g*cc wet sed^{-1}
LS	D1	Rx	1098	BS	BD	3	1.87	0.02	g*cc wet sed^{-1}

Sample Code						n	Avg.	Std. Dev	Units	Avg.	Std. Dev	Units
LN	D1	Rx	1098	BS	BD	3	1.77	0.00	g*cc wet sed^{-1}			
CD	D1	Rx	1098	BS	BD	3	1.74	0.01	g*cc wet sed^{-1}			
CL	D1	Rx	1098	BS	BD	3	1.11	0.01	g*cc wet sed^{-1}			
LL	D1	Rx	1098	BS	BD	3	1.55	0.04	g*cc wet sed^{-1}			
SP	D1	Rx	1098	BS	BD	3	1.09	0.01	g*cc wet sed^{-1}			
SS	D1	Rx	1098	BS	BD	3	1.35	0.00	g*cc wet sed^{-1}			
SC	D1	Rx	1098	BS	BD	3	1.09	0.01	g*cc wet sed^{-1}			
CS	D1	Rx	1098	BS	BD	3	1.85	0.01	g*cc wet sed^{-1}			
LB	D1	Rx	0699	BS	BD	3	1.82	0.01	g*cc wet sed^{-1}			
LB	D2	Rx	0699	BS	BD	2	1.81	0.05	g*cc wet sed^{-1}			
LB	D3	Rx	0699	BS	BD	2	1.81	0.01	g*cc wet sed^{-1}			
LB	D4	Rx	0699	BS	BD	2	1.72	0.04	g*cc wet sed^{-1}			
DR	D1	Rx	0699	BS	BD	2	1.77	0.02	g*cc wet sed^{-1}			
F1	D1	Rx	0699	BS	BD	2	1.54	0.03	g*cc wet sed^{-1}			
F1	D2	Rx	0699	BS	BD	2	1.53	0.11	g*cc wet sed^{-1}			
F1	D3	Rx	0699	BS	BD	2	1.53	0.00	g*cc wet sed^{-1}			
F1	D4	Rx	0699	BS	BD	2	1.61	0.03	g*cc wet sed^{-1}			
F2	D1	Rx	0699	BS	BD	2	1.74	0.04	g*cc wet sed^{-1}			
F3	V1	Rx	0699	BS	BD	1	1.91		g*cc wet sed^{-1}			
F3	V2	Rx	0699	BS	BD	2	1.82	0.12	g*cc wet sed^{-1}			
F3	V3	Rx	0699	BS	BD	2	1.61	0.08	g*cc wet sed^{-1}			
LS	D1	Rx	0699	BS	BD	2	1.65	0.03	g*cc wet sed^{-1}			
LS	D2	Rx	0699	BS	BD	2	1.68	0.03	g*cc wet sed^{-1}			
LS	D3	Rx	0699	BS	BD	2	1.74	0.01	g*cc wet sed^{-1}			
LS	D4	Rx	0699	BS	BD	2	1.73	0.08	g*cc wet sed^{-1}			
LN	D1	Rx	0699	BS	BD	2	1.90	0.02	g*cc wet sed^{-1}			
CD	D1	Rx	0699	BS	BD	2	1.68	0.00	g*cc wet sed^{-1}			
CL	D1	Rx	0699	BS	BD	2	1.23	0.14	g*cc wet sed^{-1}			
LL	D1	Rx	0699	BS	BD	2	1.73	0.09	g*cc wet sed^{-1}			
SP	D1	Rx	0699	BS	BD	2	1.19	0.00	g*cc wet sed^{-1}			
SS	D1	Rx	0699	BS	BD	2	1.54	0.14	g*cc wet sed^{-1}			
SC	D1	Rx	0699	BS	BD	2	1.42	0.06	g*cc wet sed^{-1}			
SC	D2	Rx	0699	BS	BD	2	1.28	0.27	g*cc wet sed^{-1}			
SC	D3	Rx	0699	BS	BD	2	1.42	0.05	g*cc wet sed^{-1}			
SC	D4	Rx	0699	BS	BD	2	1.46	0.06	g*cc wet sed^{-1}			
CS	D1	Rx	0699	BS	BD	2	1.90	0.05	g*cc wet sed^{-1}			
LB	D1	Rx	1099	BS	BD	2	1.03	0.08	g*cc wet sed^{-1}			
DR	D1	Rx	1099	BS	BD	2	0.85	0.05	g*cc wet sed^{-1}			
DY	D1	Rx	1099	BS	BD	2	0.88	0.01	g*cc wet sed^{-1}			
F1	D1	Rx	1099	BS	BD	2	0.85	0.00	g*cc wet sed^{-1}			
F1	D2	Rx	1099	BS	BD	2	0.87	0.04	g*cc wet sed^{-1}			
F1	D3	Rx	1099	BS	BD	2	0.82	0.01	g*cc wet sed^{-1}			
F1	D4	Rx	1099	BS	BD	2	0.74	0.00	g*cc wet sed^{-1}			
F2	D1	Rx	1099	BS	BD	2	0.93	0.04	g*cc wet sed^{-1}			
F3	V1	Rx	1099	BS	BD	2	0.45	0.03	g*cc wet sed^{-1}			
F3	V3	Rx	1099	BS	BD	2	0.64	0.01	g*cc wet sed^{-1}			
LS	D1	Rx	1099	BS	BD	2	0.67	0.03	g*cc wet sed^{-1}			
LN	D1	Rx	1099	BS	BD	2	0.97	0.01	g*cc wet sed^{-1}			
CD	D1	Rx	1099	BS	BD	2	0.82	0.03	g*cc wet sed^{-1}			
CL	D1	Rx	1099	BS	BD	2	0.64	0.02	g*cc wet sed^{-1}			
LL	D1	Rx	1099	BS	BD	2	0.71	0.00	g*cc wet sed^{-1}			
SP	D1	Rx	1099	BS	BD	2	0.51	0.00	g*cc wet sed^{-1}			
SS	D1	Rx	1099	BS	BD	2	0.70	0.00	g*cc wet sed^{-1}			
SC	D1	Rx	1099	BS	BD	3	0.60	0.01	g*cc wet sed^{-1}			
SC	D2	Rx	1099	BS	BD	2	0.64	0.01	g*cc wet sed^{-1}			
SC	D3	Rx	1099	BS	BD	2	0.75	0.00	g*cc wet sed^{-1}			
SC	D4	Rx	1099	BS	BD	2	0.75	0.01	g*cc wet sed^{-1}			
CS	D1	Rx	1099	BS	BD	2	0.91	0.01	g*cc wet sed^{-1}			

Sample Code						n	Avg.	Std. Dev	Units	Avg.	Std. Dev	Units
C5.Sediment Porosity												
LB	D1	Rx	1098	BS	POR	3	0.61	0.05	ml pw*cc wet sed^{-1}			
DR	D1	Rx	1098	BS	POR	3	0.47	0.01	ml pw*cc wet sed^{-1}			
F1	D1	Rx	1098	BS	POR	3	0.61	0.02	ml pw*cc wet sed^{-1}			
F2	D1	Rx	1098	BS	POR	3	0.28	0.01	ml pw*cc wet sed^{-1}			
LS	D1	Rx	1098	BS	POR	3	0.42	0.01	ml pw*cc wet sed^{-1}			
LN	D1	Rx	1098	BS	POR	3	0.47	0.01	ml pw*cc wet sed^{-1}			
CD	D1	Rx	1098	BS	POR	3	0.48	0.02	ml pw*cc wet sed^{-1}			
CL	D1	Rx	1098	BS	POR	3	0.80	0.01	ml pw*cc wet sed^{-1}			
LL	D1	Rx	1098	BS	POR	3	0.59	0.02	ml pw*cc wet sed^{-1}			
SP	D1	Rx	1098	BS	POR	3	0.86	0.01	ml pw*cc wet sed^{-1}			
SS	D1	Rx	1098	BS	POR	3	0.58	0.01	ml pw*cc wet sed^{-1}			
SC	D1	Rx	1098	BS	POR	3	0.87	0.01	ml pw*cc wet sed^{-1}			
CS	D1	Rx	1098	BS	POR	3	0.39	0.00	ml pw*cc wet sed^{-1}			
LB	D1	Rx	0699	BS	POR	3	0.48	0.01	ml pw*cc wet sed^{-1}			
LB	D2	Rx	0699	BS	POR	2	0.50	0.02	ml pw*cc wet sed^{-1}			
LB	D3	Rx	0699	BS	POR	2	0.48	0.01	ml pw*cc wet sed^{-1}			
LB	D4	Rx	0699	BS	POR	2	0.43	0.02	ml pw*cc wet sed^{-1}			
DR	D1	Rx	0699	BS	POR	2	0.48	0.01	ml pw*cc wet sed^{-1}			
F1	D1	Rx	0699	BS	POR	2	0.62	0.01	ml pw*cc wet sed^{-1}			
F1	D2	Rx	0699	BS	POR	2	0.65	0.05	ml pw*cc wet sed^{-1}			
F1	D3	Rx	0699	BS	POR	2	0.62	0.00	ml pw*cc wet sed^{-1}			
F1	D4	Rx	0699	BS	POR	2	0.54	0.02	ml pw*cc wet sed^{-1}			
F2	D1	Rx	0699	BS	POR	2	0.53	0.01	ml pw*cc wet sed^{-1}			
F3	V1	Rx	0699	BS	POR	1	0.61		ml pw*cc wet sed^{-1}			
F3	V2	Rx	0699	BS	POR	2	0.51	0.07	ml pw*cc wet sed^{-1}			
F3	V3	Rx	0699	BS	POR	2	0.30	0.02	ml pw*cc wet sed^{-1}			
LS	D1	Rx	0699	BS	POR	2	0.31	0.02	ml pw*cc wet sed^{-1}			
LS	D2	Rx	0699	BS	POR	2	0.32	0.01	ml pw*cc wet sed^{-1}			
LS	D3	Rx	0699	BS	POR	2	0.34	0.01	ml pw*cc wet sed^{-1}			
LS	D4	Rx	0699	BS	POR	2	0.31	0.02	ml pw*cc wet sed^{-1}			
LN	D1	Rx	0699	BS	POR	2	0.46	0.02	ml pw*cc wet sed^{-1}			
CD	D1	Rx	0699	BS	POR	2	0.54	0.01	ml pw*cc wet sed^{-1}			
CL	D1	Rx	0699	BS	POR	2	0.76	0.09	ml pw*cc wet sed^{-1}			
LL	D1	Rx	0699	BS	POR	2	0.67	0.04	ml pw*cc wet sed^{-1}			
SP	D1	Rx	0699	BS	POR	2	0.89	0.01	ml pw*cc wet sed^{-1}			
SS	D1	Rx	0699	BS	POR	2	0.52	0.05	ml pw*cc wet sed^{-1}			
SC	D1	Rx	0699	BS	POR	2	1.04	0.05	ml pw*cc wet sed^{-1}			
SC	D2	Rx	0699	BS	POR	2	0.73	0.16	ml pw*cc wet sed^{-1}			
SC	D3	Rx	0699	BS	POR	2	0.65	0.02	ml pw*cc wet sed^{-1}			
SC	D4	Rx	0699	BS	POR	2	0.63	0.08	ml pw*cc wet sed^{-1}			
CS	D1	Rx	0699	BS	POR	2	0.37	0.01	ml pw*cc wet sed^{-1}			
LB	D1	Rx	1099	BS	POR	2	0.22	0.02	ml pw*cc wet sed^{-1}			
DR	D1	Rx	1099	BS	POR	2	0.21	0.01	ml pw*cc wet sed^{-1}			
DY	D1	Rx	1099	BS	POR	2	0.21	0.00	ml pw*cc wet sed^{-1}			
F1	D1	Rx	1099	BS	POR	2	0.28	0.00	ml pw*cc wet sed^{-1}			
F1	D2	Rx	1099	BS	POR	2	0.28	0.01	ml pw*cc wet sed^{-1}			
F1	D3	Rx	1099	BS	POR	2	0.30	0.01	ml pw*cc wet sed^{-1}			
F1	D4	Rx	1099	BS	POR	2	0.33	0.00	ml pw*cc wet sed^{-1}			
F2	D1	Rx	1099	BS	POR	2	0.20	0.01	ml pw*cc wet sed^{-1}			
F3	V1	Rx	1099	BS	POR	2	0.01	0.00	ml pw*cc wet sed^{-1}			
F3	V3	Rx	1099	BS	POR	2	0.01	0.00	ml pw*cc wet sed^{-1}			
LS	D1	Rx	1099	BS	POR	2	0.35	0.02	ml pw*cc wet sed^{-1}			
LN	D1	Rx	1099	BS	POR	2	0.29	0.00	ml pw*cc wet sed^{-1}			
CD	D1	Rx	1099	BS	POR	2	0.27	0.03	ml pw*cc wet sed^{-1}			
CL	D1	Rx	1099	BS	POR	2	0.38	0.02	ml pw*cc wet sed^{-1}			
LL	D1	Rx	1099	BS	POR	2	0.33	0.00	ml pw*cc wet sed^{-1}			
SP	D1	Rx	1099	BS	POR	2	0.44	0.00	ml pw*cc wet sed^{-1}			
SS	D1	Rx	1099	BS	POR	2	0.31	0.00	ml pw*cc wet sed^{-1}			
SC	D1	Rx	1099	BS	POR	3	0.41	0.01	ml pw*cc wet sed^{-1}			

Sample Code						n	Avg.	Std. Dev	Units	Avg.	Std. Dev	Units
SC	D2	Rx	1099	BS	POR	2	0.36	0.01	ml pw*cc wet sed^{-1}			
SC	D3	Rx	1099	BS	POR	2	0.31	0.03	ml pw*cc wet sed^{-1}			
SC	D4	Rx	1099	BS	POR	2	0.31	0.00	ml pw*cc wet sed^{-1}			
CS	D1	Rx	1099	BS	POR	2	0.20	0.01	ml pw*cc wet sed^{-1}			

C6.Grain Size

LB	D1	Rx	1098	BS	GS	2	23.5	0.7	% < 63 um
DR	D1	Rx	1098	BS	GS	2	10.0	1.4	% < 63 um
F1	D1	Rx	1098	BS	GS	2	28.0	0.0	% < 63 um
F2	D1	Rx	1098	BS	GS	2	< 1.8		% < 63 um
LS	D1	Rx	1098	BS	GS	2	7.0	0.0	% < 63 um
LN	D1	Rx	1098	BS	GS	2	7.5	0.7	% < 63 um
CD	D1	Rx	1098	BS	GS	2	17.0	1.4	% < 63 um
CL	D1	Rx	1098	BS	GS	2	90.0	1.4	% < 63 um
LL	D1	Rx	1098	BS	GS	2	32.0	4.2	% < 63 um
SP	D1	Rx	1098	BS	GS	2	92.0	0.0	% < 63 um
SS	D1	Rx	1098	BS	GS	2	43.0	0.0	% < 63 um
SC	D1	Rx	1098	BS	GS	3	71.7	0.6	% < 63 um
CS	D1	Rx	1098	BS	GS	2	7.0	0.0	% < 63 um

LB	D1	Rx	0699	BS	GS	3	18.0	0.0	% < 63 um
LB	D2	Rx	0699	BS	GS	2	25.5	0.7	% < 63 um
LB	D3	Rx	0699	BS	GS	2	32.5	0.7	% < 63 um
LB	D4	Rx	0699	BS	GS	2	18.0	0.0	% < 63 um
F1	D1	Rx	0699	BS	GS	2	43.5	0.7	% < 63 um
F1	D2	Rx	0699	BS	GS	2	60.5	3.5	% < 63 um
F1	D3	Rx	0699	BS	GS	2	55.5	2.1	% < 63 um
F1	D4	Rx	0699	BS	GS	2	37.5	3.5	% < 63 um
LS	D1	Rx	0699	BS	GS	2	4.0	0.0	% < 63 um
LS	D2	Rx	0699	BS	GS	2	4.0	0.0	% < 63 um
LS	D3	Rx	0699	BS	GS	2	4.0	0.0	% < 63 um
LS	D4	Rx	0699	BS	GS	2	3.5	0.7	% < 63 um
SC	D1	Rx	0699	BS	GS	2	71.5	2.1	% < 63 um
SC	D2	Rx	0699	BS	GS	2	62.5	2.1	% < 63 um
SC	D3	Rx	0699	BS	GS	2	69.5	7.8	% < 63 um
SC	D4	Rx	0699	BS	GS	2	65.5	2.1	% < 63 um

C7. Redox

LB	D1	Rx	1098	BS	Eh	2	16	21	mV
DR	D1	Rx	1098	BS	Eh	2	-17	24	mV
F1	D1	Rx	1098	BS	Eh	2	-17	9	mV
F2	D1	Rx	1098	BS	Eh	2	409	24	mV
LS	D1	Rx	1098	BS	Eh	2	-27	6	mV
LN	D1	Rx	1098	BS	Eh	2	406	33	mV
CD	D1	Rx	1098	BS	Eh	2	20	3	mV
CL	D1	Rx	1098	BS	Eh	2	-26	1	mV
LL	D1	Rx	1098	BS	Eh	2	-92	4	mV
SP	D1	Rx	1098	BS	Eh	2	2	16	mV
SS	D1	Rx	1098	BS	Eh	2	-27	3	mV
SC	D1	Rx	1098	BS	Eh	3	-129	6	mV
CS	D1	Rx	1098	BS	Eh	2	209	19	mV

Note: Previously reported Eh values (10/98) in Interim Report-I were incorrect, as they were not corrected to a standard hydrogen reference electrode.

DR	D1	Rx	0699	BS	Eh	1	223		mV
F1	D1	Rx	0699	BS	Eh	2	-18	9	mV
F1	D2	Rx	0699	BS	Eh	2	58	66	mV
F1	D3	Rx	0699	BS	Eh	2	40	2	mV
F1	D4	Rx	0699	BS	Eh	2	73	8	mV
F2	D1	Rx	0699	BS	Eh	1	468		mV
F3	V1	Rx	0699	BS	Eh	1	487		mV
F3	V2	Rx	0699	BS	Eh	1	512		mV
F3	V3	Rx	0699	BS	Eh	1	474		mV
LN	D1	Rx	0699	BS	Eh	2	293	25	mV
CD	D1	Rx	0699	BS	Eh	2	-70	3	mV
CL	D1	Rx	0699	BS	Eh	2	-66	12	mV
LL	D1	Rx	0699	BS	Eh	2	-105	14	mV

Sample Code						n	Avg.	Std. Dev	Units	Avg.	Std. Dev	Units
SP	D1	Rx	0699	BS	Eh	2	-134	1	mV			
SS	D1	Rx	0699	BS	Eh	2	-50	2	mV			
SC	D1	Rx	0699	BS	Eh	2	-136	3	mV			
SC	D2	Rx	0699	BS	Eh	2	-164	0	-8.6E-02			
SC	D3	Rx	0699	BS	Eh	2	-165	3	-1.5E+00			
SC	D4	Rx	0699	BS	Eh	2	-109	8	-7.6E+00			
CS	D1	Rx	0699	BS	Eh	2	-87	10	mV			
LB	D1	Rx	1099	BS	Eh	3	-13	50	mV			
DR	D1	Rx	1099	BS	Eh	2	451	21	mV			
DY	D1	Rx	1099	BS	Eh	3	267	44	mV			
F1	D1	Rx	1099	BS	Eh	2	-57	12	mV			
F1	D2	Rx	1099	BS	Eh	3	-74	44	mV			
F1	D3	Rx	1099	BS	Eh	2	-68	26	mV			
F1	D4	Rx	1099	BS	Eh	2	-24	18	mV			
F2	D1	Rx	1099	BS	Eh	2	416	19	mV			
F3	V1	Rx	1099	BS	Eh	2						
F3	V3	Rx	1099	BS	Eh	2						
LS	D1	Rx	1099	BS	Eh	2	-70	9	mV			
LN	D1	Rx	1099	BS	Eh	2	105	17	mV			
CD	D1	Rx	1099	BS	Eh	2	-37	65	mV			
CL	D1	Rx	1099	BS	Eh	2	-57	12	mV			
LL	D1	Rx	1099	BS	Eh	2	-80	12	mV			
SP	D1	Rx	1099	BS	Eh	2	-82	4	mV			
SS	D1	Rx	1099	BS	Eh	2	-66	3	mV			
SC	D1	Rx	1099	BS	Eh	2	-132	2	mV			
SC	D2	Rx	1099	BS	Eh	2	-153	1	mV			
SC	D3	Rx	1099	BS	Eh	2	-181	0	mV			
SC	D4	Rx	1099	BS	Eh	2	-155	1	mV			
CS	D1	Rx	1099	BS	Eh	2	-151	1	mV			

C8. pH

LB	D1	Rx	1098	BS	pH	2	7.03	0.03				
DR	D1	Rx	1098	BS	pH	2	7.18	0.01				
F1	D1	Rx	1098	BS	pH	2	7.26	0.01				
F2	D1	Rx	1098	BS	pH	2	7.68	0.07				
LS	D1	Rx	1098	BS	pH	2	7.15	0.03				
LN	D1	Rx	1098	BS	pH	2	7.31	0.01				
CD	D1	Rx	1098	BS	pH	2	7.02	0.00				
CL	D1	Rx	1098	BS	pH	2	6.98	0.02				
LL	D1	Rx	1098	BS	pH	2	7.56	0.01				
SP	D1	Rx	1098	BS	pH	2	6.94	0.02				
SS	D1	Rx	1098	BS	pH	2	7.06	0.02				
SC	D1	Rx	1098	BS	pH	3	7.23	0.01				
CS	D1	Rx	1098	BS	pH	2	8.24	0.35				
DR	D1	Rx	0699	BS	pH	2	6.79	0.06				
F1	D1	Rx	0699	BS	pH	2	6.88	0.10				
F1	D2	Rx	0699	BS	pH	2	7.14	0.06				
F1	D3	Rx	0699	BS	pH	2	7.19	0.02				
F1	D4	Rx	0699	BS	pH	2	7.26	0.13				
F2	D1	Rx	0699	BS	pH	1	7.70					
F3	V1	Rx	0699	BS	pH	1	7.73					
F3	V2	Rx	0699	BS	pH	1	7.73					
F3	V3	Rx	0699	BS	pH	1	6.30					
LS	D1	Rx	0699	BS	pH	2	7.57	0.10				
LS	D2	Rx	0699	BS	pH	2	7.81	0.10				
LS	D3	Rx	0699	BS	pH	2	7.96	0.06				
LS	D4	Rx	0699	BS	pH	2	7.93	0.04				
LN	D1	Rx	0699	BS	pH	2	8.15	0.04				
CD	D1	Rx	0699	BS	pH	2	7.28	0.01				
CL	D1	Rx	0699	BS	pH	2	7.39	0.01				
LL	D1	Rx	0699	BS	pH	2	7.61	0.11				
SP	D1	Rx	0699	BS	pH	2	7.24	0.06				
SS	D1	Rx	0699	BS	pH	2	7.37	0.14				
SC	D1	Rx	0699	BS	pH	2	7.72	0.09				
SC	D2	Rx	0699	BS	pH	2	7.57	0.12				
SC	D3	Rx	0699	BS	pH	2	8.20	0.23				
SC	D4	Rx	0699	BS	pH	2	8.11	0.03				

Sample Code						n	Avg.	Std. Dev	Units	Avg.	Std. Dev	Units
CS	D1	Rx	0699	BS	pH	1	8.09					
LB	D1	Rx	1099	BS	pH	2	7.40	0.03				
DR	D1	Rx	1099	BS	pH	2	7.70	0.04				
DY	D1	Rx	1099	BS	pH	2	7.70	0.05				
F1	D1	Rx	1099	BS	pH	2	7.08	0.03				
F1	D2	Rx	1099	BS	pH	2	6.99	0.03				
F1	D3	Rx	1099	BS	pH	2	6.78	0.15				
F1	D4	Rx	1099	BS	pH	2	7.00	0.08				
F2	D1	Rx	1099	BS	pH	2	7.98	0.01				
F3	V1	Rx	1099	BS	pH	2	8.13	0.08				
F3	V3	Rx	1099	BS	pH	2	8.05	0.06				
LS	D1	Rx	1099	BS	pH	2	6.84	0.03				
LN	D1	Rx	1099	BS	pH	2	7.75	0.04				
CD	D1	Rx	1099	BS	pH	2	6.95	0.01				
CL	D1	Rx	1099	BS	pH	2	7.40					
LL	D1	Rx	1099	BS	pH	2	7.91	0.01				
SP	D1	Rx	1099	BS	pH	2	7.43	0.08				
SS	D1	Rx	1099	BS	pH	2	7.34	0.02				
SC	D1	Rx	1099	BS	pH	2	7.91	0.03				
SC	D2	Rx	1099	BS	pH	2	7.84	0.03				
SC	D3	Rx	1099	BS	pH	2	7.88	0.09				
SC	D4	Rx	1099	BS	pH	2	8.17	0.09				
CS	D1	Rx	1099	BS	pH	2	8.21	0.03				

C9. Methane

LB	D1	Rx	1098	BS	CH4	2	27.5	4.6	nmol*cc wet sed^{-1}			
DR	D1	Rx	1098	BS	CH4	2	2.2	0.0	nmol*cc wet sed^{-1}			
F1	D1	Rx	1098	BS	CH4	2	4.3	1.9	nmol*cc wet sed^{-1}			
F2	D1	Rx	1098	BS	CH4	2	< 1.0		nmol*cc wet sed^{-1}			
LS	D1	Rx	1098	BS	CH4	2	5.9	0.6	nmol*cc wet sed^{-1}			
LN	D1	Rx	1098	BS	CH4	2	1.1	0.3	nmol*cc wet sed^{-1}			
CD	D1	Rx	1098	BS	CH4	2	57.8	66.4	nmol*cc wet sed^{-1}			
CL	D1	Rx	1098	BS	CH4	2	78.1	5.7	nmol*cc wet sed^{-1}			
LL	D1	Rx	1098	BS	CH4	2	9.0	0.9	nmol*cc wet sed^{-1}			
SP	D1	Rx	1098	BS	CH4	2	40.4	4.8	nmol*cc wet sed^{-1}			
SS	D1	Rx	1098	BS	CH4	2	9.7	0.6	nmol*cc wet sed^{-1}			
SC	D1	Rx	1098	BS	CH4	3	58.4	9.4	nmol*cc wet sed^{-1}			
CS	D1	Rx	1098	BS	CH4	2	< 1.0		nmol*cc wet sed^{-1}			
LB	D1	Rx	0699	BS	CH4	3	6.3	2.4	nmol*cc wet sed^{-1}			
LB	D2	Rx	0699	BS	CH4	2	21.6	2.7	nmol*cc wet sed^{-1}			
LB	D3	Rx	0699	BS	CH4	2	6.4	2.8	nmol*cc wet sed^{-1}			
LB	D4	Rx	0699	BS	CH4	2	4.3	0.6	nmol*cc wet sed^{-1}			
F1	D1	Rx	0699	BS	CH4	2	67.2	10.2	nmol*cc wet sed^{-1}			
F1	D2	Rx	0699	BS	CH4	2	59.4	53.0	nmol*cc wet sed^{-1}			
F1	D3	Rx	0699	BS	CH4	2	109.7	59.8	nmol*cc wet sed^{-1}			
F1	D4	Rx	0699	BS	CH4	2	32.3	5.1	nmol*cc wet sed^{-1}			
LS	D1	Rx	0699	BS	CH4	2	< 1.7		nmol*cc wet sed^{-1}			
LS	D2	Rx	0699	BS	CH4	2	< 1.7		nmol*cc wet sed^{-1}			
LS	D3	Rx	0699	BS	CH4	2	< 1.7		nmol*cc wet sed^{-1}			
LS	D4	Rx	0699	BS	CH4	2	< 1.7		nmol*cc wet sed^{-1}			
SC	D1	Rx	0699	BS	CH4	2	34.8	2.8	nmol*cc wet sed^{-1}			
SC	D2	Rx	0699	BS	CH4	2	121.5	5.2	nmol*cc wet sed^{-1}			
SC	D3	Rx	0699	BS	CH4	2	14.9	2.7	nmol*cc wet sed^{-1}			
SC	D4	Rx	0699	BS	CH4	2	4.4	0.0	nmol*cc wet sed^{-1}			
F1	D1	Rx	1099	BS	CH4	2	9.1	6.7	nmol*cc wet sed^{-3}			
F1	D2	Rx	1099	BS	CH4	2	27.0	0.1	nmol*cc wet sed^{-3}			

Sample Code						n	Avg.	Std. Dev	Units	Avg.	Std. Dev	Units
F1	D3	Rx	1099	BS	CH4	2	63.9	10.9	nmol*cc wet sed^{-3}			
F1	D4	Rx	1099	BS	CH4	2	81.6	4.3	nmol*cc wet sed^{-3}			
SC	D1	Rx	1099	BS	CH4	3	6.8	1.1	nmol*cc wet sed^{-3}			
SC	D2	Rx	1099	BS	CH4	2	36.5	8.8	nmol*cc wet sed^{-3}			
SC	D3	Rx	1099	BS	CH4	2	13.0	1.1	nmol*cc wet sed^{-3}			
SC	D4	Rx	1099	BS	CH4	2	4.6	1.3	nmol*cc wet sed^{-3}			

C10. Particulate Carbon

LB	D1	Rx	1098	BS	PC	2	0.69	0.27	%C			
DR	D1	Rx	1098	BS	PC	2	0.31	0.00	%C			
F1	D1	Rx	1098	BS	PC	2	0.97	0.04	%C			
F2	D1	Rx	1098	BS	PC	2	0.06	0.02	%C			
LS	D1	Rx	1098	BS	PC	2	0.44	0.10	%C			
LN	D1	Rx	1098	BS	PC	2	0.49	0.02	%C			
CD	D1	Rx	1098	BS	PC	2	0.68	0.10	%C			
CL	D1	Rx	1098	BS	PC	2	3.75	0.32	%C			
LL	D1	Rx	1098	BS	PC	2	1.87	0.27	%C			
SP	D1	Rx	1098	BS	PC	2	2.85	0.63	%C			
SS	D1	Rx	1098	BS	PC	2	1.92	0.14	%C			
SC	D1	Rx	1098	BS	PC	3	4.75	1.84	%C			
CS	D1	Rx	1098	BS	PC	2	0.54	0.02	%C			
LB	D1	Rx	0699	BS	PC	3	0.65	0.01	%C			
LB	D2	Rx	0699	BS	PC	2	1.07	0.04	%C			
LB	D3	Rx	0699	BS	PC	2	1.11	0.07	%C			
LB	D4	Rx	0699	BS	PC	2	0.69	0.02	%C			
DR	D1	Rx	0699	BS	PC	2	0.33	0.01	%C			
F1	D1	Rx	0699	BS	PC	2	1.61	0.04	%C			
F1	D2	Rx	0699	BS	PC	2	1.55	0.04	%C			
F1	D3	Rx	0699	BS	PC	2	1.59	0.04	%C			
F1	D4	Rx	0699	BS	PC	2	1.35	0.01	%C			
F2	D1	Rx	0699	BS	PC	2	0.30	0.01	%C			
F3	V1	Rx	0699	BS	PC	1	0.48		%C			
F3	V2	Rx	0699	BS	PC	2	0.27	0.01	%C			
LS	D1	Rx	0699	BS	PC	2	1.20	0.77	%C			
LS	D2	Rx	0699	BS	PC	2	1.88	0.10	%C			
LS	D3	Rx	0699	BS	PC	2	1.67	0.57	%C			
LS	D4	Rx	0699	BS	PC	1	0.90		%C			
LN	D1	Rx	0699	BS	PC	2	0.78	0.01	%C			
CD	D1	Rx	0699	BS	PC	2	1.02	0.08	%C			
CL	D1	Rx	0699	BS	PC	2	2.87	0.07	%C			
LL	D1	Rx	0699	BS	PC	2	2.34	0.13	%C			
SP	D1	Rx	0699	BS	PC	2	2.76	0.11	%C			
SS	D1	Rx	0699	BS	PC	2	1.11	0.01	%C			
SC	D1	Rx	0699	BS	PC	2	5.70	0.06	%C			
SC	D2	Rx	0699	BS	PC	2	4.60	0.33	%C			
SC	D3	Rx	0699	BS	PC	2	3.41	0.01	%C			
SC	D4	Rx	0699	BS	PC	2	3.24	0.09	%C			
CS	D1	Rx	0699	BS	PC	2	0.56	0.04	%C			
F1	D1	Rx	1099	BS	PC	2	0.78	0.05	%C			
F1	D2	Rx	1099	BS	PC	2	0.85	0.08	%C			
F1	D3	Rx	1099	BS	PC	2	1.27	0.04	%C			

Sample Code						n	Avg.	Std. Dev	Units	Avg.	Std. Dev	Units
F1	D4	Rx	1099	BS	PC	2	1.77	0.11	%C			
SC	D1	Rx	1099	BS	PC	3	4.19	0.12	%C			
SC	D2	Rx	1099	BS	PC	2	3.94	0.04	%C			
SC	D3	Rx	1099	BS	PC	2	3.17	0.13	%C			
SC	D4	Rx	1099	BS	PC	2	2.75	0.01	%C			

C11. Particulate Nitrogen

LB	D1	Rx	0699	BS	PN	3	0.05	0.00	%N			
LB	D2	Rx	0699	BS	PN	2	0.08	0.00	%N			
LB	D3	Rx	0699	BS	PN	2	0.08	0.00	%N			
LB	D4	Rx	0699	BS	PN	2	0.05	0.00	%N			
DR	D1	Rx	0699	BS	PN	2	0.03	0.00	%N			
F1	D1	Rx	0699	BS	PN	2	0.16	0.00	%N			
F1	D2	Rx	0699	BS	PN	2	0.17	0.00	%N			
F1	D3	Rx	0699	BS	PN	2	0.18	0.00	%N			
F1	D4	Rx	0699	BS	PN	2	0.13	0.00	%N			
F2	D1	Rx	0699	BS	PN	2	0.03	0.01	%N			
F3	V1	Rx	0699	BS	PN	1	0.04		%N			
F3	V2	Rx	0699	BS	PN	2	0.02	0.00	%N			
LS	D1	Rx	0699	BS	PN	2	0.05	0.02	%N			
LS	D2	Rx	0699	BS	PN	2	0.07	0.01	%N			
LS	D3	Rx	0699	BS	PN	2	0.04	0.01	%N			
LS	D4	Rx	0699	BS	PN	1	0.04		%N			
LN	D1	Rx	0699	BS	PN	2	0.01	0.00	%N			
CD	D1	Rx	0699	BS	PN	2	0.11	0.01	%N			
CL	D1	Rx	0699	BS	PN	2	0.32	0.01	%N			
LL	D1	Rx	0699	BS	PN	2	0.15	0.01	%N			
SP	D1	Rx	0699	BS	PN	2	0.29	0.01	%N			
SS	D1	Rx	0699	BS	PN	2	0.08	0.01	%N			
SC	D1	Rx	0699	BS	PN	2	0.47	0.02	%N			
SC	D2	Rx	0699	BS	PN	2	0.33	0.00	%N			
SC	D3	Rx	0699	BS	PN	2	0.25	0.01	%N			
SC	D4	Rx	0699	BS	PN	2	0.25	0.01	%N			
CS	D1	Rx	0699	BS	PN	2	0.01	0.00	%N			
F1	D1	Rx	1099	BS	PN	2	0.06	0.00	%N			
F1	D2	Rx	1099	BS	PN	2	0.07	0.00	%N			
F1	D3	Rx	1099	BS	PN	2	0.12	0.01	%N			
F1	D4	Rx	1099	BS	PN	2	0.18	0.01	%N			
SC	D1	Rx	1099	BS	PN	3	0.33	0.01	%N			
SC	D2	Rx	1099	BS	PN	2	0.28	0.00	%N			
SC	D3	Rx	1099	BS	PN	2	0.22	0.01	%N			
SC	D4	Rx	1099	BS	PN	2	0.18	0.00	%N			

C12. Weight Loss On Ignition

LB	D1	Rx	1098	BS	LOI	1	3.0		% dry weight
DR	D1	Rx	1098	BS	LOI	1	1.6		% dry weight
F1	D1	Rx	1098	BS	LOI	1	2.4		% dry weight
F2	D1	Rx	1098	BS	LOI	1	0.6		% dry weight
LS	D1	Rx	1098	BS	LOI	1	0.9		% dry weight
LN	D1	Rx	1098	BS	LOI	1	1.5		% dry weight
CD	D1	Rx	1098	BS	LOI	1	1.7		% dry weight
CL	D1	Rx	1098	BS	LOI	1	9.2		% dry weight
LL	D1	Rx	1098	BS	LOI	1	2.7		% dry weight

Sample Code						n	Avg.	Std. Dev	Units	Avg.	Std. Dev	Units
SP	D1	Rx	1098	BS	LOI	1	8.1		% dry weight			
SS	D1	Rx	1098	BS	LOI	1	3.9		% dry weight			
SC	D1	Rx	1098	BS	LOI	1	11.6		% dry weight			
CS	D1	Rx	1098	BS	LOI	1	0.6		% dry weight			
LB	D1	Rx	0699	BS	LOI	4	2.46	0.09	% dry weight			
LB	D2	Rx	0699	BS	LOI	3	3.25	0.08	% dry weight			
LB	D3	Rx	0699	BS	LOI	2	3.42	0.25	% dry weight			
LB	D4	Rx	0699	BS	LOI	2	2.78	0.07	% dry weight			
DR	D1	Rx	0699	BS	LOI	2	1.98	0.08	% dry weight			
F1	D1	Rx	0699	BS	LOI	2	4.40	0.06	% dry weight			
F1	D2	Rx	0699	BS	LOI	2	3.82	1.71	% dry weight			
F1	D3	Rx	0699	BS	LOI	3	5.01	0.33	% dry weight			
F1	D4	Rx	0699	BS	LOI	2	3.80	0.01	% dry weight			
F2	D1	Rx	0699	BS	LOI	2	2.18	0.05	% dry weight			
F3	V1	Rx	0699	BS	LOI	2	4.32	0.68	% dry weight			
F3	V2	Rx	0699	BS	LOI	3	4.36	0.41	% dry weight			
F3	V3	Rx	0699	BS	LOI	2	0.82	0.01	% dry weight			
LS	D1	Rx	0699	BS	LOI	2	0.92	0.05	% dry weight			
LS	D2	Rx	0699	BS	LOI	2	2.13	0.92	% dry weight			
LS	D3	Rx	0699	BS	LOI	2	1.38	0.24	% dry weight			
LS	D4	Rx	0699	BS	LOI	3	1.06	0.13	% dry weight			
LN	D1	Rx	0699	BS	LOI	2	1.91	0.16	% dry weight			
CD	D1	Rx	0699	BS	LOI	3	2.41	0.15	% dry weight			
CL	D1	Rx	0699	BS	LOI	2	8.40	0.49	% dry weight			
LL	D1	Rx	0699	BS	LOI	2	2.99	0.23	% dry weight			
SP	D1	Rx	0699	BS	LOI	2	6.50	5.97	% dry weight			
SS	D1	Rx	0699	BS	LOI	2	5.24	4.13	% dry weight			
SC	D1	Rx	0699	BS	LOI	2	12.44	0.23	% dry weight			
SC	D2	Rx	0699	BS	LOI	2	9.62	0.76	% dry weight			
SC	D3	Rx	0699	BS	LOI	2	7.34	2.15	% dry weight			
SC	D4	Rx	0699	BS	LOI	2	6.30	0.04	% dry weight			
CS	D1	Rx	0699	BS	LOI	2	0.90	0.05	% dry weight			
LB	D1	Rx	1099	BS	LOI	3	1.04	0.03	% dry weight			
DR	D1	Rx	1099	BS	LOI	2	1.21	0.05	% dry weight			
DY	D1	Rx	1099	BS	LOI	2	0.94	0.05	% dry weight			
F1	D1	Rx	1099	BS	LOI	2	2.38	0.06	% dry weight			
F1	D2	Rx	1099	BS	LOI	2	2.70	0.05	% dry weight			
F1	D3	Rx	1099	BS	LOI	2	4.04	0.10	% dry weight			
F1	D4	Rx	1099	BS	LOI	2	5.12	0.04	% dry weight			
F2	D1	Rx	1099	BS	LOI	2	0.59	0.03	% dry weight			
F3	V1	Rx	1099	BS	LOI	2	4.08	0.03	% dry weight			
F3	V3	Rx	1099	BS	LOI	2	1.69	0.10	% dry weight			
LS	D1	Rx	1099	BS	LOI	3	5.85	0.12	% dry weight			
LN	D1	Rx	1099	BS	LOI	2	1.65	0.02	% dry weight			
CD	D1	Rx	1099	BS	LOI	3	2.65	0.05	% dry weight			
CL	D1	Rx	1099	BS	LOI	2	5.30	0.10	% dry weight			
LL	D1	Rx	1099	BS	LOI	3	4.04	0.12	% dry weight			
SP	D1	Rx	1099	BS	LOI	2	12.18	0.12	% dry weight			
SS	D1	Rx	1099	BS	LOI	3	4.52	0.08	% dry weight			
SC	D1	Rx	1099	BS	LOI	3	9.06	0.31	% dry weight			
SC	D2	Rx	1099	BS	LOI	2	7.97	0.06	% dry weight			
SC	D3	Rx	1099	BS	LOI	2	6.57	0.04	% dry weight			

Sample Code						n	Avg.	Std. Dev	Units	Avg.	Std. Dev	Units
SC	D4	Rx	1099	BS	LOI	2	5.80	0.23	% dry weight			
CS	D1	Rx	1099	BS	LOI	2	0.80	0.03	% dry weight			

C13. Acid Volatile Reduced Sulfur

LB	D1	Rx	1098	BS	RS	2	2.45	0.32	umol*g wet sed^{-1}			
DR	D1	Rx	1098	BS	RS	2	0.53	0.05	umol*g wet sed^{-1}			
F1	D1	Rx	1098	BS	RS	2	2.15	0.09	umol*g wet sed^{-1}			
F2	D1	Rx	1098	BS	RS	2	0.05	0.01	umol*g wet sed^{-1}			
LS	D1	Rx	1098	BS	RS	2	0.86	0.01	umol*g wet sed^{-1}			
LN	D1	Rx	1098	BS	RS	2	0.41	0.05	umol*g wet sed^{-1}			
CD	D1	Rx	1098	BS	RS	2	4.24	0.02	umol*g wet sed^{-1}			
CL	D1	Rx	1098	BS	RS	2	5.85	0.73	umol*g wet sed^{-1}			
LL	D1	Rx	1098	BS	RS	2	4.70	0.22	umol*g wet sed^{-1}			
SP	D1	Rx	1098	BS	RS	1	7.54		umol*g wet sed^{-1}			
SS	D1	Rx	1098	BS	RS	2	8.50	0.48	umol*g wet sed^{-1}			
SC	D1	Rx	1098	BS	RS	3	7.71	0.46	umol*g wet sed^{-1}			
CS	D1	Rx	1098	BS	RS	2	0.83	0.29	umol*g wet sed^{-1}			
xx	xx	EB	1098	xx	RS	2	< 0.002		umol S			
LN	D1	MS	1098	BS	RS	2	0.97	0.11	umol*g wet sed^{-1}			
LB	D1	Rx	0699	BS	RS	3	0.29	0.39	umol*g wet sed^{-1}			
LB	D2	Rx	0699	BS	RS	1	0.02		umol*g wet sed^{-1}			
LB	D3	Rx	0699	BS	RS	2	0.55	0.74	umol*g wet sed^{-1}			
LB	D4	Rx	0699	BS	RS	2	0.73	0.09	umol*g wet sed^{-1}			
DR	D1	Rx	0699	BS	RS	2	0.31	0.01	umol*g wet sed^{-1}			
F1	D1	Rx	0699	BS	RS	2	2.95	1.27	umol*g wet sed^{-1}			
F1	D2	Rx	0699	BS	RS	2	0.09	0.06	umol*g wet sed^{-1}			
F1	D3	Rx	0699	BS	RS	1	3.35		umol*g wet sed^{-1}			
F1	D4	Rx	0699	BS	RS	2	0.52	0.18	umol*g wet sed^{-1}			
F2	D1	Rx	0699	BS	RS	2	0.36	0.19	umol*g wet sed^{-1}			
F3	V1	Rx	0699	BS	RS	2	0.18	0.16	umol*g wet sed^{-1}			
F3	V2	Rx	0699	BS	RS	2	0.03	0.02	umol*g wet sed^{-1}			
F3	V3	Rx	0699	BS	RS	1	0.01		umol*g wet sed^{-1}			
LS	D1	Rx	0699	BS	RS	2	0.08	0.01	umol*g wet sed^{-1}			
LS	D2	Rx	0699	BS	RS	2	0.13	0.03	umol*g wet sed^{-1}			
LS	D3	Rx	0699	BS	RS	2	0.06	0.01	umol*g wet sed^{-1}			
LS	D4	Rx	0699	BS	RS	1	0.05	0.00	umol*g wet sed^{-1}			
LN	D1	Rx	0699	BS	RS	2	< 0.003		umol*g wet sed^{-1}			
CD	D1	Rx	0699	BS	RS	2	0.85	0.93	umol*g wet sed^{-1}			
CL	D1	Rx	0699	BS	RS	2	6.55	7.76	umol*g wet sed^{-1}			
LL	D1	Rx	0699	BS	RS	2	17.65	3.05	umol*g wet sed^{-1}			
SP	D1	Rx	0699	BS	RS	2	11.46	1.87	umol*g wet sed^{-1}			
SS	D1	Rx	0699	BS	RS	2	6.49	0.20	umol*g wet sed^{-1}			
SC	D1	Rx	0699	BS	RS	2	8.61	0.07	umol*g wet sed^{-1}			
SC	D2	Rx	0699	BS	RS	2	12.80	0.06	umol*g wet sed^{-1}			
SC	D3	Rx	0699	BS	RS	2	11.83	2.55	umol*g wet sed^{-1}			
SC	D4	Rx	0699	BS	RS	2	5.43	6.34	umol*g wet sed^{-1}			
CS	D1	Rx	0699	BS	RS	2	0.99	1.16	umol*g wet sed^{-1}			
LB	D1	Rx	1099	BS	RS	2	0.97	0.17	umol*g wet sed^{-1}			
DR	D1	Rx	1099	BS	RS	2	0.15	0.01	umol*g wet sed^{-1}			
DY	D1	Rx	1099	BS	RS	2	0.14	0.01	umol*g wet sed^{-1}			
F1	D1	Rx	1099	BS	RS	2	2.15	0.12	umol*g wet sed^{-1}			
F1	D2	Rx	1099	BS	RS	2	2.43	0.22	umol*g wet sed^{-1}			

Sample Code						n	Avg.	Std. Dev	Units	Avg.	Std. Dev	Units
F1	D3	Rx	1099	BS	RS	2	4.77	0.45	umol*g wet sed^{-1}			
F1	D4	Rx	1099	BS	RS	2	4.31	0.12	umol*g wet sed^{-1}			
F2	D1	Rx	1099	BS	RS	2	0.04	0.00	umol*g wet sed^{-1}			
F3	V1	Rx	1099	BS	RS	2	0.09	0.03	umol*g wet sed^{-1}			
F3	V3	Rx	1099	BS	RS	2	0.11	0.00	umol*g wet sed^{-1}			
LS	D1	Rx	1099	BS	RS	2	6.22	0.13	umol*g wet sed^{-1}			
LN	D1	Rx	1099	BS	RS	2	0.53	0.01	umol*g wet sed^{-1}			
CD	D1	Rx	1099	BS	RS	2	7.51	0.20	umol*g wet sed^{-1}			
CL	D1	Rx	1099	BS	RS	2	13.63	0.70	umol*g wet sed^{-1}			
LL	D1	Rx	1099	BS	RS	2	11.91	0.37	umol*g wet sed^{-1}			
SP	D1	Rx	1099	BS	RS	2	4.35	0.26	umol*g wet sed^{-1}			
SS	D1	Rx	1099	BS	RS	2	6.84	0.10	umol*g wet sed^{-1}			
SC	D1	Rx	1099	BS	RS	2	7.52	1.32	umol*g wet sed^{-1}			
SC	D2	Rx	1099	BS	RS	2	20.32	3.40	umol*g wet sed^{-1}			
SC	D3	Rx	1099	BS	RS	2	10.16	0.00	umol*g wet sed^{-1}			
SC	D4	Rx	1099	BS	RS	2	7.30	1.23	umol*g wet sed^{-1}			
CS	D1	Rx	1099	BS	RS	2	6.91	0.31	umol*g wet sed^{-1}			

C14. Iron

LB	D1	Rx	1098	BS	Fe	2	30.1	5.2	mg*g dry sed^{-1}			
DR	D1	Rx	1098	BS	Fe	2	31.0	0.2	mg*g dry sed^{-1}			
F1	D1	Rx	1098	BS	Fe	2	24.6	2.5	mg*g dry sed^{-1}			
F2	D1	Rx	1098	BS	Fe	2	13.0	1.4	mg*g dry sed^{-1}			
LS	D1	Rx	1098	BS	Fe	2	16.7	0.5	mg*g dry sed^{-1}			
LN	D1	Rx	1098	BS	Fe	2	29.3	0.8	mg*g dry sed^{-1}			
CD	D1	Rx	1098	BS	Fe	2	15.2	0.9	mg*g dry sed^{-1}			
CL	D1	Rx	1098	BS	Fe	2	30.1	0.2	mg*g dry sed^{-1}			
LL	D1	Rx	1098	BS	Fe	2	23.8	2.1	mg*g dry sed^{-1}			
SP	D1	Rx	1098	BS	Fe	2	28.6	0.6	mg*g dry sed^{-1}			
SS	D1	Rx	1098	BS	Fe	2	26.4	1.9	mg*g dry sed^{-1}			
SC	D1	Rx	1098	BS	Fe	3	32.3	0.7	mg*g dry sed^{-1}			
CS	D1	Rx	1098	BS	Fe	2	23.0	0.0	mg*g dry sed^{-1}			
xx	xx	EB	1098	xx	Fe	2	0.6	0.4	ug Fe			
LB	D1	MS	1098	BS	Fe	2	82.7	7.82	mg*g dry sed^{-1}			
CD	D1	MS	1098	BS	Fe	2	88.1	0.42	mg*g dry sed^{-1}			

LB	D1	Rx	0699	BS	Fe	3	39.0	1.6	mg*g dry sed^{-1}			
LB	D2	Rx	0699	BS	Fe	2	32.6	1.0	mg*g dry sed^{-1}			
LB	D3	Rx	0699	BS	Fe	2	36.8	1.4	mg*g dry sed^{-1}			
LB	D4	Rx	0699	BS	Fe	2	37.6	1.1	mg*g dry sed^{-1}			
DR	D1	Rx	0699	BS	Fe	2	26.3	13.8	mg*g dry sed^{-1}			
F1	D1	Rx	0699	BS	Fe	2	29.0	8.4	mg*g dry sed^{-1}			
F1	D2	Rx	0699	BS	Fe	2	32.1	1.6	mg*g dry sed^{-1}			
F1	D3	Rx	0699	BS	Fe	2	31.2	4.3	mg*g dry sed^{-1}			
F1	D4	Rx	0699	BS	Fe	2	22.6	10.7	mg*g dry sed^{-1}			
F2	D1	Rx	0699	BS	Fe	2	23.4	10.0	mg*g dry sed^{-1}			
F3	V1	Rx	0699	BS	Fe	1	38.7		mg*g dry sed^{-1}			
F3	V2	Rx	0699	BS	Fe	2	30.0	0.5	mg*g dry sed^{-1}			
F3	V3	Rx	0699	BS	Fe	2	20.3	0.7	mg*g dry sed^{-1}			
LS	D1	Rx	0699	BS	Fe	2	21.6	2.1	mg*g dry sed^{-1}			
LS	D2	Rx	0699	BS	Fe	2	25.3	1.4	mg*g dry sed^{-1}			
LS	D3	Rx	0699	BS	Fe	2	20.8	0.7	mg*g dry sed^{-1}			
LS	D4	Rx	0699	BS	Fe	1	18.5		mg*g dry sed^{-1}			
LN	D1	Rx	0699	BS	Fe	2	25.3	0.2	mg*g dry sed^{-1}			

Sample Code						n	Avg.	Std. Dev	Units	Avg.	Std. Dev	Units
CD	D1	Rx	0699	BS	Fe	2	22.2	0.7	mg*g dry sed^{-1}			
CL	D1	Rx	0699	BS	Fe	2	28.8	0.3	mg*g dry sed^{-1}			
LL	D1	Rx	0699	BS	Fe	2	24.1	1.1	mg*g dry sed^{-1}			
SP	D1	Rx	0699	BS	Fe	2	26.6	1.4	mg*g dry sed^{-1}			
SS	D1	Rx	0699	BS	Fe	2	22.9	0.8	mg*g dry sed^{-1}			
SC	D1	Rx	0699	BS	Fe	2	23.8	0.2	mg*g dry sed^{-1}			
SC	D2	Rx	0699	BS	Fe	2	24.1	0.8	mg*g dry sed^{-1}			
SC	D3	Rx	0699	BS	Fe	2	25.2	0.1	mg*g dry sed^{-1}			
SC	D4	Rx	0699	BS	Fe	2	27.5	0.1	mg*g dry sed^{-1}			
CS	D1	Rx	0699	BS	Fe	2	22.4	0.9	mg*g dry sed^{-1}			
F1	D1	Rx	1099	BS	Fe	2	28.3	0.9	mg*g dry sed^{-1}			
F1	D2	Rx	1099	BS	Fe	2	28.4	0.5	mg*g dry sed^{-1}			
F1	D3	Rx	1099	BS	Fe	2	28.7	0.4	mg*g dry sed^{-1}			
F1	D4	Rx	1099	BS	Fe	2	31.8	0.6	mg*g dry sed^{-1}			
SC	D1	Rx	1099	BS	Fe	3	24.4	1.3	mg*g dry sed^{-1}			
SC	D2	Rx	1099	BS	Fe	2	24.7	2.0	mg*g dry sed^{-1}			
SC	D3	Rx	1099	BS	Fe	2	26.8	0.7	mg*g dry sed^{-1}			
SC	D4	Rx	1099	BS	Fe	2	23.2	0.1	mg*g dry sed^{-1}			

C15. Manganese

LB	D1	Rx	1098	BS	Mn	2	0.42	0.02	mg*g dry sed^{-1}			
DR	D1	Rx	1098	BS	Mn	2	0.58	0.01	mg*g dry sed^{-1}			
F1	D1	Rx	1098	BS	Mn	2	0.50	0.01	mg*g dry sed^{-1}			
F2	D1	Rx	1098	BS	Mn	2	0.30	0.03	mg*g dry sed^{-1}			
LS	D1	Rx	1098	BS	Mn	2	0.26	0.01	mg*g dry sed^{-1}			
LN	D1	Rx	1098	BS	Mn	2	0.37	0.02	mg*g dry sed^{-1}			
CD	D1	Rx	1098	BS	Mn	2	0.17	0.01	mg*g dry sed^{-1}			
CL	D1	Rx	1098	BS	Mn	2	1.04	0.02	mg*g dry sed^{-1}			
LL	D1	Rx	1098	BS	Mn	2	0.36	0.04	mg*g dry sed^{-1}			
SP	D1	Rx	1098	BS	Mn	2	0.67	0.01	mg*g dry sed^{-1}			
SS	D1	Rx	1098	BS	Mn	2	0.83	0.07	mg*g dry sed^{-1}			
SC	D1	Rx	1098	BS	Mn	3	0.59	0.01	mg*g dry sed^{-1}			
CS	D1	Rx	1098	BS	Mn	2	0.29	0.00	mg*g dry sed^{-1}			
xx	xx	EB	1098	xx	Mn	2	**< 0.03**		ug Fe			
LB	D1	MS	1098	BS	Mn	2	1.58	0.00	mg*g dry sed^{-1}			
CD	D1	MS	1098	BS	Mn	2	1.58	0.09	mg*g dry sed^{-1}			
LB	D1	Rx	0699	BS	Mn	3	0.58	0.04	mg*g dry sed^{-1}			
LB	D2	Rx	0699	BS	Mn	2	0.65	0.00	mg*g dry sed^{-1}			
LB	D3	Rx	0699	BS	Mn	2	0.64	0.01	mg*g dry sed^{-1}			
LB	D4	Rx	0699	BS	Mn	2	0.65	0.02	mg*g dry sed^{-1}			
DR	D1	Rx	0699	BS	Mn	2	0.44	0.13	mg*g dry sed^{-1}			
F1	D1	Rx	0699	BS	Mn	2	0.87	0.03	mg*g dry sed^{-1}			
F1	D2	Rx	0699	BS	Mn	2	0.87	0.03	mg*g dry sed^{-1}			
F1	D3	Rx	0699	BS	Mn	2	0.90	0.01	mg*g dry sed^{-1}			
F1	D4	Rx	0699	BS	Mn	2	0.65	0.01	mg*g dry sed^{-1}			
F2	D1	Rx	0699	BS	Mn	2	0.42	0.05	mg*g dry sed^{-1}			
F3	V1	Rx	0699	BS	Mn	1	0.72		mg*g dry sed^{-1}			
F3	V2	Rx	0699	BS	Mn	2	1.33	0.11	mg*g dry sed^{-1}			
F3	V3	Rx	0699	BS	Mn	2	0.23	0.01	mg*g dry sed^{-1}			
LS	D1	Rx	0699	BS	Mn	2	0.40	0.01	mg*g dry sed^{-1}			
LS	D2	Rx	0699	BS	Mn	2	0.46	0.04	mg*g dry sed^{-1}			
LS	D3	Rx	0699	BS	Mn	2	0.49	0.02	mg*g dry sed^{-1}			

Sample Code						n	Avg.	Std. Dev	Units	Avg.	Std. Dev	Units
LS	D4	Rx	0699	BS	Mn	1	0.40		mg*g dry sed^{-1}			
LN	D1	Rx	0699	BS	Mn	2	0.38	0.01	mg*g dry sed^{-1}			
CD	D1	Rx	0699	BS	Mn	2	0.25	0.00	mg*g dry sed^{-1}			
CL	D1	Rx	0699	BS	Mn	2	1.02	0.04	mg*g dry sed^{-1}			
LL	D1	Rx	0699	BS	Mn	2	0.46	0.02	mg*g dry sed^{-1}			
SP	D1	Rx	0699	BS	Mn	2	0.57	0.03	mg*g dry sed^{-1}			
SS	D1	Rx	0699	BS	Mn	2	0.91	0.00	mg*g dry sed^{-1}			
SC	D1	Rx	0699	BS	Mn	2	0.48	0.01	mg*g dry sed^{-1}			
SC	D2	Rx	0699	BS	Mn	2	0.46	0.00	mg*g dry sed^{-1}			
SC	D3	Rx	0699	BS	Mn	2	0.44	0.01	mg*g dry sed^{-1}			
SC	D4	Rx	0699	BS	Mn	2	0.40	0.02	mg*g dry sed^{-1}			
CS	D1	Rx	0699	BS	Mn	2	0.28	0.02	mg*g dry sed^{-1}			
F1	D1	Rx	1099	BS	Mn	2	0.39	0.01	mg*g dry sed^{-1}			
F1	D2	Rx	1099	BS	Mn	2	0.43	0.01	mg*g dry sed^{-1}			
F1	D3	Rx	1099	BS	Mn	2	0.54	0.04	mg*g dry sed^{-1}			
F1	D4	Rx	1099	BS	Mn	2	0.84	0.02	mg*g dry sed^{-1}			
SC	D1	Rx	1099	BS	Mn	3	0.47	0.02	mg*g dry sed^{-1}			
SC	D2	Rx	1099	BS	Mn	2	0.46	0.02	mg*g dry sed^{-1}			
SC	D3	Rx	1099	BS	Mn	2	0.45	0.01	mg*g dry sed^{-1}			
SC	D4	Rx	1099	BS	Mn	2	0.44	0.00	mg*g dry sed^{-1}			

C16. Selenium

LB	D1	Rx	0699	BS	Se	3	0.31	0.03	ug*g dry sed^{-1}			
LB	D2	Rx	0699	BS	Se	2	0.36	0.01	ug*g dry sed^{-1}			
LB	D3	Rx	0699	BS	Se	2	0.37	0.02	ug*g dry sed^{-1}			
LB	D4	Rx	0699	BS	Se	2	0.32	0.05	ug*g dry sed^{-1}			
DR	D1	Rx	0699	BS	Se	2	0.31	0.06	ug*g dry sed^{-1}			
F1	D1	Rx	0699	BS	Se	2	0.45	0.10	ug*g dry sed^{-1}			
F1	D2	Rx	0699	BS	Se	2	0.46	0.04	ug*g dry sed^{-1}			
F1	D3	Rx	0699	BS	Se	2	0.48	0.02	ug*g dry sed^{-1}			
F1	D4	Rx	0699	BS	Se	2	0.44	0.01	ug*g dry sed^{-1}			
F2	D1	Rx	0699	BS	Se	2	0.32	0.03	ug*g dry sed^{-1}			
F3	V1	Rx	0699	BS	Se	1	0.40		ug*g dry sed^{-1}			
F3	V2	Rx	0699	BS	Se	2	0.41	0.01	ug*g dry sed^{-1}			
F3	V3	Rx	0699	BS	Se	2	0.21	0.01	ug*g dry sed^{-1}			
LS	D1	Rx	0699	BS	Se	1	0.25		ug*g dry sed^{-1}			
LS	D2	Rx	0699	BS	Se	1	0.27		ug*g dry sed^{-1}			
LS	D3	Rx	0699	BS	Se	2	0.25	0.03	ug*g dry sed^{-1}			
LS	D4	Rx	0699	BS	Se	1	0.28		ug*g dry sed^{-1}			
LN	D1	Rx	0699	BS	Se	2	0.41	0.01	ug*g dry sed^{-1}			
CD	D1	Rx	0699	BS	Se	2	0.30	0.04	ug*g dry sed^{-1}			
CL	D1	Rx	0699	BS	Se	2	0.81	0.02	ug*g dry sed^{-1}			
LL	D1	Rx	0699	BS	Se	2	0.51	0.01	ug*g dry sed^{-1}			
SP	D1	Rx	0699	BS	Se	2	0.59	0.06	ug*g dry sed^{-1}			
SS	D1	Rx	0699	BS	Se	2	0.47	0.05	ug*g dry sed^{-1}			
SC	D1	Rx	0699	BS	Se	1	0.71		ug*g dry sed^{-1}			
SC	D2	Rx	0699	BS	Se	1	0.50		ug*g dry sed^{-1}			
SC	D3	Rx	0699	BS	Se	2	0.53	0.02	ug*g dry sed^{-1}			
SC	D4	Rx	0699	BS	Se	2	0.55	0.01	ug*g dry sed^{-1}			
CS	D1	Rx	0699	BS	Se	2	0.28	0.01	ug*g dry sed^{-1}			

D. Sediment Pore-water Parameters

Sample Code						n	Avg.	Std. Dev	Units	Avg.	Std. Dev	Units
D1. Bioavailable Mercury via the *mer-lux* probe												
LB	D1	Rx	1098	PWc	BM	2	< 0.40		ng*l^{-1}			
DR	D1	Rx	1098	PWc	BM	2	1.34	1.69	ng*l^{-1}			
F1	D1	Rx	1098	PWc	BM	2	2.92	1.20	ng*l^{-1}			
F2	D1	Rx	1098	PWc	BM	1	< 0.40		ng*l^{-1}			
LS	D1	Rx	1098	PWc	BM	2	< 0.40		ng*l^{-1}			
LN	D1	Rx	1098	PWc	BM	2	< 0.40		ng*l^{-1}			
CD	D1	Rx	1098	PWc	BM	2	0.67	0.95	ng*l^{-1}			
CL	D1	Rx	1098	PWc	BM	2	< 0.40		ng*l^{-1}			
LL	D1	Rx	1098	PWc	BM	2	0.63	0.45	ng*l^{-1}			
SP	D1	Rx	1098	PWc	BM	2	< 0.40		ng*l^{-1}			
SS	D1	Rx	1098	PWc	BM	2	1.74	0.88	ng*l^{-1}			
SC	D1	Rx	1098	PWc	BM	2	6.11	7.53	ng*l^{-1}			
CS	D1	Rx	1098	PWc	BM	2	2.93	0.81	ng*l^{-1}			
LB	D1	Rx	0699	PWc	BM	3	< 0.20		ng*l^{-1}			
DR	D1	Rx	0699	PWc	BM	2	< 0.20		ng*l^{-1}			
F1	D1	Rx	0699	PWc	BM	2	< 0.20		ng*l^{-1}			
F2	D1	Rx	0699	PWc	BM	2	< 0.20		ng*l^{-1}			
LS	D1	Rx	0699	PWc	BM	2	< 0.20		ng*l^{-1}			
LN	D1	Rx	0699	PWc	BM	2	< 0.20		ng*l^{-1}			
CD	D1	Rx	0699	PWc	BM	2	< 0.20		ng*l^{-1}			
CL	D1	Rx	0699	PWc	BM	2	< 0.20		ng*l^{-1}			
SS	D1	Rx	0699	PWc	BM	2	< 0.20		ng*l^{-1}			
D2. Chloride												
LB	D1	Rx	1098	PWs	Cl	2	0.44	0.03	mmol*l^{-1}			
DR	D1	Rx	1098	PWs	Cl	2	0.42	0.03	mmol*l^{-1}			
F1	D1	Rx	1098	PWs	Cl	2	0.39	0.04	mmol*l^{-1}			
F2	D1	Rx	1098	PWs	Cl	2	0.33	0.00	mmol*l^{-1}			
LS	D1	Rx	1098	PWs	Cl	2	0.64	0.01	mmol*l^{-1}			
LN	D1	Rx	1098	PWs	Cl	2	0.22	0.01	mmol*l^{-1}			
CD	D1	Rx	1098	PWs	Cl	2	0.37	0.10	mmol*l^{-1}			
CL	D1	Rx	1098	PWs	Cl	2	5.91	0.05	mmol*l^{-1}			
LL	D1	Rx	1098	PWs	Cl	2	40.56	0.88	mmol*l^{-1}			
SP	D1	Rx	1098	PWs	Cl	2	6.17	0.20	mmol*l^{-1}			
SS	D1	Rx	1098	PWs	Cl	2	18.16	0.65	mmol*l^{-1}			
SC	D1	Rx	1098	PWc	Cl	3	17.74	0.46	mmol*l^{-1}			
CS	D1	Rx	1098	PWs	Cl	2	50.09	0.56	mmol*l^{-1}			
xx	xx	EB	1098	PWs	Cl	2	<0.004		mmol*l^{-1}			
xx	xx	EB	1098	PWc	Cl	2	<0.004		mmol*l^{-1}			
CL	D1	Rx	1098	PWs	Cl	2	3.26	0.13	mmol*l^{-1}			
CL	D1	Rx	1098	PWc	Cl	2	3.08	0.07	mmol*l^{-1}			
F1	D1	MS	1098	PWs	Cl	2	1.09	0.03	mmol*l^{-1}			
LB	D1	Rx	0699	PWc	Cl	2	1.51	0.07	mmol*l^{-1}			
LB	D2	Rx	0699	PWc	Cl	2	1.39	0.13	mmol*l^{-1}			
LB	D3	Rx	0699	PWc	Cl	2	0.25	0.01	mmol*l^{-1}			
LB	D4	Rx	0699	PWc	Cl	2	0.29	0.02	mmol*l^{-1}			
F1	D1	Rx	0699	PWc	Cl	2	0.13	0.02	mmol*l^{-1}			
F1	D2	Rx	0699	PWc	Cl	2	0.09	0.03	mmol*l^{-1}			
F1	D3	Rx	0699	PWc	Cl	1	0.11		mmol*l^{-1}			
F1	D4	Rx	0699	PWc	Cl	2	0.15	0.01	mmol*l^{-1}			
LS	D1	Rx	0699	PWc	Cl	2	0.21	0.01	mmol*l^{-1}			

Sample Code	n	Avg.	Std. Dev	Units	Avg.	Std. Dev	Units
LS D2 Rx 0699 PWc Cl	2	0.18	0.03	mmol*l^{-1}			
LS D3 Rx 0699 PWc Cl	2	0.10	0.01	mmol*l^{-1}			
LS D4 Rx 0699 PWc Cl	2	0.09	0.02	mmol*l^{-1}			
SC D1 Rx 0699 PWc Cl	2	17.38	0.26	mmol*l^{-1}			
SC D2 Rx 0699 PWc Cl	2	17.15	0.45	mmol*l^{-1}			
SC D3 Rx 0699 PWc Cl	2	19.79	0.35	mmol*l^{-1}			
SC D4 Rx 0699 PWc Cl	2	14.36	0.73	mmol*l^{-1}			
xx xx EB 0699 PWc Cl	2	**< 0.002**		mmol*l^{-1}			
F1 D1 Rx 1099 PWc Cl	2	0.50	0.04	mmol*l^{-1}			
F1 D2 Rx 1099 PWc Cl	2	0.43	0.04	mmol*l^{-1}			
F1 D3 Rx 1099 PWc Cl	2	0.45	0.11	mmol*l^{-1}			
F1 D4 Rx 1099 PWc Cl	2	0.37	0.04	mmol*l^{-1}			
SC D1 Rx 1099 PWc Cl	3	10.57	2.80	mmol*l^{-1}			
SC D2 Rx 1099 PWc Cl	2	7.62	2.22	mmol*l^{-1}			
SC D3 Rx 1099 PWc Cl	2	9.96	1.22	mmol*l^{-1}			
SC D4 Rx 1099 PWc Cl	1	11.22		mmol*l^{-1}			
xx xx EB 1099 PWc Cl	2	**< 0.002**		mmol*l^{-1}			

D3. Nitrate

LB D1 Rx 1098 PWs NO3	2	17.3	0.6	umol*l^{-1}			
DR D1 Rx 1098 PWs NO3	2	15.7	11.8	umol*l^{-1}			
F1 D1 Rx 1098 PWs NO3	2	9.1	4.3	umol*l^{-1}			
F2 D1 Rx 1098 PWs NO3	2	128.1	1 0	umol*l^{-1}			
LS D1 Rx 1098 PWs NO3	2	24.1	0.2	umol*l^{-1}			
LN D1 Rx 1098 PWs NO3	2	12.4	0.5	umol*l^{-1}			
CD D1 Rx 1098 PWs NO3	2	1.8	0.3	umol*l^{-1}			
CL D1 Rx 1098 PWs NO3	2	13.0	0.6	umol*l^{-1}			
LL D1 Rx 1098 PWs NO3	2	16.8	5.9	umol*l^{-1}			
SP D1 Rx 1098 PWs NO3	2	9.4	3.2	umol*l^{-1}			
SS D1 Rx 1098 PWs NO3	2	9.0	7.2	umol*l^{-1}			
SC D1 Rx 1098 PWc NO3	3	8.1	5.9	umol*l^{-1}			
CS D1 Rx 1098 PWs NO3	2	37.5	3.6	umol*l^{-1}			
xx xx EB 1098 PWs NO3	2	**< 0.8**		umol*l^{-1}			
xx xx EB 1098 PWc NO3	2	**< 0.8**		umol*l^{-1}			
CL D1 Rx 1098 PWs NO3	2	48.9	2.2	umol*l^{-1}			
CL D1 Rx 1098 PWc NO3	2	9.7	6.7	umol*l^{-1}			
F1 D1 MS 1098 PWs NO3	2	56 4	1.8	umol*l^{-1}			
LB D1 Rx 0699 PWc NO3	2	253.7	10.9	umol*l^{-1}			
LB D2 Rx 0699 PWc NO3	2	216 3	42.5	umol*l^{-1}			
LB D3 Rx 0699 PWc NO3	2	6.6	0.6	umol*l^{-1}			
LB D4 Rx 0699 PWc NO3	2	18.0	2.6	umol*l^{-1}			
F1 D1 Rx 0699 PWc NO3	2	1.7	1.5	umol*l^{-1}			
F1 D2 Rx 0699 PWc NO3	2	1.5	0.2	umol*l^{-1}			
F1 D3 Rx 0699 PWc NO3	1	0 7		umol*l^{-1}			
F1 D4 Rx 0699 PWc NO3	2	0.4	0.2	umol*l^{-1}			
LS D1 Rx 0699 PWc NO3	2	4.5	1 7	umol*l^{-1}			
LS D2 Rx 0699 PWc NO3	2	7.9	1.5	umol*l^{-1}			
LS D3 Rx 0699 PWc NO3	2	860.5	15.5	umol*l^{-1}			
LS D4 Rx 0699 PWc NO3	2	11 2	2.7	umol*l^{-1}			
SC D1 Rx 0699 PWc NO3	2	2.3	0.6	umol*l^{-1}			
SC D2 Rx 0699 PWc NO3	2	8.2	0 6	umol*l^{-1}			
SC D3 Rx 0699 PWc NO3	2	1.6	0.9	umol*l^{-1}			

Sample Code	n	Avg.	Std. Dev	Units	Avg.	Std. Dev	Units
SC D4 Rx 0699 PWc NO3	2	5,664 6	337 3	umol*l^{-1}			
xx xx EB 0699 PWc NO3	2	0 4	0 6	umol*l^{-1}			
F1 D1 Rx 1099 PWc NO3	2	0 4		umol*l^{-1}			
F1 D2 Rx 1099 PWc NO3	2	0 7	0 1	umol*l^{-1}			
F1 D3 Rx 1099 PWc NO3	2	1 5	0 6	umol*l^{-1}			
F1 D4 Rx 1099 PWc NO3	2	1 9	1 4	umol*l^{-1}			
SC D1 Rx 1099 PWc NO3	2	1 1		umol*l^{-1}			
SC D2 Rx 1099 PWc NO3	2	1 9	0 4	umol*l^{-1}			
SC D3 Rx 1099 PWc NO3	2	2 2		umol*l^{-1}			
SC D4 Rx 1099 PWc NO3	2	2 0		umol*l^{-1}			
xx xx EB 1099 PWc NO3	2	**< 0.4**		umol*l^{-1}			

D4 Sulfate

LB	D1	Rx	1098	PWs	SO4	2	18	3	umol*l^{-1}	
DR	D1	Rx	1098	PWs	SO4	2	27	16	umol*l^{-1}	
F1	D1	Rx	1098	PWs	SO4	2	94	0	umol*l^{-1}	
F2	D1	Rx	1098	PWs	SO4	2	569	3	umol*l^{-1}	
LS	D1	Rx	1098	PWs	SO4	2	55	0	umol*l^{-1}	
LN	D1	Rx	1098	PWs	SO4	2	18	0	umol*l^{-1}	
CD	D1	Rx	1098	PWs	SO4	2	271	5	umol*l^{-1}	
CL	D1	Rx	1098	PWs	SO4	2	19	1	umol*l^{-1}	
LL	D1	Rx	1098	PWs	SO4	2	32	7	umol*l^{-1}	
SP	D1	Rx	1098	PWs	SO4	2	65	8	umol*l^{-1}	
SS	D1	Rx	1098	PWs	SO4	2	227	38	umol*l^{-1}	
SC	D1	Rx	1098	PWc	SO4	3	5	2	umol*l^{-1}	
CS	D1	Rx	1098	PWs	SO4	2	641	76	umol*l^{-1}	
xx	xx	EB	1098	PWs	SO4	2	1	0	umol*l^{-1}	
xx	xx	EB	1098	PWc	SO4	2	**< 0.5**		umol*l^{-1}	
CL	D1	Rx	1098	PWs	SO4	2	58	1	umol*l^{-1}	
CL	D1	Rx	1098	PWc	SO4	2	2	2	umol*l^{-1}	
F1	D1	MS	1098	PWs	SO4	2	479	11	umol*l^{-1}	
LB	D1	Rx	0699	PWc	SO4	2	643	27	umol*l^{-1}	
LB	D2	Rx	0699	PWc	SO4	2	494	51	umol*l^{-1}	
LB	D3	Rx	0699	PWc	SO4	2	224	124	umol*l^{-1}	
LB	D4	Rx	0699	PWc	SO4	2	256	11	umol*l^{-1}	
F1	D1	Rx	0699	PWc	SO4	2	145	20	umol*l^{-1}	
F1	D2	Rx	0699	PWc	SO4	2	30	1	umol*l^{-1}	
F1	D3	Rx	0699	PWc	SO4	1	66	37	umol*l^{-1}	
F1	D4	Rx	0699	PWc	SO4	2	15	5	umol*l^{-1}	
LS	D1	Rx	0699	PWc	SO4	2	646	35	umol*l^{-1}	
LS	D2	Rx	0699	PWc	SO4	2	368	237	umol*l^{-1}	
LS	D3	Rx	0699	PWc	SO4	2	157	8	umol*l^{-1}	
LS	D4	Rx	0699	PWc	SO4	2	149	35	umol*l^{-1}	
SC	D1	Rx	0699	PWc	SO4	2	2,130	46	umol*l^{-1}	
SC	D2	Rx	0699	PWc	SO4	2	561	95	umol*l^{-1}	
SC	D3	Rx	0699	PWc	SO4	2	1,080	43	umol*l^{-1}	
SC	D4	Rx	0699	PWc	SO4	2	2,082	133	umol*l^{-1}	
xx	xx	EB	0699	PWc	SO4	2	5	5	umol*l^{-1}	
F1	D1	Rx	1099	PWc	SO4	2	457	10	umol*l^{-1}	
F1	D2	Rx	1099	PWc	SO4	2	45	4	umol*l^{-1}	
F1	D3	Rx	1099	PWc	SO4	2	25		umol*l^{-1}	

Sample Code	n	Avg.	Std. Dev	Units	Avg.	Std. Dev	Units
F1 D4 Rx 1099 PWc SO4	2	11		umol*l^{-1}			
SC D1 Rx 1099 PWc SO4	3	747	25	umol*l^{-1}			
SC D2 Rx 1099 PWc SO4	2	193	107	umol*l^{-1}			
SC D3 Rx 1099 PWc SO4	2	291	13	umol*l^{-1}			
SC D4 Rx 1099 PWc SO4	2	204	11	umol*l^{-1}			
xx xx EB 1099 PWc SO4	2	6		umol*l^{-1}			

D5 Phosphate

LB D1 Rx 1098 PWs PO4	2	**< 0.5**		umol*l^{-1}			
DR D1 Rx 1098 PWs PO4	2	6 4	0 9	umol*l^{-1}			
F1 D1 Rx 1098 PWs PO4	2	3 5	0 5	umol*l^{-1}			
F2 D1 Rx 1098 PWs PO4	2	11 6	2 1	umol*l^{-1}			
LS D1 Rx 1098 PWs PO4	2	**< 0.5**		umol*l^{-1}			
LN D1 Rx 1098 PWs PO4	2	**< 0.5**		umol*l^{-1}			
CD D1 Rx 1098 PWs PO4	2	**< 0.5**		umol*l^{-1}			
CL D1 Rx 1098 PWs PO4	2	92 1	4 7	umol*l^{-1}			
LL D1 Rx 1098 PWs PO4	2	55 6	2 3	umol*l^{-1}			
SP D1 Rx 1098 PWs PO4	2	98 4	3 3	umol*l^{-1}			
SS D1 Rx 1098 PWs PO4	2	131 7	4 6	umol*l^{-1}			
SC D1 Rx 1098 PWc PO4	3	93 0	17 4	umol*l^{-1}			
CS D1 Rx 1098 PWs PO4	2	13 0	0 7	umol*l^{-1}			
xx xx EB 1098 PWs PO4	2	**< 0.5**		umol*l^{-1}			
xx xx EB 1098 PWc PO4	2	**< 0.5**		umol*l^{-1}			
CL D1 Rx 1098 PWs PO4	2	125 9	5 6	umol*l^{-1}			
CL D1 Rx 1098 PWc PO4	2	163 3	2 3	umol*l^{-1}			
F1 D1 MS 1098 PWs PO4	2	12 1	2 0	umol*l^{-1}			
LB D1 Rx 0699 PWc PO4	2	6 4	0 3	umol*l^{-1}			
LB D2 Rx 0699 PWc PO4	2	1 8	1 6	umol*l^{-1}			
LB D3 Rx 0699 PWc PO4	2	5 2	3 2	umol*l^{-1}			
LB D4 Rx 0699 PWc PO4	1	1 3		umol*l^{-1}			
F1 D1 Rx 0699 PWc PO4	2	1 7	0 0	umol*l^{-1}			
F1 D2 Rx 0699 PWc PO4	2	1 0	0 1	umol*l^{-1}			
F1 D3 Rx 0699 PWc PO4	2	**< 0.6**		umol*l^{-1}			
F1 D4 Rx 0699 PWc PO4	1	2 4		umol*l^{-1}			
LS D1 Rx 0699 PWc PO4	2	5 3	0 6	umol*l^{-1}			
LS D2 Rx 0699 PWc PO4	2	3 9	1 8	umol*l^{-1}			
LS D3 Rx 0699 PWc PO4	2	**< 0.6**		umol*l^{-1}			
LS D4 Rx 0699 PWc PO4	2	7 5	1 8	umol*l^{-1}			
SC D1 Rx 0699 PWc PO4	2	26 7	0 6	umol*l^{-1}			
SC D2 Rx 0699 PWc PO4	2	36 6	4 0	umol*l^{-1}			
SC D3 Rx 0699 PWc PO4	2	24 9	1 1	umol*l^{-1}			
SC D4 Rx 0699 PWc PO4	2	117 4	4 4	umol*l^{-1}			
xx xx EB 0699 PWc PO4	2	**< 0.6**		umol*l^{-1}			
F1 D1 Rx 1099 PWc PO4	2	1 6	0 3	umol*l^{-1}			
F1 D2 Rx 1099 PWc PO4	2	1 1	0 1	umol*l^{-1}			
F1 D3 Rx 1099 PWc PO4	2	1 3	1 1	umol*l^{-1}			
F1 D4 Rx 1099 PWc PO4	2	**< 0.6**		umol*l^{-1}			
SC D1 Rx 1099 PWc PO4	3	37 9	0 7	umol*l^{-1}			
SC D2 Rx 1099 PWc PO4	2	48 9	0 7	umol*l^{-1}			
SC D3 Rx 1099 PWc PO4	2	48 4	0 5	umol*l^{-1}			
SC D4 Rx 1099 PWc PO4	2	47 4	0 4	umol*l^{-1}			
xx xx EB 1099 PWc PO4	2	**< 0.6**		umol*l^{-1}			

Sample Code	n	Avg.	Std. Dev	Units	Avg.	Std. Dev	Units

D6 Sulfide

LB	D1	Rx	1098	PWs	SU	2	1 7	1 1	umol*l^{-1}	
DR	D1	Rx	1098	PWs	SU	2	2 0	0 2	umol*l^{-1}	
F1	D1	Rx	1098	PWs	SU	2	**< 0 3**		umol*l^{-1}	
F2	D1	Rx	1098	PWs	SU	2	**< 0.3**		umol*l^{-1}	
LS	D1	Rx	1098	PWs	SU	2	0 5	0 3	umol*l^{-1}	
LN	D1	Rx	1098	PWs	SU	2	0 6	0 1	umol*l^{-1}	
CD	D1	Rx	1098	PWs	SU	2	1 1	0 1	umol*l^{-1}	
CL	D1	Rx	1098	PWs	SU	2	2 2	1 1	umol*l^{-1}	
LL	D1	Rx	1098	PWs	SU	2	143 4	5 1	umol*l^{-1}	
SP	D1	Rx	1098	PWs	SU	2	20 8	4 1	umol*l^{-1}	
SS	D1	Rx	1098	PWs	SU	2	3 0	2 2	umol*l^{-1}	
SC	D1	Rx	1098	PWc	SU	3	966 8	68 2	umol*l^{-1}	
CS	D1	Rx	1098	PWs	SU	2	6 4	3 0	umol*l^{-1}	
xx	xx	EB	1098	PWs	SU	2	**< 0.3**		umol*l^{-1}	
xx	xx	EB	1098	PWc	SU	2	**< 0.3**		umol*l^{-1}	
LL	D1	MS	1098	PWs	SU	1	190 7		umol*l^{-1}	
CL	D1	Rx	1098	PWs	SU	2	7 6	2 6	umol*l^{-1}	
CL	D1	Rx	1098	PWc	SU	2	4 3	1 0	umol*l^{-1}	

LB	D1	Rx	0699	PWc	SU	2	0 5	0 6	umol*l^{-1}	
LB	D2	Rx	0699	PWc	SU	2	1 0	0 4	umol*l^{-1}	
LB	D3	Rx	0699	PWc	SU	2	**< 0.5**		umol*l^{-1}	
LB	D4	Rx	0699	PWc	SU	2	**< 0.5**		umol*l^{-1}	
F1	D1	Rx	0699	PWc	SU	1	0 7		umol*l^{-1}	
F1	D2	Rx	0699	PWc	SU	2	**< 0.5**		umol*l^{-1}	
F1	D3	Rx	0699	PWc	SU	2	0 7	0 3	umol*l^{-1}	
F1	D4	Rx	0699	PWc	SU	1	0 8	0 0	umol*l^{-1}	
LS	D1	Rx	0699	PWc	SU	2	2 0	0 8	umol*l^{-1}	
LS	D2	Rx	0699	PWc	SU	2	1 5	0 2	umol*l^{-1}	
LS	D3	Rx	0699	PWc	SU	2	**< 0.5**		umol*l^{-1}	
LS	D4	Rx	0699	PWc	SU	2	1 7	0 6	umol*l^{-1}	
SC	D1	Rx	0699	PWc	SU	2	144 5	9 5	umol*l^{-1}	
SC	D2	Rx	0699	PWc	SU	2	925 9	13 7	umol*l^{-1}	
SC	D3	Rx	0699	PWc	SU	2	573 5	11 5	umol*l^{-1}	
SC	D4	Rx	0699	PWc	SU	2	31 9	1 2	umol*l^{-1}	
xx	xx	EB	0699	PWc	SU	2	**< 0.5**		umol*l^{-1}	

F1	D1	Rx	1099	PWc	SU	2	**< 0.8**		umol*l^{-1}	
F1	D2	Rx	1099	PWc	SU	2	**< 0.8**		umol*l^{-1}	
F1	D3	Rx	1099	PWc	SU	2	**< 0.8**		umol*l^{-1}	
F1	D4	Rx	1099	PWc	SU	2	**< 0.8**		umol*l^{-1}	
SC	D1	Rx	1099	PWc	SU	3	93 5	16 0	umol*l^{-1}	
SC	D2	Rx	1099	PWc	SU	2	633 6	158 9	umol*l^{-1}	
SC	D3	Rx	1099	PWc	SU	2	441 3	71 5	umol*l^{-1}	
SC	D4	Rx	1099	PWc	SU	2	123 1	2 5	umol*l^{-1}	
xx	xx	EB	1099	PWc	SU	2	**< 0.8**		umol*l^{-1}	

D7. Dissolved Organic Carbon

LB	D1	Rx	1098	PWs	DOC	2	37 1	0 3	mg*l^{-1}	
DR	D1	Rx	1098	PWs	DOC	2	24 7	2 3	mg*l^{-1}	
F1	D1	Rx	1098	PWs	DOC	2	13 6	0 6	mg*l^{-1}	
F2	D1	Rx	1098	PWs	DOC	2	4 8	0 7	mg*l^{-1}	

Sample Code	n	Avg.	Std. Dev	Units	Avg.	Std. Dev	Units
LS D1 Rx 1098 PWs DOC	2	25 8	0 0	mg*l^{-1}			
LN D1 Rx 1098 PWs DOC	2	57 9	3 1	mg*l^{-1}			
CD D1 Rx 1098 PWs DOC	2	13 3	2 1	mg*l^{-1}			
CL D1 Rx 1098 PWs DOC	2	29 2	2 3	mg*l^{-1}			
LL D1 Rx 1098 PWs DOC	2	39 9	2 7	mg*l^{-1}			
SP D1 Rx 1098 PWs DOC	2	14 4	0 3	mg*l^{-1}			
SS D1 Rx 1098 PWs DOC	2	26 6	1 0	mg*l^{-1}			
SC D1 Rx 1098 PWc DOC	3	26 6	1 7	mg*l^{-1}			
CS D1 Rx 1098 PWs DOC	2	27 8	1 1	mg*l^{-1}			
xx xx EB 1098 PWs DOC	2	4 7	0 5	mg*l^{-1}			
xx xx EB 1098 PWc DOC	2	0 9	0 0	mg*l^{-1}			
CL D1 Rx 1098 PWc DOC	2	30 9	1 8	mg*l^{-1}			
CL D1 Rx 1098 PWs DOC	2	27 5	0 9	mg*l^{-1}			
F1 D1 MS 1098 PWs DOC	2	28 5	1 7	mg*l^{-1}			
LB D1 Rx 0699 PWc DOC	3	16 1	2 8	mg*l^{-1}			
LB D2 Rx 0699 PWc DOC	2	43 9	8 8	mg*l^{-1}			
LB D3 Rx 0699 PWc DOC	1	48 3		mg*l^{-1}			
LB D4 Rx 0699 PWc DOC	2	41 9	14	mg*l^{-1}			
F1 D1 Rx 0699 PWc DOC	1	36 2	8 6	mg*l^{-1}			
F1 D2 Rx 0699 PWc DOC	2	29 7	1	mg*l^{-1}			
F1 D3 Rx 0699 PWc DOC	2	39 1	3 9	mg*l^{-1}			
F1 D4 Rx 0699 PWc DOC	2	36 0	10 3	mg*l^{-1}			
LS D1 Rx 0699 PWc DOC	1	100 0		mg*l^{-1}			
LS D2 Rx 0699 PWc DOC	1	60 1		mg*l^{-1}			
LS D3 Rx 0699 PWc DOC	2	38 1	22	mg*l^{-1}			
LS D4 Rx 0699 PWc DOC	2	46 6	26 2	mg*l^{-1}			
SC D1 Rx 0699 PWc DOC	2	39 1	4 8	mg*l^{-1}			
SC D2 Rx 0699 PWc DOC	2	44 1	1 4	mg*l^{-1}			
SC D3 Rx 0699 PWc DOC	2	38 7	6 8	mg*l^{-1}			
SC D4 Rx 0699 PWc DOC	2	90 3	27 6	mg*l^{-1}			
xx xx EB 0699 PWc DOC	2	**< 1.7**		mg*l^{-1}			
SC D1 MS 0699 PWc DOC	3	124 9	2 6	mg*l^{-1}			
F1 D1 Rx 1099 PWc DOC	2	23 9	1 5	mg*l^{-1}			
F1 D2 Rx 1099 PWc DOC	2	26 7	5 9	mg*l^{-1}			
F1 D3 Rx 1099 PWc DOC	2	31 6	4 0	mg*l^{-1}			
F1 D4 Rx 1099 PWc DOC	2	34 6	7 9	mg*l^{-1}			
SC D1 Rx 1099 PWc DOC	3	27 1	4 0	mg*l^{-1}			
SC D2 Rx 1099 PWc DOC	2	32 6	1 8	mg*l^{-1}			
SC D3 Rx 1099 PWc DOC	2	35 1	1 6	mg*l^{-1}			
SC D4 Rx 1099 PWc DOC	2	42 7	0 4	mg*l^{-1}			
xx xx EB 1099 PWc DOC	2	**< 0.7**		mg*l^{-1}			

D8 Iron

LB D1 Rx 1098 PWs Fe	2	14 0	1 1	mg*l^{-1}			
DR D1 Rx 1098 PWs Fe	2	4 6	6 0	mg*l^{-1}			
F1 D1 Rx 1098 PWs Fe	2	11 7	0 6	mg*l^{-1}			
F2 D1 Rx 1098 PWs Fe	2	0 0	0 0	mg*l^{-1}			
LS D1 Rx 1098 PWs Fe	2	11 6	1 3	mg*l^{-1}			
LN D1 Rx 1098 PWs Fe	2	3 4	0 2	mg*l^{-1}			
CD D1 Rx 1098 PWs Fe	2	5 4	0 3	mg*l^{-1}			
CL D1 Rx 1098 PWs Fe	2	10 6	0 9	mg*l^{-1}			
LL D1 Rx 1098 PWs Fe	2	0 7	0 2	mg*l^{-1}			

Sample Code	n	Avg.	Std. Dev	Units	Avg.	Std. Dev	Units
SP D1 Rx 1098 PWs Fe	2	0 4	0.1	$mg*l^{-1}$			
SS D1 Rx 1098 PWs Fe	2	2.4	0 1	$mg*l^{-1}$			
SC D1 Rx 1098 PWc Fe	3	0.0	0 0	$mg*l^{-1}$			
CS D1 Rx 1098 PWs Fe	2	0 3	0 0	$mg*l^{-1}$			
xx xx EB 1098 PWs Fe	2	0.03	0.00	$mg*l^{-1}$			
xx xx EB 1098 PWc Fe	2	**< 0.01**		$mg*l^{-1}$			
CL D1 Rx 1098 PWc Fe	2	9 1	0.3	$mg*l^{-1}$			
CL D1 Rx 1098 PWs Fe	2	8 2	0 8	$mg*l^{-1}$			
SP D1 MS 1098 PWs Fe	2	1 1	0.0	$mg*l^{-1}$			
LB D1 Rx 0699 PWc Fe	3	2 3	1 5	$mg*l^{-1}$			
LB D2 Rx 0699 PWc Fe	2	1 1	0 2	$mg*l^{-1}$			
LB D3 Rx 0699 PWc Fe	1	0 6	0 1	$mg*l^{-1}$			
LB D4 Rx 0699 PWc Fe	2	2 2	1 6	$mg*l^{-1}$			
F1 D1 Rx 0699 PWc Fe	2	1 3	1 0	$mg*l^{-1}$			
F1 D2 Rx 0699 PWc Fe	2	3 5	0 5	$mg*l^{-1}$			
F1 D3 Rx 0699 PWc Fe	2	1.9	0 0	$mg*l^{-1}$			
F1 D4 Rx 0699 PWc Fe	2	19 1	3 6	$mg*l^{-1}$			
LS D1 Rx 0699 PWc Fe	2	6.0	1 2	$mg*l^{-1}$			
LS D2 Rx 0699 PWc Fe	1	8.5		$mg*l^{-1}$			
LS D3 Rx 0699 PWc Fe	2	1.0	0 1	$mg*l^{-1}$			
LS D4 Rx 0699 PWc Fe	2	22.6	0 3	$mg*l^{-1}$			
SC D1 Rx 0699 PWc Fe	2	0.5	0 1	$mg*l^{-1}$			
SC D2 Rx 0699 PWc Fe	2	0 6	0 0	$mg*l^{-1}$			
SC D3 Rx 0699 PWc Fe	2	1.0	0.4	$mg*l^{-1}$			
SC D4 Rx 0699 PWc Fe	2	9 0	2.9	$mg*l^{-1}$			
xx xx EB 0699 PWc Fe	2	1 2	0.0	$mg*l^{-1}$			
F1 D1 Rx 1099 PWc Fe	2	6 4	0 2	$mg*l^{-1}$			
F1 D2 Rx 1099 PWc Fe	2	30 7	0 0	$mg*l^{-1}$			
F1 D3 Rx 1099 PWc Fe	2	43 4	8.2	$mg*l^{-1}$			
F1 D4 Rx 1099 PWc Fe	2	34 2	0.7	$mg*l^{-1}$			
SC D1 Rx 1099 PWc Fe	3	0 2	0 1	$mg*l^{-1}$			
SC D2 Rx 1099 PWc Fe	2	0 7	0 0	$mg*l^{-1}$			
SC D3 Rx 1099 PWc Fe	2	0 9	0 1	$mg*l^{-1}$			
SC D4 Rx 1099 PWc Fe	2	0 5	0 0	$mg*l^{-1}$			
xx xx EB 1099 PWc Fe	2	**< 0.003**		$mg*l^{-1}$			

D9. Manganese

LB D1 Rx 1098 PWs Mn	2	10 97	0 97	$mg*l^{-1}$			
DR D1 Rx 1098 PWs Mn	2	17.04	13.95	$mg*l^{-1}$			
F1 D1 Rx 1098 PWs Mn	2	12.53	0.04	$mg*l^{-1}$			
F2 D1 Rx 1098 PWs Mn	2	0 02	0.00	$mg*l^{-1}$			
LS D1 Rx 1098 PWs Mn	2	9.09	0.36	$mg*l^{-1}$			
LN D1 Rx 1098 PWs Mn	2	5 82	0.32	$mg*l^{-1}$			
CD D1 Rx 1098 PWs Mn	2	2 21	0.06	$mg*l^{-1}$			
CL D1 Rx 1098 PWs Mn	2	12.04	0.04	$mg*l^{-1}$			
LL D1 Rx 1098 PWs Mn	2	0.77	0.08	$mg*l^{-1}$			
SP D1 Rx 1098 PWs Mn	2	3 44	0 12	$mg*l^{-1}$			
SS D1 Rx 1098 PWs Mn	2	11 86	0 88	$mg*l^{-1}$			
SC D1 Rx 1098 PWc Mn	3	0 43	0.10	$mg*l^{-1}$			
CS D1 Rx 1098 PWs Mn	2	0 23	0 03	$mg*l^{-1}$			
xx xx EB 1098 PWs Mn	2	**< 0.004**		$mg*l^{-1}$			
xx xx EB 1098 PWc Mn	2	**< 0.004**		$mg*l^{-1}$			

Sample Code	n	Avg.	Std. Dev	Units	Avg.	Std. Dev	Units
CL D1 Rx 1098 PWc Mn	2	10.27	0.28	$mg*l^{-1}$			
CL D1 Rx 1098 PWs Mn	2	9 39	0.32	$mg*l^{-1}$			
F2 D1 MS 1098 PWs Mn	2	0.04	0.00	$mg*l^{-1}$			
LB D1 Rx 0699 PWc Mn	3	0 6	0.1	$mg*l^{-1}$			
LB D2 Rx 0699 PWc Mn	2	4 9	0 7	$mg*l^{-1}$			
LB D3 Rx 0699 PWc Mn	2	3.5	0 6	$mg*l^{-1}$			
LB D4 Rx 0699 PWc Mn	2	5 0	1 7	$mg*l^{-1}$			
F1 D1 Rx 0699 PWc Mn	2	10 1	1 2	$mg*l^{-1}$			
F1 D2 Rx 0699 PWc Mn	2	12 6	1 4	$mg*l^{-1}$			
F1 D3 Rx 0699 PWc Mn	2	14.3	0 0	$mg*l^{-1}$			
F1 D4 Rx 0699 PWc Mn	2	26 4	1.4	$mg*l^{-1}$			
LS D1 Rx 0699 PWc Mn	2	1 2	0.5	$mg*l^{-1}$			
LS D2 Rx 0699 PWc Mn	1	1 3		$mg*l^{-1}$			
LS D3 Rx 0699 PWc Mn	2	2.2	0.6	$mg*l^{-1}$			
LS D4 Rx 0699 PWc Mn	2	1.8	0 2	$mg*l^{-1}$			
SC D1 Rx 0699 PWc Mn	2	0 3	0.0	$mg*l^{-1}$			
SC D2 Rx 0699 PWc Mn	2	0 1	0 0	$mg*l^{-1}$			
SC D3 Rx 0699 PWc Mn	2	0 2	0.0	$mg*l^{-1}$			
SC D4 Rx 0699 PWc Mn	2	0 6	0.1	$mg*l^{-1}$			
xx xx EB 0699 PWc Mn	2	0 0	0.0	$mg*l^{-1}$			
F1 D1 Rx 1099 PWc Mn	2	5 0	0.4	$mg*l^{-1}$			
F1 D2 Rx 1099 PWc Mn	2	10 7	0.4	$mg*l^{-1}$			
F1 D3 Rx 1099 PWc Mn	2	25 3	1 0	$mg*l^{-1}$			
F1 D4 Rx 1099 PWc Mn	2	27.7	1 1	$mg*l^{-1}$			
SC D1 Rx 1099 PWc Mn	2	0 04	0 0	$mg*l^{-1}$			
SC D2 Rx 1099 PWc Mn	2	0 10	0.0	$mg*l^{-1}$			
SC D3 Rx 1099 PWc Mn	2	0.09	0 0	$mg*l^{-1}$			
SC D4 Rx 1099 PWc Mn	2	0.10	0 0	$mg*l^{-1}$			
xx xx EB 1099 PWc Mn	2	**< 0.001**		$mg*l^{2}$			

E. Overlying Water Parameters

E1. Water Temperature / Incubation Temperature

LB	D1	Rx	0699	BW	TMP	1	10 0		°C		
DR	D1	Rx	0699	BW	TMP	1	12 0		°C		
F1	D1	Rx	0699	BW	TMP	1	10.0		°C		
F2	D1	Rx	0699	BW	TMP	1	10.0		°C		
F3	D1	Rx	0699	BW	TMP	1	10 0		°C		
LS	D1	Rx	0699	BW	TMP	1	11 0		°C		
LN	D1	Rx	0699	BW	TMP	1	15 0		°C		
CD	D1	Rx	0699	BW	TMP	1	15 0		°C		
CL	D1	Rx	0699	BW	TMP	1	16 0		°C		
LL	D1	Rx	0699	BW	TMP	1	17 0		°C		
SP	D1	Rx	0699	BW	TMP	1	17.5		°C		
SS	D1	Rx	0699	BW	TMP	1	15 0		°C		
SC	D1	Rx	0699	BW	TMP	1	16 5		°C		
CS	D1	Rx	0699	BW	TMP	1	14 0		°C		
LB	D1	Rx	1099	BW	TMP	1	15 0		°C		
DR	D1	Rx	1099	BW	TMP	1	14.0		°C		
DY	D1	Rx	1099	BW	TMP	1	14 0		°C		
F1	D1	Rx	1099	BW	TMP	1	13 0		°C		
F2	D1	Rx	1099	BW	TMP	1	12 0		°C		

Sample Code	n	Avg.	Std. Dev	Units	Avg.	Std. Dev	Units
LS D1 Rx 1099 BW TMP	1	17.0		°C			
LN D1 Rx 1099 BW TMP	1	16 0		°C			
CD D1 Rx 1099 BW TMP	1	12 0[a]		°C			
CL D1 Rx 1099 BW TMP	1	12.0[a]		°C			
LL D1 Rx 1099 BW TMP	1	13.0[a]		°C			
SP D1 Rx 1099 BW TMP	1	13 0		°C			
SS D1 Rx 1099 BW TMP	1	13 0[a]		°C			
SC D1 Rx 1099 BW TMP	1	11 0		°C			
CS D1 Rx 1099 BW TMP	1	11.5		°C			

[a] - *Thermometer lost. In-situ temperature not recorded.* Value indicates incubation used for all microbial transformation assays.